

Dissertation zur Erlangung des Doktorgrades

der Fakultät für Chemie und Pharmazie

der Ludwig-Maximilians-Universität München

# Contributions to the Chemistry of Polyhydroxylated Aromatic Compounds

Methodology, Natural Products and Materials Science

Florian Wolfgang Löbermann

aus München, Deutschland

2013



## **Erklärung**

Diese Dissertation wurde im Sinne von §7 der Promotionsordnung vom 28. November 2011 durch Herrn Prof. Dr. Dirk Trauner betreut.

## **Eidesstaatliche Versicherung**

Diese Dissertation wurde eigenständig und ohne unerlaubte Hilfe erarbeitet.

München, den 28.02.2013

Florian Löbermann

Dissertation eingereicht am 05.03.2013

1. Gutachter: Prof. Dr. Dirk Trauner

2. Gutachter: Prof. Dr. Manfred Heuschmann

Mündliche Prüfung am 22.03.2013



# Acknowledgments

Amongst many other things I have learned during my PhD research, Dirk Trauner – my supervisor – taught me how to unravel the complexity of cluttered problems and to think of elegant and compelling solutions. Also his sense for the beauty of unapparent symmetry always was a huge source of inspiration during my research.

First I would like to express my gratitude to Dr. Laura Salonen who invested a lot of her free time to carefully and critically examine the many drafts of this. Because criticism and discussions are the fuel for scientific development, I would like to thank all my colleagues that helped me to improve as a scientist during my PhD research – in particular: Johannes Broichhagen, Dr. Mesut Cakmak, Dr. Ingrid Chen, Dr. Henry “the Dude” Dube, Pascal Ellerbrock, Dr. Nicolas Guimond, Dr. Michael Kienzler, Dr. Christian “Kutti” Kuttruff, Dr. Eddie Myers, Dr. Albert Schröckeneder and Dr. Rob Webster.

I also benefited a lot from the motivated and dedicated students I was supervising in the past years (listed in order of appearance): Martina Wild, Robert Greiner, Tobias Stürzer, Marina Ilg, Felix Hartrampf, Moritz Pendzialek, Silvia Laube, Katrin Fenzke, Jan Schmidt, Oliver Richter, Adriana Grossmann, Lara Weisheit.

Working on a broad variety of chemical problems was very interesting but also challenging. The results presented in this thesis would not have been possible without the hard work and dedication of: Dr. Albert Schröckeneder (Chapter 1); Prof. Wolfgang Steglich (Chapter 2); Prof. Thomas Bein, Dr. Laura Salonen, Dr. Yan Li, Dr. Mirjam Dogru, Mona Calik, (all Chapter 3).

Of course I would like to mention many more names of friends, colleagues and family, who all supported me during the PhD time and helped me to continue to the end. However, I would be forced to compile a list that could never be complete and go beyond the scope of the acknowledgements for a scientific thesis. So please forgive me for saying it in general terms: Thank you for all the discussions, love, support, drinks, dinners, chats, quiet times, nights out, trips, fights, friendship, advise, coffee- lunch- and ice-cream breaks! I would not have made it without you all!

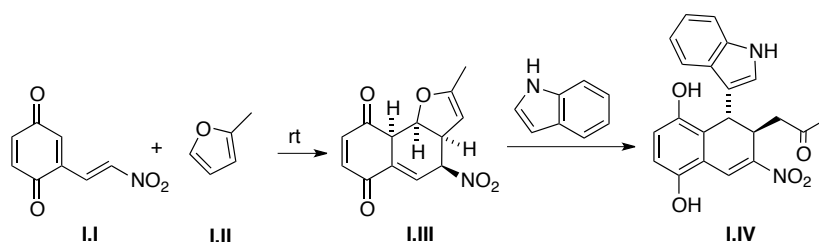


To my Family

# Abstract

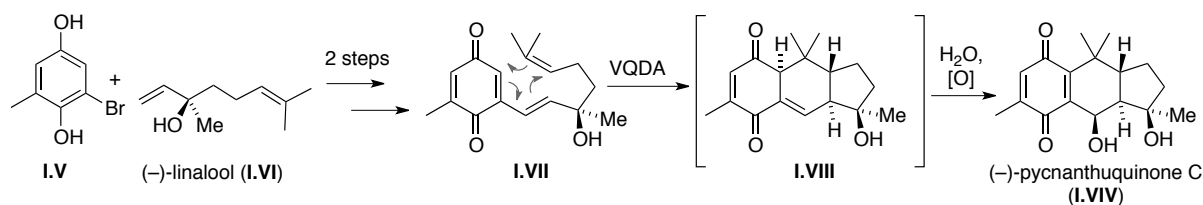
## Chapter 1: Vinyl Quinone DIELS-ALDER Reactions – Method Development and Application in Total Synthesis

DIELS-ALDER (DA) reactions involving vinyl quinones give access to polycyclic structures in a concise and diastereoselective fashion. The goal was to expand the synthetic scope of the vinyl quinone DIELS-ALDER (VQDA) reaction and to achieve an asymmetric variant through LEWIS-acid catalysis. In addition to investigations of literature-known systems, VQDA reactions of several substrates were examined. However, the high instability of the corresponding DA adducts proved to be a limiting factor for further studies. The literature-reported DA reaction of vinyl quinone **I.I** with 2-methylfuran (**I.II**) (Scheme I.I) gave isoquinone methide **I.III**. Interestingly, an unprecedented cleavage of cyclic enol ether resulting in hydroquinone **I.IV** was observed, when isoquinone methide **I.III** was reacted with indole.



**Scheme I.I.** VQDA reaction between **I.I** and **I.II** to isoquinone methide **I.III** and subsequent reactivity with indole to hydroquinone **I.IV**.

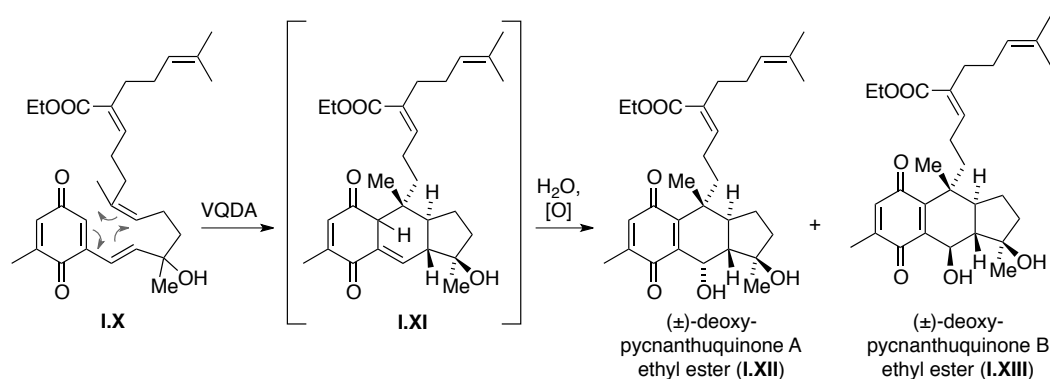
Intramolecular VQDA reactions were applied in the biomimetic synthesis of complex natural products by exploiting the synthetic potential of the initially formed isoquinone methide through interception with nucleophiles. Such cascade reactions allow a fast and diastereoselective construction of highly functionalised polycyclic ring systems.



**Scheme I.III.** Protecting-group free, three-step biomimetic synthesis of pycnanthuquinone C (**I.IV**).

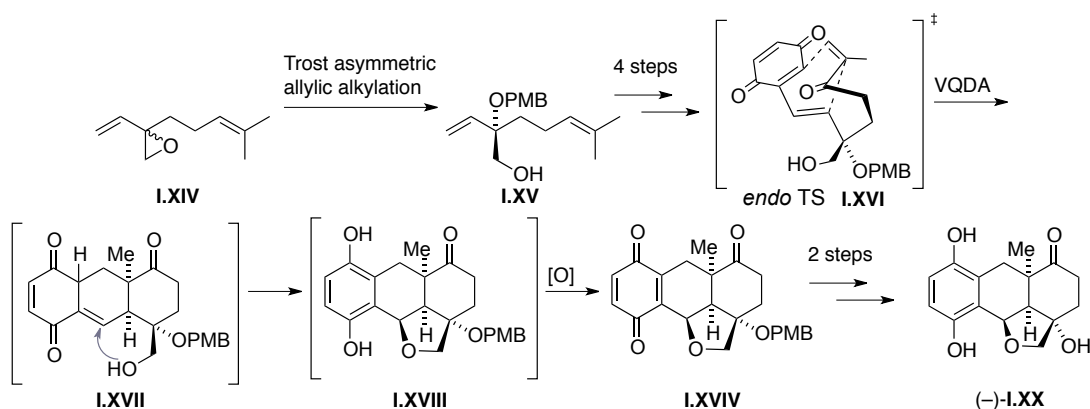


A concise, asymmetric synthesis of pycnanthuquinone C (**I.VIV**) was achieved starting from (–)-linalool (**I.VI**) and bromo hydroquinone **I.V** in three steps (Scheme I.II). Reactive vinyl quinone **I.VII** was converted through a VQDA reaction to putative isoquinone methide **I.VIII**, which then immediately reacted with water and was oxidised by air to give pycnanthuquinone C. VQDA reactions were shown to be applicable for more complex substrates in an approach towards the synthesis of pycnanthuquinones A and B. The VQDA reaction of vinyl quinone **I.X** resulted in isoquinone methide **I.XI**, which then gave deoxy-pycnanthuquinone A and B ethyl ester **I.XII** and **I.XIII** upon nucleophilic attack of water and oxidation by air (Scheme I.III).



**Scheme I.III.** Synthesis of deoxy-pycnanthuquinone A and B ethyl esters (**I.XII**) and (**I.XIII**).

A short and asymmetric entry into the core structure of the cordiachromes was developed, giving access to (–)-*iso*-glaziovianol **I.XX** in seven steps (Scheme I.IV). The synthesis includes the enantioselective opening of vinyl epoxide **I.XIV** through a highly efficient Pd-catalysed TROST asymmetric allylic alkylation. Additionally, this sequence features a reaction cascade triggered by an intramolecular neutral electron demand DIELS-ALDER reaction involving vinyl quinone **I.XVI**.

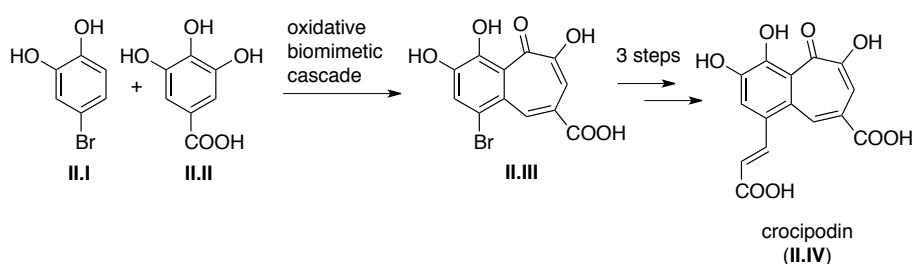


**Scheme I.IV.** Concise synthesis of (–)-*iso*-glaziovianol (**I.XX**) through a VQDA cascade reaction.

## Chapter 2: Mushroom Metabolite – Crocipodin, a Benzotropolone Pigment from the Mushroom *Leccinum Crocipodium* (Boletales)

Total synthesis of crocipodin was performed to confirm the proposed chemical structure. This natural product has been isolated from the fruit bodies of the mushroom *Leccinum crocipodium* by Lydia KERSCHENSTEINER in the group of Prof. Dr. W. STEGLICH.

Bromo catechol **II.I** and gallic acid (**II.II**) were reacted in a biomimetic oxidative cascade to give bromo benzotropolone **II.III**, which was subsequently converted into crocipodin (**II.IV**) in three steps.



**Scheme II.1.** Synthesis of crocipodin (**II.IV**) from bromocatechol **II.I** and gallic acid (**II.II**).

The synthetic product was identical with natural crocipodin by comparison of the IR, NMR and mass spectra, as well as co-chromatography in the HPLC.

## Chapter 3: Organic Photovoltaics: Porphyrin- and Phthalocyanine-based Periodic-Porous Frameworks

Highly ordered 3D polymeric structures hold great potential for application in electronic devices, such as organic photovoltaics (OPVs). Covalent organic frameworks (COFs) are a new class of porous materials formed through self-assembly of building blocks with reversible linkages. The properties of the COFs can be fine-tuned towards specific applications through the modular construction of those structures, because the length and relative orientation of the building groups determine the lattice structure.

Porphyrin and phthalocyanine dyes are suitable molecules for the construction of the photoactive layer in a photovoltaic device, due to their optical properties. Together with Dr. L. SALONEN multiple gram quantities of phthalocyanine and porphyrin COF linkers **III.I** and **III.II** have been synthesised (Figure III.I).

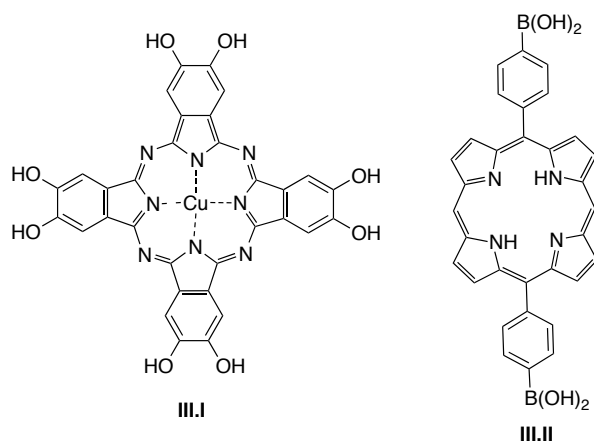


**Figure III.I.** Porphyrin- and phthalocyanine-based COF precursors.

The precursors were applied in the synthesis of COF materials in cooperation with the group of Prof. Dr. T. BEIN. However, despite considerable efforts no novel material with the required crystallinity has been obtained thus far.

Periodic mesoporous organosilica (PMOs) allow the tailor-made design of nanoscale structures. Hence, this class of materials holds promise for the development of 3D heterojunctions for OPVs. For the synthesis of PMO materials, porphyrin- and phthalocyanine-based precursors **III.III** and **III.IV** were prepared (Figure III.II) and incorporated into novel PMO structures by Y. LI in the group of Prof. Dr. T. BEIN.

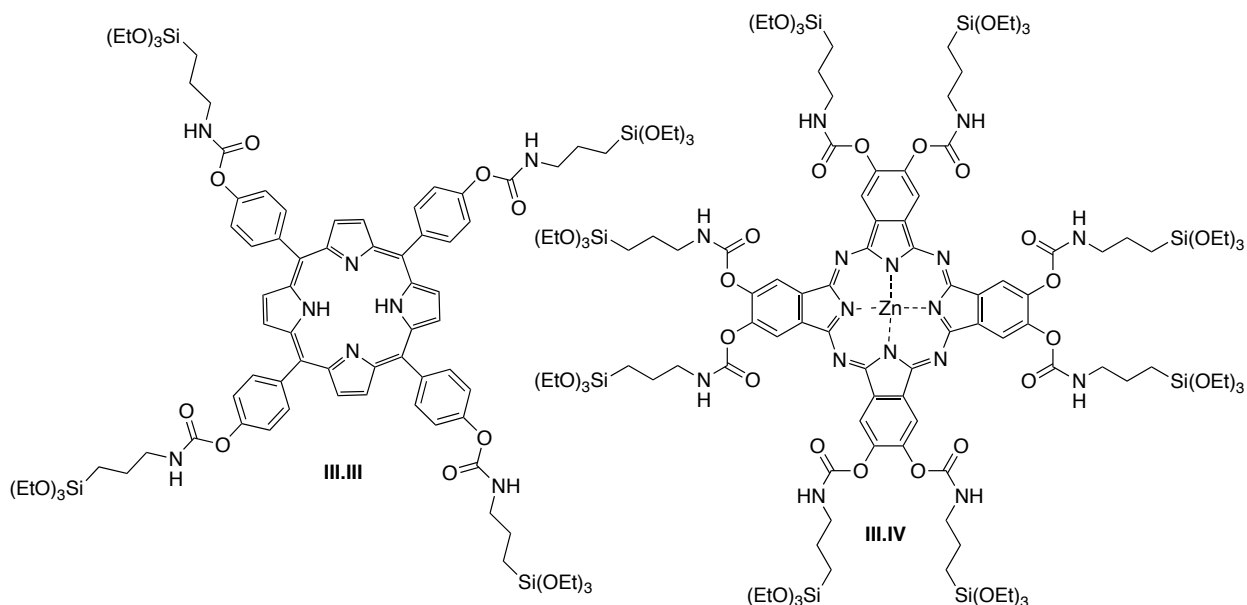


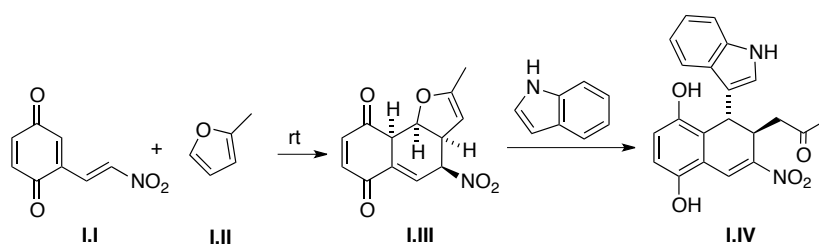
**Figure III.II.** Porphyrin and phthalocyanine-based PMO precursors.

Functional devices were fabricated of both PMO materials, exhibiting up to a ten-fold higher efficiency than their amorphous bi-layer counterparts.

# Zusammenfassung

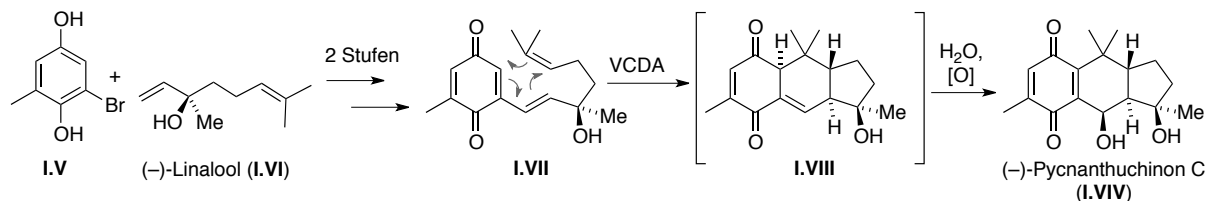
## Kapitel 1: Vinylchinon-DIELS-ALDER Reaktionen – Methodische Studien und Anwendung in Totalsynthese

Vinylchinon DIELS-ALDER Reaktionen (VCDA) ermöglichen einen effizienten Zugang zu funktionalisierten bi- und polycyclischen Systemen. Um das Anwendungsspektrum dieser Reaktion zu erweitern, war es das Ziel, durch LEWIS-Säure-Katalyse eine asymmetrische Version zu entwickeln. Zunächst wurden Literaturbekannte VCDA-Systeme genauer untersucht sowie die Limitierung der intermolekularen VCDA-Reaktion durch zahlreiche weitere Substrate erforscht. Die hohe Instabilität der entsprechenden DA Addukte stellte sich als größtes Hindernis für weitere Studien heraus. Die Literaturbekannte DA Reaktion zwischen Vinylchinon **I.I** mit 2-Methylfuran (**I.II**) ergab Isochinonmethid (**I.III**) als stabiles Produkt. Interessanterweise wurde bei Umsetzung von **I.III** mit Indol eine bisher unbekannte Öffnung des zyklischen Enoethers beobachtet.



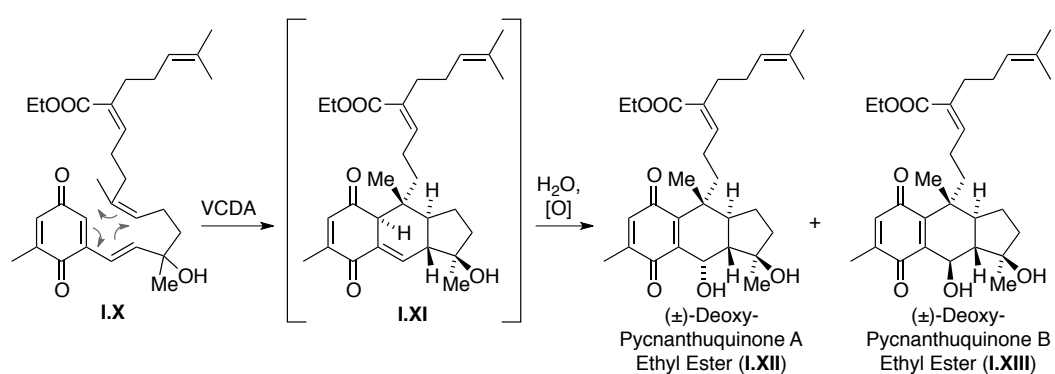
**Schema I.I.** VCDA Reaktion zwischen **I.I** und **I.II** ergab Isochinonmethid **I.III**; Umsetzung des Produkts mit Indol zu Hydrochinon **I.IV**.

Weiterhin wurden intramolekulare Varianten der VCDA in der Totalsynthese von komplexen Naturstoffen angewendet. Hierbei wurde das synthetische Potenzial des anfänglich gebildeten Isochinonmethids durch Abfangen mit geeigneten Nucleophilen ausgenutzt. Derartige Dominoreaktionen ermöglichen einen schnellen und eleganten Zugang zu komplexen polycyclischen Ringsystemen.



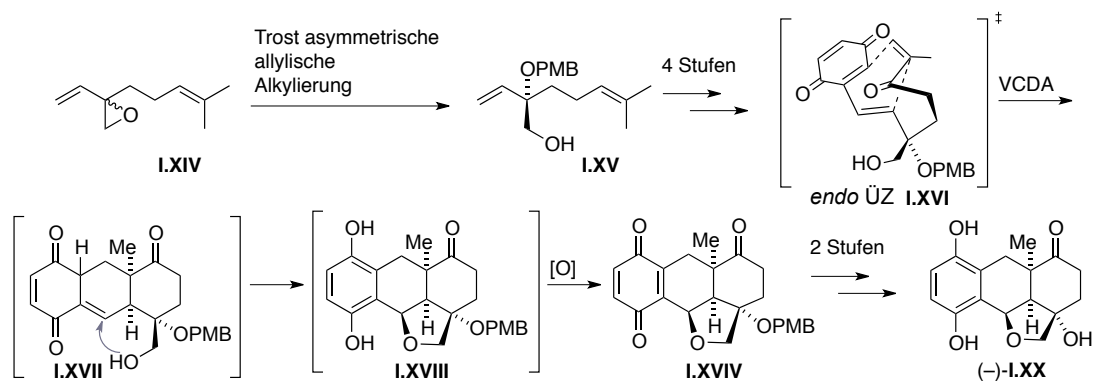
**Schema I.II.** Schutzgruppenfreie, dreistufige, biomimetische Synthesesequenz zu Pycnanthuchinon C (**I.IV**).

Die effiziente und asymmetrische Synthese von Pycnanthuchinon C wurde beginnend von (-)-Linalool (**I.VI**) und Bromhydrochinon **I.V** in drei Stufen ausgeführt (Schema I.II). Vinylchinon **I.VII** reagierte in einer VCDA-Reaktion zu Isochinonmethid **I.VIII**, welches anschließend sofort durch Wasser nukleophil angegriffen und durch Luftsauerstoff zu Pycnanthuchinon C oxidiert wurde. In einer Studie über die Synthese der Pycnanthuchinone A und B wurde gezeigt, dass die VCDA-Reaktion auch in sehr komplexen Substraten für den Aufbau von quartären Stereozentren anwendbar ist. Die VCDA-Reaktion von Vinylchinon **I.X** ergab Isochinonmethid **I.XI**, was sofort zu Deoxy-Pycnanthuchinon Ethylester A (**I.XII**) und B (**I.XIII**) weiter reagierte (Schema I.III).



**Schema I.III.** Synthese von Deoxy-Pycnanthuchinon Ethyl Ester A (**I.XII**) und B (**I.XIII**).

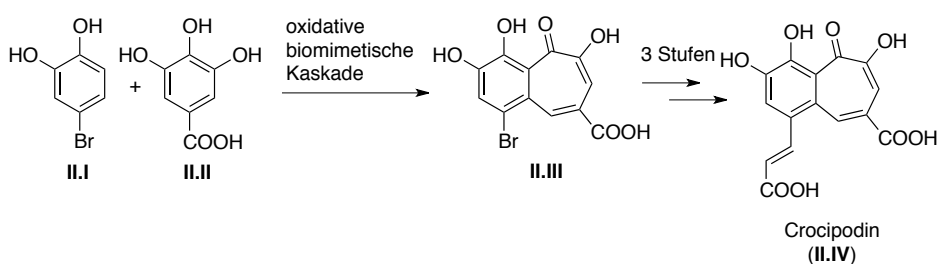
Basierend auf einer intramolekularen VCDA Reaktion wurde ein kurzer und asymmetrischer Zugang zu dem Grundgerüst der Cordiachrome entwickelt. Die Synthesesequenz ergab (-)-*Iso*-Glaziovianol (**I.XX**) in nur sieben Stufen (Schema I.IV). Über eine enantioselektive Epoxidöffnung mittels effizienter Palladium-katalysierter TROST Chemie wurde das Stereozentrum des tertiären Alkohols eingeführt. Ein weiteres Highlight der Synthese ist eine Dominoreaktion, welche durch eine intramolekulare VCDA-Reaktion mit neutralem Elektronenbedarf ausgelöst wird.



**Schema I.IV.** Synthese von (-)-*Iso*-Glaziovianol (**I.XX**) mittels einer VCDA-Dominoreaktion.

## Kapitel 2: Pilz Metabolit – Crocipodin, ein Benzotropolon Pigment aus dem Pilz *Leccinum Crocipodium* (Boletales)

Die Totalsynthese von Crocipodin wurde durchgeführt, um die vorgeschlagene chemische Struktur zu bestätigen. Der Naturstoff wurde aus dem Fruchtkörper des Pilzes *Leccinum Crocipodium* von L. KERSCHENSTEINER aus der Gruppe von Prof. Dr. W. STEGLICH gewonnen. Eine oxidative, biomimetische Kaskadenreaktion zwischen Bromocatechol **II.I** und Gallussäure (**II.II**) ergab Bromobenzotropolon **II.III**, was schließlich in drei Stufen in Crocipodin (**II.IV**) umgewandelt wurde.



**Schema II.1.** Synthese von Crocipodin (**II.IV**) aus Bromocatechol **II.I** und Gallussäure (**II.II**).

Die IR-, NMR- und Massenspektren des synthetischen Materials waren identisch mit denen des natürlichen Crocipodin.

## Kapitel 3: Organische Photovoltaik: Porphyrin- und Phthalocyanin-basierte Periodische Poröse Materialien

Hochgeordnete 3D polymere Strukturen haben großes Potential für Anwendungen in elektronischen funktionalen Bauteilen, wie beispielsweise organischen Photovoltaiks (OPVs). Covalent Organic Frameworks (COFs) sind eine neue Klasse poröser Materialien, die sich durch Self-Assembly aus Bausteinen mit reversiblen Verknüpfungen bilden. Die Eigenschaften der COF-Materialien können durch den modularen Aufbau für spezifische Anwendungen abgestimmt werden, da die Länge und relative Ausrichtung der Bausteine die Gitterstruktur bestimmen.

Wegen ihrer optischen und chemischen Eigenschaften sind Porphyrin und Phthalocyanin Farbstoffe geeignete Moleküle für den Aufbau der photoaktiven Schicht in einem OPV. In Zusammenarbeit mit Dr. L. SALONEN wurden mehrere Gramm von Phthalocyanin und Porphyrin-COF-Linker **III.I** und **III.II** synthetisiert (Abbildung III.1).

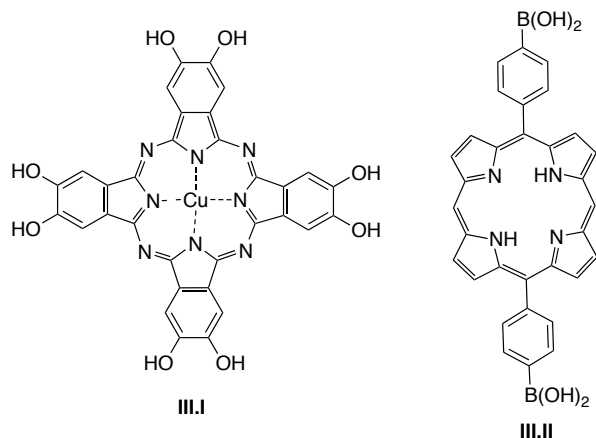


**Abbildung III.I.** Porphyrin und Phthalocyanin COF Bausteine.

Die Bausteine wurden in Kooperation mit der Arbeitsgruppe von Prof. Dr. T. BEIN in der COF-Synthese eingesetzt. Trotz erheblicher Anstrengungen ist es bisher nicht gelungen, neue COF-Materialien mit der notwendigen Kristallinität zu erhalten.

Periodische Mesoporöse Organosilica (PMOs) ermöglichen das Design von maßgeschneiderten Strukturen im Nanometerbereich. Daher sind diese Materialien vielversprechende Kandidaten für die Entwicklung von geordneten 3D-Heteroübergänge für OPVs. Porphyrin- und Phthalocyanin-basierte Ausgangsstoffe wurden für die Synthese von PMO Materialien hergestellt (Abbildung III.II). Diese Moleküle wurden von Y. LI aus der Gruppe von Prof. Dr. T. BEIN erfolgreich in PMO Strukturen eingebaut. Funktionale Devices aus diesen Materialien zeigten einen bis zu 10fach höheren Wirkungsgrad als das entsprechende amorphe doppelschichtige Gegenstück.

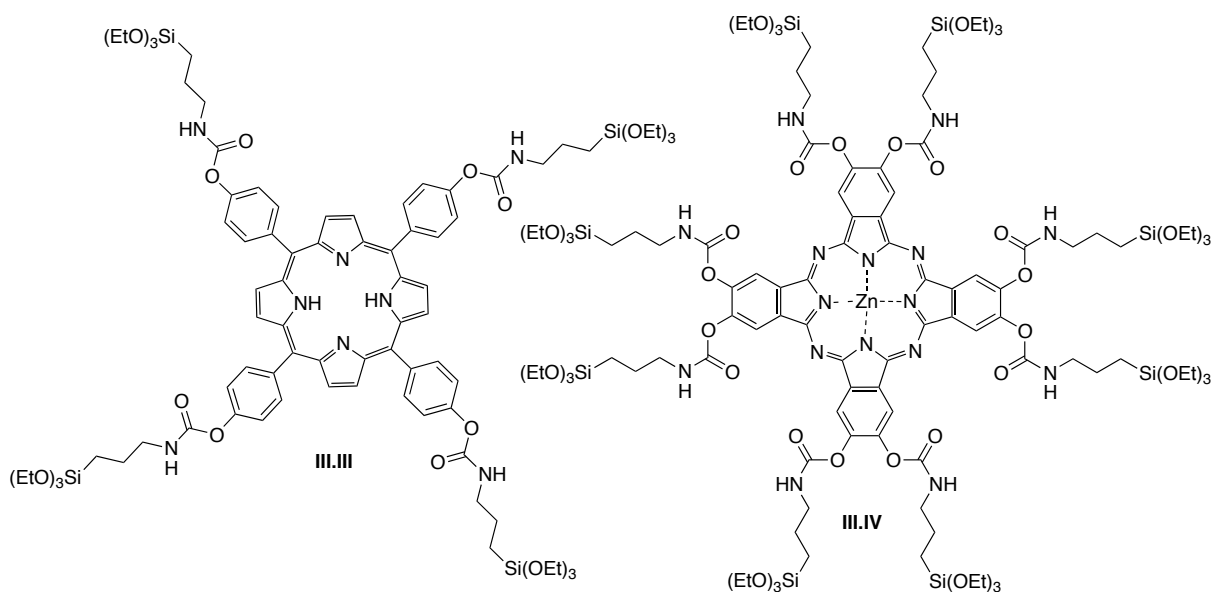


**Abbildung III.II.** Porphyrin und Phthalocyanin-basierte PMO-Ausgangsstoffe.

# Abbreviations

°C	degrees Celsius
Ac	acetate
aq	aqueous
atm	atmosphere
b.o.r.s.m.	based on recovered starting material
BAIB	bisacetoxiodobenzene
Bn	benzyl
ca.	circa
calc.	calculated
CAM	ceric ammonium molybdate
CAN	ceric ammonium nitrate
CLA	chiral LEWIS acid
cy	cyclohexane
DA	DIELS-ALDER
dba	dibenzylidene acetone
DDQ	2,3-dichloro-5,6-dicyano-1,4-benzoquinone
decomp.	decomposition
DHP	dihydropyrene
DIPA	diisopropylamine
DIPEA	<i>N,N</i> -diisopropylethylamine
DMAP	dimethylaminopyridin
DMF	dimethylformamide
DMP	DESS-MARTIN periodinane
DMS	dimethylsulfide
<i>eq.</i>	equivalent(s)
Et	ethyl
Et <sub>2</sub> O	diethylether
EtOAc	ethyl acetate
EtOH	ethanol
FTIR	FOURIER-transform-infrared spectrometer
g	gram
GC	gas chromatography
GPa	giga Pascal
h	hour(s)
HMDS	hexamethyldisilazane
HOMO	highest occupied molecular orbital
HPLC	high pressure liquid chromatography
HWE	HORNER-WADSWORTH-EMMONS
Hz	Hertz
hν	light
<i>i</i> -PrOH	isopropanol
im	imidazole
l	large



LA	LEWIS acid
LUMO	lowest unoccupied molecular orbital
m	medium
M	molarity/ molar
Me	methyl
MeCN	acetonitrile
MeOH	methanol
min	minute(s)
mL	millilitre
MS	mass spectroscopy
<i>n</i> -BuLi	<i>n</i> -butyllithium
NMR	nuclear magnetic resonance
OTf	triflate
PCC	pyridinium chlorochromate
Ph	phenyl
PhH	benzene
PMB	<i>para</i> -methoxybenzyl
ppm	parts per million
PPTS	pyridinium <i>para</i> -toluenesulfonate
py	pyridine
rt	room temperature
s	small
sat.	saturated
<i>T</i>	temperature
t	time
TBS	<i>tert</i> -butyldimethylsilyl
TBSCl	<i>tert</i> -butyldimethylsilylchloride
TBSOTf	<i>tert</i> -butyldimethylsilyltriflate
TEA	triethylamine
TESOTf	triethylsilyltriflate
THF	tetrahydrofuran
TLC	thin layer chromatography
TMSOTf	trimethylsilyltriflate
TS	transition state
TsOH	<i>para</i> -toluenesulfonic acid
VQDA	vinyl quinone DIELS-ALDER
μg	microgram
NMR:	
s	singlet
d	doublet
t	triplet
q	quartet
m	multiplet
ppm	parts per million

COSY	correlated spectroscopy
HMBC	heteronuclear multiple bond correlation
HSQC	heteronuclear single quantum coherence spectroscopy
NOESY	nuclear OVERHAUSER enhancement spectroscopy
m	medium
s	strong

# Table of Contents

Acknowledgments .....	iii
Abstract	vi
Zusammenfassung.....	x
Abbreviations .....	xiv
Table of Contents.....	xvii
Chapter 1: Vinyl Quinone DIELS-ALDER Reactions.....	1
1.1 Introduction.....	3
1.1.2 Previous Application of the VQDA Reaction in Total Synthesis .....	5
1.1.3 Project Aims.....	6
1.2 Method Development.....	8
1.2.1 The Scope of VQDA Reactions .....	8
1.2.2 Alternative Precursors and Oxidation Methods.....	17
1.2.3 Catalysis attempts .....	21
1.2.4 Method Development: Summary and Outlook.....	26
1.3 Intramolecular VQDA Reaction in the Total Synthesis of the Pycnanthuquinones .	27
1.3.1 Introduction .....	27
1.3.2 Biosynthetic Pathways of the Pycnanthuquinones .....	29
1.3.4 Previous Synthetic Approaches Towards Rossinone B and Pycnanthuquinone C .....	35

1.3.5 Biomimetic Synthesis of (-)-Pycnanthuquinone C.....	37
1.3.6 Towards the Biomimetic Synthesis of Pycnanthuquinones A and B .....	41
1.4 Towards the Bioinspired Total Synthesis of Glaziovianol.....	46
1.4.1 Introduction.....	46
1.4.2 Proposed Biosynthetic Pathway for Glaziovianol .....	47
1.4.3 Synthesis of <i>Isø</i> -Glaziovianol.....	48
1.5 Experimental Section .....	57
1.5.1 General Experimental Details.....	57
1.5.2 Method Development .....	59
1.5.3 Biomimetic Total Synthesis of Pycnanthuquinone C.....	71
1.5.4 Towards the Total Synthesis of Pycnanthuquinones A and B.....	91
1.5.5 Towards the Total Synthesis of Glaziovianol.....	107
1.6 Bibliography.....	146
Chapter 2: Mushroom Metabolite.....	151
2.1 Project Aims .....	151
2.2 Benzotropolones.....	151
2.3 Isolation and Structure Determination.....	152
2.4 Total synthesis of Crocipodin.....	155
2.5 Experimental Section .....	158
2.5.1 General Experimental Details.....	158
2.5.2 Synthesis of Crocipodin.....	159
2.6 Bibliography.....	172

Chapter 3: Organic Photovoltaics.....	173
3.1 Project Aims .....	175
3.2 Introduction.....	176
3.2.1 The Working Principle and General Architectures of Organic Photovoltaic Cells .....	176
3.2.2 Molecular Self-Assembly.....	178
3.2.3 Optical Properties of Porphyrins and Phthalocyanines .....	179
3.3 Towards Novel Electroactive Covalent Organic Frameworks.....	181
3.3.1 Introduction to Covalent Organic Frameworks.....	181
3.3.2 Towards the Synthesis of Phthalocyanine and Porphyrin Containing COFs....	184
3.4 Opto-Electronically Active Periodic Mesoporous Organosilica .....	191
3.4.1 Introduction to Periodic Mesoporous Organosilica.....	191
3.4.2 Synthesis of Functional Phthalocyanine PMO .....	192
3.4.3 Synthesis of a Porphyrin-based 3D Donor-Acceptor Interpenetrating System	199
3.5 Summary and Outlook.....	205
3.6 Experimental Section .....	208
3.6.1 General Experimental Details .....	208
3.6.2 Towards Novel Electroactive Covalent Organic Frameworks .....	209
3.6.3 Synthesis of a Porphyrin-based 3D Donor-Acceptor Interpenetrating System	216
3.7 Bibliography .....	219



# Chapter 1

## Vinyl Quinone DIELS-ALDER Reactions: Method Development\* and Application in Total Synthesis

F. Löbermann, P. Mayer, D. Trauner, *Angew. Chem. Int. Ed.* **2010**, *49*, 6199–202.

F. Löbermann, L. Weisheit, D. Trauner, *Manuscript in Preparation*.

---

\* This part of the work was conducted in collaboration with Dr. ALBERT SCHRÖCKENEDER and can also be found in his thesis: A. Schröckeneder, PhD Thesis, Ludwig-Maximilians-Universität München, **2013**. Both authors contributed equally.



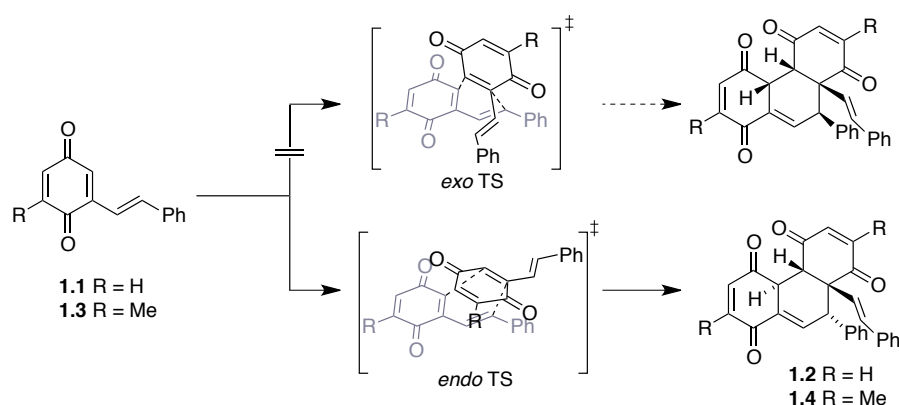


## 1.1 Introduction

### 1.1.1 DIELS-ALDER Reactions Involving Vinyl Quinones

The DIELS-ALDER (DA) reaction is a [4+2] cycloaddition reaction between a diene and a dienophile, which was discovered almost eight decades ago, and to this day continues to attract synthetic organic chemists.<sup>[1]</sup> This is largely due to the great synthetic potential of this atom-economic reaction. With its broad substrate scope the DA reaction allows the creation of up to four contiguous stereocenters with usually remarkably high regio- and diastereoselectivity. A wide range of examples of DA reactions proceeding with normal, inverse and neutral electron demand have been showcased in literature.<sup>[2,3]</sup>

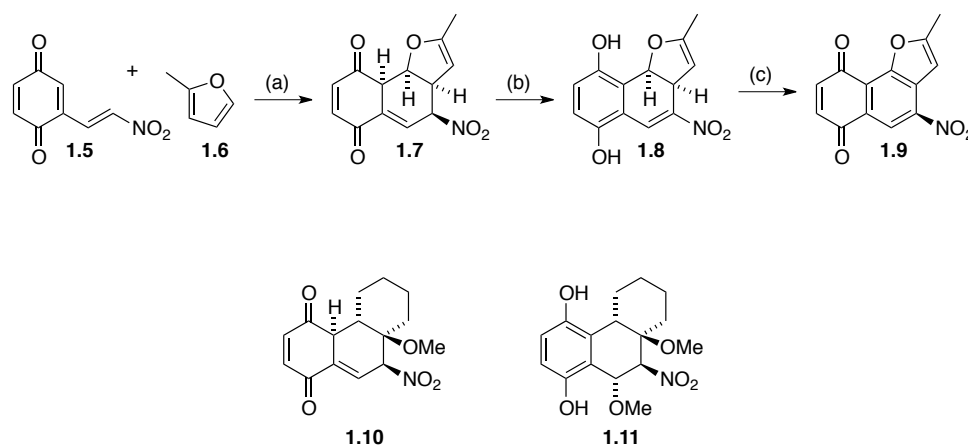
The first DA reaction involving vinyl quinones as dienes was reported by IRNGARTINGER *et al.*<sup>[4]</sup> When examining the chemistry of electron-rich alkenyl-substituted quinone **1.1**, a dimerisation was observed, yielding hydrophenanthrene **1.2** in excellent regio- and diastereoselectivity (Scheme 1.1). The products were unambiguously assigned by NMR spectroscopy and X-ray crystallography. The stereochemical outcome suggests that this inverse electron demand DA reaction proceeds *via* an *endo*-type transition state, where the most electron-rich double bond in the quinone system reacts with the vinyl quinone diene. Later, IWAMOTO *et al.* reported a similar reaction of vinyl quinone **1.3** to DA-type product **1.4** using UV light, with the same remarkable regio- and diastereoselectivity (Scheme 1.1).<sup>[5]</sup>



**Scheme 1.1.** Dimerisation of vinyl *para*-quinones.

The scope of this reaction was further extended by NOLAND and KEDROWSKI, when they showed that the electron-poor nitrovinyl quinone **1.5** smoothly undergoes [4+2] cycloaddition reactions with electron-rich dienophiles, such as 2-methylfuran (**1.6**) to give

dihydronaphthoquinones **1.7** in excellent regio- and diastereoselectivity (Scheme 1.2).<sup>[6,7]</sup> However, the initial isoquinone methide DA products were not isolated in all cases, because they easily tautomerise to the aromatic phenol form. Only when a thoroughly dried, non-polar solvent was employed for the reaction, precipitation of the quinoid cycloadduct **1.7** could be observed. Contact with polar solvents or base almost immediately caused tautomerisation to the corresponding hydroquinone **1.8**.



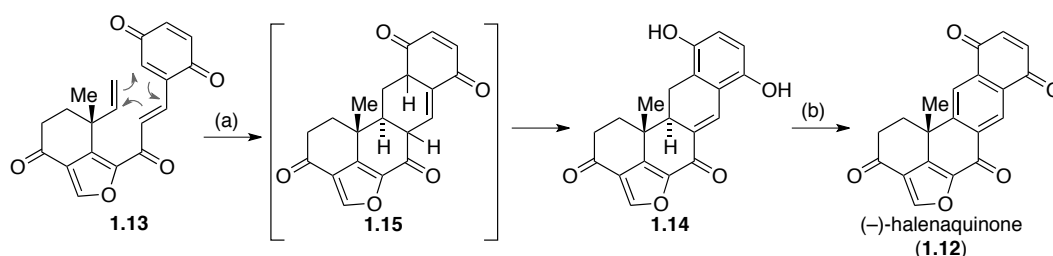
Reagents and conditions: (a) rt, neat, 22 h, 83% of **1.7**; (b) 10% Et<sub>3</sub>N/THF, benzene, then (c) MnO<sub>2</sub>, reflux, 54% of **1.9** over 2 steps; (d) MeOH/MeCN, reflux, 68% of **1.11**.

**Scheme 1.2.** Reaction of nitrovinyl quinone **1.5** with 2-methylfuran (**1.6**) and reactivity of initially formed isoquinone methides.

It was shown that the resulting hydroquinones and isoquinone methides can be further functionalised into more complex molecules or alternatively be fully aromatised. Heating hydroquinone **1.8** with MnO<sub>2</sub> as the dehydrogenating agent resulted in aromatic quinone **1.9**. The synthetic potential of isoquinone methides can be exploited by intercepting this reactive intermediate with nucleophiles such as MeOH, as shown in the conversion of **1.10** to **1.11**. In this case, the 1,4-addition of methanol only yielded one single diastereoisomer.<sup>[6]</sup>

## 1.1.2 Previous Application of the VQDA Reaction in Total Synthesis

The first example of an intramolecular version of the VQDA reaction was reported by KIENZLER and TRAUNER in the total synthesis of (–)-halenaquinone (**1.12**).<sup>[8]</sup> This short and elegant synthesis was also the first reported DA reaction involving a vinyl *para*-quinone in total synthesis. Halenaquinone (**1.12**) has attracted considerable interest of the synthetic community due to its multifaceted biological profile.<sup>[9,10]</sup> Precursor **1.13** underwent the desired [4+2] cycloaddition reaction under LEWIS-acid catalysis or upon heating in toluene. However, the highest yield was obtained when a very high pressure of almost 1 GPa was applied, affording vinyl hydroquinone **1.14** in 78% yield (Scheme 1.3). Isoquinone methide **1.15** could not be isolated in any case. Subsequently, the natural product **1.12** was obtained upon oxidation with MnO<sub>2</sub>. However, the synthetic value of the *ortho*-quinone methide remained unexploited in this synthesis.



Reagents and conditions: (a) 1 GPa, CH<sub>2</sub>Cl<sub>2</sub>, 2 days, 78% of **1.14**; (b) CH<sub>2</sub>Cl<sub>2</sub>, MnO<sub>2</sub>, 60% of **1.12**.

**Scheme 1.3.** Synthesis of (–)-halenaquinone (**1.12**) via an intramolecular VQDA reaction.

Given the abundance of quinones in nature, it is entirely possible that VQDA reactions bear some biosynthetic relevance. Indeed, many natural products can be identified to contain the corresponding retrons. These include pycnanthuquinones A – C (**1.16–1.18**),<sup>[11,12]</sup> glaziovianol (**1.19**),<sup>[13]</sup> pleurotin (**1.20**),<sup>[14]</sup> and, in a modified form, rossinone B (**1.21**) (Figure 1.1).<sup>[15]</sup> In most of these, the retrosynthetic application of the VQDA reaction would lead to simple meroterpenoid quinones, which are common natural products themselves.

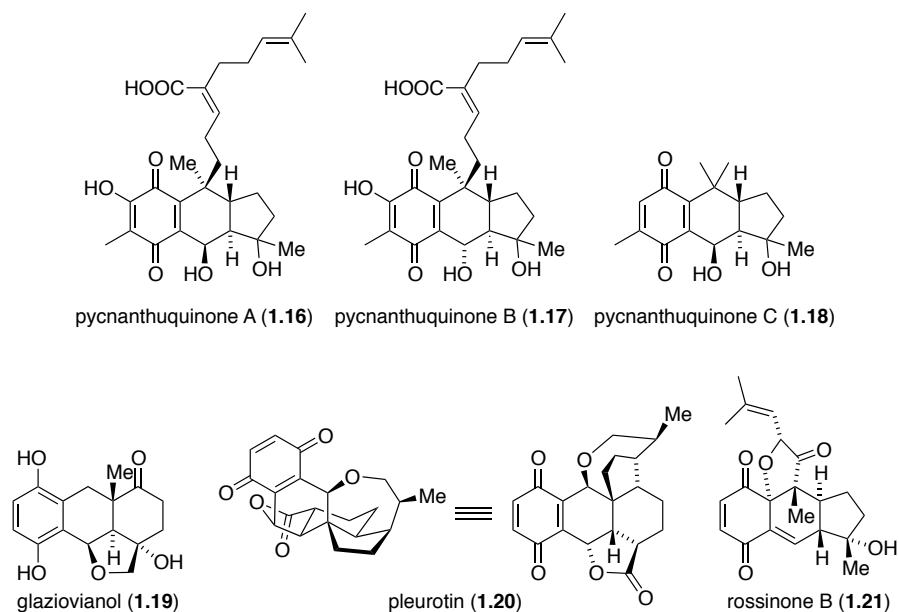
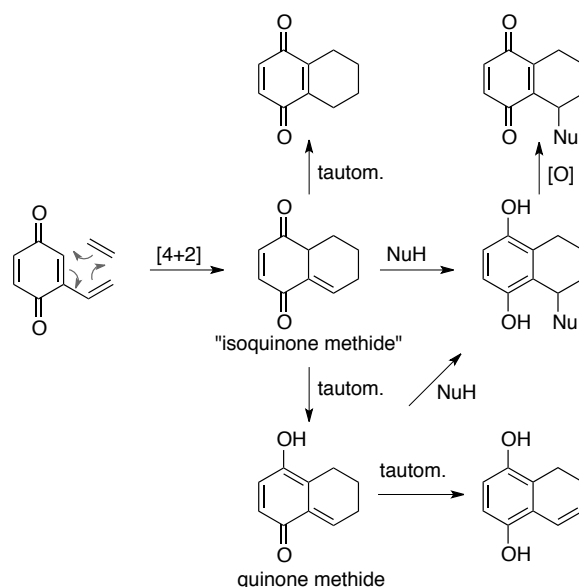


**Figure 1.1.** Natural products bearing the VQDA retron.

Recently, two biomimetic syntheses, both showing the synthetic value of the initially formed isoquinone methide, were reported. LÖBERMANN and TRAUNER suggested biosynthetic pathways for the formation of pycnanthuquinone C (1.18) and rossinone B (1.21), involving a VQDA reaction as the key transformation.<sup>[16]</sup> The total synthesis of rossinone B, reported by ZHANG, will be discussed in Chapter 1.3.4.<sup>[17]</sup> The results of the biomimetic synthesis of pycnanthuquinone C will be discussed in Chapter 1.3.5 of this thesis.

### 1.1.3 Project Aims

The DIELS-ALDER (DA) reaction of vinyl quinones provides a rapid entry to highly functionalised bi- and polycyclic ring systems. This reaction involves the inverse electron demand cycloaddition of an electron-rich dienophile to a vinyl quinone, which presumably generates an “isoquinone methide” (Scheme 1.4). This reactive intermediate could then tautomerise in several ways to yield quinone methides, bicyclic quinones or hydroquinones. If the isoquinone methide or quinone methide is intercepted by a nucleophile inter- or intramolecularly, a functionalised tetraline hydroquinone may result.<sup>[16]</sup>



**Scheme 1.4.** DIELS-ALDER reactions of vinyl quinones and possible subsequent transformations.

In comparison to classical DA reactions involving quinones and electron-rich dienes, which have been extensively used in synthesis,<sup>[18,19]</sup> VQDA reactions still remain largely unexplored and underutilised. In this context, an asymmetric intermolecular version would further enhance the usability and largely extend the scope of this mode of DA reactions. Hence, exploiting the synthetic potential of the VQDA reaction could give access to many potentially bioactive natural and non-natural products enantioselectively in a swift and elegant fashion. One aim of this project was to further extend the substrate scope and achieve an enantioselective variant of the VQDA reaction through asymmetric LEWIS-acid (LA) catalysis.

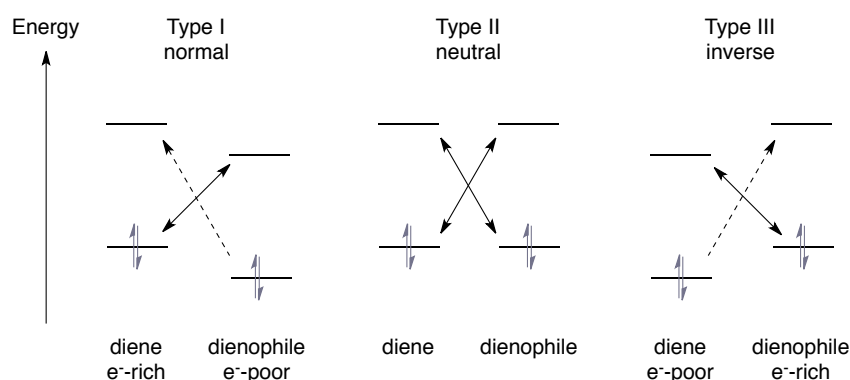
A very effective way to demonstrate the usefulness and practicability of an underexplored reaction mode is the application of the reaction in the total synthesis of natural products. Hence, four natural products pycnanthuquinones A – C and glaziovianol were chosen as synthetic targets to showcase the power of intramolecular VQDA reactions as the key bond-forming event, while further exploiting the synthetic value of *in situ* generated isoquinone methides.

## 1.2 Method Development\*

### 1.2.1 The Scope of VQDA Reactions

In the past several years, mainly intramolecular DIELS-ALDER (DA) reactions involving vinyl quinones have been successfully employed to develop highly functionalised and complex molecules. It was the aim of this research was to extend the scope of the intermolecular VQDA reaction, with respect to potential dienes and dienophiles. In addition, the possibility of using catalysis to promote this reaction was briefly explored.

The concept of orbital energy controlled cycloaddition reactivity was developed by SUSTMANN.<sup>[20]</sup> He considered the possible overlaps of the highest occupied molecular orbitals (HOMO) with the lowest unoccupied molecular orbitals (LUMO) for cycloaddition reactions and classified them accordingly (Scheme 1.5). In general the HOMO-LUMO pair with the lowest energy difference will react. When the HOMO of an electron-rich diene overlaps with the LUMO of an electron-poor dienophile, a so-called Type I DA reaction takes place. In the case of a DA reaction with neutral electron demand (Type II) the HOMOs and LUMOs of both reactants overlap with each other, due to the equal energy difference. When an electron-poor diene reacts with an electron-rich dienophile, the energy difference between  $\text{HOMO}_{\text{dienophile}}$  and  $\text{LUMO}_{\text{diene}}$  is the smallest, which will result in a DA reaction with inverse electron demand (Type III).

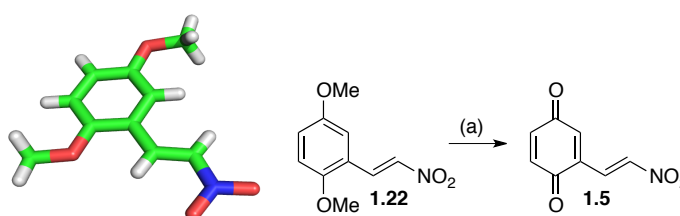


**Scheme 1.5.** DIELS-ALDER cycloaddition reactivity according to HOMO-LUMO interactions.

\* Unpublished results. This work was conducted together with Dr. A. SCHRÖCKENEDER and can also be found in his PhD thesis: A. Schröckeneder, PhD Thesis, Ludwig-Maximilians-Universität München, 2013. Both authors contributed equally.

The first DA reaction involving a vinyl quinone was reported by NOLAND and co-workers.<sup>[7]</sup> They showed that the electron-poor nitro substituted vinyl quinone **1.5** reacts smoothly with electron-rich dienophiles, such as sylvan (**1.6**) to quinoid heterocycle **1.7** (Chapter 1.1.1, Scheme 1.2). Hence, this DA reaction proceeds with inverse electron demand. To further expand the scope of the VQDA reaction it was decided to first study the system reported by NOLAND and gain deeper insights into the reactivity of nitro vinyl quinone **1.5**.

The synthesis of **1.5** was achieved through the oxidation of methoxyhydroquinone **1.22** with CAN on a multi gram scale (Scheme 1.6). In the course of this work it was possible to obtain an X-ray structure of compound **1.22**.

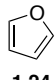
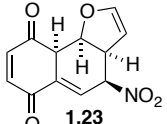
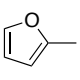
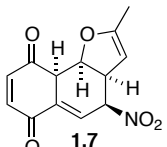


Reagents and conditions: (a) CAN, MeCN/H<sub>2</sub>O (3:1), 55% of **1.5**.

**Scheme 1.6.** Synthesis of vinyl quinone **1.6** and X-ray crystal structure of **1.22**.

With large amounts of **1.5** in hand, reactivity with dienophiles in a VQDA reaction with different electronic and steric properties was examined. While electron-rich furans and vinyl ethers reacted with vinyl quinone **1.5** in almost all cases, it was only possible to isolate the corresponding cycloaddition adducts, when they precipitated from the reaction mixture (Table 1.1).

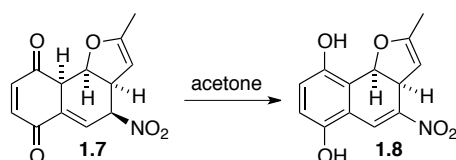
**Table 1.1.** Screening with furans and enol ethers

entry	dienophile	anticipated product	observation
1	 <b>1.24</b>	 <b>1.23</b>	decomposition
2	 <b>1.6</b>	 <b>1.7</b>	quinone methide <b>1.7</b> 98%

## 1.2. Method Development

entry	dienophile	anticipated product	observation
3			decomposition upon work up
4			complex mixture; decomposition upon work up
5			isolation of hydroquinone <b>1.31</b> ; 83%
6			mixture of hydroquinone and by-products/ decomposition upon work up

For all entries in Table 1.1 complete consumption of VQDA precursor **1.5** was observed by TLC analysis. Crude proton NMR indicated the formation of DA adduct **1.23** in small amounts, when reacting **1.5** with furan (**1.24**) (entry 1). However, the very unstable product quickly decomposed and could not be isolated or further characterized. The introduction of a methyl group to the dienophile resulted in a very clean reaction between **1.5** and **1.6** as isoquinone methide **1.7** precipitated from the reaction mixture and could be collected by filtration as reported by NOLAND (entry 2).<sup>[7]</sup> Presumably the isolation of this DA adduct was possible due to stabilisation through steric effects of the methyl group. However, while stable in unpolar solvents such as benzene or CH<sub>2</sub>Cl<sub>2</sub>, isoquinone methide **1.7** quickly tautomerised to the corresponding hydroquinone **1.8** within minutes when taken up in polar solvents such as EtOAc, DMSO or acetone (Scheme 1.7).<sup>[6,7]</sup>



**Scheme 1.7.** Tautomerisation of **1.7** to the corresponding hydroquinone **1.8** in a polar solvent.

Adding more steric bulk to the system, using dimethyl furan (**1.25**) (entry 3) or changing the electronics of the dienophile through addition of a hydroxyl group **1.26** (entry 4), did not yield isolable DA adducts. A novel product was obtained when employing vinyl ether



**1.29** (entry 5) in the reaction. The isolated product was not isoquinone methide **1.30**, but its tautomer hydroquinone **1.31**. A similarly high tautomerisation rate of isoquinone methide **1.32** obtained from VQDA reaction with indole (**1.33**) (entry 6) was observed (Figure 1.2).

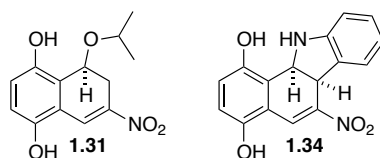


**Figure 1.2.** Stable tautomers from VQDA reactions: novel isopropylvinyl ether derived hydroquinone **1.31** and with indole derived product **1.34** (as described by NOLAND).

Possibly, the presence of a heteroatom in pseudo benzylic position, renders the cycloaddition adducts very unstable. Hence, the VQDA reaction with various substituted alkenes was examined. For all reactions described in Table 1.2, using alkenes **1.35**–**1.41** consumption of vinyl quinone **1.5** was observed. However, none of the anticipated cycloaddition adducts were observed, due to decomposition.

**Table 1.2.** Screening with substituted alkenes

entry	dienophile	anticipated product	outcome
1			decomposition
2			decomposition
3			decomposition
4			decomposition

## 1.2. Method Development

The reaction of vinyl quinone **1.5** with 2-methylfuran (**1.6**) in  $\text{CDCl}_3$  at room temperature was followed by 200 MHz  $^1\text{H}$  NMR spectroscopy (Figure 1.3).

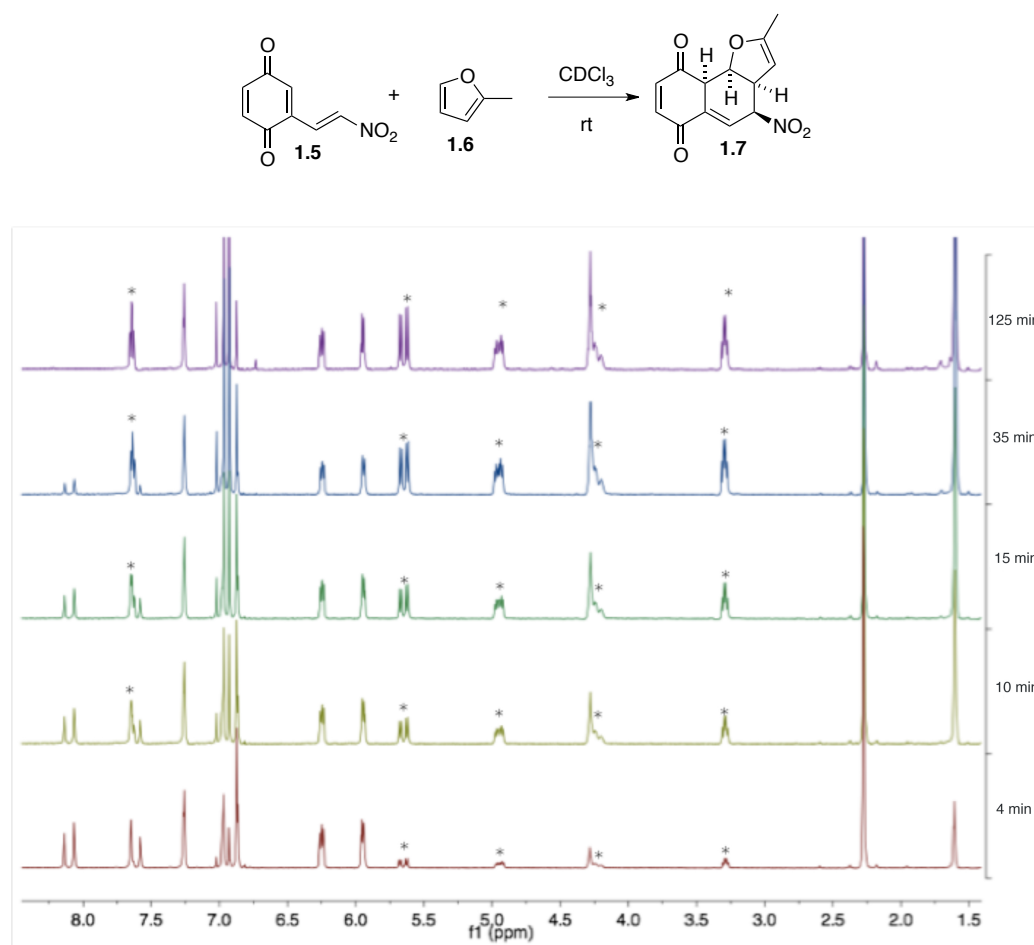


**Figure 1.3.** Progress of VQDA in  $\text{CDCl}_3$ , 2 eq. of **1.6**; characteristic product peaks are marked with an asterisk.

Over the course of 125 minutes, proton spectra were recorded every five minutes. As can be seen in Figure 1.3, vinyl quinone **1.5** reacts smoothly with sylvan (**1.6**) to the corresponding isoquinone methide **1.7**. By means of 200 MHz NMR no significant formation of any side-product could be observed under these reaction conditions. The progress of the reaction is plotted as a chronological sequence in Figure 1.4. Relative conversion was determined by peak integral ratios. In this set up the relation between starting quinone **1.5** and dienophile **1.6** were determined. With two equivalents dienophile, the reaction proceeds smoothly within one hour, whereby a 50% conversion is achieved after approximately 10 minutes.

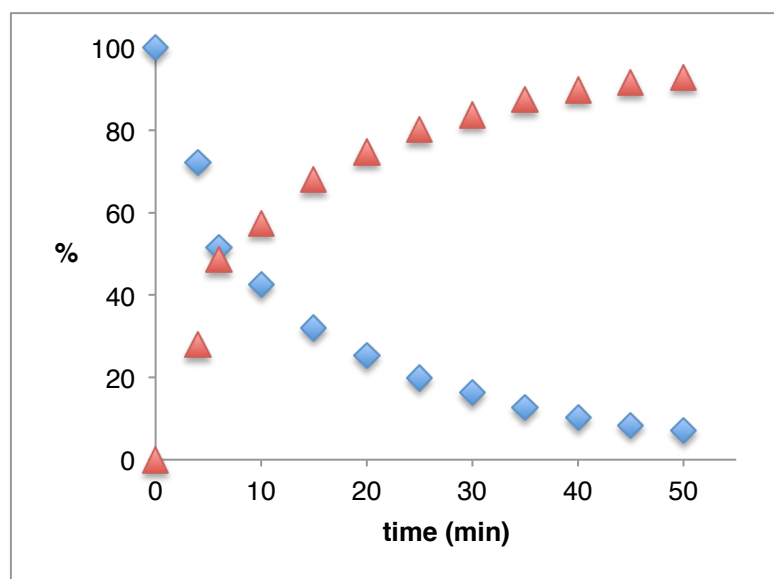
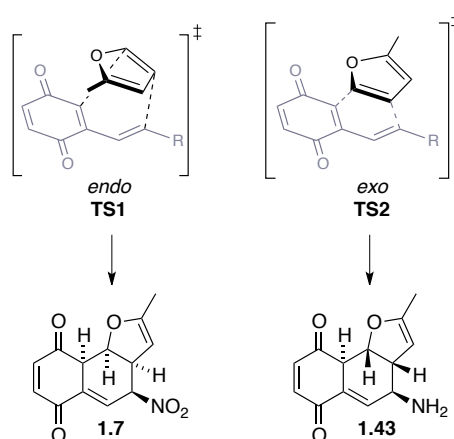


**Figure 1.4.** Conversion in VQDA reaction of nitrovinyl quinone (**1.5**) (blue rhombi) to the corresponding isoquinone methide (**1.7**) (red triangles).

The stereochemistry in the only obtained product **1.7** was determined by NMR spectroscopy. Formation of this product indicates that this VQDA reaction proceeds *via* an *endo* transition state (**TS1**) as opposed to an alternate *exo* transition state (**TS2**), which would lead to product **1.43**.

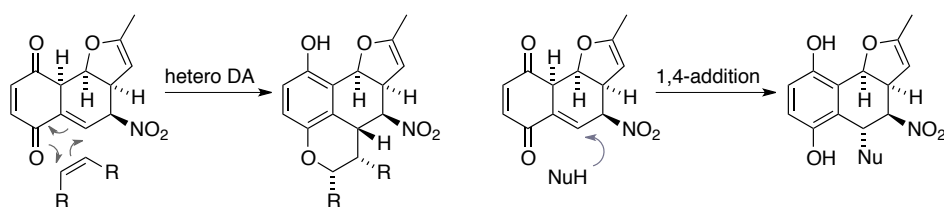


**Scheme 1.8.** The *endo* and *exo* transition states for the VQDA reaction between **1.5** and **1.6**.

As depicted in Scheme 1.8, the *endo* transition state would lead to an all-*syn* alignment of the protons on the newly generated stereogenic centres, resulting in comparably small coupling constants, following the KARPLUS curve.<sup>[21]</sup> In contrast, an *exo* transition state would lead to an *anti-syn-anti* configuration. Hence, larger coupling constants for the *anti*-oriented protons on the newly created stereocenters would be expected. <sup>1</sup>H NMR analysis indeed showed that corresponding coupling constants of the respective protons are found in a range

between 2.2–3.0 Hz, which correlates to dihedral angles between 60° and 70°, providing evidence for the *endo* transition state and the resulting all-*syn* orientation. The thus determined relative configuration of the molecule structure was confirmed by a NOESY experiment.

It is well known, that the reactive *ortho*-quinone methides are valuable dienophiles for hetero DA reactions or alternatively can be intercepted by nucleophiles.<sup>[22]</sup> To further investigate the potential of the VQDA reaction and its products as a tool in modern organic synthesis, the reactivity of isoquinone methide **1.7** towards electron-rich dienes and suitable nucleophiles was studied (Scheme 1.9)

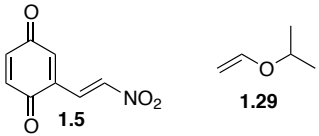
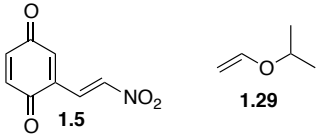
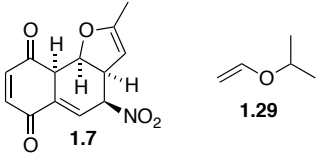
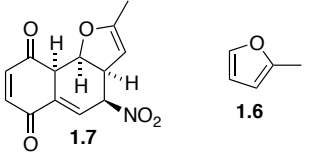
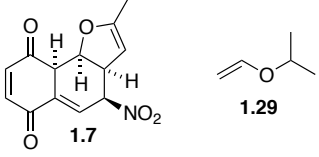
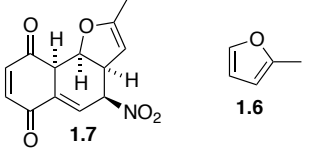
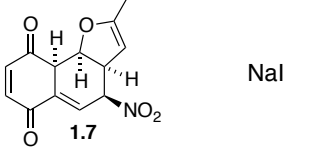
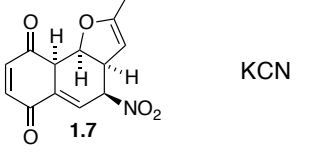


**Scheme 1.9.** Investigating further reactivity of isoquinone methide **1.7** in hetero DA reactions or MICHAEL addition.

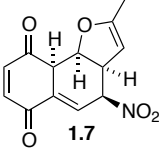
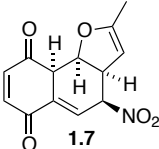
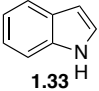
To examine the outlined reactivity suitable nucleophiles, such as iodide and cyanate, as well as dienophiles, such as 2-methylfuran (**1.6**) and isopropylvinylether (**1.29**) were tested (Table 1.3; entries 1–4 and 7–9). Additionally a VQDA hetero DA tandem reaction starting from vinyl quinone (**1.5**) was investigated (entries 5 and 6). Indole (**1.33**) (entry 10) could either react as a nucleophile or dienophile.

Reaction of isoquinone methide **1.7** with additional or excess dienophile did not result in the isolation of any new product because of decomposition or no reaction. Reacting **1.7** with nucleophiles resulted in decomposition in all cases.

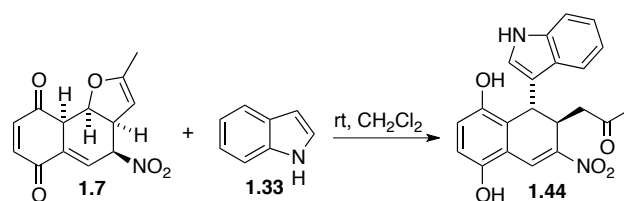
**Table 1.3.** Reactivity of isoquinone methide **1.7** towards dienophiles and nucleophiles.

entry	reactant 2	solvent	conditions	observation
1	 <chem>C=CC(=O)OC</chem> <b>1.29</b>	CH <sub>2</sub> Cl <sub>2</sub>	rt, 0.5 h	decomposition
2	 <chem>C=CC(=O)OC</chem> <b>1.29</b>	neat	55 °C, 0.5 h	decomposition
3	 <chem>C=CC(=O)OC</chem> <b>1.29</b>	CH <sub>2</sub> Cl <sub>2</sub>	rt, 0.5 h	no reaction
4	 <chem>C1=CC=CO1</chem> <b>1.6</b>	CH <sub>2</sub> Cl <sub>2</sub>	rt, 0.5 h	no reaction
5	 <chem>C=CC(=O)OC</chem> <b>1.29</b>	neat	60 °C, 12 h	decomposition
6	 <chem>C1=CC=CO1</chem> <b>1.6</b>	neat	60 °C, 12 h	decomposition
7	 NaI	THF	rt, 12 h	decomposition
8	 KCN	THF	rt, 12 h	decomposition

## 1.2. Method Development

entry	reactant 2	solvent	conditions	observation
9	 KCN      2.5 eq 18-crown-6      2.5 eq	THF	rt, 12 h	decomposition
10	  2 eq	CH <sub>2</sub> Cl <sub>2</sub>	rt, 0.5 h	<b>1.44</b>

However, when attempting a hetero DA reaction with indole (**1.33**), the formation of an unexpected product was observed. Careful NMR analysis suggested the formation of a compound, obtained from the opening of the furan-ring through nucleophilic attack of indole (Scheme 1.10).



**Scheme 1.10.** Nucleophilic attack of indole (**1.33**) on isoquinone methide **1.7**.

An X-ray crystal analysis confirmed the structure assigned to **1.44** by NMR (Figure 1.5), indicating the opening of the furan moiety upon attack of indole from the opposite face.

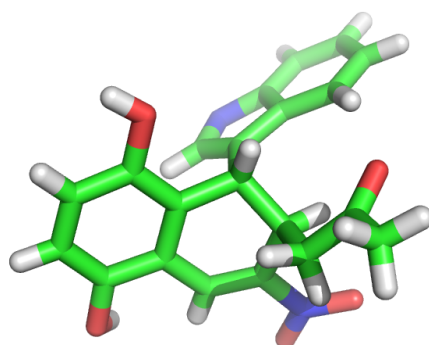


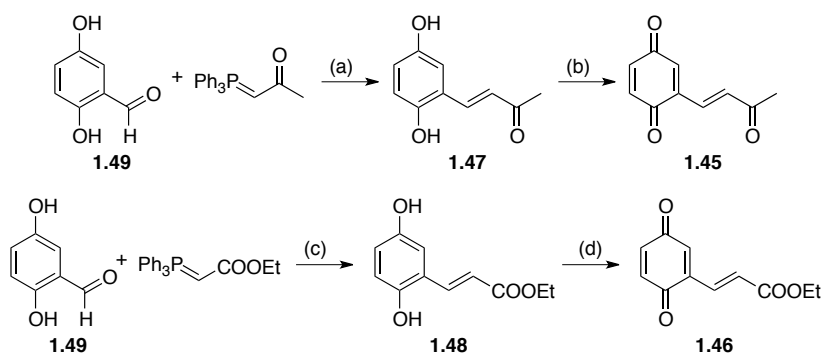
**Figure 1.5.** X-ray crystal structure of **1.44**.

The high instability of the DA adducts might be explained with the fact, that enol ethers are very reactive under acidic conditions. When the VQDA adduct tautomerises, an acidic phenol is formed, which could contribute to the activation of the enol ether and thus result in decomposition.

## 1.2.2 Alternative Precursors and Oxidation Methods

After having further explored the reactivity of nitrovinyl quinones as DA dienes, the attention was next turned on extending the substrate scope of the VQDA reaction. Because nitro-substituted vinyl quinones, such as the parent system studied by NOLAND and KEDROWSKI,<sup>[6,7]</sup> are very electron-poor and thus very reactive towards electron-rich dienophiles, the VQDA reaction precedes within minutes (see Figure 1.4). Enabling a DA reaction with different vinyl quinones would allow to study the influence of electronics on the reaction performance and at the same time introduce a broader variety of synthetic handles into the products. Both of which would further increase the usability of the VQDA reaction.

Replacing the nitro moiety with carbonyl functionalities in vinyl system would render the resultant diene less electron-poor than the nitro-substituted counterpart, but still setting the stage for a DA reaction with inverse electron demand. To explore whether such a significantly less electron-poor system would indeed still be suited for a DA reaction, quinones **1.45** and **1.46** were targeted for synthesis. Both hydroquinones **1.47** and **1.48** were obtained in good yield through a WITTIG-reaction with the corresponding phosphoylide and subsequently oxidised with activated silver oxide to give the desired vinyl quinones **1.45** and **1.46** (Scheme 1.11).

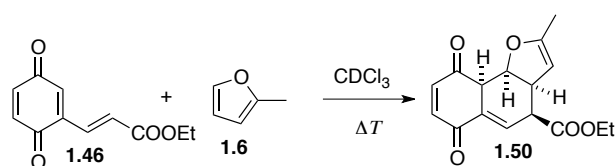


Reagents and conditions: (a) toluene, reflux, 81% of **1.47**; (b) AgO, dipicolinic acid, MeCN/H<sub>2</sub>O, 99% of **1.45**; (c) toluene, reflux, 83% of **1.48**; (d) AgO, dipicolinic acid, MeCN/H<sub>2</sub>O, 90% of **1.46**.

**Scheme 1.11.** Synthesis of VQDA-precursors **1.45** and **1.46**.

Both vinyl quinones were then subjected to DA conditions with excess methyl-furan as the electron-rich dienophile. However no precipitation of a [4+2] cycloadduct could be observed and TLC analysis of the crude reaction mixtures always revealed a complex

mixture, presumably due to the high instability of any formed reaction products. Only when heating a sample of **1.46** and methyl-furan in  $\text{CDCl}_3$  the formation of isoquinone methide **1.50** could be observed (Scheme 1.12; Figure 1.6). Attempts to force the reaction to completion through prolonged reaction times and higher temperatures as well as attempted isolation of the product through precipitation with non-polar solvents or chromatography all lead to decomposition. For this reason the observed product could not unambiguously be assigned, but the signals marked with an asterisk suggest the formation of DA adduct **1.50**.



**Scheme 1.12.** VQDA reaction of vinyl quinone **1.46**.

Due to fast decomposition of the instable VQDA precursor no product was observed upon heating of **1.45** in the presence of 2-methylfuran (**1.6**).

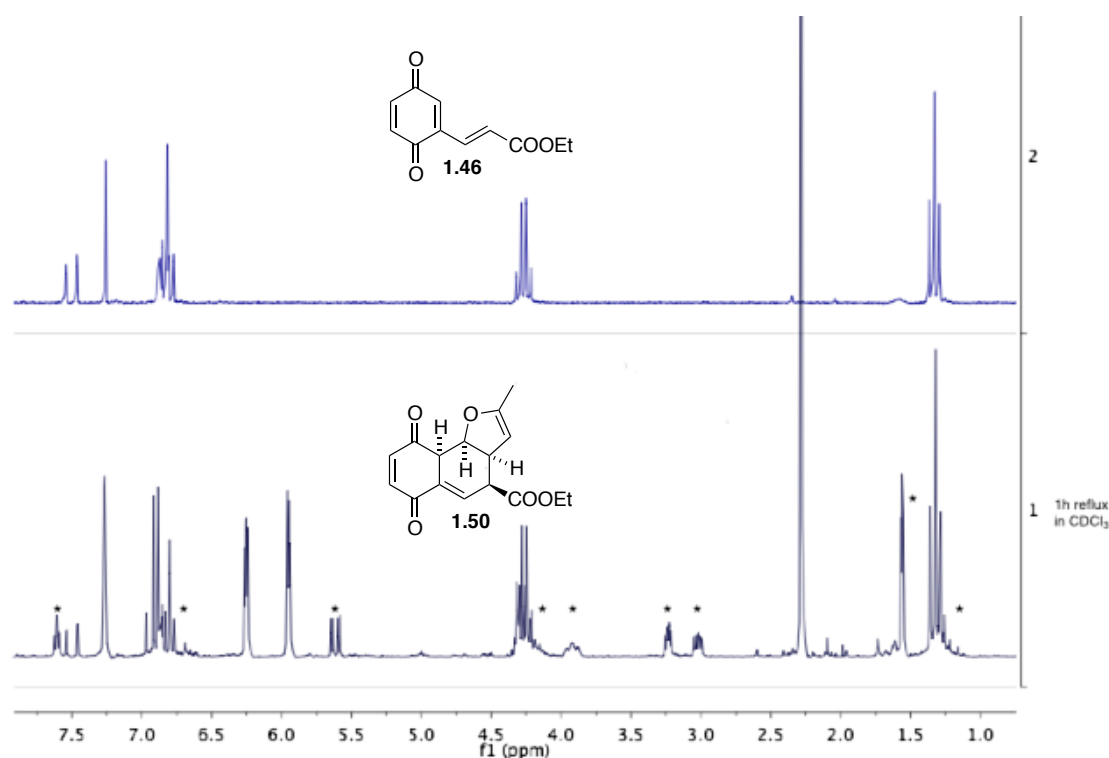
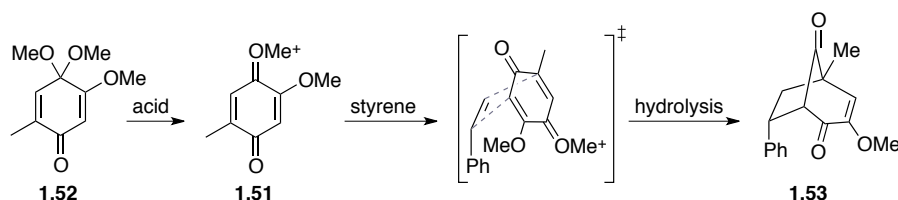


**Figure 1.6.** Crude NMR analysis of the VQDA reaction between 2-methylfuran **1.6** and vinyl quinone **1.46**; characteristic product peaks are indicated with an asterisk.



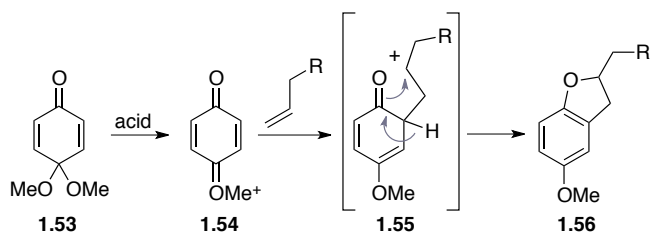
These results suggest that a diene system bearing ester substituents, is not activated enough anymore to effectively undergo a [4+2] cycloaddition before decomposition occurs.

Hence, the diene system has to be activated further, which could be achieved by introducing further electron withdrawing substituents or a positive charge. GRIECO and co-workers first showed that quinone monoketals readily undergo [5+2] cycloaddition reactions in highly polar media (Scheme 1.13).<sup>[23,24]</sup> The reaction presumably commences with the formation of an oxonium ion **1.51**, which is generated from quinone monoketal **1.52** in acidic environment. This sets the stage for an intermolecular [5+2] cycloaddition with styrene, giving diketones such as **1.53** in good to excellent yields.



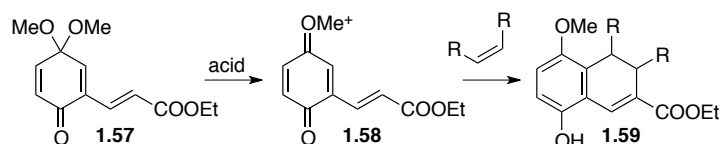
**Scheme 1.13.** An acid-promoted intermolecular [5+2] cycloaddition reaction between quinone monoketal **1.52** and styrene.

Another example of a formal cycloaddition reaction involving quinone monoketals was recently described by KITA and co-workers (Scheme 1.14). They reported a BRØNSTED-acid promoted, formal [3+2] cycloaddition of alkenes to quinone monoketal **1.53** *via* the oxonium ion **1.54** which then coupled to various alkenes. The formal [3+2] reaction presumably proceeds step-wise *via* charged intermediate **1.55** to finally result in hydrobenzofuran **1.56**.



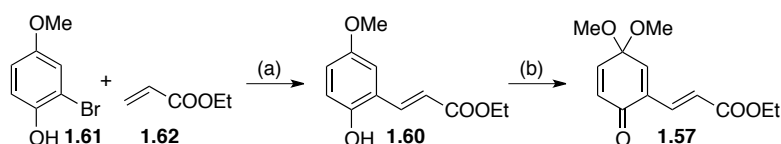
**Scheme 1.14.** A BRØNSTED-acid promoted formal [3+2] cycloaddition reaction involving quinone monoketal **1.53** resulting in hydrobenzofuran **1.56**.

To explore the reactivity of vinyl quinone monoketals towards electron-rich alkenes, compound **1.57** was chosen as a test system (Scheme 1.15). If a vinyl quinone monoketal such as **1.57** is treated with acid, a positively charged vinyl quinone type intermediate **1.58** is generated, in which the diene system is activated through the positive charge. Hence, it might well be possible that a cationic [4+2]-type cycloaddition, giving DA adduct **1.59**, might proceed faster than the corresponding [5+2] or [3+2] competing reactions.



**Scheme 1.15.** Envisaged cationic VQDA reaction from quinone monoketal **1.57**.

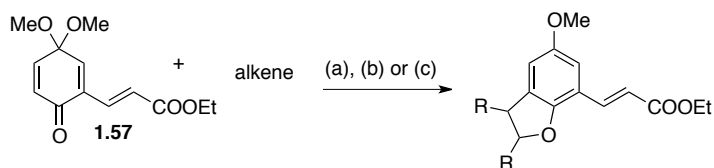
Vinyl methoxyphenol **1.60** was obtained after HECK coupling between arylbromide **1.61** and ethyl acrylate (**1.62**), which was transformed into the desired vinyl quinone monoketal **1.57** by treatment with bis(acetoxy)iodobenzene (BAIB) in anhydrous methanol (Scheme 1.16).



Reagents and conditions: (a) Pd<sub>2</sub>(dba)<sub>3</sub> (3%), *t*-Bu<sub>3</sub>P (20%), cy<sub>2</sub>NMe, dioxane, 90 °C, 99% of **1.60**; (b) BAIB, MeOH, 79% of **1.57**.

**Scheme 1.16.** Synthesis of vinyl quinone monoketal **1.57**.

Next, vinyl quinone monoketal **1.57** was subjected to acidic conditions, as reported by GRIECO and KITA, in the presence of electron-rich alkenes (Table 1.4).<sup>[23–25]</sup> In all cases the reaction proceeded very sluggishly and the resulting products were very unstable and could not be isolated. However, crude NMR and HRMS data suggest that a formal [3+2] reaction instead of the anticipated [4+2] cycloaddition occurred under all conditions tested.

**Table 1.4** Reactivity of vinyl quinone monoketal **1.57** towards various alkenes under acidic conditions.

Reagents and Conditions: (a) 3.0 M LiClO<sub>4</sub>, TMSOTf, -15°C; (b) BF<sub>3</sub>·OEt<sub>2</sub>, CH<sub>2</sub>Cl<sub>2</sub>, -78°C;  
 (c) Montmorillonite K-10, CH<sub>2</sub>Cl<sub>2</sub>, -78°C.

entry	alkene	reaction conditions	observation by NMR and MS
1	 1.6	(a)	decomposition
2	 1.37	(a)	 1.63
3	 1.29	(a), (b), (c)	 1.64

### 1.2.3 Catalysis attempts

The addition of catalytic or stoichiometric amounts of LEWIS acid (LA) is well known to enhance the reaction rate of DA reactions.<sup>[26–28]</sup> In the case of a LA catalysed cycloaddition, the LA can selectively coordinate to heteroatoms of one of the reaction components.<sup>[29,30]</sup> This interaction strongly influences the electronic environment of the molecule. Not only the HOMO and LUMO orbital energies are lowered, but also the size of orbital coefficients is changed.<sup>[27,31]</sup> In the case of the VQDA reaction, the LA could coordinate to the carbonyl moiety of the quinone as shown in Figure 1.7. Lowering the orbital energies of the diene consequently also lowers the energy gap between the HOMO<sub>dienophile</sub> and LUMO<sub>diene</sub>, which results in higher reactivity and often in improved regio- and diastereoselectivity.

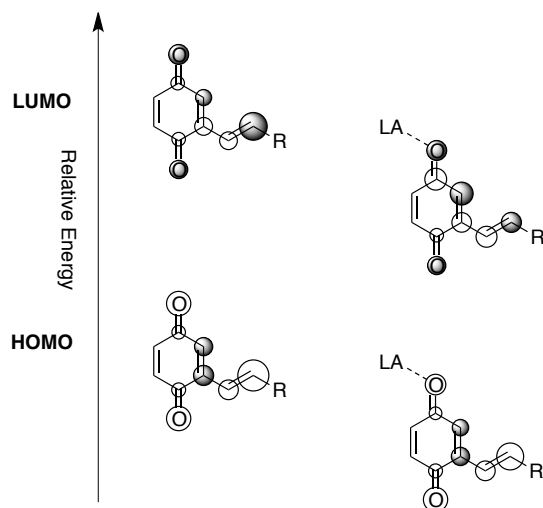


**Figure 1.7.** Coordination of a Lewis-acid to a vinyl quinone and the influence on the energy levels of its HOMO and LUMO.

When utilizing chiral Lewis-acids (CLA) for the catalysis of DA reactions, additionally high enantioselectivity can be achieved.<sup>[30]</sup> Upon coordination to one of the substrates, the CLA and the two reactants can form diastereomeric transition states (TS-1\* and TS-2\*) (Figure 1.8). As both enantiomeric products have the same relative energy, the reaction needs to proceed under kinetic control to achieve high enantioselectivity.

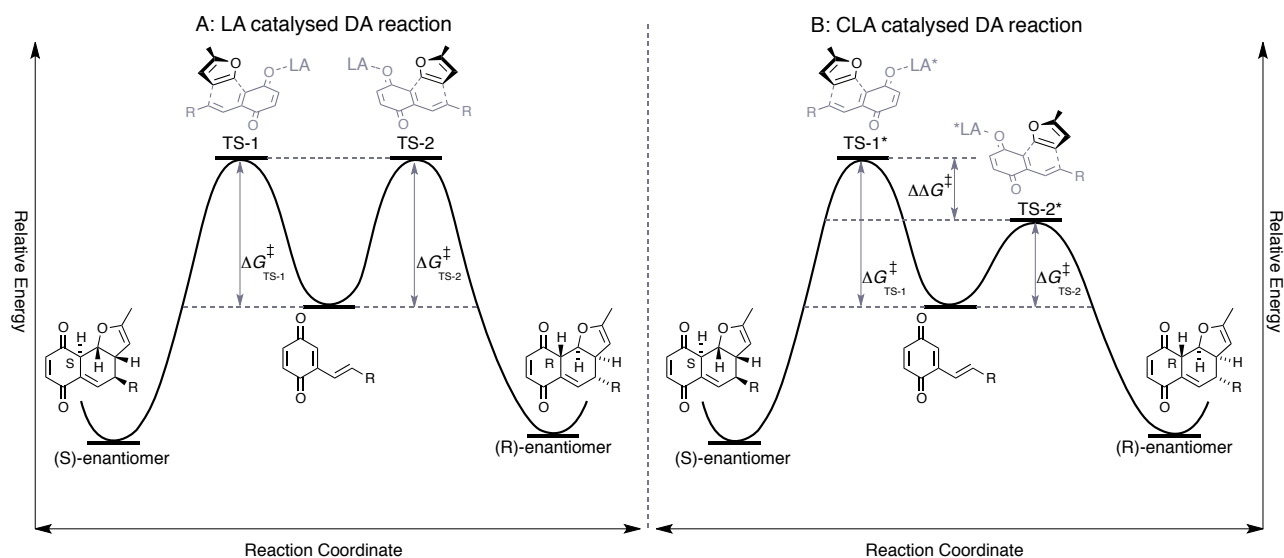


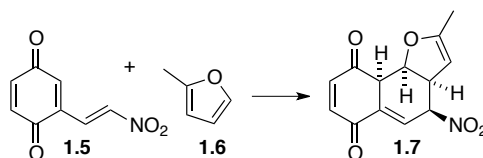
**Figure 1.8.** Transition states of a DA reaction catalysed with LA and CLA.

Hence, the activation barrier for one of the diastereomeric transition states needs to be substantially lower in energy relative to the competing diastereomeric transition states. The example in Figure 1.6.B shows a CLA-catalysed DA reaction, which would proceed through TS-2\* due to kinetic control and thus give predominantly the corresponding (R)-

enantiomer as product. In order to favour one diastereomeric transition state over another, the CLA should activate one component selectively and at the same time provide a well defined stereochemical environment that results in a significantly lower activation barrier of one of the diastereomeric transition states.

The nitrovinyl quinone **1.5** has proven as a reliable diene in VQDA reactions. As described in chapter 1.3.2, the reactions proceed smoothly with a variety of dienophiles in usually good to excellent yield. Additionally, the products were isolable in some cases. Therefore, nitrovinyl quinone **1.5** was chosen as the test-diene to investigate activation through LA catalysis and ultimately whether an enantioselective version can be achieved. To explore whether the VQDA reaction can be catalysed, several LA were applied as additives in the reaction between **1.5** and 2-methylfuran (**1.6**) (Table 1.5). While stirring **1.5** and **1.6** in CH<sub>2</sub>Cl<sub>2</sub> at low temperature did not result in any reaction, employing triflate LAs only led to decomposition products. But also other LAs such as BF<sub>3</sub>OEt<sub>2</sub> did not give any isolable product under the conditions shown in Table 1.5.

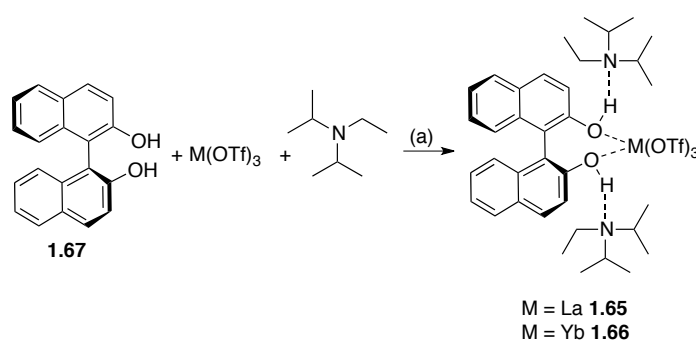
**Table 1.5.** Influence of achiral LA on the DA reaction between **1.5** and **1.6**.



Entry	LA	Reaction Conditions	Observation
1	None	CH <sub>2</sub> Cl <sub>2</sub> , -78 °C	no reaction
2	BF <sub>3</sub> OEt <sub>2</sub> (5%)	CH <sub>2</sub> Cl <sub>2</sub> , -78 °C	decomposition
3	Et <sub>2</sub> AlCl (10%)	toluene, -20 °C	decomposition
4	Ti( <i>i</i> -PrO <sub>4</sub> ) (5%)	CH <sub>2</sub> Cl <sub>2</sub> , -78 °C	decomposition
5	Yb(OTf) <sub>3</sub> (5%)	CH <sub>2</sub> Cl <sub>2</sub> , -78 °C	decomposition
6	Eu(OTf) <sub>3</sub> (5%)	CH <sub>2</sub> Cl <sub>2</sub> , -78 °C	decomposition
7	Sc(OTf) <sub>3</sub> (5%)	CH <sub>2</sub> Cl <sub>2</sub> , -78 °C	decomposition
8	La(OTf) <sub>3</sub> (5%)	CH <sub>2</sub> Cl <sub>2</sub> , -78 °C	decomposition
9	SnCl <sub>4</sub> (5%)	toluene, 0 °C	decomposition

All triflate LAs only lead to decomposition, which might be due to the acid sensitivity of the vinyl quinone and the cycloaddition adducts.

The binol LA complexes reported by YAMAMOTO (Scheme 1.17) are chiral and significantly less acidic.<sup>[32,33]</sup> Hence it was anticipated that directly an asymmetric version of the VQDA reaction could be achieved. The chiral lanthanide binol complexes **1.65** and **1.66** were obtained by reacting (*S*)-binol (**1.67**) with the corresponding lanthanide triflates in the presence of a base.

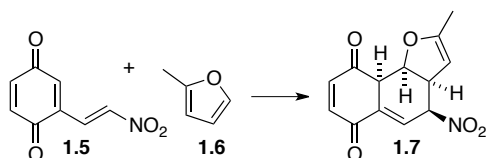


Reagents and conditions: (a) CH<sub>2</sub>Cl<sub>2</sub>, 0 °C.

**Scheme 1.17.** Preparation of binol-based CLAs **1.65** and **1.66**.

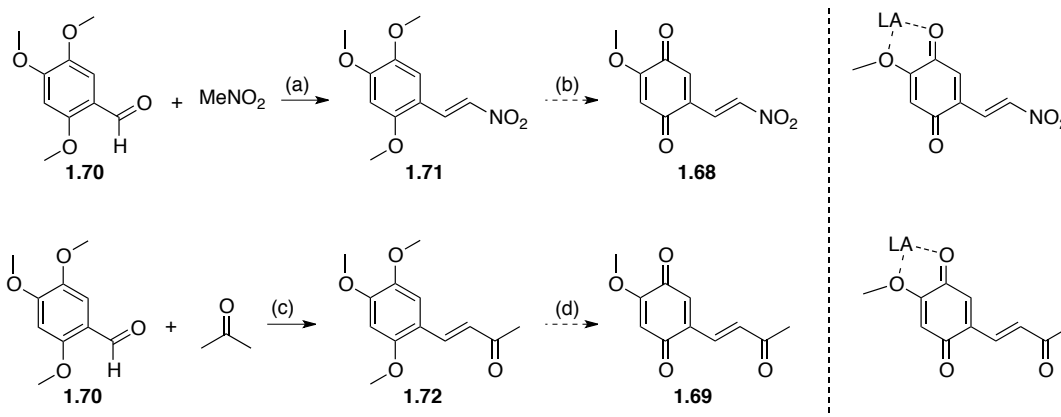
Those CLAs were always freshly prepared to test them for catalysis of a VQDA reaction between **1.5** and **1.6** (Table 1.6). However, addition of the LA at 0 °C led to decomposition of the starting material in both cases.

**Table 1.6.** Influence of CLAs on the DA reaction between **1.5** and **1.6**.



Entry	LA	Reaction Conditions	Observation
1	<b>1.65</b> (30%)	CH <sub>2</sub> Cl <sub>2</sub> , 0 °C	decomposition
2	<b>1.66</b> (30%)	CH <sub>2</sub> Cl <sub>2</sub> , 0 °C	decomposition

All tested conditions and LA did not result in a rate accelerated VQDA reaction, but in decomposition. One potential issue could be that the LAs do not coordinate in a well-defined fashion to the vinyl quinone. To test this hypothesis, vinyl quinones **1.68** and **1.69**, bearing an additional methoxy moiety to aid coordination of the LA were designed (Scheme 1.18).

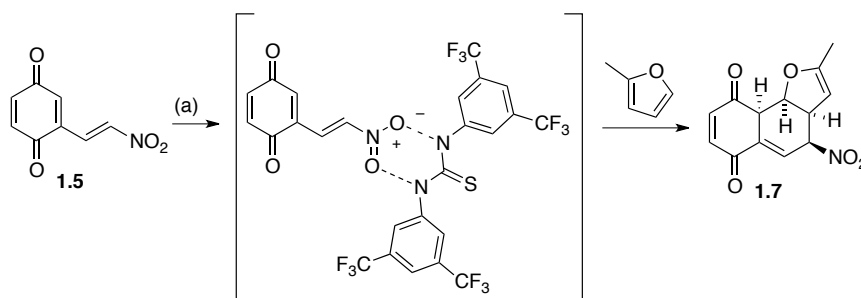


Reagents and conditions: (a) NaOH, MeCN/H<sub>2</sub>O, 64% of **1.71**; (b) CAN, MeCN/H<sub>2</sub>O, decomposition; (c) NaOH, acetone/H<sub>2</sub>O, 86% of **1.72**; (d) CAN, MeCN/H<sub>2</sub>O, decomposition.

**Scheme 1.18.** Attempted synthesis of vinyl quinones **1.68** and **1.69** bearing an extra coordination site.

Aldol condensation of aldehyde **1.70** with nitromethane or acetone gave the corresponding vinyl methoxyhydroquinone derivatives **1.71** and **1.72** in good yield. However, it was not possible to obtain the corresponding quinones by oxidation with CAN, as the products quickly decomposed upon aqueous workup.

Since it was not possible to activate the vinyl quinone system with traditional LAs, presumably due to the high instability of both, the products and starting materials under acidic conditions, the possibility of mild organocatalysis was investigated. It is well known that electron-poor thioureas can coordinate to nitro functionalities and also accelerate DA reactions (Scheme 1.19).<sup>[34,35]</sup> However, no rate accelerating effect could be detected, when adding 1,3-bis(3,5-bis(trifluoromethyl)phenyl)thiourea to the reaction mixture



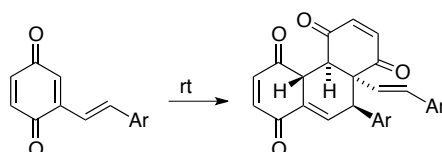
Reagents and conditions: (a) 1,3-bis(3,5-bis(trifluoromethyl)phenyl)thiourea, THF, -78°C, no reaction.

**Scheme 1.19.** Influence of an electron-poor-thiourea on the VQDA reaction.

### 1.2.4 Method Development: Summary and Outlook

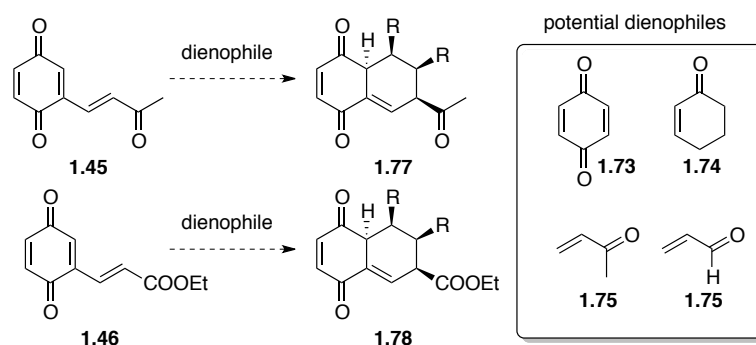
In summary, the intermolecular VQDA chemistry originally developed by NOLAND was studied in greater detail. Time-resolved NMR studies revealed that the DA reaction between vinyl quinone **1.5** and 2-methylfuran (**1.6**) is very clean and efficient. All efforts to further extend the scope of the intermolecular DA reaction were unsuccessful until now, mostly due to unstable products. However, it was possible to further functionalise isoquinone methide **1.7** through an unusual opening of the furan-ring. This interesting result might allow a more systematic study on the reactivity of isoquinone methides towards nucleophiles such as indole.

It is known that vinyl quinones with the appropriate electronics tend to dimerise and give DA-type adducts (Scheme 1.20).<sup>[4]</sup> This dimerisation presumably proceeds with neutral electron demand. This mode of the VQDA reaction still remains unexplored and until today there is no intermolecular VQDA reaction, other than this dimerisation, with electron-poor dienes reported in literature



**Scheme 1.20.** Dimerisation of vinyl quinones.

No dimerisation reaction was observed for the very electron-poor nitrovinyl quinone **1.5**. It might well be the case that the electronics are not matched in this case and the nitro group is too electron withdrawing. Hence, in order to further explore the feasibility of neutral electron demand VQDA reactions, vinyl quinones like **1.45** and **1.46** should be reacted with several electron-poor dienophiles, such as quinone (**1.73**), cyclohexenone (**1.74**), acrolein (**1.75**) and methyl vinyl ketone (**1.76**) (Scheme 1.21), to give products like **1.77** and **1.78**. Achieving such a cycloaddition would significantly broaden the scope of VQDA reactions.



**Scheme 1.21.** Potential neutral electron demand VQDA reactions.



## 1.3 Intramolecular VQDA Reaction in the Total Synthesis of the Pycnanthuquinones

### 1.3.1 Introduction

The pycnanthuquinones are members of a family of natural products, which have been isolated from various biological sources. Following an ethnomedical drug discovery program, SHAMAN PHARMACEUTICALS, a pharmaceutical company that ceased to exist, focussed on the isolation of bioactive molecules from tropical plants, which have been used in traditional indigenous medicine.<sup>[11]</sup> In the course of this program they found that *Pycnanthus angolensis* (Welw.) Warb. (Myristicaceae), a tree which can be found in western Africa, is used by traditional healers to treat a variety of symptoms often caused by type 2 diabetes mellitus.<sup>[11]</sup> From the extracts of the trees leaves and stems they reported the isolation of the two novel natural products pycnanthuquinone A (**1.16**) and B (**1.17**), along with other known terpenoid quinol derivatives. Structure elucidation revealed a linearly fused unprecedented 6,6,5-tricyclic system with an unusual oxidation pattern (Figure 1.9). Compounds **1.16** and **1.17** are diastereoisomers with respect to the secondary alcohol, featuring five contiguous stereocenters, one of which is quaternary. Both compounds were found to exhibit significant antihyperglycemic activities in a mouse model for type 2 diabetes mellitus.<sup>[11]</sup>

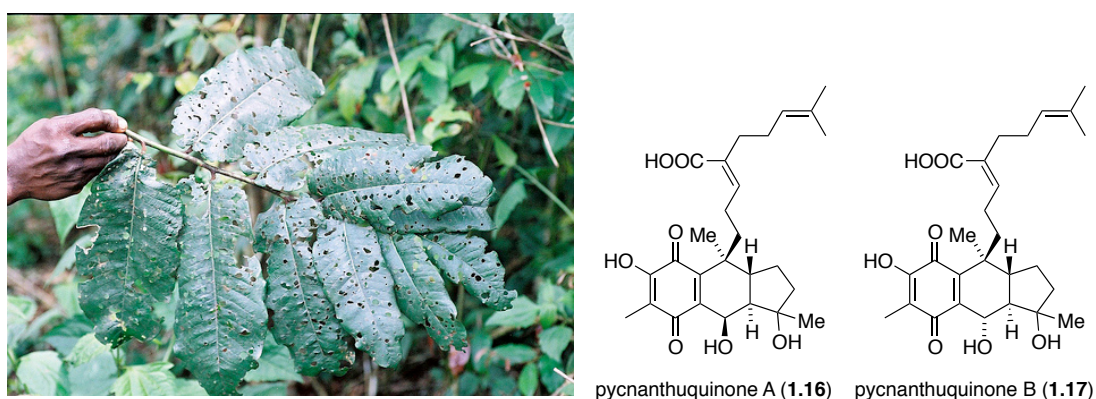


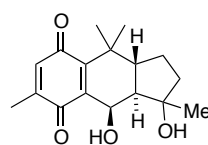
**Figure 1.9.** Leaves of *Pycnanthus angolensis* and the structures of pycnanthuquinones A (**1.16**) and B (**1.17**).<sup>\*</sup>

<sup>\*</sup> Photography by P. LATHAM. Image used with the permission of the author.

### 1.3. Application in the Total Synthesis of the Pycnanthuquinones

---

In 2006, the structurally less complex pycnanthuquinone C (**1.18**) was isolated from the western Australian brown alga *Cystophora harveyi* Womersley (Cystoseiraceae) in addition to four previously reported geranyltoquinol derivatives (Figure 1.10).<sup>[12]</sup> Pycnanthuquinone C exhibits four contiguous stereocenters. Despite considerable efforts, the relative configuration with respect to the C3 carbon atom of the pycnanthuquinones could not be elucidated in all cases. Hence, their absolute configuration has not thus far been established either. In contrast to the pycnanthuquinones A and B, no bioactivity has been reported for pycnanthuquinone C, because it was obtained only in minute quantities from the natural source and no testing was done.



pycnanthuquinone C (**1.18**)

**Figure 1.10.** Image of *Cystophora harveyi* and the structure of pycnanthuquinone C (**1.18**).<sup>\*</sup>

The pycnanthuquinones A and B are so called meroditerpenoids, whereas **1.18** is a meromonoterpenoid. Meroterpenoids (ancient greek *meros*, “part, portion”) are classified as compounds that feature a partial terpenoid structure. Additionally the quinoid core of pycnanthuquinone C is not further oxidised.

Rossinone B (**1.21**), another meroterpenoid natural product featuring this unusual 6,6,5-tricyclic core skeleton, was isolated from a marine organism. It was found in the Antarctic ascidian, *Aplidium* species,<sup>[15]</sup> which is unusual for this kind of natural source, as most metabolites found in ascidian are derived from amino acids.<sup>[36]</sup> The main difference of this intriguing structure to those of pycnanthuquinones A – C is not only the highly unusual oxidation pattern of the terpenoid fragment, but also the less substituted quinoid core, which occurs in the form of a stabilised isoquinone methide. Furthermore, rossinone B features five contiguous stereo centres, one of which is quaternary (Figure 1.11).

---

<sup>\*</sup> Photography by J. M. HUISMAN. Image used with the permission of the Western Australian Herbarium, Department of Environment and Conservation (<http://florabase.dec.wa.gov.au/help/copyright>). Accessed on Friday, 31 August 2012.



**Figure 1.11.** Image of ascidian (*Aplidium sp.*) and the structure of rossinone B (**1.21**).

The very interesting biological profile of rossinone B can be speculated to stem from the highly unusual stabilised isoquinone methide. In biological *in vitro* assays it showed some antiviral and antibacterial activity, but more interestingly exhibited potent antiproliferative activity towards a leukemia cell-line and good activity towards a neuroblastoma cell-line, while not targeting normal human liver cells.<sup>[15]</sup>

### 1.3.2 Biosynthetic Pathways of the Pycnanthuquinones

When the isolation of pycnanthuquinones A and B were reported by FORT *et al.*, no suggestions on the biogenesis of these complex natural products were made.<sup>[11]</sup> However, VAN ALTENA and co-workers proposed a plausible pathway for the biosynthesis of pycnanthuquinone C (**1.18**).<sup>[12]</sup> Their considerations were based on the conjoint isolation of pycnanthuquinone C with four other compounds **1.79–1.82** of the same class from a single source organism (Figure 1.12). Since alkylated toluquinols are well known to be easily oxidised to the corresponding quinones, it seems likely that toluquinone **1.79** is an isolation artefact. Hence, the actual metabolite from *C. harveyi* is suggested to be toluquinol **1.83**,<sup>[37]</sup> which they anticipate as a common precursor for the isolated congeners (Scheme 1.21).<sup>[12]</sup> In this case **1.83** presumably originates from a mixed biosynthetic pathway. The quinone portion most likely originates from a shikimate derivative, which is prenylated during terpene biosynthesis.

\*Photography by DANIEL VAULOT.

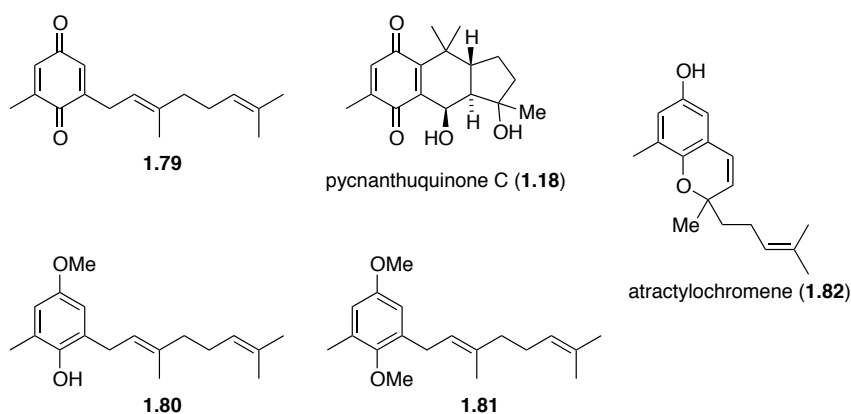
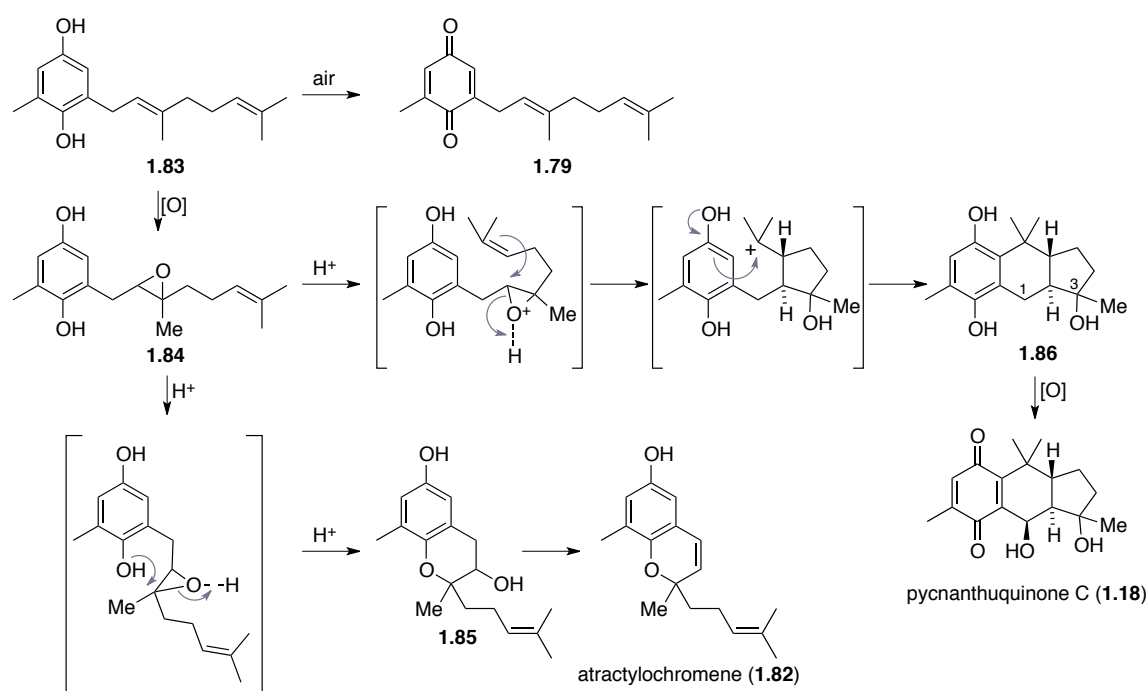


**Figure 1.12.** Congeners of pycnanthuquinone C.

Methoxyquinols **1.80** and **1.81** are proposed to be products of alkylation by *S*-adenosyl methionine (SAM). In the proposed biosynthetic pathway, to obtain atractylochromene (**1.82**) and pycnanthuquinone C (**1.18**), quinol **1.83** is epoxidised at the 2,3-double bond to common precursor **1.84**. Epoxide opening and nucleophilic attack of the C-1' hydroxyl at the C-3 position would result in cyclic ether **1.85**. Elimination of water would then form the benzylic double bond of atractylochromene (**1.82**).



**Scheme 1.22.** Proposed biosynthesis of pycnanthuquinone C from known congeners.<sup>[12]</sup>

Pycnanthuquinone C would arise, when epoxide **1.84** is opened through an alternative pathway (Scheme 1.22). Nucleophilic attack of the terminal double bond on the epoxide would result in a stabilised cyclopentyl tertiary carbocation, which upon electrophilic

aromatic substitution yields tricyclic structure **1.86**. Selective oxidation of intermediate **1.86** at the C-1 position, followed by oxidation of the quinol finally gives rise to pycnanthuquinone C (**1.18**). This proposed biosynthetic pathway could also be applied to the biosynthesis of the pycnanthuquinones A and B.

However, because pycnanthuquinones A and B are diastereoisomers with respect to the secondary hydroxyl group at the C-1 position, a more sophisticated biosynthetic hypothesis can be developed. This revised biosynthesis also takes into account that **1.16** and **1.17** were isolated together with the meroditerpenoids kombic acid (**1.87**) and sargachromenol (**1.88**) (Figure 1.13).

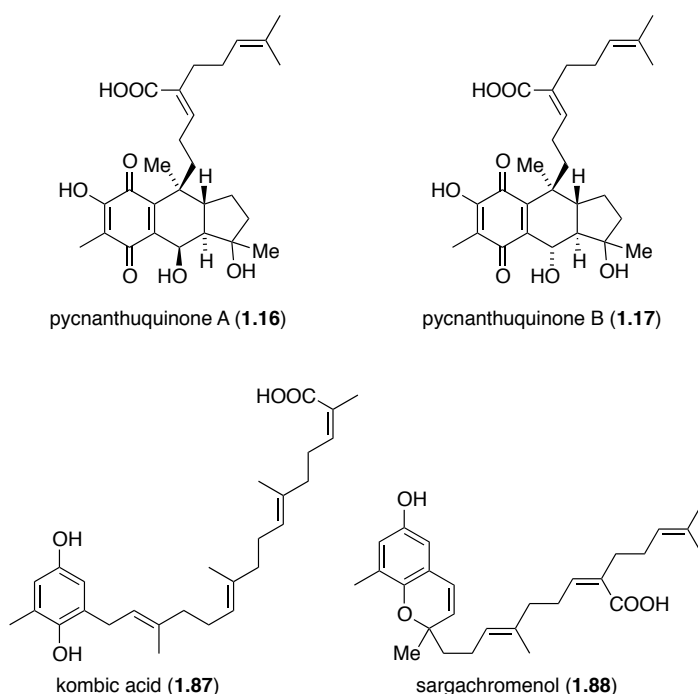
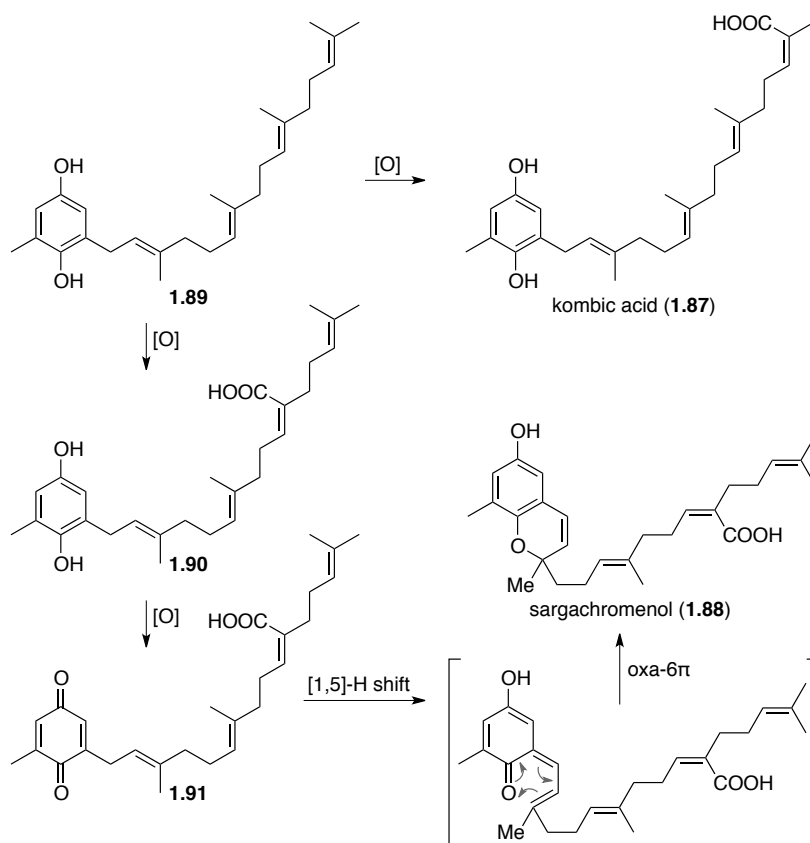


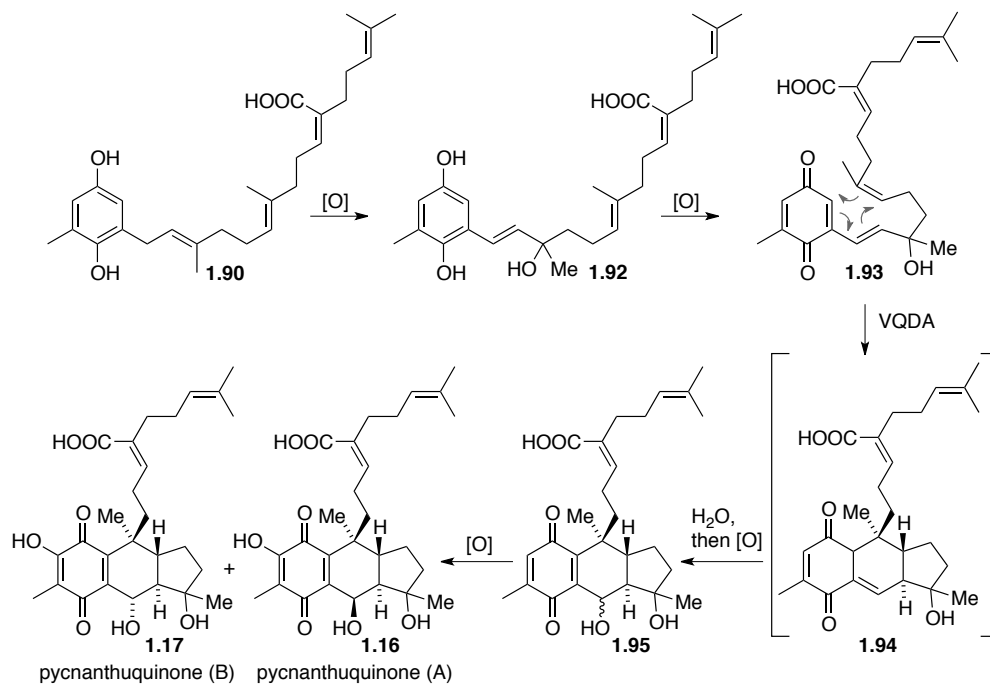
**Figure 1.13.** Congeners of pycnanthuquinones A and B.

The proposed biosynthesis commences with common prenylated shikimate **1.89**, which is selectively oxidised to either kombic acid (**1.87**), or to carboxylic acid **1.90** (Scheme 1.23). This compound can then be oxidised to give alkylated toluquinone **1.91** as a precursor for sargachromenol (**1.88**): a [1,5]-H shift gives rise to the precursor of an oxa- $\pi$  electrocyclisation reaction, which results in the formation of the natural product sargachromenol (**1.88**).



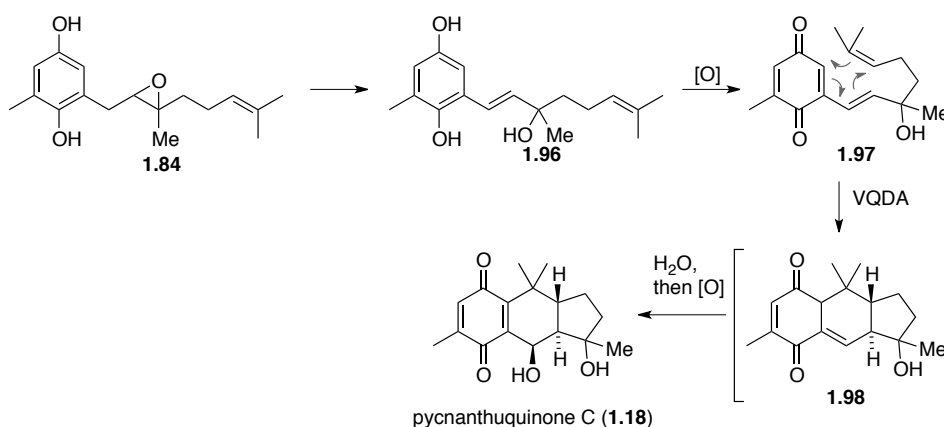
**Scheme 1.23.** Revised proposal for the biosynthesis of kombic acid, sargachromenol.

However, epoxidation of vinyl quinone **1.89** (Scheme 1.24), followed by epoxide opening would give rise to alkenyl hydroquinone **1.92**. Oxidation to the corresponding vinyl quinone **1.93** sets the stage for an intramolecular VQDA reaction, which forms isoquinone methide **1.94** as a reactive intermediate. Nucleophilic attack of water would initially afford quinone **1.95**, as a mixture of diastereoisomers. Late stage hydroxylation of the quinone core finally results in the natural products pycnanthuquinone A (**1.16**) and B (**1.17**).



**Scheme 1.24.** Revised proposal for the biosynthesis of pycnanthuquinones A and B *via* VQDA reaction.

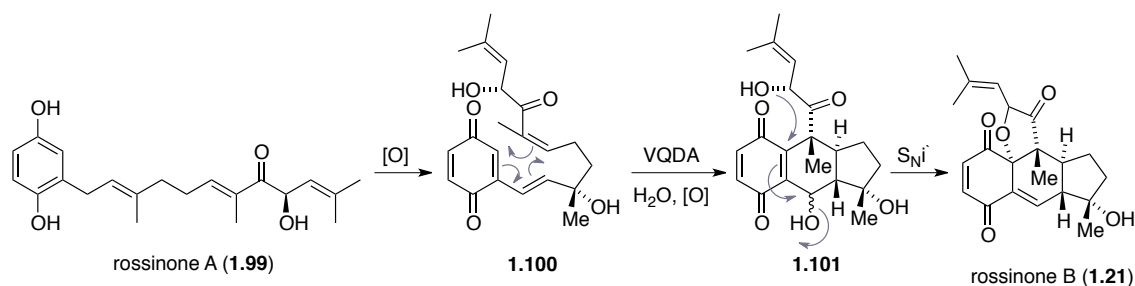
The same biosynthetic concept can be employed to develop a revised biosynthesis of pycnanthuquinone C (**1.18**) (Scheme 1.25). Starting from intermediate **1.84**, as suggested by VAN ALTENA and co-workers,<sup>[12]</sup> opening of the epoxide will result in alkenylated hydroquinone **1.96**, which is converted upon oxidation into the corresponding vinyl quinone **1.97**. This precursor for a VQDA reaction then undergoes [4+2] cycloaddition, giving rise to an isoquinone methide intermediate **1.98**, which is transferred into the natural product **1.18** by conjugate addition of water, followed by oxidation.



**Scheme 1.25.** Revised proposal for the biosynthesis of pycnanthuquinone C *via* VQDA reaction.

### 1.3. Application in the Total Synthesis of the Pycnanthuquinones

When considering the structural similarity and conjoint isolation of rosinone A (**1.99**) and B (**1.21**), it seems plausible that they might share a common biosynthetic origin (Scheme 1.26).<sup>[16]</sup>



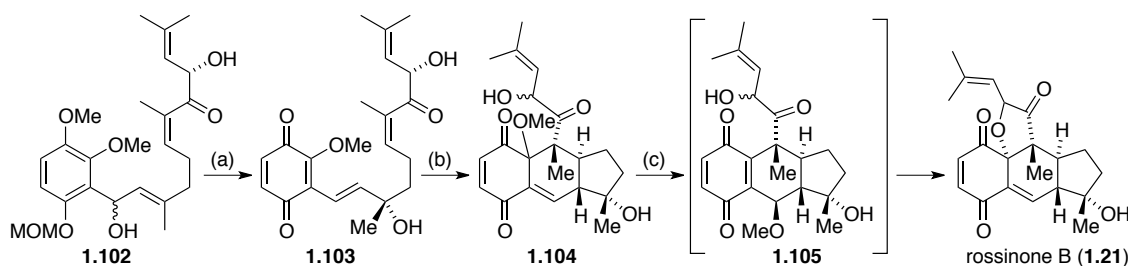
**Scheme 1.26.** Biosynthetic proposal for the transformation of rosinone A (**1.99**) into rosinone B (**1.21**).

Rosinone A (**1.99**) is transformed into vinyl quinone **1.100** through a similar sequence of oxidation steps, as discussed in the biosynthesis of pycnanthuquinones A – C (schemes 1.24 and 1.25). This electron-poor VQDA precursor then undergoes a diastereoselective [4+2] cycloaddition reaction, which presumably proceeds with neutral electron demand, giving rise to a quinone methide intermediate. This reactive species is then immediately intercepted by non-selective attack of water, yielding quinone **1.101** as a mixture of diastereoisomers, closely resembling the pycnanthuquinones A and B. In this case, however, the VQDA sequence is followed by an intramolecular S<sub>N</sub>i' reaction that yields the tetracyclic framework of rosinone B **1.21**.



### 1.3.4 Previous Synthetic Approaches Towards Rossinone B and Pycnanthuquinone C

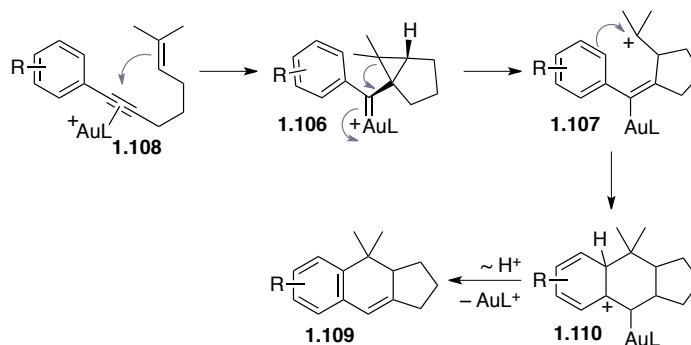
In the course of this work two approaches towards the 6,6,5-tricyclic skeleton of the pycnanthuquinones were published by ZHANG and ECHAVARREN. The biosynthetic relevance of the VQDA reaction was further underlined by a biomimetic total synthesis. ZHANG *et al.* completed a racemic synthesis of rossinone B (**1.21**) by following the biosynthetic proposal of TRAUNER and co-workers.<sup>[16,17]</sup> The total synthesis closely resembles the proposed biosynthetic pathway as discussed in Chapter 1.4.3. Advanced intermediate **1.102** was transformed into DA precursor **1.103** under acidic, oxidative conditions (Scheme 1.27). After VQDA reaction with normal electron demand, an inconsequential diastereomeric mixture of **1.104** was obtained, which then reacted in the presence of TsOH *via* intermediate **1.105** to give rossinone B (**1.21**).<sup>[17]</sup>



Reagents and conditions: (a) 6 N HNO<sub>3</sub>, then AgO, 90% of **1.103**; (b) toluene, 150 °C, 50% of **1.104**; (c) MeOH/H<sub>2</sub>O, TsOH, 31% of **1.21** over two steps.

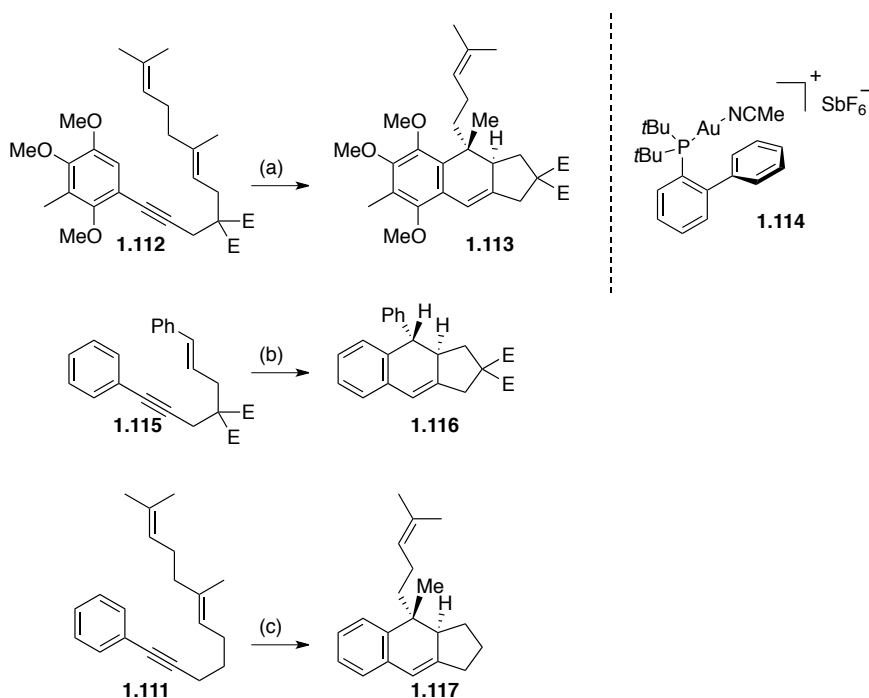
**Scheme 1.27.** Bioinspired synthesis of rossinone B (**1.21**).<sup>[17]</sup>

The group of ECHAVARREN has recently developed interesting Au(I)-catalysed cyclisation reactions of 1,5-enynes to give the 6,6,5-tricyclic scaffold of the pycnanthuquinones (Scheme 1.28).<sup>[38–40]</sup> Due to the low reactivity of alkenyl or phenyl substituted enynes, it was necessary to employ bulky phosphine ligands for Au(I) to catalyse a formal [4+2] type cycloaddition yielding linearly fused tricyclic systems.<sup>[38]</sup> According to DFT calculations, the mechanism of this reaction proceeds as a step-wise process, commencing with a 5-*exo*-dig cyclisation, which results in an *anti*-cyclopropyl Au(I)-carbene **1.106**. This reactive intermediate is subsequently opened to form a stabilised carbocation **1.107**, which undergoes a FRIEDEL-CRAFTS-type reaction with the aryl ring to furnish compound **1.109** *via* carbocation **1.110**.<sup>[39]</sup>



**Scheme 1.28.** Proposed mechanism for the Au(I) catalyzed formation of tetrahydrocyclopentanaphthalenes **1.109**.<sup>[38–40]</sup>

Several scaffolds, closely resembling the carbon skeletons of the pycnanthuquinones, as well as rossinone B, were prepared using this methodology (Scheme 1.29). Remarkably even cyclisations of substrates without a gem-substituted tether (THORPE-INGOLD effect), such as enyne **1.111**, were accomplished in very good yield. However, further derivatisation of these scaffolds to the corresponding natural products was not successful.



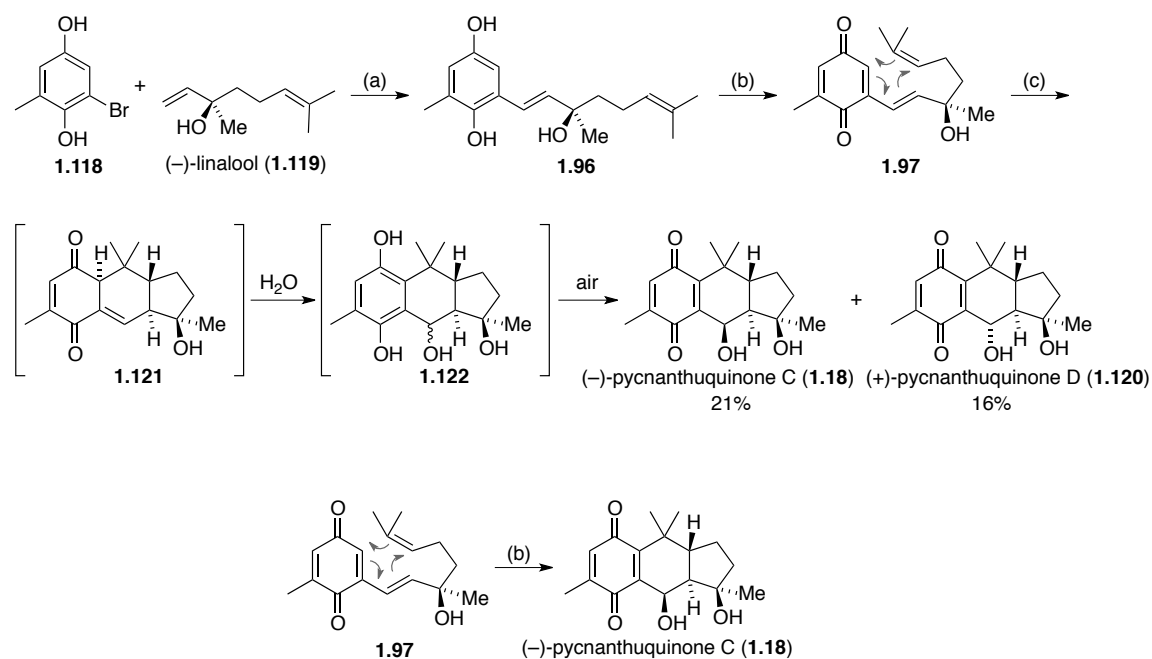
Reagents and conditions: (a)  $\text{CH}_2\text{Cl}_2$ , **1.114** (2 mol%), rt then 40 °C, 35% of **1.113**; (b)  $\text{CH}_2\text{Cl}_2$ , **1.114** (2 mol%), 150 °C, 50% of **1.116**; (c)  $\text{CH}_2\text{Cl}_2$ , **1.114** (5 mol%) rt, 18 h, 80% of **1.117**.

**Scheme 1.29.** Au(I)-catalysed enyne cyclisations to 6,6,5-tricyclic scaffolds.<sup>[39]</sup>

## 1.3.5 Biomimetic Synthesis of (–)-Pycnanthuquinone C\*

In order to explore the avenues of a synthesis based on the revised biosynthetic proposal described in Scheme 1.11 and to further extend the scope of the intramolecular VQDA reaction, a biomimetic total synthesis of pycnanthuquinone C was devised.

The total synthesis started with a HECK-type coupling reaction between bromohydroquinone **1.118** and commercially available monoterpene alcohol (–)-linalool (**1.119**; Scheme 1.30). This reaction proceeded well under JEFFERY conditions to afford alkenyl hydroquinone **1.96** in 81% yield.<sup>[41,42]</sup> Remarkably, only one HECK reaction involving an unprotected *ortho*-halohydroquinone appears to have been reported previously in the literature.<sup>[42]</sup> Reactions of this type provide an excellent entry into vinyl quinones. Since the absolute configuration of pycnanthuquinone C was not known at the outset of this study, the more readily available enantiomer of linalool was chosen, which ultimately translated to the unnatural levorotatory enantiomer of pycnanthuquinone C.



Reagents and conditions: (a) Pd(OAc)<sub>2</sub> (5%), TBACl, K<sub>2</sub>CO<sub>3</sub>, DMF, 50 °C, 81% of **1.96**; (b) MnO<sub>2</sub>, CH<sub>2</sub>Cl<sub>2</sub>, 65% of **1.97**; (c) toluene/H<sub>2</sub>O, 60 °C, 21% of (–)-**1.18** and 16% of **1.120** over three steps; (d) citrate-phosphate buffer, RT, 8% of (–)-**1.18**.

**Scheme 1.30.** Synthesis of (–)-pycnanthuquinone C (**1.18**) via a biomimetic VQDA reaction.

\* Published in: F. Löbermann, P. Mayer, D. Trauner, *Angew. Chem. Int. Ed.* **2010**, *49*, 6199–202.

Oxidation of hydroquinone **1.96** with manganese dioxide gave the sensitive vinyl quinone **1.97** and set the stage for the key reaction of the synthesis: Heating of a solution of **1.97** in a biphasic toluene/water mixture to 60 °C gave pycnanthuquinone C as a 5:4 mixture with its epimer **1.120** in 37% yield (Scheme 1.30). This reaction presumably involves a highly diastereoselective intramolecular VQDA reaction to afford the putative isoquinone methide **1.121**. The reactive intermediate **1.121** is then attacked by water in a non-stereoselective fashion to yield hydroquinone **1.122**, which is subsequently oxidised to (–)-**1.18** and its diastereomer **1.120** under the biomimetic reaction conditions.

Synthetic (–)-pycnanthuquinone C (**1.18**) proved to be identical to the natural product in all respects with the notable exception of its optical rotation, which had the opposite sign and a higher absolute value. The relative, and thus absolute, configuration of its isomer **1.120** was elucidated by X-ray crystallography (Figure 1.14). This compound has not yet been isolated from natural sources but in light of the biosynthetic hypothesis (Scheme 1.25), and given the joint isolation of pycnanthuquinone A and B, it seems likely that **1.120** exists in nature as well. It may well prove to be another case of “natural product anticipation” through total synthesis,<sup>[43–45]</sup> in which case **1.120** should be called “pycnanthuquinone D”.

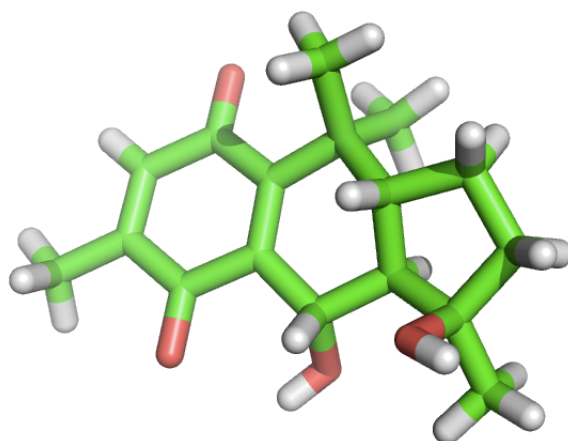
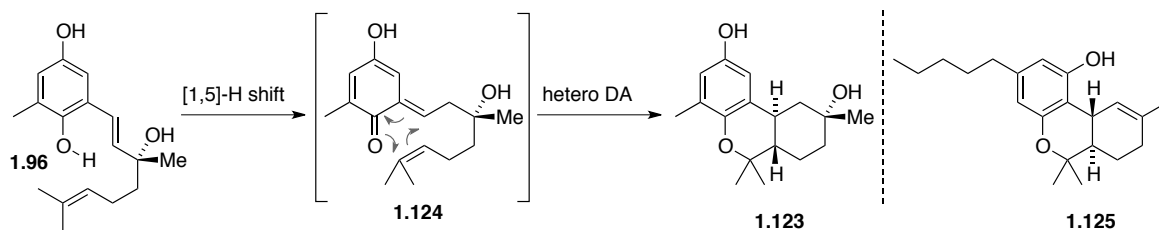


**Figure 1.14.** X-ray structure of “pycnanthuquinone D” (**1.120**).

Additionally, an interesting product was observed when a solution of vinyl hydroquinone **1.96** was concentrated on a rotary evaporator at elevated temperature: under such conditions, it isomerised to afford benzopyrane **1.123** as the only identifiable product (Scheme 1.31). This reaction presumably proceeds through an intramolecular 1,5-hydrogen shift to give intermediate **1.124**, followed by a highly diastereoselective intramolecular cycloaddition of the resultant *ortho*-quinone methide **1.124**.



**Scheme 1.31.** Formation of “cannabinoid” **1.123** from hydroquinone **1.96**.

Benzopyrane **1.123**, whose structure was confirmed by X-ray crystallography (Figure 1.15), bears a strong resemblance to  $\Delta^9$ -tetrahydrocannabinol ( $\Delta^9$ -THC) (**1.125**). Indeed domino reactions of this type have been used to synthesise cannabinoids, and those results could provide an asymmetric entry to this class of natural products.<sup>[43–45]</sup>

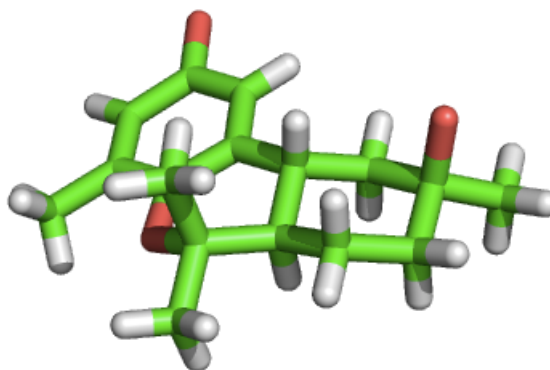


**Figure 1.15.** X-ray crystal structure of benzopyrane **1.125**.

Having developed a concise asymmetric synthesis of pycnanthuquinone C, the focus of attention was turned to the issue of the relative and absolute configuration of the natural product. Since the absolute configuration of (–)-linalool is known, it was possible to determine the absolute configuration of the synthetic material at carbon C-3. In addition, the structure of isomer **1.120** was established by X-ray crystallography, and the *trans*-configuration of the hydrindane moiety could be gleaned from the literature.<sup>[11,12]</sup> This left two possible isomers, compounds **1.126** and (–)-**1.18** (Figure 1.16). Compounds (–)-**1.18** and **1.120** would arise as a pair from a highly diastereoselective DA reaction and an unselective attack of water, whereas **1.120** and **1.126** would be formed through an unselective DA reaction and a highly diastereoselective addition of water. Given the relative configuration of pycnanthuquinones A (**1.16**) and B (**1.17**), the latter seemed unlikely, but could not be ruled out.

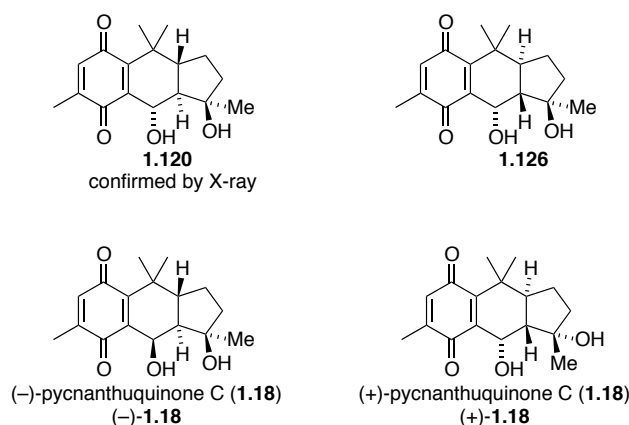


**Figure 1.16.** Elucidation of the relative and absolute configuration of pycnanthuquinone C.

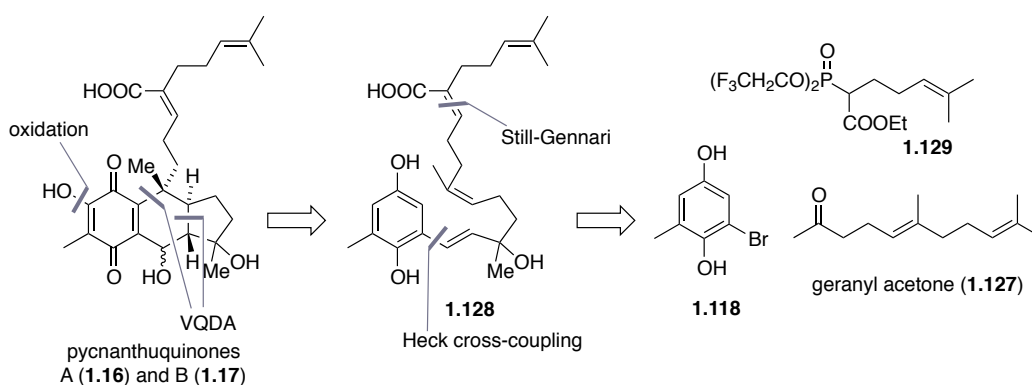
After several unsuccessful attempts to prove the relative configuration of pycnanthuquinone C through chemical derivatisation or interconversion, the efforts were focused on nOe measurements, which had reportedly given inconclusive results in the initial investigations.<sup>[11,12]</sup> However, with ample material at hand, nOe signals between the protons of both hydroxy groups and the methine hydrogen at C-6 in anhydrous DMSO-*d*<sub>6</sub> were observed. This is possible only if unnatural (–)-pycnanthuquinone C has the relative configuration indicated in Figure 1.8. Hence, the natural product (+)- pycnanthuquinone C has the all-*S* configuration. This total synthesis provides evidence that pycnanthuquinone C arises biosynthetically from its known congener **1.83** by means of epoxidation ( $\rightarrow$ **1.84**), followed by formation of the vinyl quinone ( $\rightarrow$ **1.97**), VQDA reaction, addition of water and aerobic reoxidation (Scheme 1.25). The fact that pycnanthuquinones A (**1.16**) and B (**1.17**) are diastereomers with respect to the secondary hydroxy group also supports this hypothesis, since an enzymatic hydroxylation would be expected to be highly diastereoselective.

In summary a three-step, protecting-group free synthesis of (–)-pycnanthuquinone C, which extends the reach of vinyl quinone Diels–Alder reactions was developed. It also provides strong evidence for the formation of the pycnanthuquinone skeleton through a biosynthetic cycloaddition and enabled the full elucidation of the stereochemistry of the natural product. The VQDA chemistry developed herein could be extended in a straightforward way towards the synthesis of pycnanthuquinones A and B as well as glaziovianol, which will be discussed in the next sections.

### 1.3.6 Towards the Biomimetic Synthesis of Pycnanthuquinones A and B

Having shown the effectiveness of the biomimetic VQDA reaction through the synthesis of pycnanthuquinone C, the goal was to extend the scope of this reaction to the construction of more complex systems. Hence, pycnanthuquinones A (**1.16**) and B (**1.17**) with five contiguous stereocenters, one of which is quaternary, were chosen as the target for total synthesis.

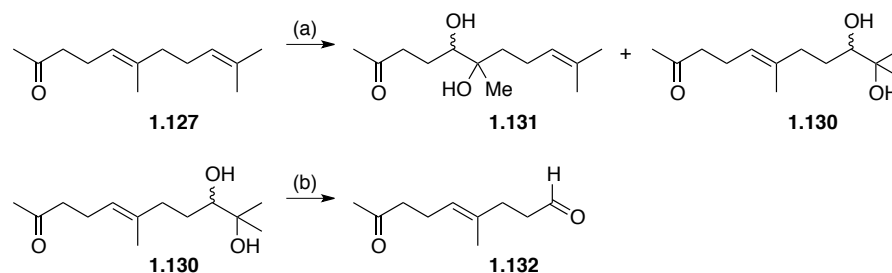
Retrosynthetic analysis (Scheme 1.32) was based on the proposed biosynthesis (Chapter 1.3.2), leading to simple starting materials, such as geranyl acetone (**1.127**) for the terpenoid side chain and literature-known bromo toluhydroquinone **1.118**.<sup>[46]</sup>



**Scheme 1.32.** Retrosynthetic analysis of pycnanthuquinones A (**1.16**) and B (**1.17**).

The synthesis of the side chain fragment commenced with the dihydroxylation of geranylacetone (**1.127**), which is commercially available as a mixture of *cis*- and *trans*-stereoisomers (Scheme 1.33). Treatment of **1.127** with  $K_2OsO_4$  and NMO resulted in the dihydroxylation of both, the internal and terminal double bond, yielding a mixture of the two regio-isomers **1.130** and **1.131**, which were easily separable by column chromatography.<sup>[47]</sup> At this stage it was also possible to separate the initial double bond isomers through HPLC to give pure diol **1.130**. Glycol cleavage with sodium periodate resulted in volatile aldehyde **1.132** (scheme 1.33).<sup>[48]</sup>

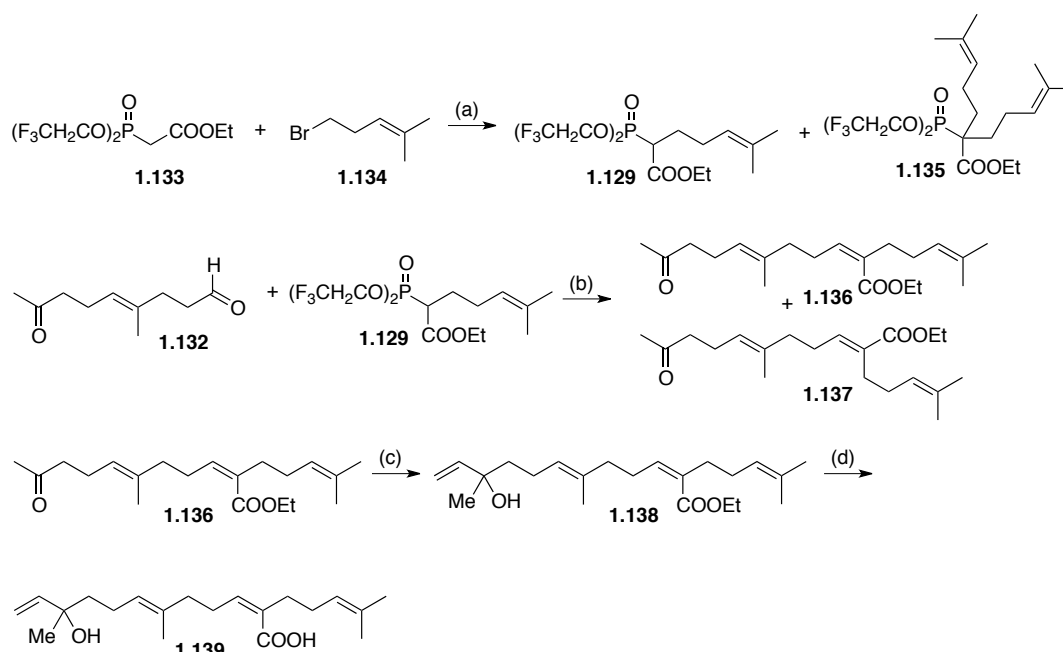
### 1.3. Application in the Total Synthesis of the Pycnanthuquinones



Reagents and conditions: (a)  $\text{K}_2\text{OsO}_4$  (mol 1%), NMO, acetone/ $\text{H}_2\text{O}$ , 29% of **1.131** and 35% of **1.130**; (b)  $\text{NaIO}_4$ , THF/ $\text{H}_2\text{O}$  99% of **1.132**.

**Scheme 1.33.** Synthesis of aldehyde **1.132**.

Alkylation of commercial phosphonate **1.133** with 5-bromo-2-methylpent-2-ene (**1.134**) gave desired phosphonate **1.129** and the doubly alkylated side product **1.135** (Scheme 1.34).<sup>[49]</sup> However, despite considerable optimisation efforts double alkylation was observed in all cases with relatively low overall yield for desired phosphonate **1.129**. When reacting aldehyde **1.132** with phosphonate **1.129** in the presence of KHMDS and 18-crown-6 ether under optimised conditions, a 1.3:1 ratio of a mixture of *Z/E* stereoisomers **1.136** and **1.137** was obtained. Moreover, employing an unfluorinated WITTIG-type phosphonate reagent in this reaction resulted in almost exclusive formation of the undesired *E*-isomer **1.137**. Addition of vinylmagnesium bromide to ketone **1.136** gave allylic alcohol **1.138**, which was saponified to carboxylic acid **1.139**.

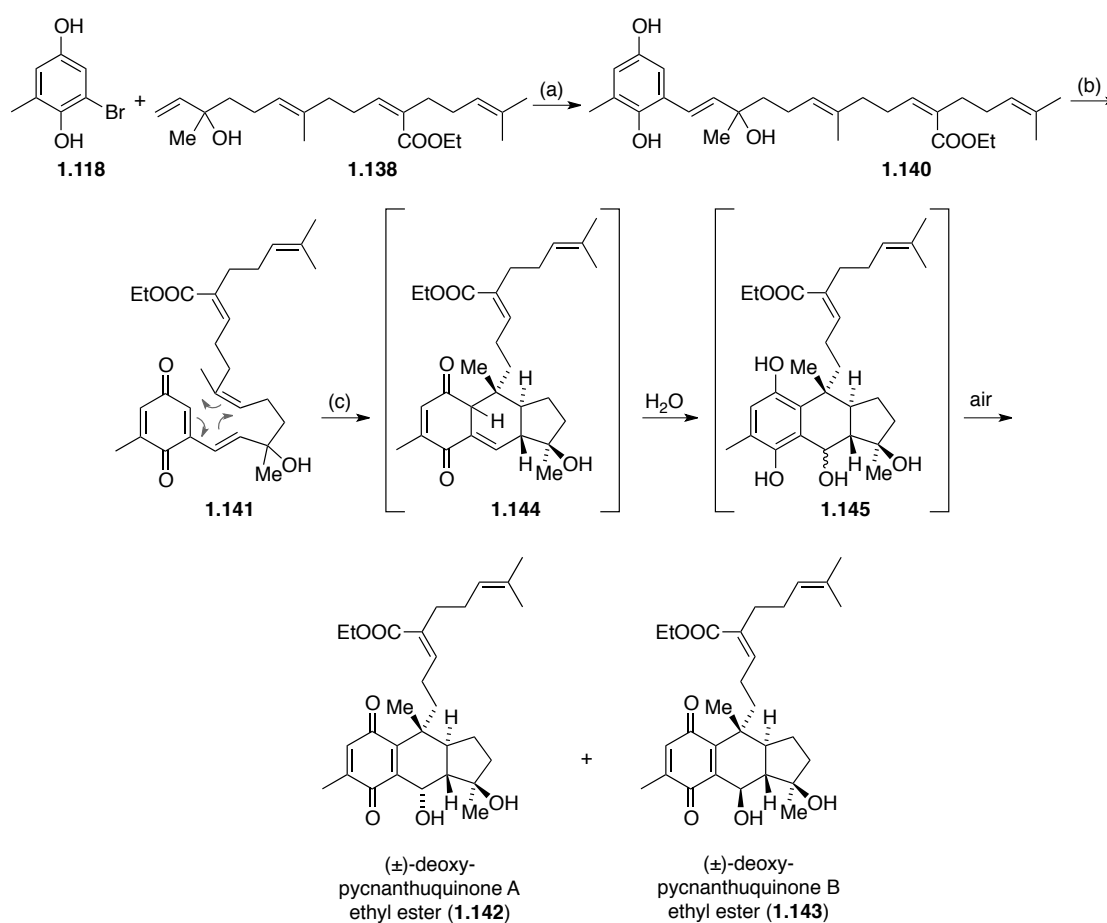


Reagents and conditions: (a) NaH, DMSO, 35% of **1.129** and 6% of **1.135**; (b) KHMDS, 18-crown-6, THF,  $-78\text{ }^\circ\text{C}$  to  $-10\text{ }^\circ\text{C}$ , 40% of **1.136** and 29% of **1.137**; (c) vinylmagnesium bromide, THF,  $0\text{ }^\circ\text{C}$ , 60% of **1.138**; (d) NaOH, THF,  $60\text{ }^\circ\text{C}$ , 83% of **1.139**.

**Scheme 1.34.** Synthesis of terpenoid side chain **1.139** for pycnanthuquinones A and B.



Subsequently, HECK coupling between allylic alcohol **1.138** and bromohydroquinone **1.118** under the conditions previously reported in the total synthesis of pycnanthuquinone C<sup>[16]</sup> yielded alkenyl hydroquinone **1.140** (Scheme 1.35). Oxidation with manganese dioxide gave highly sensitive vinyl quinone **1.141**, which was used as a substrate in the following VQDA reaction. When heating the quinone in a mixture of toluene and water to 60 °C, deoxy-pycnanthuquinone ethyl esters A (**1.142**) and B (**1.143**) were isolated as a 1:1 mixture, which was separable by HPLC.



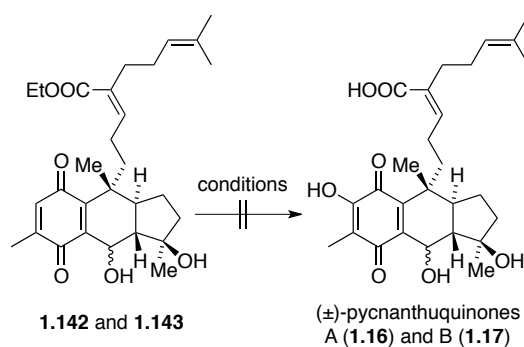
Reagents and conditions: (a) Pd(OAc)<sub>2</sub> (5%), TBACl, K<sub>2</sub>CO<sub>3</sub>, DMF, 50 °C, 81% of **1.140**; (b) MnO<sub>2</sub>, CH<sub>2</sub>Cl<sub>2</sub>, 51% of **1.141**; (c) toluene/H<sub>2</sub>O, 60 °C, 18% of (±)-**1.142** and 19% of (±)-**1.143** over three steps.

**Scheme 1.35.** Biomimetic synthesis of (±)-deoxy-pycnanthuquinone ethyl esters A and B.

This cascade reaction presumably proceeds analogously to that described for the synthesis of pycnanthuquinone C.<sup>[16]</sup> It supposedly commences with a diastereoselective intramolecular VQDA reaction yielding alleged isoquinone methide intermediate **1.144**, which then is immediately attacked in a non-stereoselective fashion by water to give hydroquinone **1.145** as a mixture of diastereoisomers. This relatively electron-rich quinol is subsequently oxidised by air to deoxy-pycnanthuquinone ethyl esters A (**1.142**) and

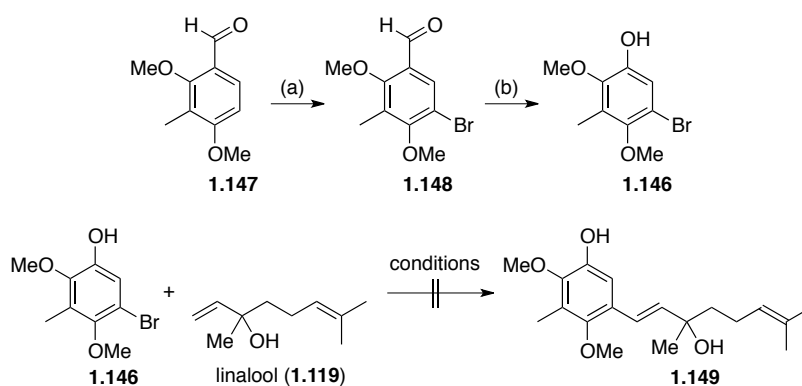
B (**1.143**), which already closely resemble the natural products.

It was then attempted to introduce the hydroxy functionality at the quinone core, followed by *in situ* saponification of the ethyl ester, to finally furnish both natural products (Scheme 1.36). At first sight, this might seem like a relatively simple transformation, because only one position is available for the hydroxylation of the quinone. However, compounds **1.142** and **1.143** are both very sensitive to light, heat, acid, base and temperatures above 30 °C, which immediately rules out a manifold of conditions. Even at lower temperatures or very short reaction times only decomposition was observed when subjecting **1.142** and **1.143** to various literature known procedures for the hydroxylation of quinones, such as ferric sulphate,<sup>[50]</sup> potassium superoxide<sup>[51]</sup> or *tert*-butyl hydroperoxide.<sup>[52]</sup>



**Scheme 1.36.** Attempted late-stage hydroxylation of **1.142** and **1.143** to  $(\pm)$ -pycnanthuquinones A (**1.16**) and B (**1.17**).

As the late stage-hydroxylation strategy failed due to instability of the substrate, the introduction of the hydroxy functionality at an earlier stage was pursued (Scheme 1.37).



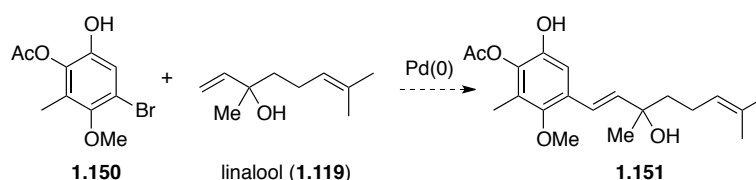
Reagents and conditions: (a) Br<sub>2</sub>, NaOAc, AcOH, 88% of **1.148**; (b) *m*CPBA, CH<sub>2</sub>Cl<sub>2</sub>, then KOH, MeOH, 58% of **1.146**.

**Scheme 1.37.** Early-stage hydroxylation strategy.

Brominated trihydroxybenzene **1.146** was synthesised starting from 2,4-dimethoxy-3-methylbenzaldehyde (**1.147**), which brominated in the first step to give compound **1.148**. Bromide **1.148** was then treated with *m*CPBA, followed by KOH in MeOH to give 5-bromo-2,4-dimethoxy-3-methylphenol (**1.146**) (Scheme 1.37).

With bromohydroquinone **1.146** in hand, linalool (**1.119**) was chosen as the coupling partner to investigate the reactivity of this electron-rich aromatic bromide in a HECK reaction. However, it was not possible to achieve a palladium-catalysed coupling reaction between **1.146** and linalool (**1.119**) under a broad variety of ligand-free conditions, such as those reported by JEFFERY (scheme 1.37).<sup>[41,42]</sup> Presumably oxidative addition of Pd(0) into the carbon-halogen bond is not possible in this very electron-rich system. Hence pycnanthuquinones A (**1.16**) and B (**1.17**) were not yet obtained.

In summary a bioinspired synthesis of the ( $\pm$ )-deoxy-pycnanthuquinone ethyl esters A and B has been developed, which showcases the versatility of the VQDA reaction even in very complex substrates. To achieve the synthesis of pycnanthuquinones A and B, the early-stage hydroxylation strategy should be pursued. Since the HECK coupling presumably failed due to the electron rich coupling partner, the introduction of electron withdrawing substituents could enable such a coupling reaction. An acetyl protecting-group, instead of a methoxy-ether could achieve the required electronics at the aryl ring (Scheme 1.38).



**Scheme 1.38.** Suggested HECK coupling partner with the right substitution-pattern and electronics.

## 1.4 Towards the Bioinspired Total Synthesis of Glaziovianol

### 1.4.1 Introduction

The cordiachromes (**1.152–1.160**) are an interesting class of meroterpenoids that have been isolated either in the quinone or quinol form (Figure 1.17) They all feature a hydroanthracene skeleton and some of them exhibit unusual oxidation patterns.<sup>[13,53–57]</sup>

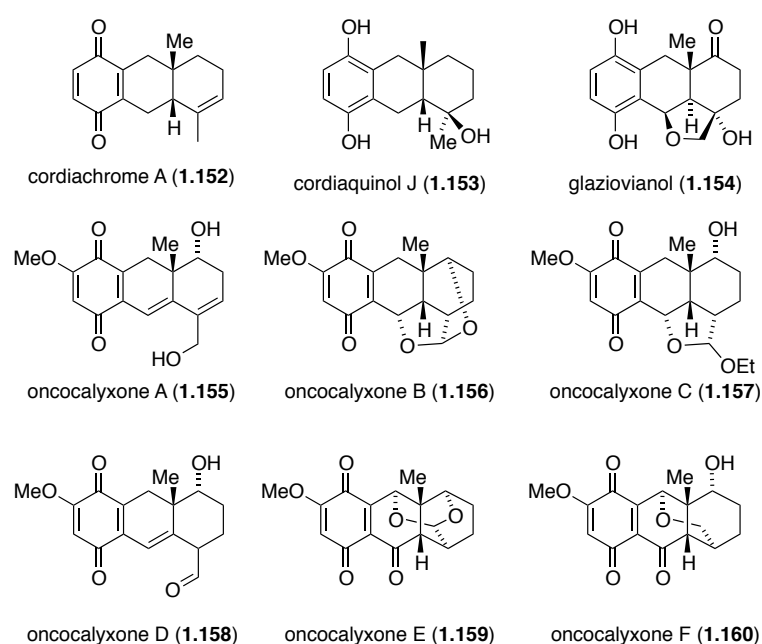


**Figure 1.17.** Examples demonstrating the structural diversity of the cordiachromes.

No asymmetric access to this class of natural products has been reported to this date. The cordiachromes almost exclusively possess a *cis*-fused decalin system; one remarkable exception being glaziovianol (**1.154**), which is a cordiaquinol with a *trans*-fused decalin. It was isolated from the trunk heartwood of *Auxemma glazioviana* Taub., a tree endemic in the region of north-eastern Brazil.<sup>[13]</sup> The wood of this tree is resistant to fungi and termite attacks, and thus often used in civil construction. Additionally, in folk medicine cuts and wounds are treated with the trunk bark.<sup>[58]</sup> The intriguing tetracyclic structure of glaziovianol includes four contiguous stereocenters (Figure 1.18), one of which is quaternary, thus rendering it a challenging target for total synthesis. Until now no data regarding the biological activity of glaziovianol (**1.154**) has been published.

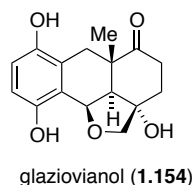


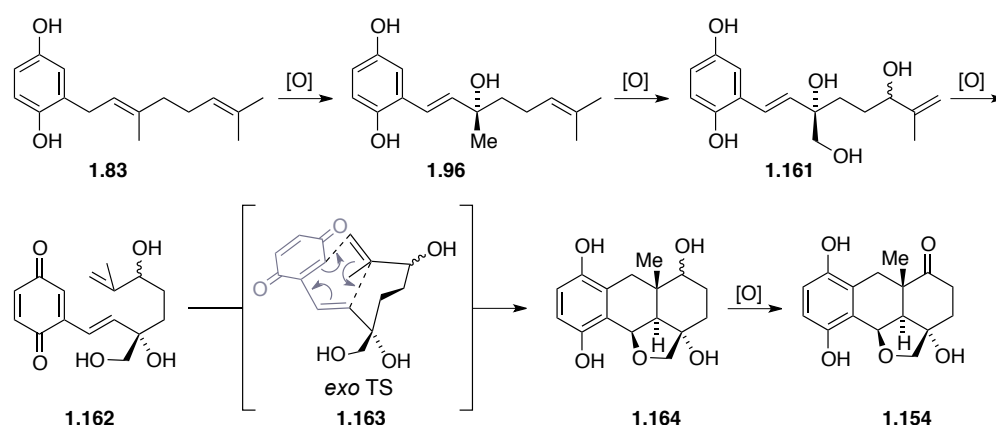
**Figure 1.18.** Image of the tree *Auxemma Glazioviana* Taub. and the structure of glaziovianol (1.154).\*

### 1.4.2 Proposed Biosynthetic Pathway for Glaziovianol

When LEMOS *et al.* reported the isolation of glaziovianol, they did not speculate about the biogenesis.<sup>[13]</sup> However, in analogy to the biosynthesis of the pycnanthuquinone C (see Chapter 1.3.2, Scheme 1.25) hydroquinone **1.83** is a likely biosynthetic precursor for the cordiachromes.

Thus, the following biosynthetic proposal can be formulated (Scheme 1.39). Epoxidation of **1.83**, followed by epoxide opening gives hydroquinone **1.96**, which is a natural product itself. It has been isolated from the root bark of *Cordia Alliodora*,<sup>[59]</sup> a common source for several cordiachromes.<sup>[60]</sup> Further oxidation of **1.96** is followed by an ALDER-ene reaction with singlet oxygen to give **1.161**. Oxidation to the corresponding VQDA precursor **1.162** sets the stage for a [4+2] cycloaddition proceeding through *exo*-transition state **1.163** gives a tricyclic isoquinone methide, which is then transformed into the natural product by intramolecular conjugate addition of the primary alcohol to **1.164**, followed by oxidation of the secondary alcohol.

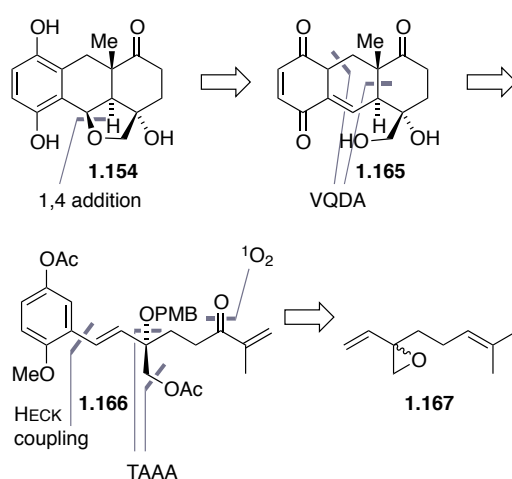
\*Image by Banco de Dados de Plantas do Nordeste, Brazil; <http://www.cnip.org.br/bdnp/>. Accessed on Monday, 28 January, 2013.



**Scheme 1.39.** Biosynthetic proposal for the formation of glaziovianol (**1.154**).

### 1.4.3 Synthesis of *Iso*-Glaziovianol\*

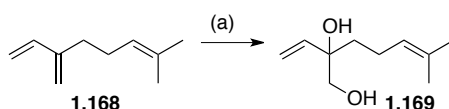
The retrosynthetic analysis of glaziovianol (**1.154**) (Scheme 1.40) commences with the disconnection of the tetrahydrofuran ring at the benzylic position, resulting in isoquinone methide **1.165**. Intermediate **1.165** bears the retron of an intramolecular vinyl quinone DIELS-ALDER (VQDA) reaction with neutral electron demand, leading back to alkenyl hydroquinone **1.166**. The enone functionality in **1.167** can be introduced through a singlet oxygen ene reaction in the side chain, while the tertiary allylic alcohol would be introduced *via* a Pd-catalysed enantioselective opening of vinyl epoxide **1.168**, followed by joining the side chain with the aromatic moiety through a HECK-type coupling reaction.



**Scheme 1.40.** Retrosynthetic analysis of glaziovianol (**1.154**).

\* The experimental work in this chapter was performed together with M. ILG and L. WEISHEIT; undergraduate researchers in the Trauner laboratory supervised by F. L.

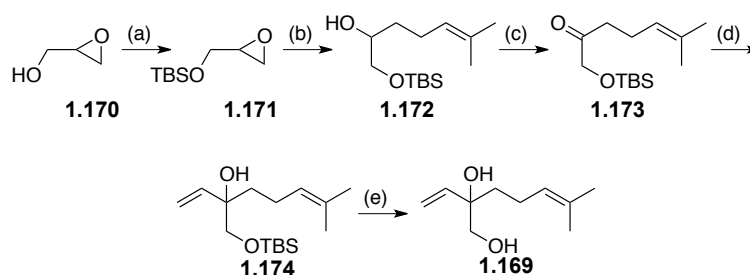
The preparation of myrcene epoxide (**1.167**) (Scheme 1.41) has been reported by FAUCHET *et al.* starting with the dihydroxylation from myrcene (**1.168**).<sup>[61]</sup> While this procedure would provide access to diol **1.169** in only one step, it was not possible to reproduce the reported yield and purification of the product proved to be a major issue. Additionally scale-up of this selective dihydroxylation procedure to multiple gram scale resulted in significantly reduced yields.



Reagents and conditions: (a)  $\text{BnBu}_3\text{NCl}$ ,  $\text{KMnO}_4$ ,  $\text{CH}_2\text{Cl}_2$ , 16% of **1.169** (Lit. 25%).<sup>[61]</sup>

**Scheme 1.41.** Synthesis of dihydroxymyrcene (**1.169**).

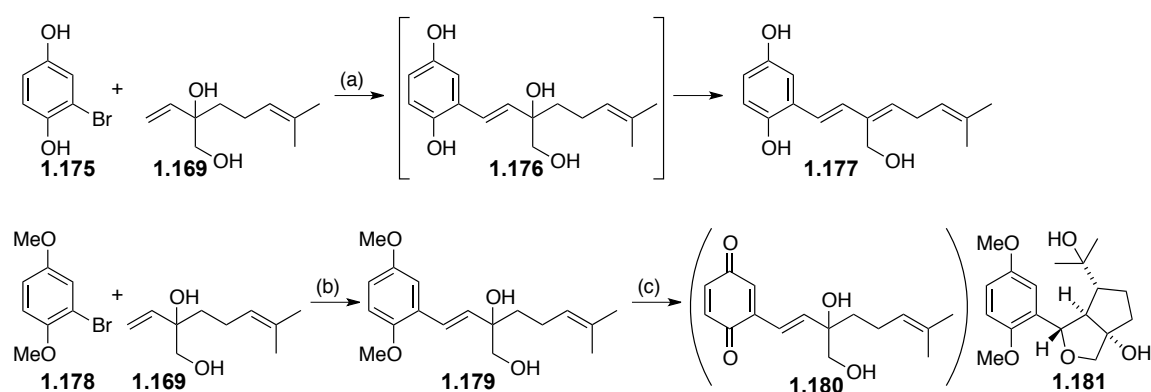
Since diol **1.169** could not be easily obtained in larger quantities using the literature-known synthetic procedure, an alternative route was devised (Scheme 1.42). The synthesis commenced with the TBS protection of glycidol (**1.170**). The epoxide **1.171** was then opened by addition of a cuprate formed from prenylmagnesium chloride.<sup>[62]</sup> Oxidation of the thus obtained alcohol **1.172** through SWERN oxidation resulted in ketone **1.173**, which was then reacted with vinylmagnesium bromide to furnish allylic alcohol **1.174**. The protecting group was then removed through treatment with TBAF, giving rise to dihydroxymyrcene (**1.169**). Although this reaction sequence is longer, the product was obtained in significantly higher over all yield, 77% over five steps compared to 15% for the shorter pathway.



Reagents and conditions: (a) TBSCl, imidazole, THF, 95% of **1.171**; (b) prenyl magnesium chloride,  $\text{CuI}$ , THF, 99% of **1.172**; (c) oxalyl chloride, DMSO,  $\text{NEt}_3$ , 99% of **1.173**; (d) vinyl magnesium chloride, THF, 98% of **1.174**; (e) TBAF, THF, 84% of **1.169**.

**Scheme 1.42.** Revised synthesis of dihydroxymyrcene (**1.169**).

The development of a robust synthesis for myrcenediol opened up the possibility to explore the synthetic pathway towards glaziovianol. HECK coupling between bromo hydroquinone (**1.175**) and **1.169** under the conditions reported by JEFFERY<sup>[41]</sup> did not result in isolation of anticipated alkenyl hydroquinone **1.176** but instead the corresponding elimination product **1.177** in good yield (Scheme 1.43). Protection of the phenolic hydroxy-groups as methoxy ethers **1.178**, resulted in the desired HECK product **1.179**. This result suggests that the tertiary allylic alcohol is sensitive to even weak acids, such as phenols. Indeed, oxidation hydroquinone methyl ether (**1.179**) with slightly acidic reagents like CAN without complete decomposition of the starting material. Hence, it was then attempted to obtain the corresponding quinone **1.180** under mild and non-acidic conditions. When employing neutral single electron transfer reagents such as DDQ or buffered CAN, clean conversion to one single product was observed. However, the formation of **1.180** was not observed; instead only the formation of tricyclic compound **1.181** was obtained in good yield.



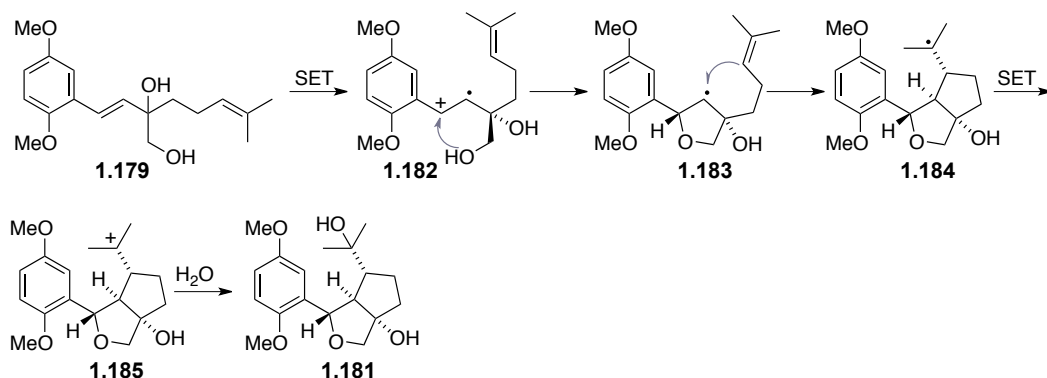
Reagents and conditions: (a) Pd(OAc)<sub>2</sub> (10%), TBACl, NaHCO<sub>3</sub>, DMF, 100 °C, 75% of **1.177**; (b) PdCl<sub>2</sub>(PPh<sub>3</sub>)<sub>2</sub> (10%), dppp (20%), NaHCO<sub>3</sub>, DMF, 60% of **1.179**; (c) DDQ, CH<sub>2</sub>Cl<sub>2</sub>/H<sub>2</sub>O, 55% of **1.181**.

**Scheme 1.43.** Studies on the HECK coupling of the dihydroxylated side chain **1.169**.

The formation of this unexpected side product can be explained with an oxidative radical cyclisation cascade, as suggested in Scheme 1.44.<sup>[63–65]</sup> In the first step, a single electron transfer (SET) reagent (e.g. DDQ) abstracts an electron from the electron-rich vinyl hydroquinone methyl ether **1.179**. The thus obtained positively charged radical **1.182**, which is stabilised through mesomeric effects, can be localised in the benzylic position, where it is intercepted through nucleophilic attack by the primary alcohol to give free radical intermediate **1.183**. This radical **1.183** then reacts with the substituted double bond, resulting in the formation of the *cis*-fused bicycle, giving a highly stabilised tertiary radical

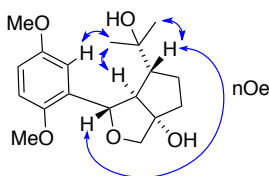


**1.184.** One further equivalent of oxidant abstracts another electron to give tertiary carbocation **1.185**, which is intercepted by a water molecule to furnish **1.181**. The formation of this compound suggests that the oxidation of protected vinyl hydroquinones to the corresponding vinyl quinone should be accomplished through an ionic pathway, to avoid this undesired side reactions.



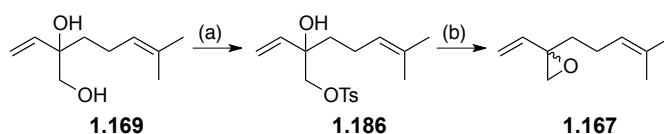
**Scheme 1.44.** Proposed mechanism for the oxidative radical cyclisation cascade reaction.

The relative configuration of **1.181** was determined by 2D NMR experiments. Key NOESY signals are shown in Figure 1.19.



**Scheme 1.19.** Relative configuration of **1.181** determined by NOESY analysis.

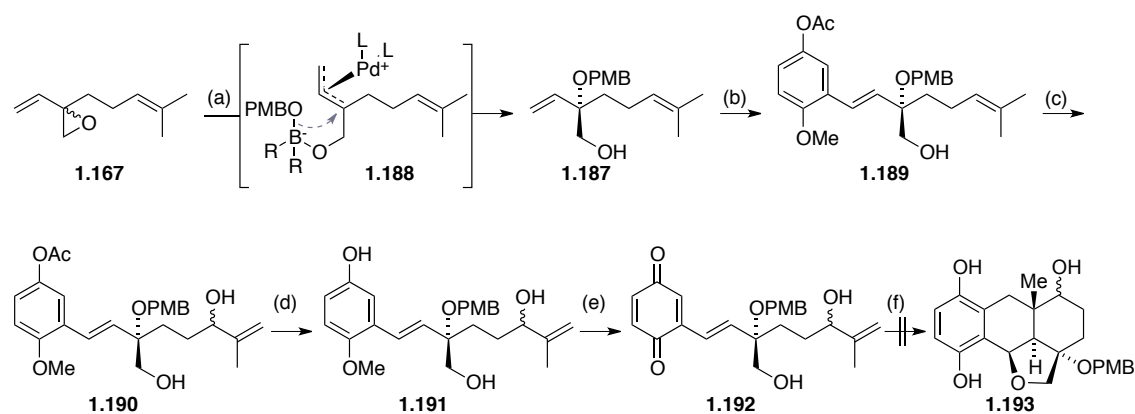
Next, focus was turned to the synthesis of an asymmetric version of dihydroxymyrce. Diol **1.169** was converted into tosylate **1.186** (Scheme 1.45). Conditions reported by FAUCHET did not result in formation of the desired epoxide **1.167** from tosylate **1.186** with high conversion.<sup>[61]</sup> Treatment of tosylate **1.186** with KOH in  $\text{Et}_2\text{O}$  yielded volatile, racemic epoxide **1.167** in excellent yield.



Reagents and conditions: (a) *p*-TosCl, pyridine, 75% of **1.186**; (b) KOH,  $\text{Et}_2\text{O}$ , 91% of **1.167**.

**Scheme 1.45.** Formation of myrcene epoxide (**1.167**).

Subjecting vinyl epoxide **1.167** to a palladium- and boron-cocatalysed asymmetric allylic alkylation (AAA) conditions as reported by TROST *et al.* resulted in allylic ether **1.187** in a highly regio- and enantioselective fashion (81% isolated yield, 93% ee) (Scheme 1.46).<sup>[66]</sup> This reaction presumably proceeds *via* transition state **1.188**, in which the alcohol nucleophile is delivered intramolecularly by a boronate complex. It is important for this reaction to rigorously degas all solvents and always prepare a fresh stock solution of Et<sub>3</sub>B, due to the high reactivity of Et<sub>3</sub>B with oxygen. Subsequently HECK arylation under optimised conditions gave protected vinyl hydroquinone **1.189** in 71% yield. However, reproducibility of this reaction proved to be capricious, because reaction vessels with scratched surfaces or fast stirring of the reaction mixture easily resulted in precipitation of palladium black. In such cases the reaction could be driven towards completion by slow addition of further catalyst. Continuous addition of a catalyst solution via a syringe pump over the course of the reaction did not affect the turnover in the desired fashion. Photosensitised singlet oxygen reaction of **1.189**, followed by reductive work-up gave allylic alcohol **1.190**. Saponification with K<sub>2</sub>CO<sub>3</sub> in methanol resulted in free phenol **1.191** in almost quantitative yield, followed by oxidation with (bis(trifluoroacetoxy)iodo)benzene (PIFA) to vinyl quinone **1.192**.<sup>[67]</sup> However, heating **1.192** in anhydrous toluene only resulted in decomposition of starting material.

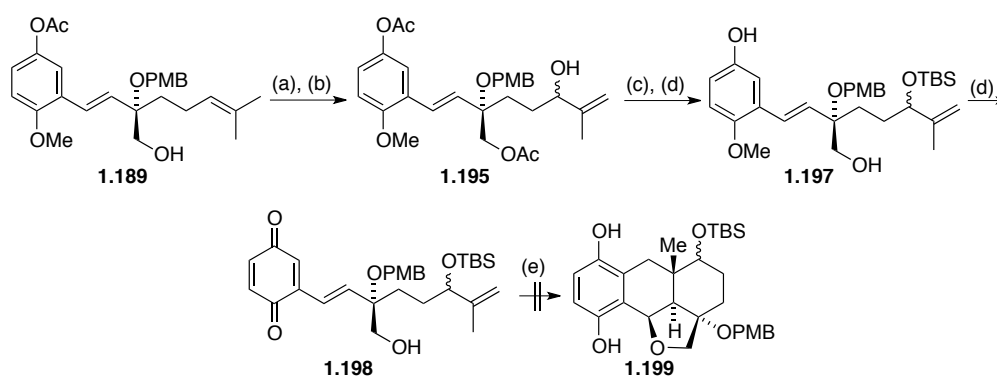


Reagents and conditions: (a) Pd<sub>2</sub>(dba)<sub>3</sub> (1 mol%), (*S,S*)-DACH-phenyl TROST ligand (3 mol%), Et<sub>3</sub>B (1 mol%), PMBOH, CH<sub>2</sub>Cl<sub>2</sub>, 81% of **1.187**, 93% ee; (b) 3-bromo-4-methoxyphenyl acetate, Pd(OAc)<sub>2</sub>, P(*o*-Tol)<sub>3</sub>, NEt<sub>3</sub>/toluene, 71% of **1.189**; (c) O<sub>2</sub>, TPP, UV lamp, CH<sub>2</sub>Cl<sub>2</sub>, then Me<sub>2</sub>S, 33% of **1.190**; (d) K<sub>2</sub>CO<sub>3</sub>, MeOH, 99% of **1.191**; (e) PIFA, THF/H<sub>2</sub>O, crude of **1.192**; (f) benzene, heat, decomposition.

**Scheme 1.46.** Attempted synthesis of glaziovianol (**1.154**).

In theory, the envisaged intramolecular inverse electron demand DA reaction between electron-poor diene and electron-rich dienophile should be electronically matched. However unprotected allylic alcohol in **1.192** could cause side reactions at elevated

temperatures, resulting in decomposition of the material. Hence, a TBS protected version was synthesised. Acetylation of primary alcohol **1.189** gave **1.194**, which was then subjected to photosensitised singlet oxygen reaction resulting in free allylic alcohol **1.195** upon reductive workup with DMS.<sup>[68]</sup> Protection of the allylic alcohol with TBSCl ( $\rightarrow$ **1.196**), followed by de-acetylation with  $K_2CO_3$  in methanol gave free phenol **1.197**, which was then oxidised to the corresponding sensitive vinyl quinone **1.198** by treatment with PIFA.<sup>[67]</sup> Again heating the VQDA cascade precursor in solvents such as toluene and EtOAc did not result in the formation of any cyclised product, but decomposition of starting material (Scheme 1.47).



Reagents and conditions: (a)  $Ac_2O$ , DMAP, pyridine,  $CH_2Cl_2$ , 99% of **1.194**; (b)  $O_2$ , TPP, UV lamp,  $CH_2Cl_2$ , then  $Me_2S$ , 32% of **1.195**; (c) TBSCl, imidazole, DMAP,  $CH_2Cl_2$ , 99% of **1.196**; (d)  $K_2CO_3$ , MeOH, 99% of **1.197**; (e) PIFA, THF/ $H_2O$ , crude of **1.198**; (f) benzene, heat, decomposition.

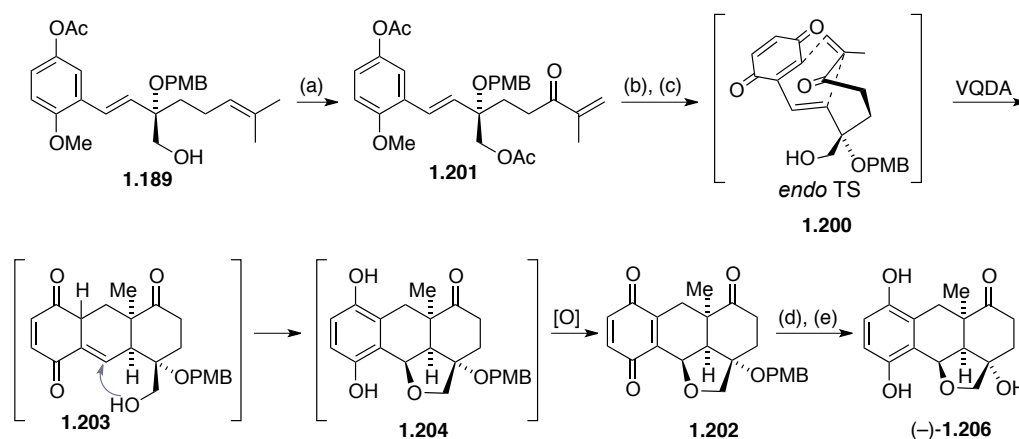
**Scheme 1.47.** Attempted synthesis of glaziopianol (**1.154**) via TBS protected VQDA precursor **1.198**.

Vinyl quinones are known to dimerise through DA reactions with neutral electron demand,<sup>[4]</sup> it was hence attempted to achieve such a neutral electron demand VQDA reaction intramolecularly. Introduction of an enone as the dienophile would render both, the diene and the dienophile electron poor. The synthesis VQDA precursor **1.200** started with a TPP-sensitized singlet oxygen ene reaction of compound **1.189** (Scheme 1.48). This ene-reaction initially resulted in an allylhydroperoxide, which was acetylated *in situ* and then formally dehydrated to the corresponding  $\alpha,\beta$ -unsaturated ketone **1.201** by elimination of acetic acid.<sup>[69]</sup>

Removal of the acetyl protecting groups under ZEMPLÉN deacetylation conditions lead to a complex, dynamic mixture of the free alcohol and intramolecular diastereomeric acetals, which was impossible to fully characterise. Oxidation of this mixture with PIFA to quinone **1.200**,<sup>[67]</sup> triggered the key cascade reaction of this synthesis: Work-up of the oxidation reaction resulted in the isolation of tetracyclic quinone **1.202** in 39% yield (Scheme 1.48).

This cascade reaction presumably involves a highly diastereoselective intramolecular VQDA reaction proceeding with neutral electron demand through an *endo*-transition state, resulting in putative *cis*-fused isoquinone methide **1.203**. This reactive intermediate is then intercepted intramolecularly by the primary alcohol giving rise to the tetracyclic ringsystem **1.204**. However, this reaction has only been performed on very small scale and presumably needs further optimisation to be carried out on larger scale (e.g. screening of different oxidants). This is the first example of an intramolecular VQDA reaction with neutral electron demand is at the same time the first intramolecular interception of an isoquinone methide generated through a VQDA reaction. The resulting hydroquinone **1.204** is subsequently oxidised to quinone **1.202** by the reaction conditions.

Oxidative cleavage of the PMB-protecting group with DDQ furnished **1.205** in 87% yield.<sup>[70]</sup> Stirring this quinone in a solution of sodium dithionite in acetone/water at 0 °C finally resulted in (–)-*iso*-glaziovianol (**1.206**) in good yield.<sup>[71]</sup>



Reagents and conditions: (a) Ac<sub>2</sub>O, DMAP, pyridine, CH<sub>2</sub>Cl<sub>2</sub>, then O<sub>2</sub>, TPP, UV lamp, then Me<sub>2</sub>S, 32% of **1.201**; (b) K<sub>2</sub>CO<sub>3</sub>, MeOH, 99% of **1.207**; (c) PIFA, THF/H<sub>2</sub>O, 39% of **1.202**; (d) DDQ, CH<sub>2</sub>Cl<sub>2</sub>/H<sub>2</sub>O, 67% of **1.205**; (e) Na<sub>2</sub>S<sub>2</sub>O<sub>4</sub>, acetone/H<sub>2</sub>O, 0 °C, 92% of **1.206**.

**Scheme 1.48.** Synthesis of *iso*-glaziovianol (**1.206**).

The *cis*-decalin junction along with the relative configuration of (–)-**1.206** was elucidated through nOe measurements. NOESY signals between the methine protons at C1 and C2, as well as signals between C2 and the tertiary methyl group (Figure 1.19), were observed.

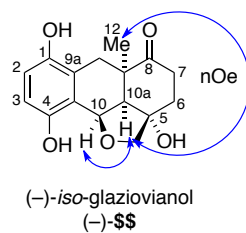


**Figure 1.19.** Relative configuration of *iso*-glaziovianol (**1.206**).

Comparison of the  $^{13}\text{C}$  NMR spectrum of *iso*-glaziovianol **1.206** with that of the natural product **1.154** shows that the carbon atoms in direct vicinity of the decalin junction exhibit the greatest deviation in chemical shift (Figure 1.20). The methyl group C-12 at the *cis*-decalin junction of *iso*-glaziovianol is shifted almost 6 ppm downfield in comparison to that of glaziovianol in a *trans*-junction. The downfield shift is due to the larger ring-strain of *cis*-decalins. The chemical shifts observed for all other carbons are very similar in both molecules.

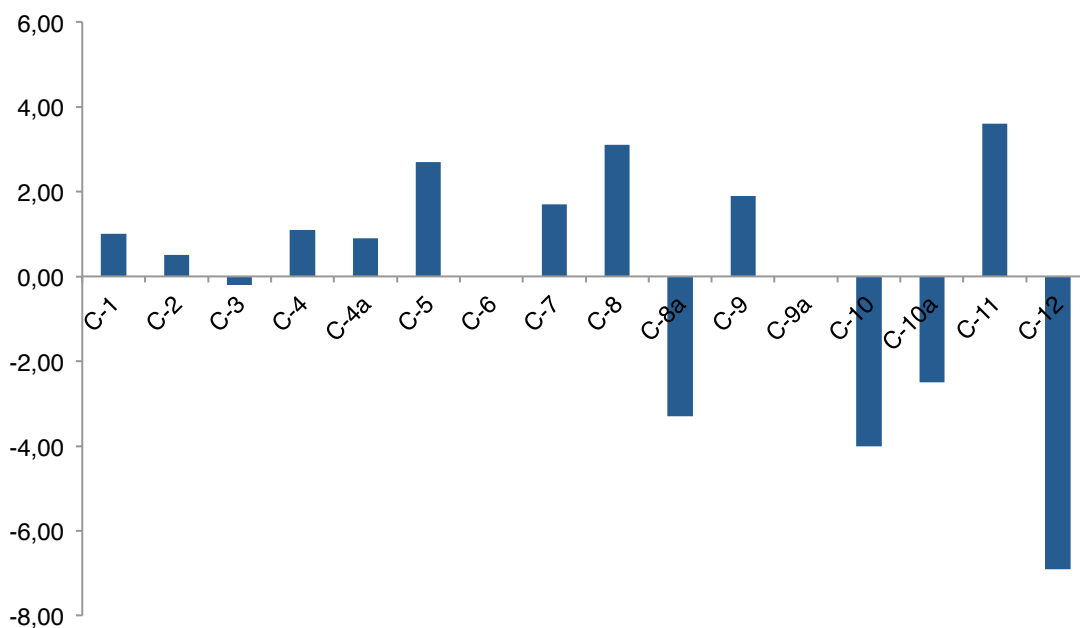
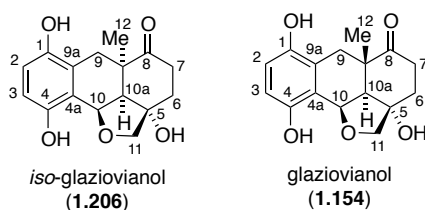


**Figure 1.20.** Difference of chemical shifts in the  $^{13}\text{C}$  spectra of *iso*-glaziovianol (**1.206**) and glaziovianol (**1.154**). Note: **1.206** was measured in acetone- $d_6$ ; **1.154** was measured in DMSO- $d_6$ .

In conclusion the first asymmetric synthesis of the cordiachromes skeleton was achieved, involving the efficient TROST asymmetric allylic alkylation of vinyl epoxide **1.167**. An intramolecular VQDA cascade reaction, involving the intramolecular interception of an isoquinone methide, constructed the tetracyclic core. This reaction sequence proceeded through an *endo* DA transition-state, giving rise to *iso*-glaziovianol (**1.206**) with a *cis*-fused decalin system. Attempts to achieve an *exo* type transition state, which would result in a *trans*-decalin, proved to be unsuccessful. Since all other cordiachromes that have been described in literature thus far exhibit a *cis*-fused decalin, this chemistry might be applied in a straight forward fashion towards the synthesis of complex cordiachromes such as oncocalyxone A (**1.155**).<sup>[55]</sup>

## 1.5 Experimental Section

### 1.5.1 General Experimental Details

**Chemicals and chromatography.** Unless otherwise noted, all reagents were purchased from commercial suppliers and used without further purification. Unless otherwise noted, all reaction mixtures were magnetically stirred in oven-dried glassware under a blanket of argon. External bath temperatures were used to record all reaction mixture temperatures. Analytical thin layer chromatography (TLC) was carried out on Merck silica gel 60 F<sub>254</sub> TLC plates. TLC visualisation was accomplished using 254 nm UV light or charring solutions of KMnO<sub>4</sub> and ceric ammonium molybdenate. All organic extracts were washed with brine, dried over sodium sulfate and filtered; solvents were then removed with a rotary evaporator at aspirator pressure. Flash chromatography was performed on Merck KGaA Geduran<sup>®</sup> Silica Gel (40–63 μm particle size) using a forced flow of eluent at 1.3–1.5 bar pressure. Yields refer to chromatographically and spectroscopically (<sup>1</sup>H NMR and <sup>13</sup>C NMR) homogenous material.

**NMR spectroscopy.** NMR spectra were recorded on Bruker AC 300, WH 400, or AMX 600 instruments (operating at 300 MHz, 400 MHz and 600 MHz for proton nuclei and 75 MHz, 100 MHz, 150 MHz for carbon nuclei, respectively). Chemical shifts are reported in ppm with the solvent resonance employed as the internal standard (CDCl<sub>3</sub> at 7.26 and 77.0 ppm; DMSO at 2.50 and 39.5 ppm). Additionally to standard <sup>1</sup>H and <sup>13</sup>C NMR measurements, 2D NMR techniques such as homonuclear correlation spectroscopy (COSY), heteronuclear single quantum coherence (HSQC) and heteronuclear multiple bond coherence (HMBC) was used to assign signals. The following abbreviations are used to explain the multiplicities: s = singlet, d = doublet, t = triplet, q = quartet, m = multiplet, br = broad.

**IR spectroscopy.** IR spectra were recorded 4000–400 cm<sup>-1</sup> on a Perkin Elmer Spectrometer BY FT-IR-System with a Smith Dura sample IR II ATR-unit. Samples were measured as neat materials (ATR). The absorption bands are reported in wave numbers (cm<sup>-1</sup>).

**Mass spectroscopy.** Mass spectra were recorded on a Varian MAT CH 7A for electron impact ionisation (EI) and high-resolution mass spectra (HRMS) on a Varian MAT 711 spectrometer.

**Chiral HPLC.** Chiral HPLC spectra were recorded on a high performance liquid chromatography (HPLC) system from the Shimadzu 20A series (DGU-20A3R degasser, LC-20AD Binary Pump VL, SIL-20AHT auto sampler, CTO-20A thermostatted column compartment, SPD-M20A DAD diode array detector), which was computer controlled through Shimadzu LabSolutions Software (Version 5.42 SP5). Enantiomeric excess (ee) was calculated by using the following equation;  $m_1$  refers to the integral of the major peak and  $m_2$  to the integral of the minor peak:

$$ee = \frac{|m_1 - m_2|}{m_1 + m_2} \cdot 100\%$$

**Infrared spectroscopy (IR).** Infrared spectra (IR) were recorded on a Perkin Elmer Spectrum BX II (FTIR System) equipped with an attenuated total reflection (ATR) measuring unit. IR data is reported in frequency of absorption ( $\text{cm}^{-1}$ ). The IR bands are characterized as: w = weak, m = medium, s = strong, br = broad, or combinations thereof.

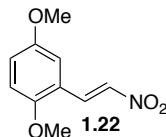
**Optical rotation.** Optical rotation values were recorded on a polarimeter. The specific rotation was calculated according to the following formula:

$$[\alpha]_{\lambda}^{\theta} = \frac{[\alpha] \times 100}{c \times d}$$

Wavelength  $\lambda$  is reported in nm and the measuring temperature  $\theta$  in  $^{\circ}\text{C}$ ;  $\alpha$  resembles the recorded optical rotation at the apparatus,  $c$  the concentration of the analyte in 10 mg/mL and  $d$  the length of the cuvette in dm. Thus, the specific rotation is given in  $10^{-1} \cdot \text{deg} \cdot \text{cm}^2 \cdot \text{g}^{-1}$ . Usage of the sodium D line ( $\lambda = 589 \text{ nm}$ ) is indicated by D instead of the wavelength in nm. The respective concentration as well as the solvent is reported in the relevant section of the experimental description.

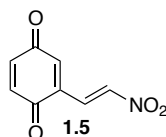


## 1.5.2 Method Development



**(E)-1,4-Dimethoxy-2-(2-nitrovinyl)benzene (1.22).** A solution of 2,5-dimethoxybenzaldehyde (**S1.1**, 33.2 g, 200 mmol, 1.0 *eq.*) and MeNO<sub>2</sub> (12.2 g, 200 mmol, 1.0 *eq.*) in MeCN (15 mL) was cooled to 5 °C internal temperature using an ice-bath. A solution of NaOH (8.80 g, 220 mmol, 1.1 *eq.*) in H<sub>2</sub>O (65 mL) was added drop wise at such a rate that the internal temperature did not rise above 20 °C. After stirring for 5 minutes, the reaction mixture was slowly poured into 5 N HCl (500 mL). The formed precipitate was washed with H<sub>2</sub>O (100 mL), filtered off, dissolved in acetone, dried over Na<sub>2</sub>SO<sub>4</sub> and concentrated *in vacuo*. Recrystallisation from *i*-PrOH/H<sub>2</sub>O yielded 26 g (62%) of **1.22** as bright orange needles.

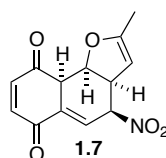
**Data for 1.22:** IR (ATR):  $\tilde{\nu}$  = 3104, 2839, 1618, 1489, 1422, 1348, 1295, 1250, 1220, 1184 cm<sup>-1</sup>; <sup>1</sup>H NMR (300 MHz, CDCl<sub>3</sub>):  $\delta$  = 8.10 (d, *J* = 6.9, 1H), 7.84 (d, *J* = 6.9, 1H), 7.00 (dd, *J* = 4.7, 1.7, 1H), 6.95 (d, *J* = 1.5, 1H), 6.89 (d, *J* = 4.4, 1H), 3.89 (s, 3H), 3.79 (s, 3H); <sup>13</sup>C NMR 75 MHz, CDCl<sub>3</sub>)  $\delta$  = 153.9, 151.5, 138.5, 135.2, 119.5, 119.1, 116.3, 112.4, 56.0, 55.8; HRMS (EI) calc. for C<sub>10</sub>H<sub>11</sub>NO<sub>4</sub> (M<sup>+</sup>): 209.0684; found: 209.0687.



**(E)-2-(2-Nitrovinyl)cyclohexa-2,5-diene-1,4-dione (1.5).** A solution of CAN (28.8 g, 52.3 mmol, 2.2 *eq.*) in MeCN/H<sub>2</sub>O (50 mL, 3:1) was poured into a solution of compound **1.22** (5 g, 23.9 mmol, 1.0 *eq.*) in MeCN (400 mL) under vigorous stirring. After 5 min the reaction mixture was diluted with brine (25 mL) and extracted with EtOAc (2 × 25 mL). The organic phases were combined and concentrated *in vacuo* down to ca. 5 ml of residual solvent (bath temperature below 30 °C). The resulting slurry was partitioned between CHCl<sub>3</sub> (125 mL) and H<sub>2</sub>O (50 mL) and the aqueous layer extracted with CHCl<sub>3</sub> (50 mL).

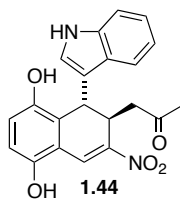
Combined organic phases were washed with H<sub>2</sub>O (25 mL), dried over Na<sub>2</sub>SO<sub>4</sub> and all volatiles removed *in vacuo*. The resulting brown solid was recrystallised from THF/cyclohexane twice to yield 2.35 g (55%) of vinyl quinone **1.5** as yellow needles.

**Data for 1.5:** IR (ATR):  $\tilde{\nu}$  = 3125, 3065, 2857, 1752, 1651, 1575, 1520, 1342, 1290, 1208, 1092 cm<sup>-1</sup>; <sup>1</sup>H NMR (300 MHz, CDCl<sub>3</sub>)  $\delta$  = 8.13 (d, *J* = 13.7, 1H), 7.65 (dd, *J* = 13.7, 0.8, 1H), 7.00 (m, 1H) 6.95-6.87 (m, 2H); <sup>13</sup>C NMR (75 MHz, CDCl<sub>3</sub>)  $\delta$  = 186.0, 184.8, 144.5, 137.9, 137.4, 136.8, 136.4, 130.1; HRMS (EI) calc. for C<sub>8</sub>H<sub>5</sub>NO<sub>4</sub> (M<sup>+</sup>): 179.0219; found: 179.0221.



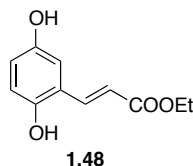
**(3a*S*,4*S*,9a*R*,9b*S*)-2-Methyl-4-nitro-3a,4-dihydronaphtho[1,2-*b*]furan-6,9(9a*H*,9b*H*)-dione (1.7).** Quinone **1.5** (0.50 g, 2.8 mmol, 1.0 *eq.*) was suspended in toluene (5 mL) and 2-methylfuran (**1.6**) (0.46 g, 5.6 mmol, 2.0 *eq.*) was added. After stirring for 16 h at ambient temperature, a yellow precipitate had formed. The solid was filtered off and washed with dry hexanes (3 mL). After drying 720 mg (98%) of title compound **1.7** were obtained as a pale yellow solid.

**Data for 1.7:** IR (ATR):  $\tilde{\nu}$  = 1739 (w), 1690 (s), 1668 (s), 1620 (s), 1600 (w), 1552 (vs), 1371 (s), 1345 (w), 1335 (w), 1303 (s) 1287 (s), 1258 (w), 1251 (w), 1206 (w), 1184 (s), 1126 (w), 1083 (s), 942 (vs); <sup>1</sup>H NMR (300 MHz, CDCl<sub>3</sub>)  $\delta$  = 7.66 (td, *J* = 2.9, 1.0, 1H), 7.03 – 6.88 (m, 2H), 5.66 (dd, *J* = 9.6, 3.4, 1H), 4.98 – 4.90 (m, 1H), 4.32 – 4.20 (m, 2H), 3.28 (dd, *J* = 5.3, 3.1, 1H), 1.62 (t, *J* = 1.4, 3H); <sup>13</sup>C NMR (75 MHz, CDCl<sub>3</sub>)  $\delta$  = 192.6, 181.8, 160.2, 142.5, 141.6, 133.6, 131.0, 92.9, 82.9, 79.7, 48.1, 47.6, 13.1; HRMS (EI) calc. for C<sub>13</sub>H<sub>11</sub>NO<sub>5</sub> (M<sup>+</sup>): 261.0637; found 261.0631.



**1-((1*S*,2*R*)-5,8-Dihydroxy-1-(1*H*-indol-3-yl)-3-nitro-1,2-dihydronaphthalen-2-yl)propan-2-one (1.44).** To a suspension of isoquinone methide **1.7** (63 mg, 0.24 mmol, 1.0 *eq.*) in anhydrous CH<sub>2</sub>Cl<sub>2</sub> (1 mL) was added indole (**1.33**) (56 mg, 0.48 mmol, 2.0 *eq.*) at rt. After stirring the reaction for 30 minutes, a bright red precipitate had formed. The solid was centrifuged off and washed with hexanes (1 mL). After drying under high vacuum, 40 mg (44%) of title compound **1.44** were obtained as red crystals.

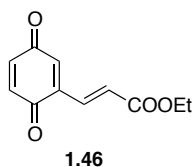
**Data for 1.44:** IR (ATR):  $\tilde{\nu}$  = 3364, 1685, 1618, 1482, 1458, 1356, 1330, 1309, 1245, 1158, 1100 cm<sup>-1</sup>; <sup>1</sup>H NMR (400 MHz, acetone-*d*<sub>6</sub>)  $\delta$  = 9.82 (s, 1H), 8.82 (s, 1H), 8.35 – 8.30 (m, 2H), 7.93 (s, 1H), 7.37 – 7.26 (m, 1H), 7.14 – 7.05 (m, 2H), 6.97 – 6.79 (m, 3H), 6.34 (d, *J* = 1.6, 1H), 4.23 (d, *J* = 9.3, 1H), 2.69 (dd, *J* = 17.7, 2.8, 1H), 2.22 (d, *J* = 7.7, 3H); <sup>13</sup>C NMR (100 MHz, acetone-*d*<sub>6</sub>)  $\delta$  = 206.2, 149.7, 148.2, 148.0, 137.1, 126.7, 126.5, 123.7, 122.5, 121.4, 121.1, 119.6, 118.7, 117.7, 115.7, 114.8, 111.3, 43.00, 35.1, 34.5, 29.6; HRMS (EI) calc. for C<sub>21</sub>H<sub>17</sub>N<sub>2</sub>O<sub>5</sub> (M–H<sup>+</sup>): 377.1143; found: 377.1144.



**Ethyl 3-(2,5-Dihydroxyphenyl)acrylate (1.48).** 2,5-dihydroxybenzaldehyde (**1.49**) (6.63 g, 48.0 mmol, 1.0 *eq.*) and ethyl 2-(triphenylphosphoranylidene)acetate (20.1 g, 57.6 mmol, 1.2 *eq.*) were dissolved in anhydrous toluene (250 mL) and heated to reflux for 3 h. After cooling to room temperature, the reaction mixture was washed with brine (2 × 100 mL). Combined organic phases were concentrated *in vacuo* and the resulting residue purified by silica gel chromatography (14% EtOAc in hexanes) to yield 8.3 g (83%) of title compound **1.48** as a colourless solid.

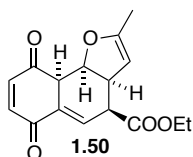
**Data for 1.48:** IR (ATR):  $\tilde{\nu}$  = 3360 (br), 1682 (vs), 1622 (w), 1523 (w), 1473 (w), 1456 (s), 1445 (w), 1373 (w), 1367 (w), 1284 (s), 1264 (w), 1156 (s), 1038 (vs), 864 (vs); <sup>1</sup>H NMR (400 MHz, DMSO-*d*<sub>6</sub>)  $\delta$  = 9.53 (s, 1H), 8.89 (s, 1H), 7.77 (d, *J* = 16.1, 1H), 6.89 (d, *J* = 2.7, 1H), 6.71 (d, *J* = 8.7, 1H), 6.67 (dd, *J* = 2.7, 8.7, 1H), 6.41 (d, *J* = 16.1, 1H), 4.14

(q,  $J = 7.1$ , 2H), 1.22 (t,  $J = 7.1$ , 3H);  $^{13}\text{C}$  NMR (100 MHz,  $\text{DSMO}-d_6$ )  $\delta = 167.06, 150.34, 150.11, 140.49, 121.26, 119.74, 117.40, 117.18, 113.85, 60.21, 14.68$ ; HRMS (ESI) calcd for:  $\text{C}_{11}\text{H}_{11}\text{O}_4$  ( $\text{M}-\text{H}^+$ ): 207.0663; found: 207.0665.

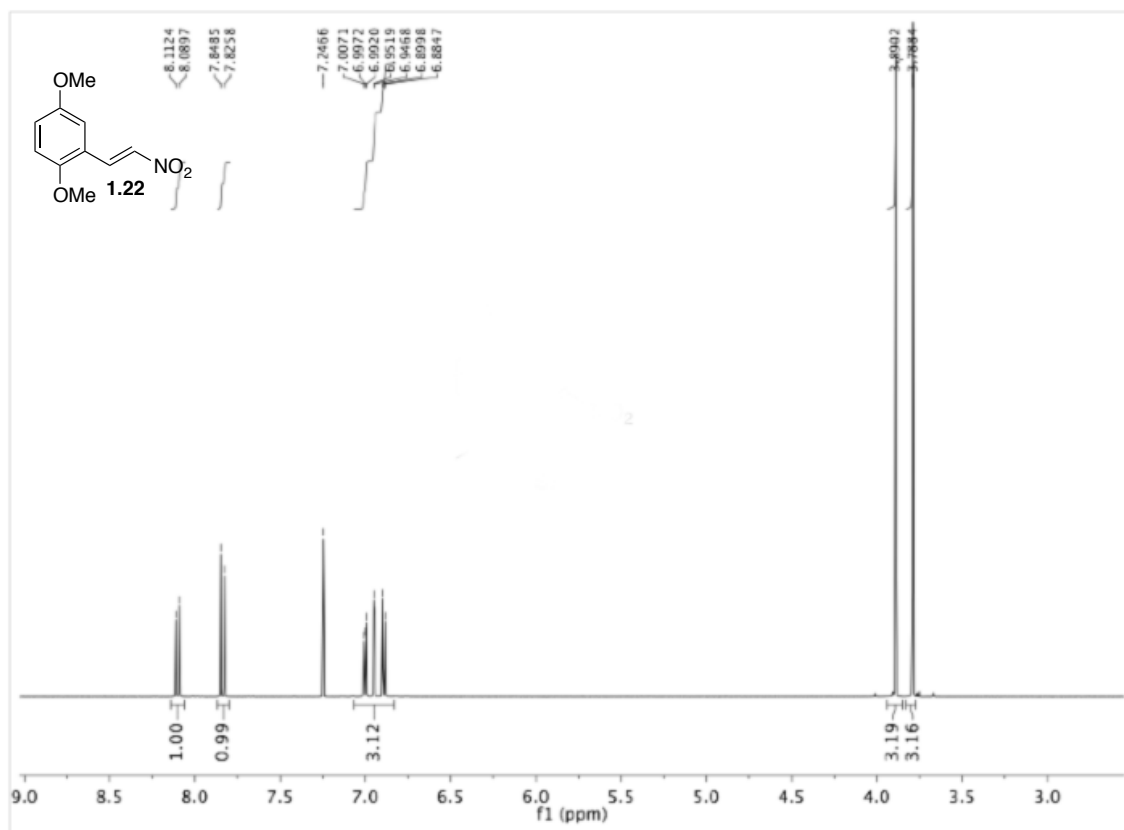
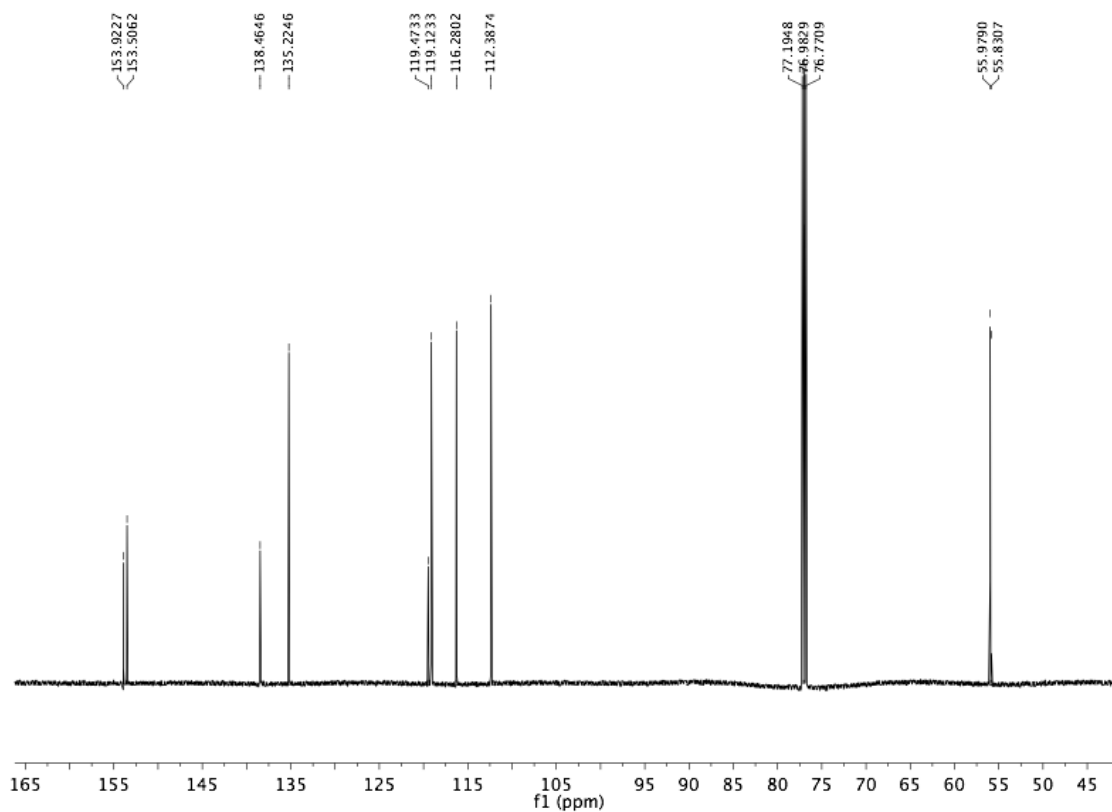


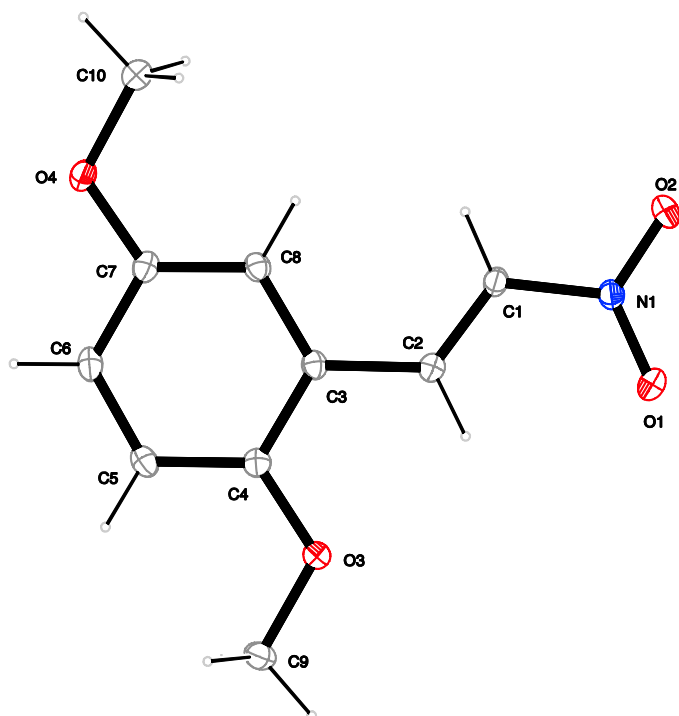
**(E)-Ethyl 3-(3,6-Dioxocyclohexa-1,4-dien-1-yl)acrylate (1.46).** To a solution of hydroquinone **1.48** (208 mg, 1.0 mmol, 1.0 *eq.*) in a mixture of MeCN and  $\text{H}_2\text{O}$  (24 mL, 4:1), 2,6-pyridinedicarboxylic acid (418 mg, 2.5 mmol, 2.5 *eq.*) was added. After sonication for 30 seconds silver(II)oxide (310 mg, 2.5 mmol, 2.5 *eq.*) was added and the reaction mixture sonicated for another 30 seconds upon which the colour changed from dark green to yellow. After 5 minutes of vigorous stirring, the reaction mixture was diluted with EtOAc (20 mL) and filtered over a plug of celite. The organic phase was washed with saturated  $\text{NaHCO}_3$  ( $4 \times 30\text{mL}$ ),  $\text{H}_2\text{O}$  ( $2 \times 30\text{mL}$ ) and brine ( $3 \times 30\text{mL}$ ). The combined organic phases were dried over  $\text{Na}_2\text{SO}_4$  and concentrated under reduced pressure to give 185 mg (90%) of title compound **1.46** as yellow solid.

**Data for 1.46:** IR (ATR):  $\tilde{\nu} = 2360, 2336, 1738, 1707, 1654, 1472, 1367, 1307, 1265, 1188\text{ cm}^{-1}$ ;  $^1\text{H}$  NMR (200 MHz,  $\text{CDCl}_3$ )  $\delta = 7.49$  (dd,  $J = 16.0, 1, 1\text{H}$ ), 6.86-6.85 (m, 1H), 6.80 (d,  $J = 16.0, 1\text{H}$ ), 6.80-6.79 (m, 2H), 4.25 (q,  $J = 7.2, 2\text{H}$ ), 1.31 (t,  $J = 7.2, 3\text{H}$ );  $^{13}\text{C}$  NMR (125 MHz,  $\text{CDCl}_3$ )  $\delta = 187.4, 185.9, 165.8, 139.7, 137.2, 136.8, 135.4, 133.4, 128.1, 61.4, 14.4$ ; HRMS (EI) calc. for  $\text{C}_{11}\text{H}_{10}\text{O}_4$  ( $\text{M}^+$ ): 206.0579; found: 206.0581.



**Ethyl 2-Methyl-6,9-dioxo-3a,4,6,9,9a,9b-hexahydronaphtho[1,2-*b*]furan-4-carboxylate (1.50).** Quinone **1.46** (50 mg, 0.242 mmol, 1.0 *eq.*) was dissolved in  $\text{CDCl}_3$  (3.5 mL) and 2-methylfuran (0.131 mL, 1.45 mmol, 6.0 *eq.*) was added. The reaction mixture was heated to reflux for 1 h. Crude NMR analysis indicated partial conversion to desired DA adduct **1.50**. Longer reaction times, as well as any attempt to isolate the product lead to decomposition.

$^1\text{H}$  NMR,  $\text{CDCl}_3$ , 300 MHz $^{13}\text{C}$  NMR,  $\text{CDCl}_3$ , 150 MHz

**Figure S1.1:** X-ray crystal structure of (*E*)-1,4-dimethoxy-2-(2-nitrovinyl)benzene (**1.22**).**Table S1.1:** Crystallographic data for (*E*)-1,4-dimethoxy-2-(2-nitrovinyl)benzene (**1.22**).

<i>(E)</i> -1,4-dimethoxy-2-(2-nitrovinyl)benzene		<b>1.22</b>	
netto formula		C <sub>10</sub> H <sub>11</sub> NO <sub>4</sub>	
molecular mass/ g mol <sup>-1</sup>		209.199	
Crystal size/ mm		0.25 × 0.20 × 0.12	
temperature/ K		173(2)	
radiation		MoKα	
diffractometer		'KappaCCD'	
crystal system		monoclinic	
space group		<i>P2<sub>1</sub>/c</i>	
<i>a</i> / Å	3.90880(10)	<i>α</i> / °	90
<i>b</i> / Å	18.9082(5)	<i>β</i> / °	94.6963(17)
<i>c</i> / Å	13.0295(3)	<i>γ</i> / °	90
<i>V</i> / Å <sup>3</sup>		959.76(4)	

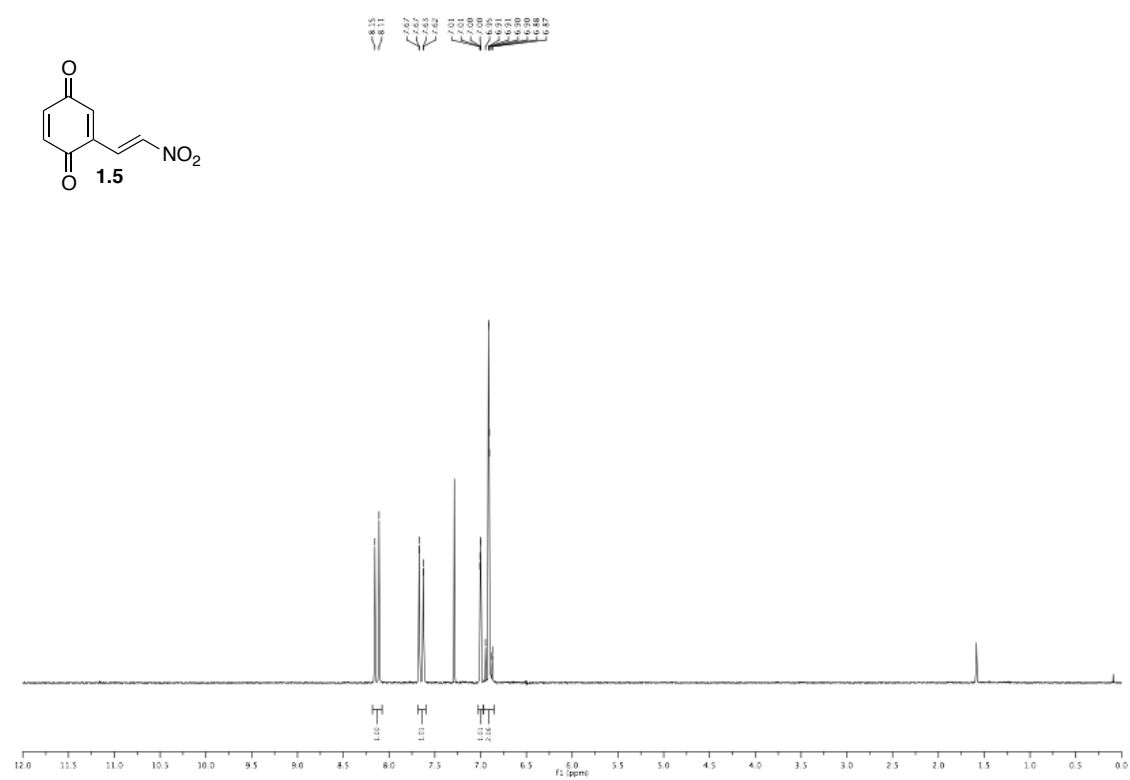
---

Z	4
calc. density/g cm <sup>-3</sup>	1.44781(6)
μ/mm <sup>-1</sup>	0.113
absorption correction	none
refls. measured	7436
<i>R</i> <sub>int</sub>	0.0275
mean σ( <i>I</i> )/ <i>I</i>	0.0254
θ range	3.14–27.46
observed refls.	1715
<i>x</i> , <i>y</i> (weighting scheme)	0.0531, 0.3309
hydrogen refinement	constr
refls in refinement	2174
parameters	138
restraints	0
<i>R</i> ( <i>F</i> <sub>obs</sub> )	0.0418
<i>R</i> <sub>w</sub> ( <i>F</i> <sup>2</sup> )	0.1106
<i>S</i>	1.040
shift/error <sub>max</sub>	0.001
max electron density/e Å <sup>-3</sup>	0.217
min electron density/e Å <sup>-3</sup>	-0.295

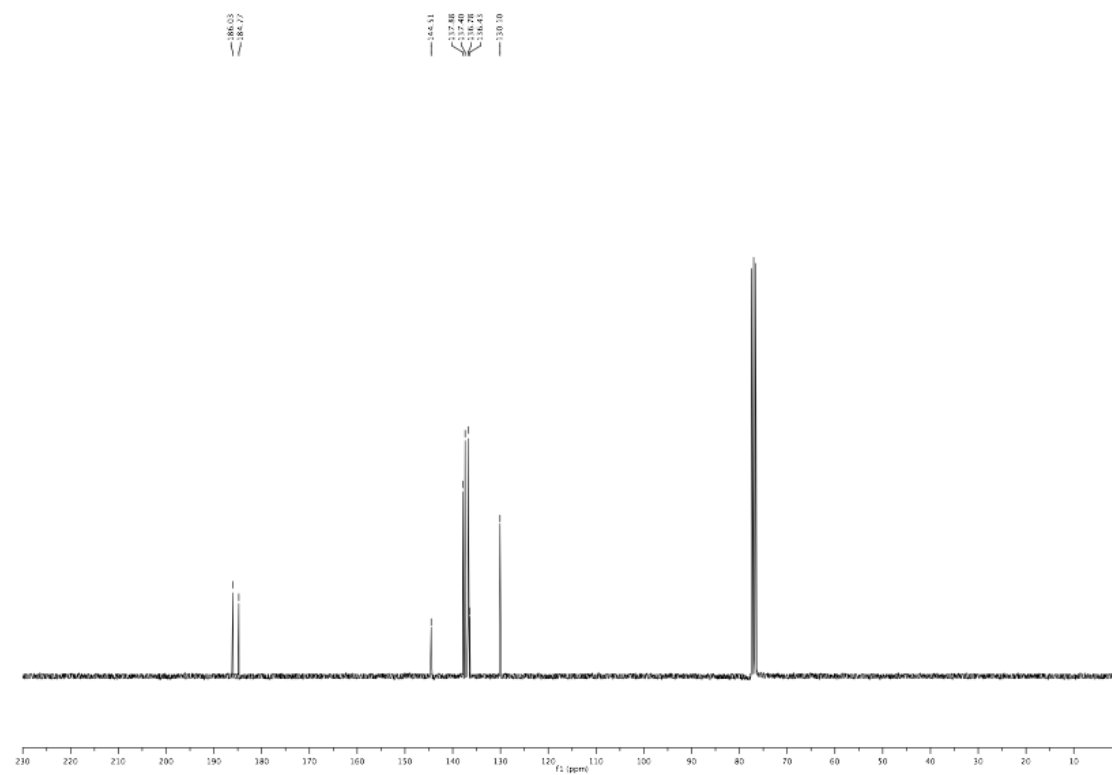
---

## 1.5. Experimental Section

$^1\text{H}$  NMR,  $\text{CDCl}_3$ , 300 MHz



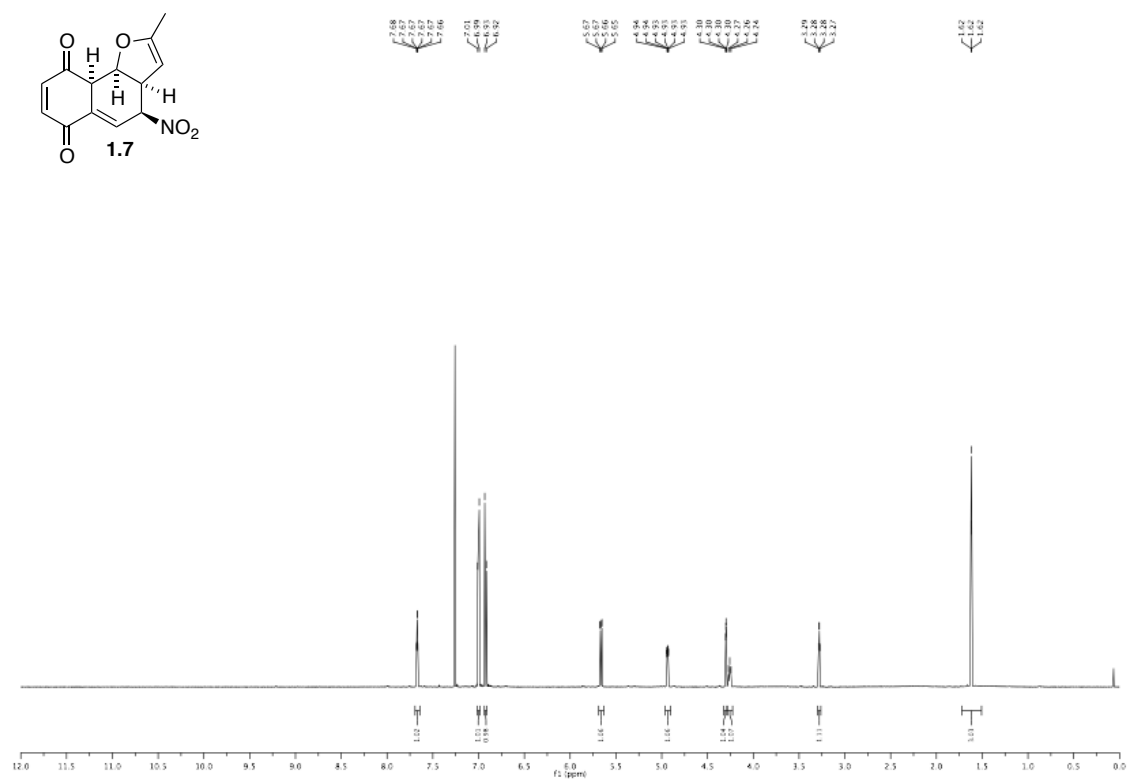
$^{13}\text{C}$  NMR,  $\text{CDCl}_3$ , 150 MHz



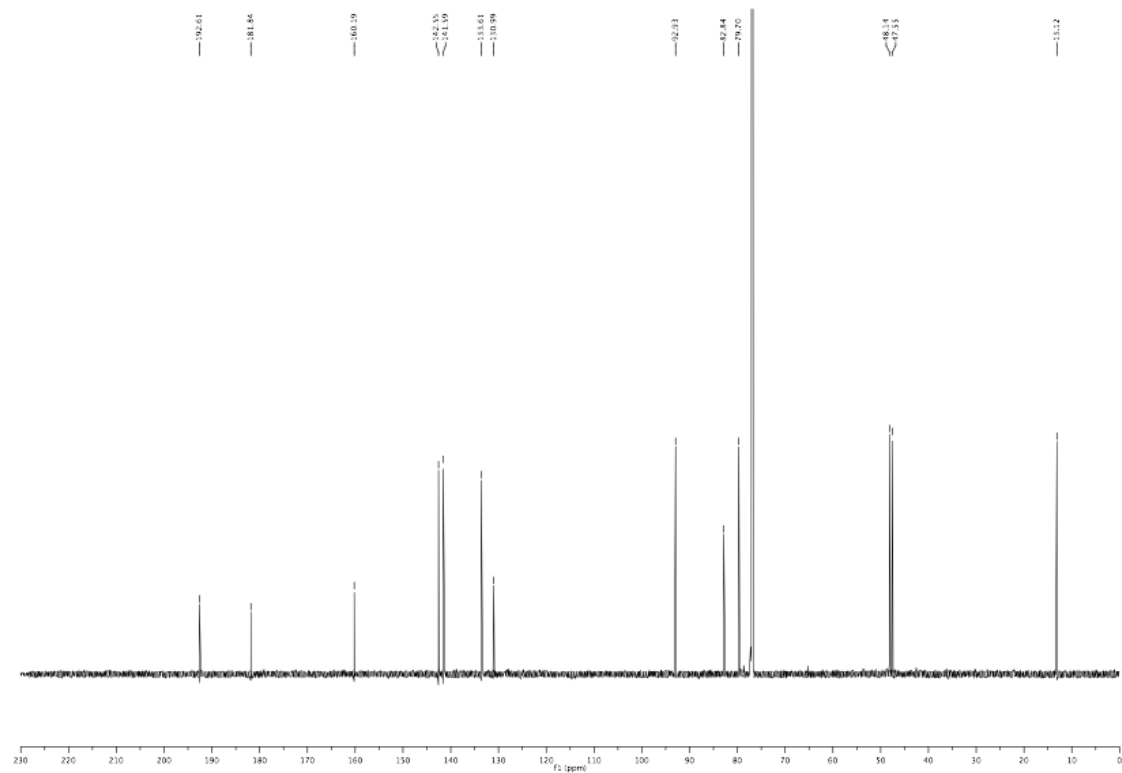


# 1. VINYL QUINONE DIELS-ALDER REACTIONS

$^1\text{H}$  NMR,  $\text{CDCl}_3$ , 300 MHz

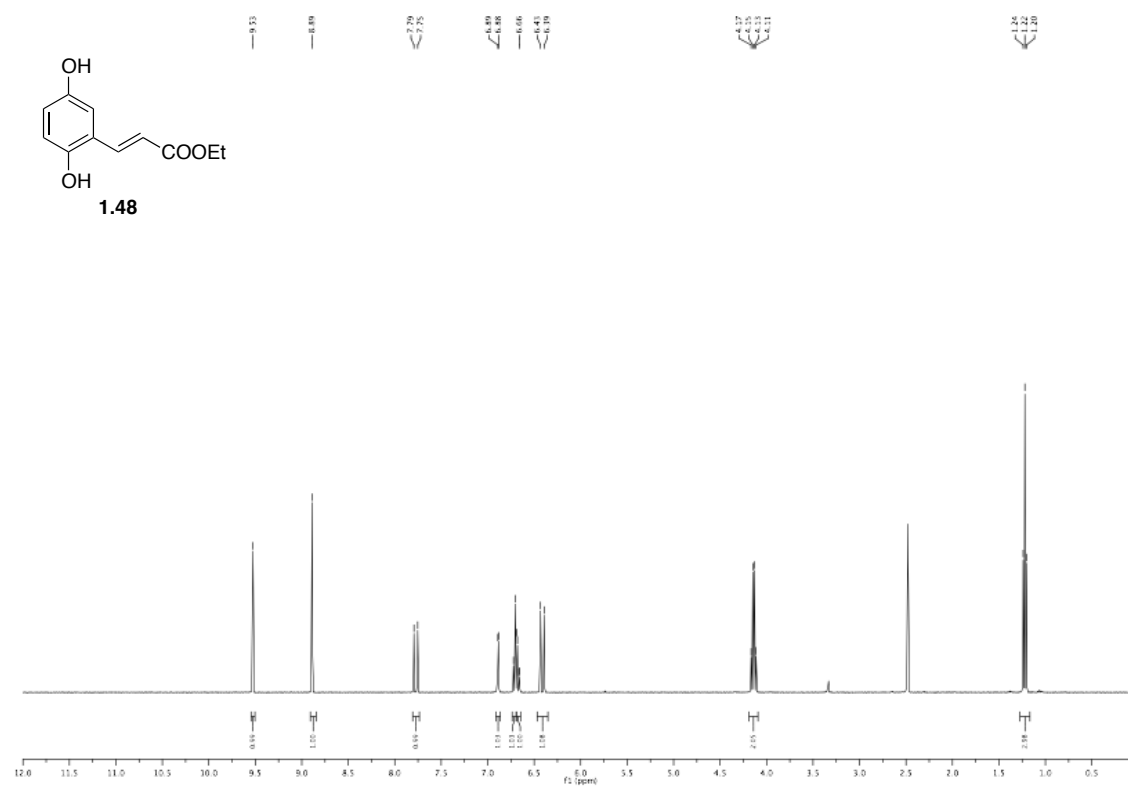


$^{13}\text{C}$  NMR,  $\text{CDCl}_3$ , 150 MHz

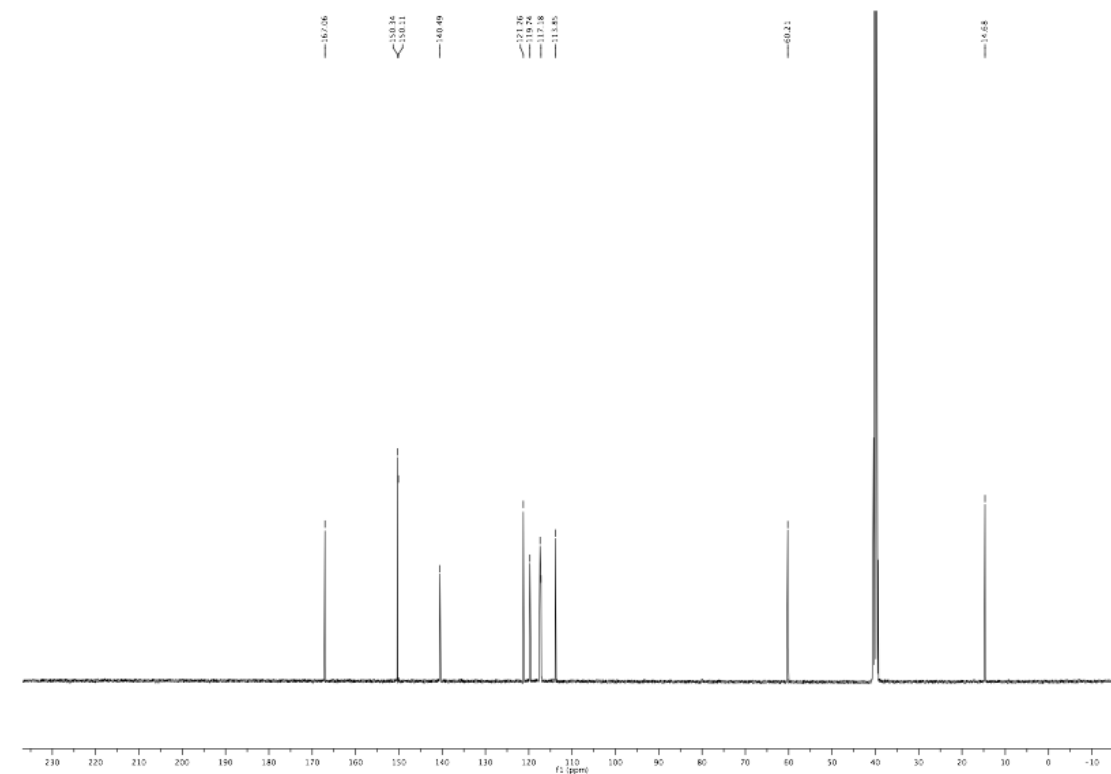


## 1.5. Experimental Section

$^1\text{H}$  NMR,  $\text{DMSO-}d_6$ , 400 MHz

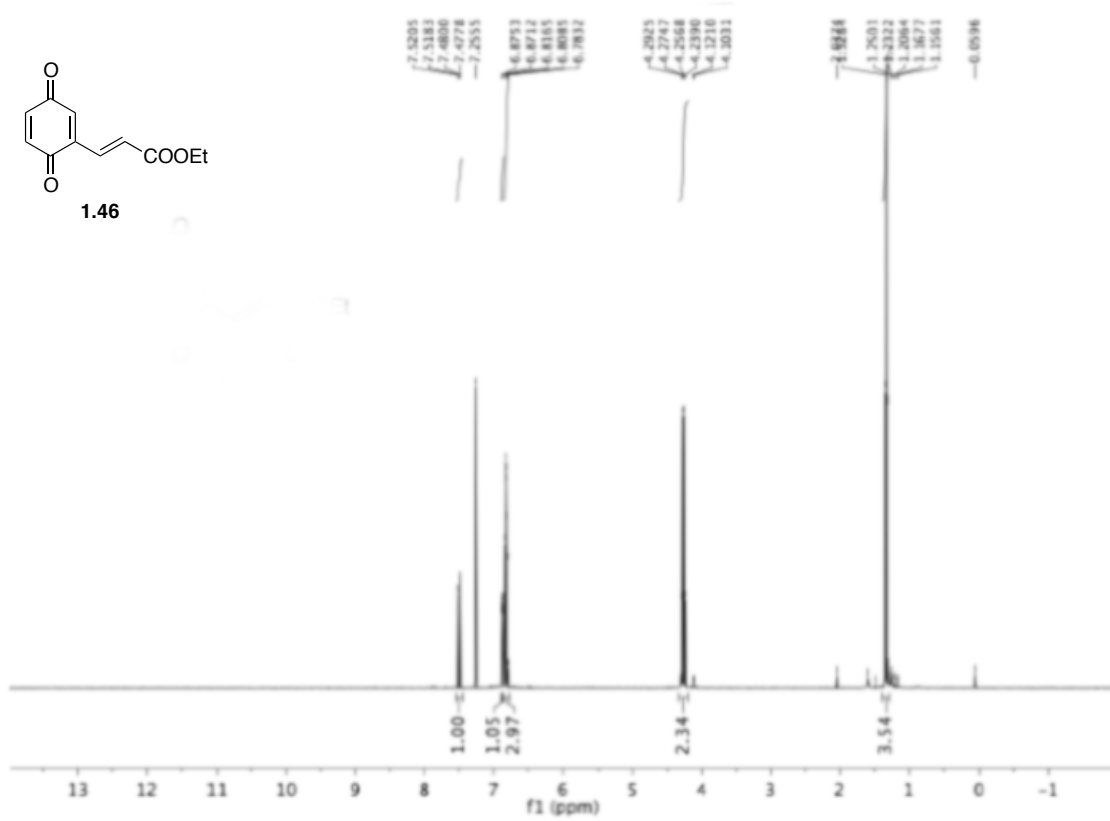


$^{13}\text{C}$  NMR,  $\text{DMSO-}d_6$ , 100 MHz

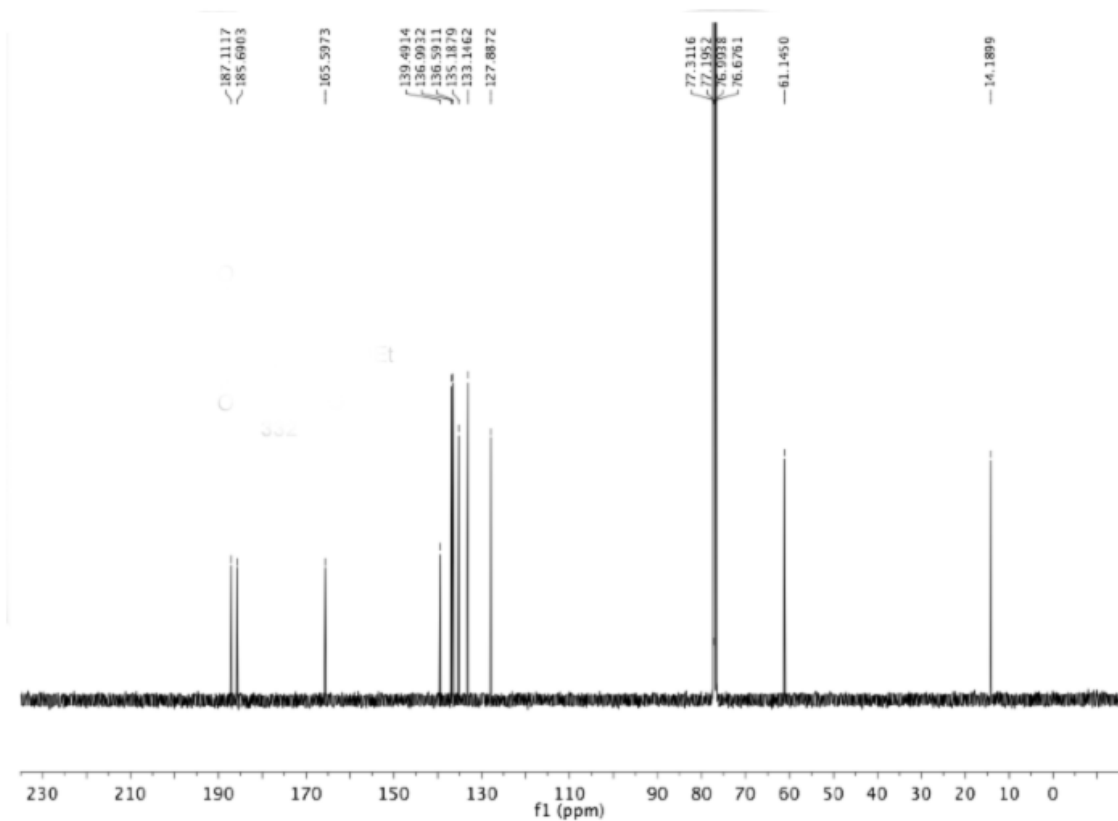


# 1. VINYL QUINONE DIELS-ALDER REACTIONS

$^1\text{H}$  NMR,  $\text{CDCl}_3$ , 300 MHz

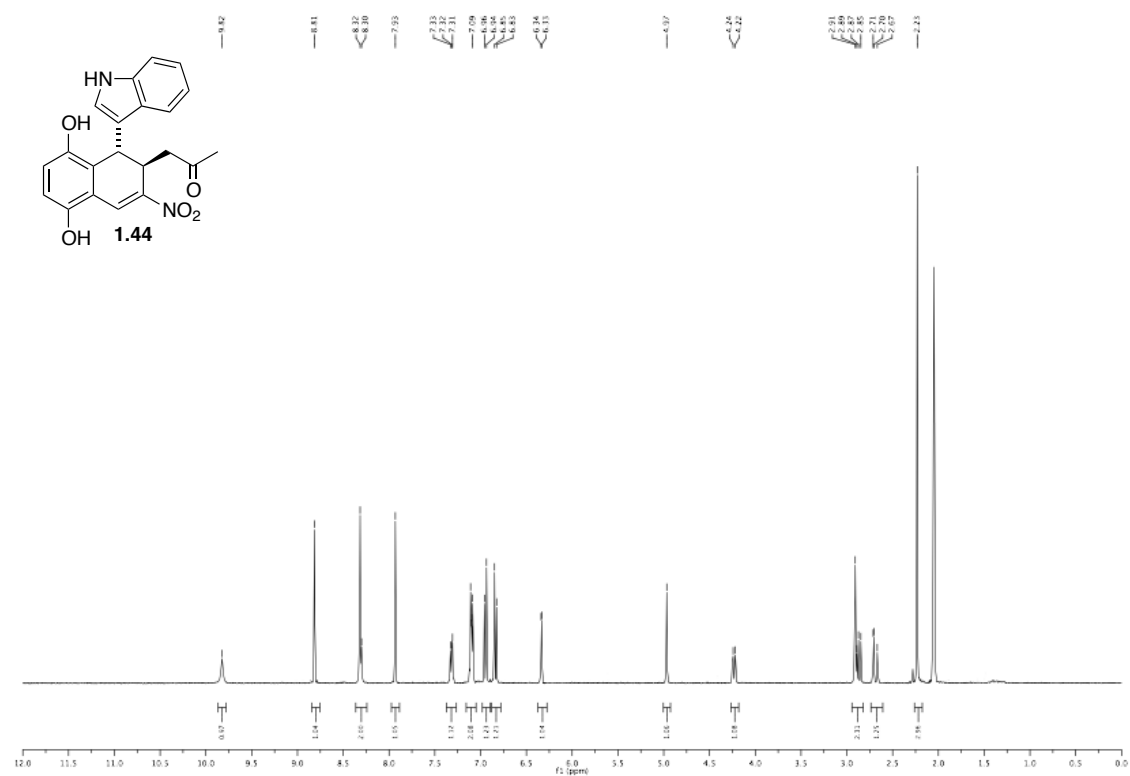


$^{13}\text{C}$  NMR,  $\text{CDCl}_3$ , 150 MHz

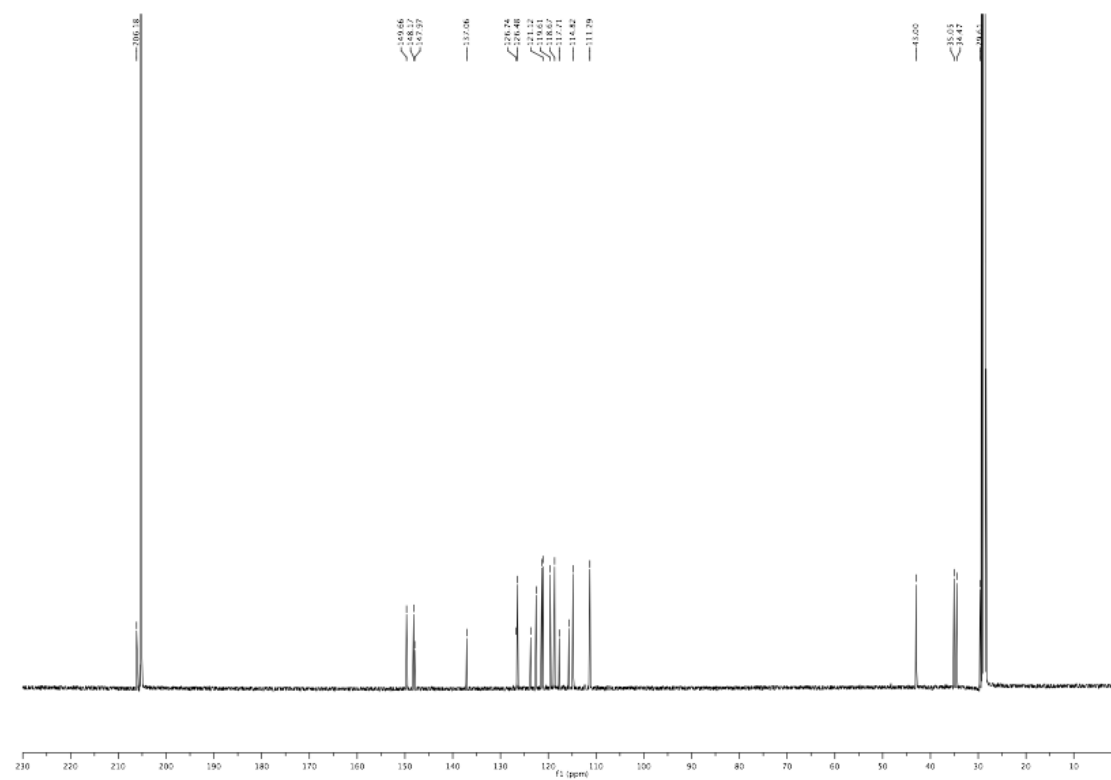


## 1.5. Experimental Section

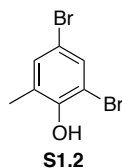
$^1\text{H}$  NMR, acetone- $d_6$ , 300 MHz



$^{13}\text{C}$  NMR, acetone- $d_6$ , 100 MHz

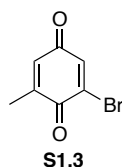


## 1.5.3 Biomimetic Total Synthesis of Pycnanthuquinone C



**2,4-Dibromo-6-methylphenol (S1.2).** To an ice cold solution of *o*-cresol (10.8 g, 100 mmol, 1.0 *eq.*) in 90% acetic acid (100 mL), bromine (32.0 g, 200 mmol, 2.0 *eq.*) was added drop wise over 15 min. After stirring at room temperature for 1 h, the reaction mixture was poured on cold H<sub>2</sub>O (500 mL). The colourless precipitate was filtered off and washed excessively with water to provide 26 g (96%) of title compound **S1.2** as a colourless solid, which was used without further purification.

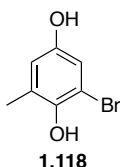
**Data for (S1.2):** IR (ATR):  $\tilde{\nu}$  = 3499, 3412, 3080, 1590, 1567, 1462, 1396, 1379, 1315, 1278, 1221 cm<sup>-1</sup>; <sup>1</sup>H NMR (300 MHz, CDCl<sub>3</sub>):  $\delta$  = 7.46 – 7.43 (m, 1H), 7.24 – 7.20 (m, 1H), 5.55 (s, 1H), 2.29 (t, 3H, *J* = 0.7); <sup>13</sup>C NMR (150 MHz, CDCl<sub>3</sub>)  $\delta$  = 149.8, 133.1, 131.3, 127.7, 112.0, 110.4, 16.5; HRMS (EI) calcd for C<sub>7</sub>H<sub>6</sub>Br<sub>2</sub>O (M<sup>+</sup>): 263.8765; found: 263.8779.



**2-Bromo-6-methylcyclohexa-2,5-diene-1,4-dione (S1.3).** To a suspension of **S1.2** (25.3 g, 95.0 mmol, 1.0 *eq.*) in acetic acid anhydride (50 mL) and MeCN (25 mL) was added a solution of CrO<sub>3</sub> (10.4 g, 105 mmol, 1.1 *eq.*) in H<sub>2</sub>O (25 mL), upon which the solution turned black. The reaction mixture was heated to 60 °C for 1.5 h. After cooling to room temperature the mixture was diluted with H<sub>2</sub>O (400 mL) and extracted with CH<sub>2</sub>Cl<sub>2</sub> (3 × 150 mL). The combined organic phases were washed with brine (2 × 200 mL), dried and concentrated to obtain 19 g (99%) of title compound **S1.3** as orange needles, which was used without further purification.

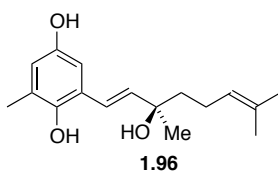
**Data for (S1.3):** IR (ATR):  $\tilde{\nu}$  = 3055, 1677, 1649, 1630, 1595, 1423, 1282 cm<sup>-1</sup>; <sup>1</sup>H NMR (300 MHz, CDCl<sub>3</sub>):  $\delta$  = 7.25 (d, 1H, *J* = 2.4), 6.66 (dq, 1H, *J* = 3.2, 1.6), 2.15 (d,

3H,  $J = 1.6$ );  $^{13}\text{C}$  NMR (75 MHz,  $\text{CDCl}_3$ )  $\delta = 184.8, 179.9, 145.7, 138.1, 137.3, 133.4, 16.8$ ; HRMS calcd for  $\text{C}_7\text{H}_6\text{BrO}_2$  ( $\text{M}^-$ ): 200.9546; found: 200.9533.



**2-Bromo-6-methylbenzene-1,4-diol (1.118).** A solution of **S1.3** (12.2 g, 60.7 mmol, 1.0 *eq.*) in EtOH (120 mL) and  $\text{H}_2\text{O}$  (20 mL) was heated to 50 °C. Subsequently sodium dithionite (12.7 g, 72.8 mmol, 1.2 *eq.*) was added and the mixture was stirred at 50 °C for 1.5 h. The reaction mixture was concentrated under reduced pressure and the resulting residue was taken up in EtOAc (200 mL), washed with  $\text{H}_2\text{O}$  ( $2 \times 150$  mL), dried and concentrated. The resulting brown solid was washed with cold  $\text{CH}_2\text{Cl}_2$  to provide 8.8 g (71%) of hydroquinone **1.118** as a colourless solid.

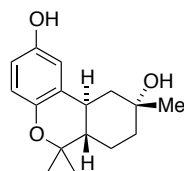
**Data for 1.118:** IR (ATR):  $\tilde{\nu} = 3230, 1610, 1585, 1471, 1361, 1189$   $\text{cm}^{-1}$ ;  $^1\text{H}$  NMR (300 MHz,  $\text{CDCl}_3$ ):  $\delta = 6.84$  (d, 1H,  $J = 2.9$ ), 6.62 (d, 1H,  $J = 2.8$ ), 5.20 (s, 1 H), 4.66 (s, 1H), 2.27 (s, 3H);  $^{13}\text{C}$  NMR (75 MHz,  $\text{CDCl}_3$ )  $\delta = 184.8, 144.8, 126.5, 117.7, 115.8, 109.6, 16.8$ ; HRMS calcd for  $\text{C}_7\text{H}_8\text{BrO}_2$  ( $\text{M}^-$ ): 202.9702; found: 202.9663.



**(R,E)-2-(3-Hydroxy-3,7-dimethylocta-1,6-dien-1-yl)-6-methylbenzene-1,4-diol (1.96).** To a solution of 2-bromo-6-methylbenzene-1,4-diol (**1.118**) (500 mg, 2.50 mmol, 1.0 *eq.*) in dry DMF (8 mL) were added  $\text{Pd}(\text{OAc})_2$  (28.9 mg, 0.13 mmol, 0.05 *eq.*), dry sodium carbonate (1.06 g, 10.0 mmol, 4.0 *eq.*), tetrabutylammonium chloride (0.90 g, 3.25 mmol, 1.3 *eq.*) and (–)-linalool (**1.119**) (1.16 g, 1.34 mL, 7.50 mmol, 3.0 *eq.*). The mixture was degassed with argon for 15 min. Subsequently the reaction mixture was heated in a sealed tube in an oil-bath (preheated to 50 °C) to 50 °C for 1 h. The dark brown reaction mixture was dissolved in  $\text{Et}_2\text{O}$  (15 mL) and then filtered through a pad of

of silica gel (EtOAc as eluent), concentrated and purified by silica gel chromatography (25% EtOAc in hexanes) to yield 560 mg (81%) of title vinyl hydroquinone **1.96** as an orange oil.

**Data for 1.96:**  $R_f$  0.43 (50% EtOAc in hexanes); IR (ATR):  $\tilde{\nu}$  = 3285, 2970, 2926, 1608, 1493, 1450, 1374, 1342, 1300, 1253, 1193, 1153, 1104  $\text{cm}^{-1}$ ;  $^1\text{H}$  NMR (300 MHz,  $\text{CDCl}_3$ ):  $\delta$  = 6.80 (d, 1H,  $J$  = 16.1), 6.70 (d, 1H,  $J$  = 3.1), 6.58 (s, 1H), 6.22 (d, 1H,  $J$  = 16.1), 5.16 (t, 1H,  $J$  = 7.1), 4.72 (s, 1H), 4.61 (s, 1H), 2.23 (s, 3H), 2.14 – 2.01 (m, 2H), 1.92 – 1.85 (m, 1H), 1.70 (d, 3H,  $J$  = 1.1), 1.75 – 1.66 (m, 1H), 1.64 (s, 1H), 1.62 (s, 3H), 1.40 (s, 3H);  $^{13}\text{C}$  NMR (150 MHz,  $\text{CDCl}_3$ )  $\delta$  = 148.9, 145.2, 138.9, 132.3, 125.5, 124.8, 124.2, 121.5, 116.9, 111.0, 73.8, 42.5, 28.4, 25.7, 23.0, 17.8, 16.2; HRMS calcd for  $\text{C}_{17}\text{H}_{25}\text{O}_3$  ( $\text{M}^+$ ): 276.1725; found: 276.1730.

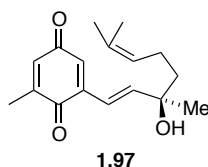


**1.123**

**Benzopyrane 1.123.** To a solution of 2-bromo-6-methylbenzene-1,4-diol (**1.118**) (2.50 g, 12.0 mmol, 1.0 *eq.*) in dry DMF (25 mL) were added  $\text{Pd}(\text{OAc})_2$  (28.9 mg, 0.13 mmol, 0.05 *eq.*), dry sodium carbonate (5.30 g, 48.0 mmol, 4.00 *eq.*), tetrabutylammonium chloride (4.50 g, 15.6 mmol, 1.3 *eq.*) and ( $\pm$ )-linalool (**1.119**) (5.80 g, 6.70 mL, 38.0 mmol, 3.0 *eq.*). The mixture was degassed with argon for 15 min. Subsequently the reaction mixture was heated to 80 °C with an oil-bath (preheated to 80 °C) in a sealed tube for 2 h. The cooled mixture was diluted with EtOAc (100 mL) and  $\text{H}_2\text{O}$  (400 mL). After phase separation, the aqueous phase was extracted with EtOAc (3  $\times$  400 mL). Combined organic phases were dried and concentrated at reduced pressure and 50 °C. Purification by silica gel chromatography (25% EtOAc in hexanes) provided 2.2 g (67%) of benzopyrane **1.123** as a brown solid.

**Data for 1.123:**  $R_f$  0.43 (50% EtOAc in hexanes); IR (ATR):  $\tilde{\nu}$  = 3216, 2972, 2930, 2361, 2338, 1457, 1368, 1304, 1251, 1213, 1152, 1137, 1117  $\text{cm}^{-1}$ ;  $^1\text{H}$  NMR (300 MHz,  $\text{CDCl}_3$ ):  $\delta$  = 6.51 (s, 2H), 2.79 (td, 1H,  $J$  = 11.3, 3.6), 2.33 – 2.24 (dt, 1H,  $J$  = 11.3, 3.7), 2.13 (s, 3H), 1.85 – 1.77 (m, 1H), 1.72 – 1.62 (m, 2H), 1.54 – 1.28 (m, 4H), 1.40 (s, 3H), 1.33 (s, 3H), 1.12 (s, 3H);  $^{13}\text{C}$  NMR (150 MHz,  $\text{CDCl}_3$ )  $\delta$  = 147.9, 145.5, 127.2, 125.2,

115.8, 109.6, 76.4, 70.0, 46.9, 43.7, 38.6, 31.8, 31.5, 28.00, 23.3, 20.2, 16.3; HRMS calcd for  $C_{17}H_{25}O_3$  ( $M^+$ ): 276.1725; found: 276.1721.

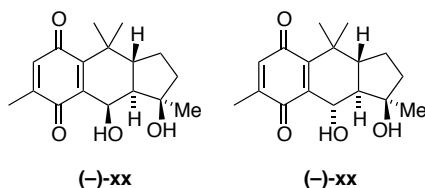


**(*R,E*)-2-(3-Hydroxy-3,7-dimethylocta-1,6-dien-1-yl)-6-methylcyclohexa-2,5-diene-1,4-dione (1.97).** A solution of hydroquinone **1.96** (95.0 mg, 0.34 mmol, 1.0 *eq.*) in  $CH_2Cl_2$  (10 mL) was treated with  $MnO_2$  (897 mg, 10.3 mmol, 30.0 *eq.*) for 15 min at room temperature. The reaction mixture was diluted with  $CH_2Cl_2$  (50 mL) and filtered through a pad of celite. The filtrate was concentrated and the resulting oil was purified by silica gel chromatography (25%  $Et_2O$  in hexanes) to provide 61 mg (65%) of vinyl quinone **1.97** as bright yellow oil. **One-pot procedure for 1.97.** To a stirred solution of 2-bromo-6-methylbenzene-1,4-diol (**1.118**) (500 mg, 2.50 mmol, 1.0 *eq.*) in dry DMF (8 mL) were added  $Pd(OAc)_2$  (28.9 mg, 0.13 mmol, 0.05 *eq.*), dry sodium carbonate (1.06 g, 10.0 mmol, 4.0 *eq.*), tetrabutylammonium chloride (0.903 g, 3.25 mmol, 1.3 *eq.*) and (–)-linalool (**1.96**) (1.16 g, 1.34 mL, 7.5 mmol, 3.0 *eq.*). The mixture was degassed with argon for 15 min. Subsequently the reaction mixture was heated to 80 °C with an oil-bath (preheated to 80 °C) in a sealed tube for 2 h. After cooling to room temperature, the reaction mixture was treated with  $MnO_2$  (6.52 g, 75.0 mmol, 30.0 *eq.*) for 15 min at room temperature. Subsequently the reaction mixture was filtered through a plug of celite. The concentrated filtrate was then filtered through a plug of silica. After concentration the resulting oil was diluted with  $Et_2O$  (50 mL) and washed with water (3 × 25 mL), brine (25 mL), dried, concentrated and purified by silica gel chromatography (25%  $Et_2O$  in hexanes) to provide 516 mg (75%) of vinyl quinone **1.97** as a bright yellow oil.

**Data for 1.97:**  $R_f$  0.65 (25%  $EtOAc$  in hexanes);  $[a]_D^{20} +36$  ( $c$  0.83,  $CHCl_3$ ), IR (ATR):  $\tilde{\nu} = 3348, 2966, 2920, 1651, 1604, 1462, 1375, 1198$   $cm^{-1}$ ;  $^1H$  NMR (600 MHz,  $CDCl_3$ ):  $\delta = 6.66$  (d, 1H,  $J = 16.61$ ), 6.66 (dd, 1H,  $J = 2.6, 0.4$ ), 6.63 – 6.59 (m, 1H), 6.59 – 6.57 (m, 1H), 5.11 (t, 1H,  $J = 7.2$ ), 2.07 (d, 3H,  $J = 1.5$ ), 2.14 – 1.95 (m, 2H), 1.81 (s, 1H), 1.67 (s, 3H), 1.66 – 1.62 (m, 2H), 1.58 (s, 3H), 1.35 (s, 3H);  $^{13}C$  NMR (150 MHz,  $CDCl_3$ )  $\delta = 187.8, 187.4, 146.6, 145.7, 142.0, 133.3, 132.5, 128.9, 123.9, 119.2, 73.9, 42.1, 28.2, 25.7, 22.9, 17.8,$



16.1; HRMS calcd for  $C_{17}H_{22}O_3$  ( $M^-$ ): 273.1496; found: 273.1485.



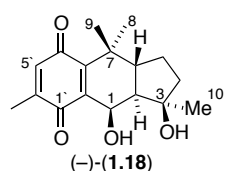
**(-)-pycnanthuquinone C (-)-1.18** and **(+)-pycnanthuquinone D (1.120)**. A solution of vinyl quinone **1.97** (686 mg, 2.50 mmol, 1.0 *eq.*) in toluene (2 mL) was diluted with  $H_2O$  (5 mL). The resulting biphasic mixture was heated in a sealed tube to 60 °C for 16 h. The reaction mixture was diluted with EtOAc (10 mL). After phase separation the aqueous phase was extracted with EtOAc ( $3 \times 10$  mL). The combined organic phases were dried, filtered, concentrated and purified by silica gel chromatography (25% EtOAc in hexanes) to yield 108 mg (37%) of a mixture of (-)-**1.18** and (+)-**1.120** as a yellow oil. Separation of the diastereomers was achieved by reversed phase HPLC (50 to 65% MeOH in  $H_2O$  linear gradient over 35 minutes, preparative RP column, Dynamax Microsorb 60  $C_{18}$ , 8  $\mu m$  particle size) provided 151 mg (21%) of pycnanthuquinone C (-)-**1.18** and 116 mg (16%) of its diastereomer **1.120** as yellow oils. X-ray quality crystals of compound **1.120** were obtained by crystallisation from  $CHCl_3$  (slow evaporation of solvent). **Biomimetic procedure for compounds (-)-1.18 and 1.120:** A solution of vinyl quinone **1.97** (69 mg, 0.25 mmol, 1.0 *eq.*) in THF (4 mL) was treated with phosphate/citrate buffer (1.5 mL, pH 5). The reaction mixture was stirred at room temperature for 52 h. After the usual workup and purification by silica gel chromatography 5 mg (8%) of title compound (-)-**1.18** and 4 mg (6%) **1.120** were obtained as a yellow oil.

**Data for pycnanthuquinone C (-)-1.18:**  $R_f$  0.33,  $[a]_D^{20}$  -53 ( $c$  0.33,  $CHCl_3$ ), IR (ATR):  $\tilde{\nu}$  = 3272, 2961, 2928, 1647, 1591, 1457, 1379, 1360, 1280, 1249, 1157  $cm^{-1}$ ;  $^1H$  NMR (600 MHz, DMSO)  $\delta$  = 6.63 (s, 1H), 5.68 (d, 1H,  $J$  = 3.5), 5.11 (s, 1H), 4.99 (t, 1H,  $J$  = 3.5), 3.29 (s, 1H), 2.35 (dt, 1H,  $J$  = 13.7, 9.0), 1.94 (s, 3H), 1.79 – 1.69 (m, 1H), 1.69 – 1.59 (m, 1H), 1.56 – 1.44 (m, 2H), 1.33 (s, 3H), 1.27 (dd, 2H,  $J$  = 13.5, 3.6) 1.27 (s, 3H), 1.07 (s, 3H);  $^{13}C$  NMR (150 MHz,  $CDCl_3$ )  $\delta$  = 189.4, 187.9, 151.4, 144.2, 141.1, 135.5, 80.3, 63.7, 46.7, 43.5, 40.6, 38.1, 26.8, 26.5, 20.7, 19.5, 15.0; HRMS calcd for  $C_{17}H_{21}O_4$  ( $M-H^+$ ): 289.1445; found: 289.1442. **Data for pycnanthuquinone D (1.120):**  $R_f$  0.33,  $[a]_D^{20}$  +138 ( $c$  0.35,  $CHCl_3$ ), IR (ATR):  $\tilde{\nu}$  = 3466, 2961, 2929, 2874, 1600, 1587, 1458, 1414, 1380, 1363, 1291, 1253, 1169, 1116  $cm^{-1}$ ;  $^1H$  NMR (600 MHz,  $CDCl_3$ ):  $\delta$  = 6.48 (q, 1H,  $J$  = 1.5), 4.97 (dd, 1H,  $J$  = 9.6, 1.8), 3.75 (d, 1H,  $J$  = 1.8), 2.00 (d, 3H,  $J$  = 1.5), 1.85 (m, 1H), 1.78

## 1.5. Experimental Section

(dd, 2H,  $J = 10.5, 4.7$ ), 1.64 (s, 1H), 1.59 (dd, 1H,  $J = 12.7, 9.6$ ), 1.54 – 1.43 (m, 2H), 1.51 (s, 3H), 1.27 (s, 3H), 1.25 (s, 3H);  $^{13}\text{C}$  NMR (150 MHz,  $\text{CDCl}_3$ )  $\delta = 190.8, 187.7, 151.1, 144.4, 143.3, 135.2, 79.0, 67.4, 50.3, 48.3, 40.7, 38.1, 29.6, 27.06, 22.3, 20.6, 15.1$ ; HRMS calcd for  $\text{C}_{17}\text{H}_{21}\text{O}_4$  ( $\text{M}-\text{H}^+$ ): 289.1445; found: 289.1443.

**Table S1.2.** Comparison of analytical data for pycnanthuquinone C.



Comparison of optical rotations:

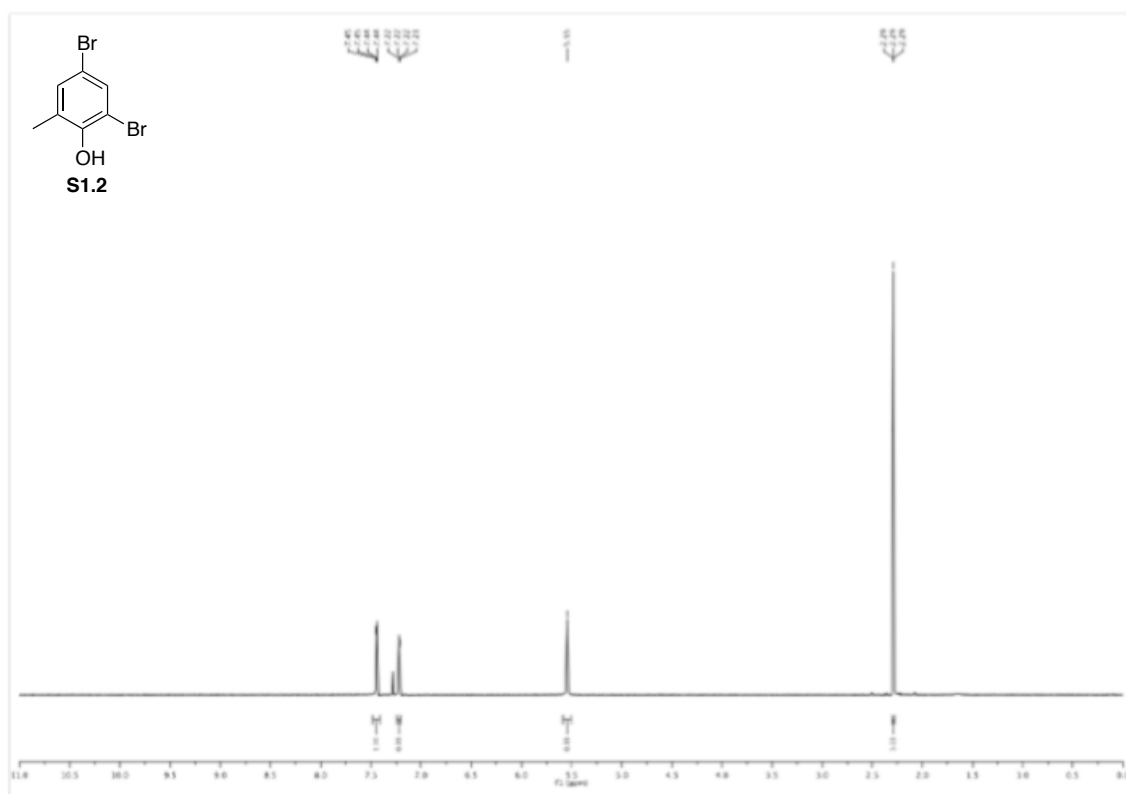
isolation:  $[\alpha]_D^{21} = +41$  ( $c$  0.16,  $\text{CHCl}_3$ )

synthetic:  $[\alpha]_D^{21} = -53$  ( $c$  0.33,  $\text{CHCl}_3$ )

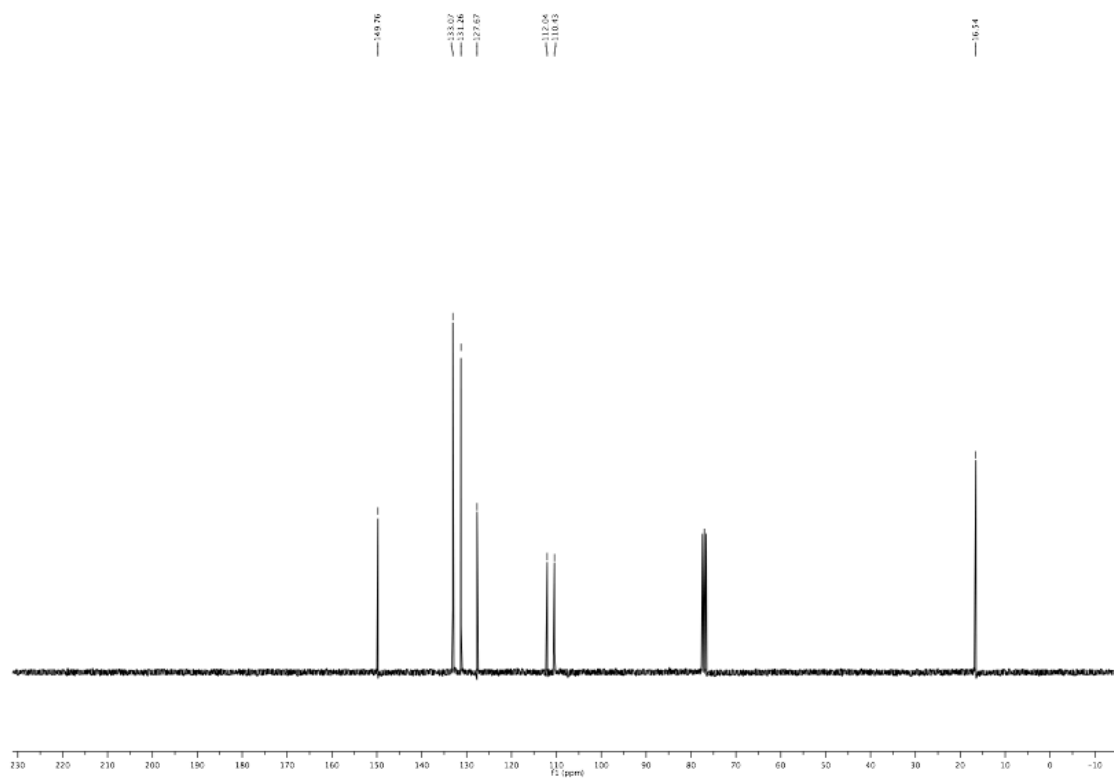
Comparison of NMR data:      isolation: 300 MHz,      isolation: 600 MHz,  $\text{CDCl}_3$

position	mult.	dC		dH ( $J$ in Hz)	
		isolation	synthetic	isolation	synthetic
1	CH	63.7	63.7	5.11, d (4.3)	
2	CH	46.7	46.7	1.36, dd (13.9, 4.3)	
3	qC	80.3	80.3		
4	$\text{CH}_2$	40.6	40.6	1.81, m	1.82, m
				1.55, m	1.56, m
5	$\text{CH}_2$	20.7	20.7	1.88, m	1.91, m
				1.54, m	1.55, m
6	CH	43.5	43.5	2.46, ddd (13.9, 9.7, 7.4)	
7	qC	38.1	38.1		
8	$\text{CH}_3$	19.5	19.5	1.13, s	1.14, s
9	$\text{CH}_3$	26.8	26.8	1.34, s	1.34, s
10	$\text{CH}_3$	26.5	26.5	1.44, s	1.45, s
1'	qC	189.5	189.4		
2'	qC	141.2	141.2		
3'	qC	151.5	151.4		
4'	qC	187.9	187.9		
5'	CH	135.5	135.5	6.49, q (1.5)	6.50, dd (2.9, 1.3)
6'	qC	144.2	144.1		
6'-Me	$\text{CH}_3$	15.0	15.0	1.99, d (1.5)	2.00, d (1.5)
1-OH				4.05, bs	4.27, bs
3-OH				3.25, bs	3.56, bs

$^1\text{H}$  NMR,  $\text{CDCl}_3$ , 300 MHz

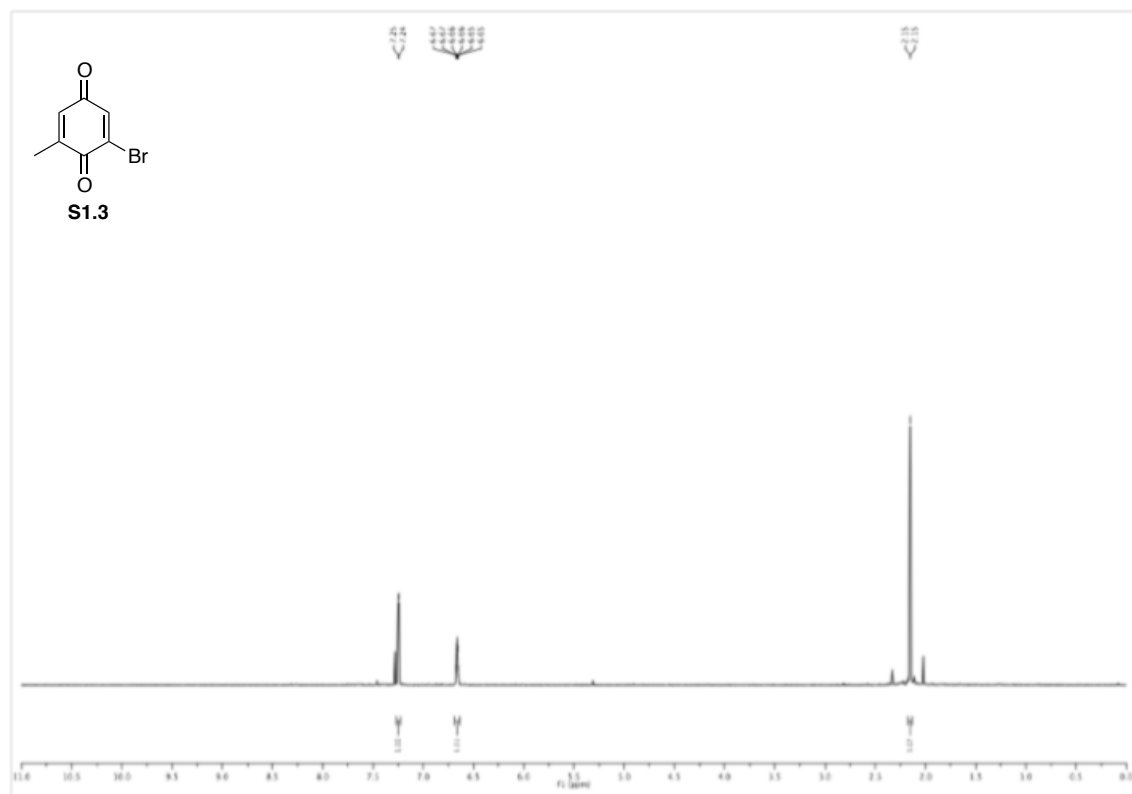


$^{13}\text{C}$  NMR,  $\text{CDCl}_3$ , 75 MHz

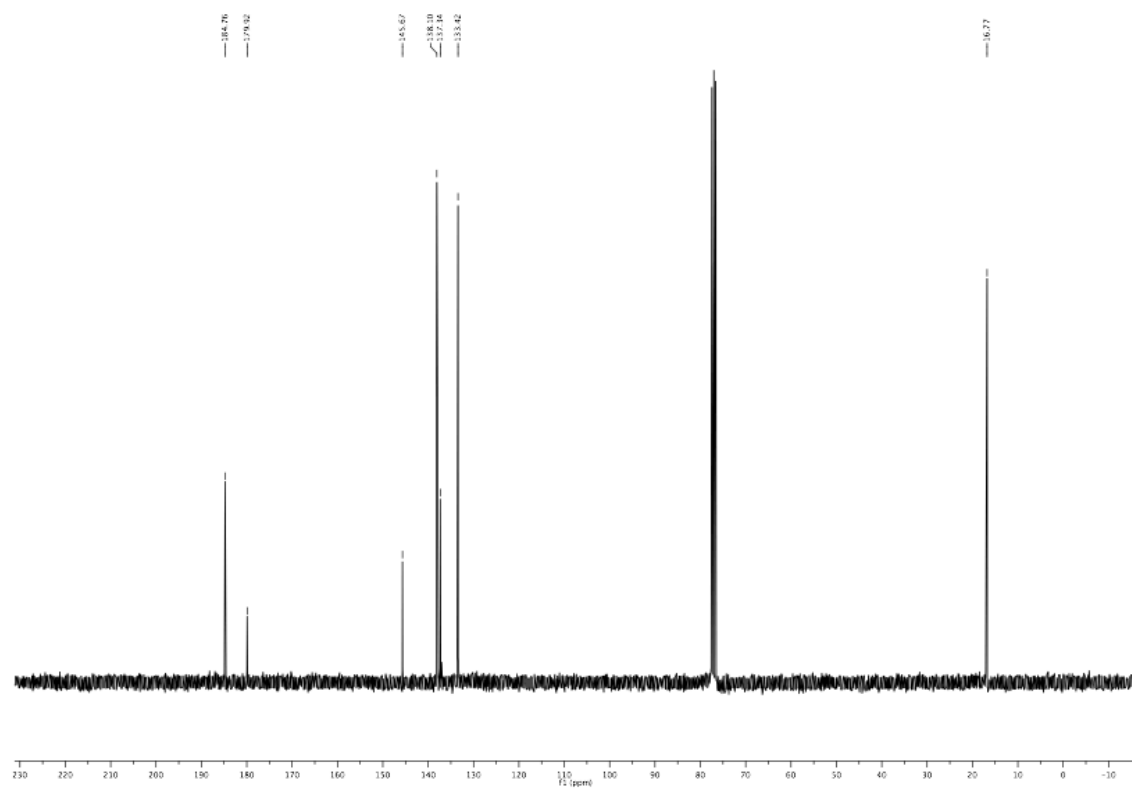


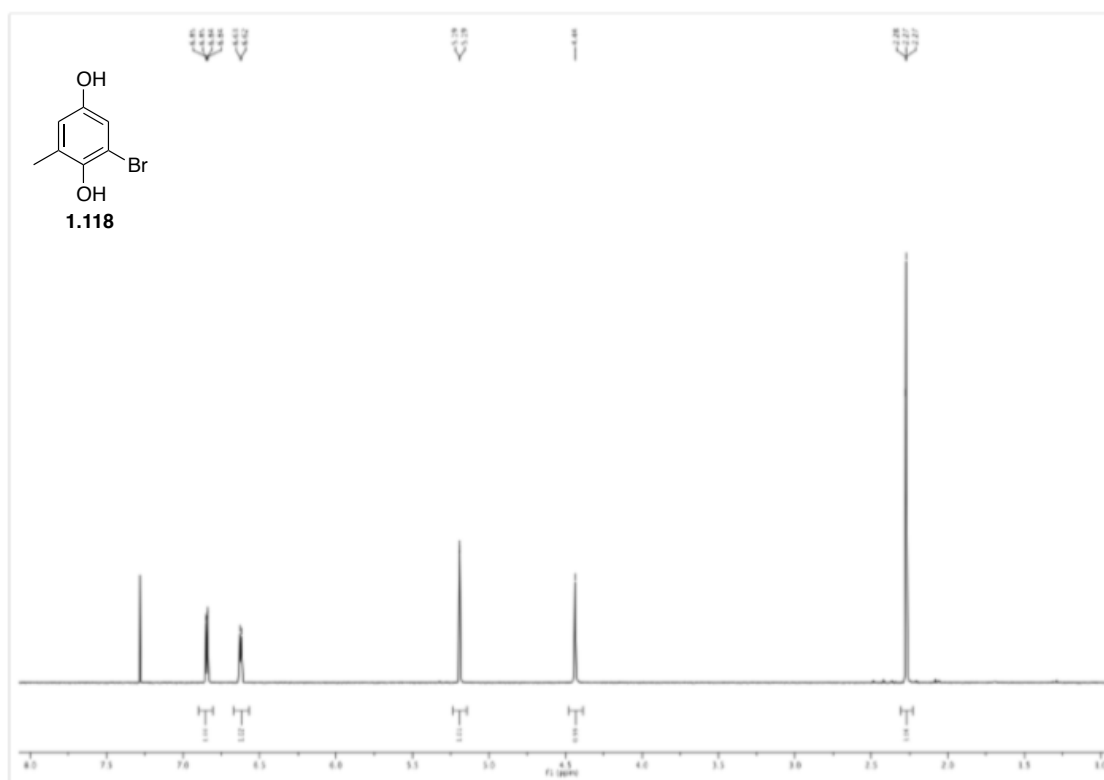
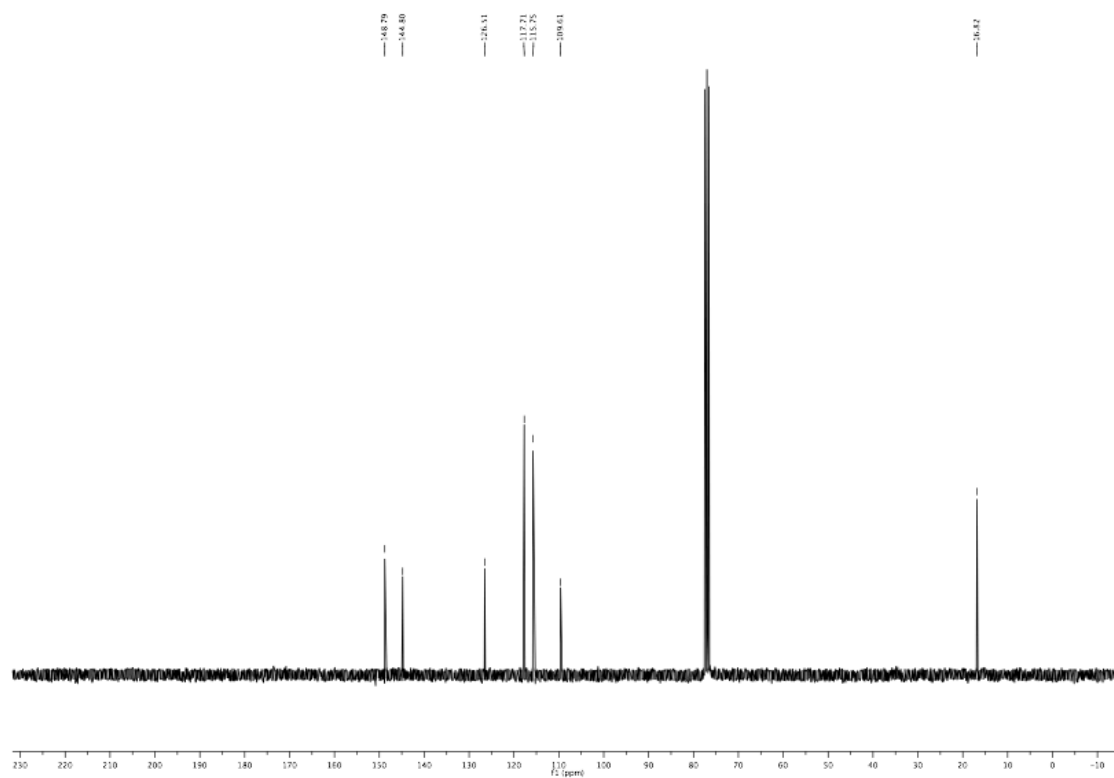
## 1.5. Experimental Section

$^1\text{H}$  NMR,  $\text{CDCl}_3$ , 300 MHz



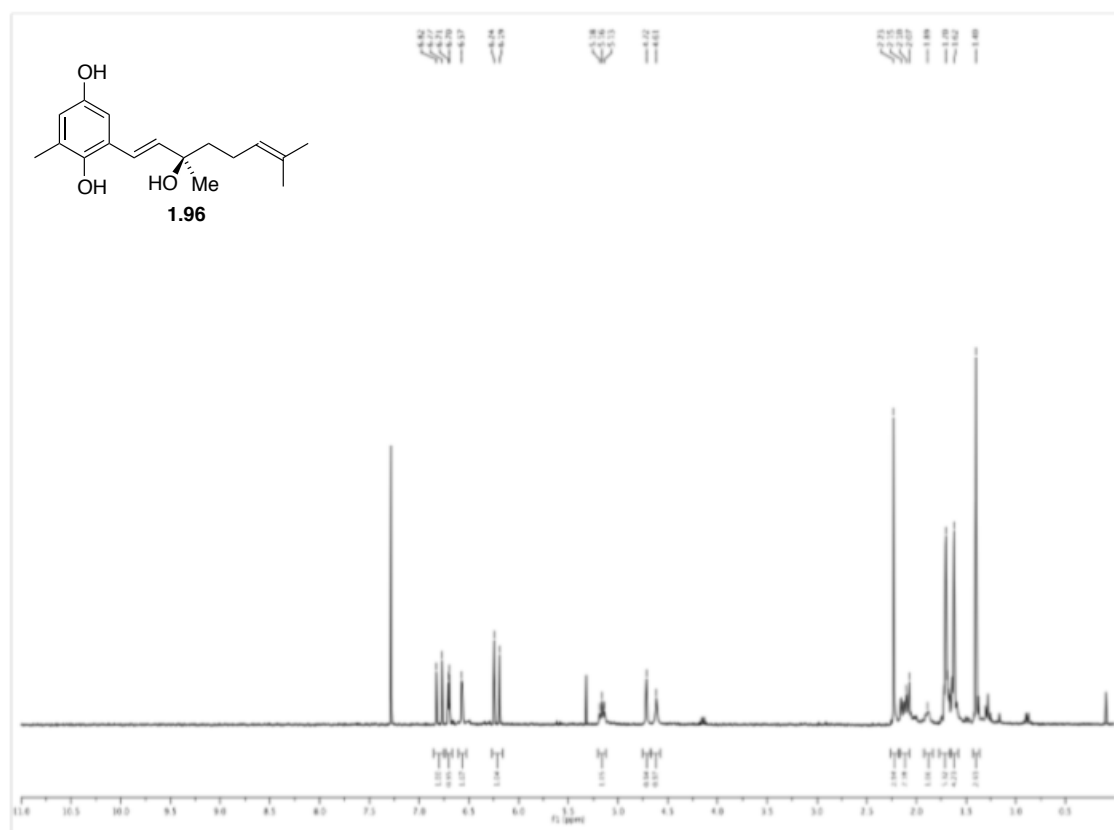
$^{13}\text{C}$  NMR,  $\text{CDCl}_3$ , 75 MHz



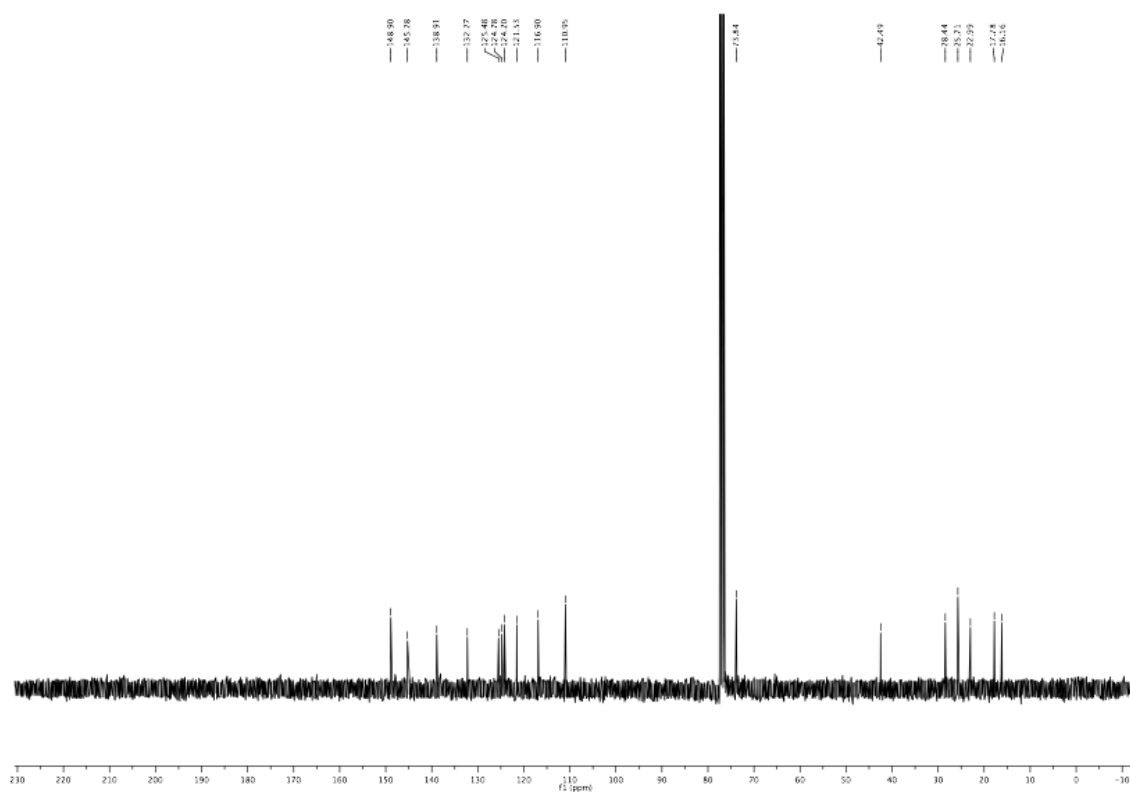
$^1\text{H}$  NMR,  $\text{CDCl}_3$ , 300 MHz $^{13}\text{C}$  NMR,  $\text{CDCl}_3$ , 75 MHz

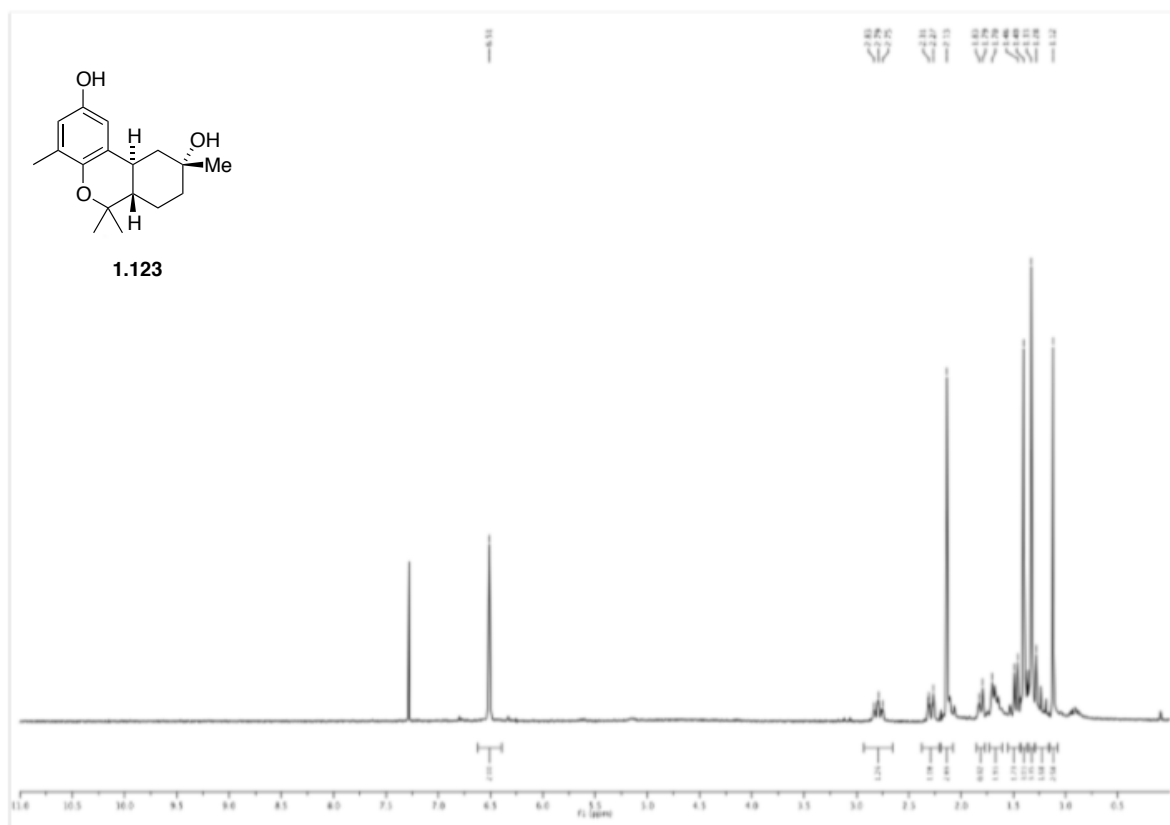
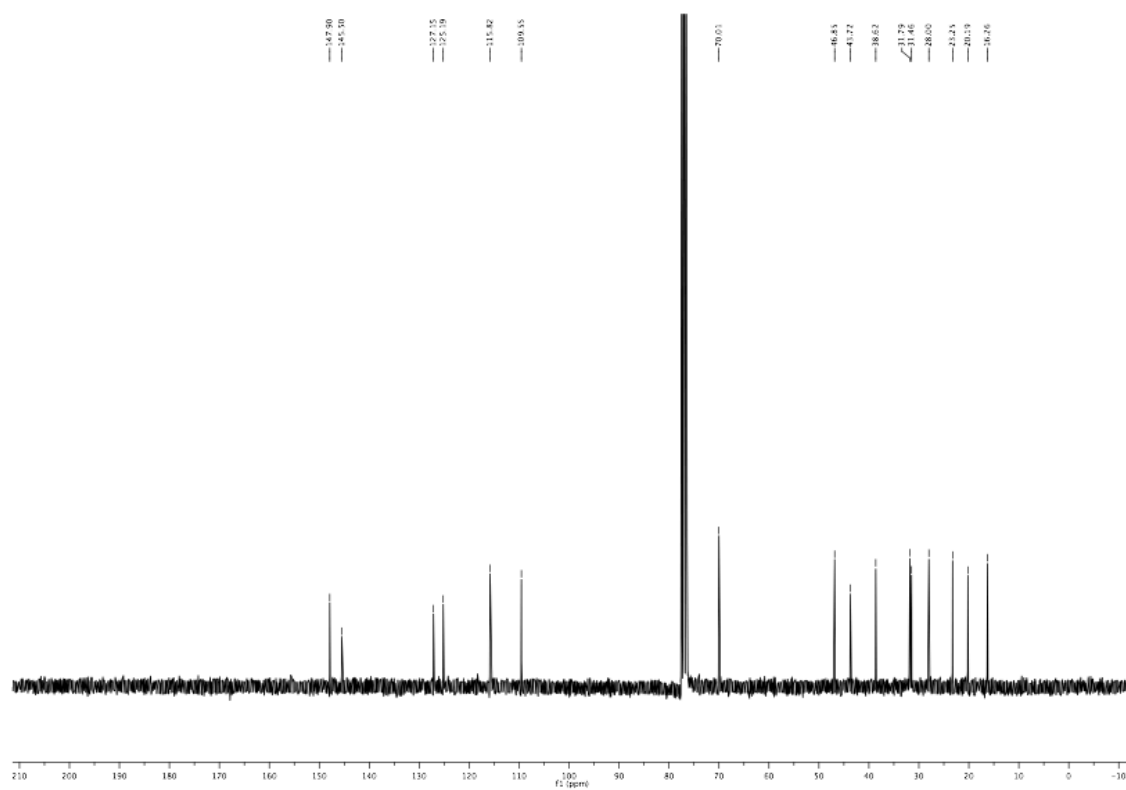
## 1.5. Experimental Section

$^1\text{H}$  NMR,  $\text{CDCl}_3$ , 300 MHz

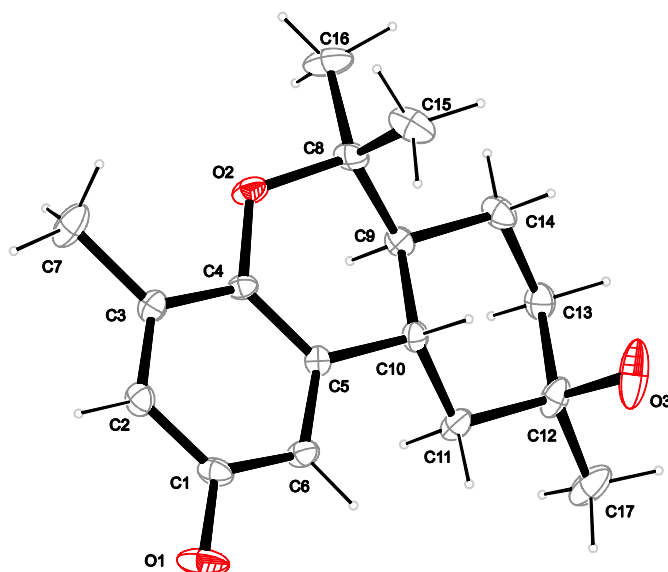


$^{13}\text{C}$  NMR,  $\text{CDCl}_3$ , 75 MHz



$^1\text{H}$  NMR,  $\text{CDCl}_3$ , 300 MHz $^{13}\text{C}$  NMR,  $\text{CDCl}_3$ , 75 MHz

**Figure S1.2:** X-ray crystal structure of (6*aS*,9*R*,10*aS*)-4,6,6,9-tetramethyl-6*a*,7,8,9,10,10*a*-hexahydro-6*H*-benzo[*d*]chromene-2,9-diol (**1.123**).



Hydrogen atoms bound to O1 and O3 not considered in the refinement.

**Table S1.3:** Crystallographic data for (6*aS*,9*R*,10*aS*)-4,6,6,9-tetramethyl-6*a*,7,8,9,10,10*a*-hexahydro-6*H*-benzo[*d*]chromene-2,9-diol (**1.123**).

net formula	C <sub>17</sub> H <sub>24</sub> O <sub>3</sub>
<i>M<sub>r</sub></i> /g mol <sup>-1</sup>	276.371
crystal size/mm	0.29 × 0.24 × 0.12
<i>T</i> /K	200(2)
radiation	MoKα
diffractometer	'Oxford XCalibur'
crystal system	triclinic
space group	<i>P</i> 1bar
<i>a</i> /Å	9.3595(4)
<i>b</i> /Å	16.4320(8)
<i>c</i> /Å	20.5378(8)
α/°	91.999(4)
β/°	101.834(4)
γ/°	100.485(4)
<i>V</i> /Å <sup>3</sup>	3031.3(2)
<i>Z</i>	8



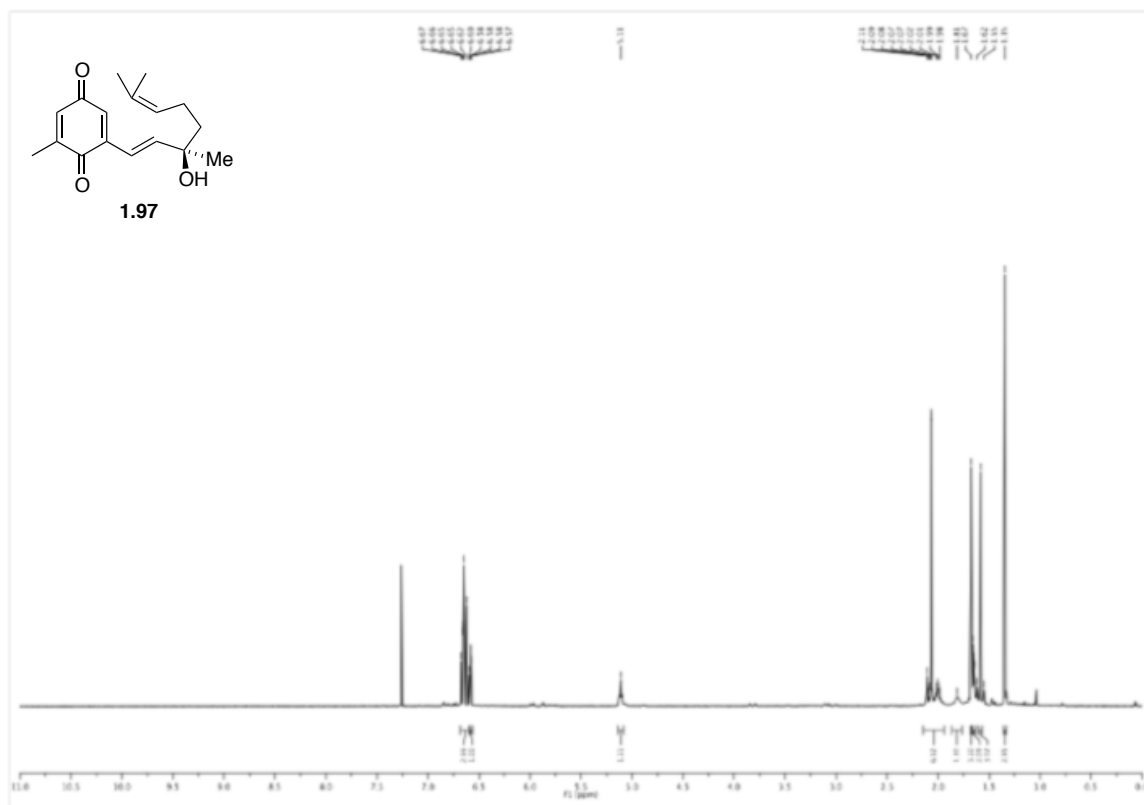
---

calc. density/g cm <sup>-3</sup>	1.21118(8)
$\mu/\text{mm}^{-1}$	0.081
absorption correction	'multi-scan'
transmission factor range	0.95502–1.00000
refls. measured	19503
$R_{\text{int}}$	0.0373
mean $\sigma(I)/I$	0.1276
$\theta$ range	4.17–25.37
observed refls.	5501
$x, y$ (weighting scheme)	0.0562, 0
hydrogen refinement	mixed
refls in refinement	11042
parameters	737
restraints	0
$R(F_{\text{obs}})$	0.0624
$R_w(F^2)$	0.1466
$S$	0.961
shift/error <sub>max</sub>	0.001
max electron density/e Å <sup>-3</sup>	0.327
min electron density/e Å <sup>-3</sup>	-0.261

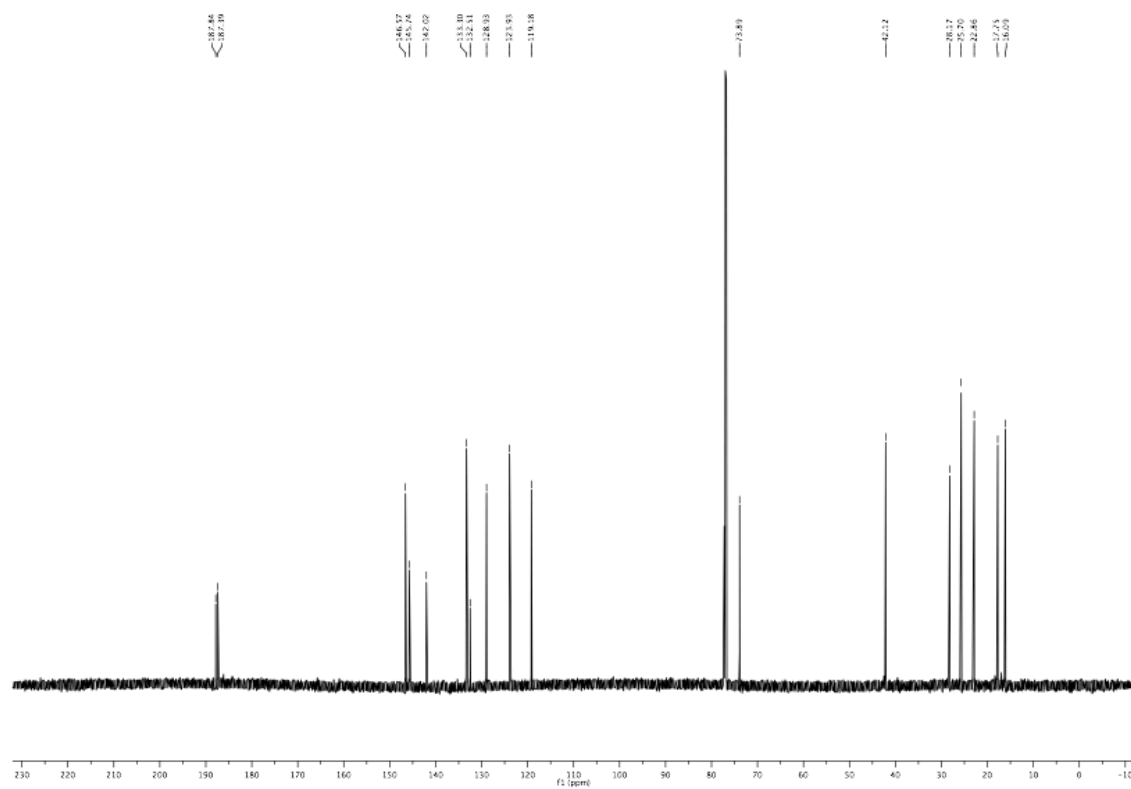
C-bound H: constr., O-bound H: not considered, because a reasonable hydrogen bonding system could not be obtained.

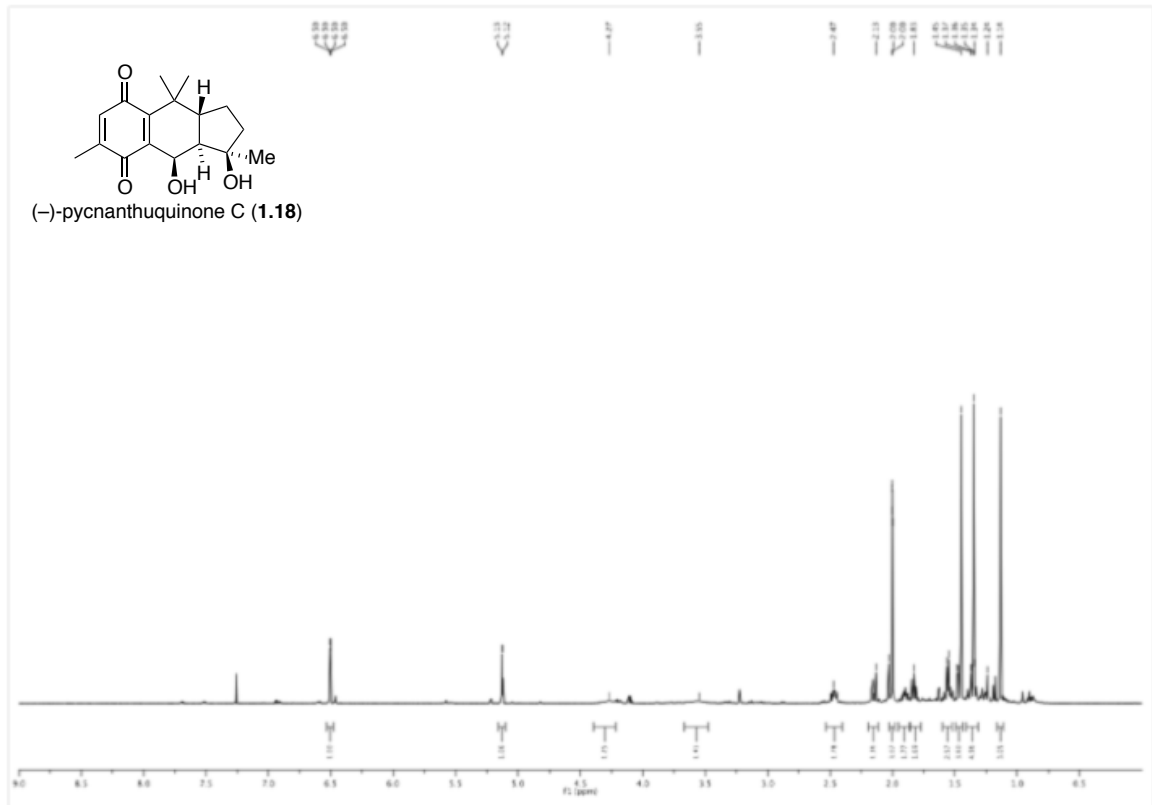
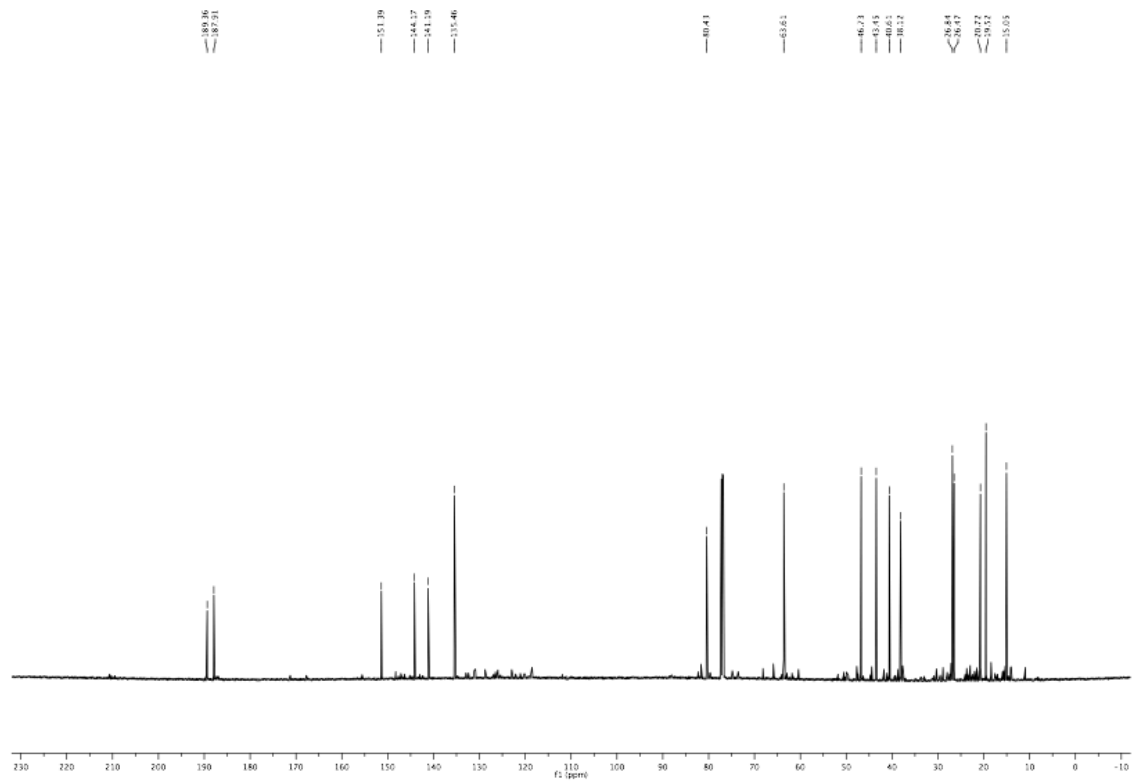
## 1.5. Experimental Section

$^1\text{H}$  NMR,  $\text{CDCl}_3$ , 300 MHz



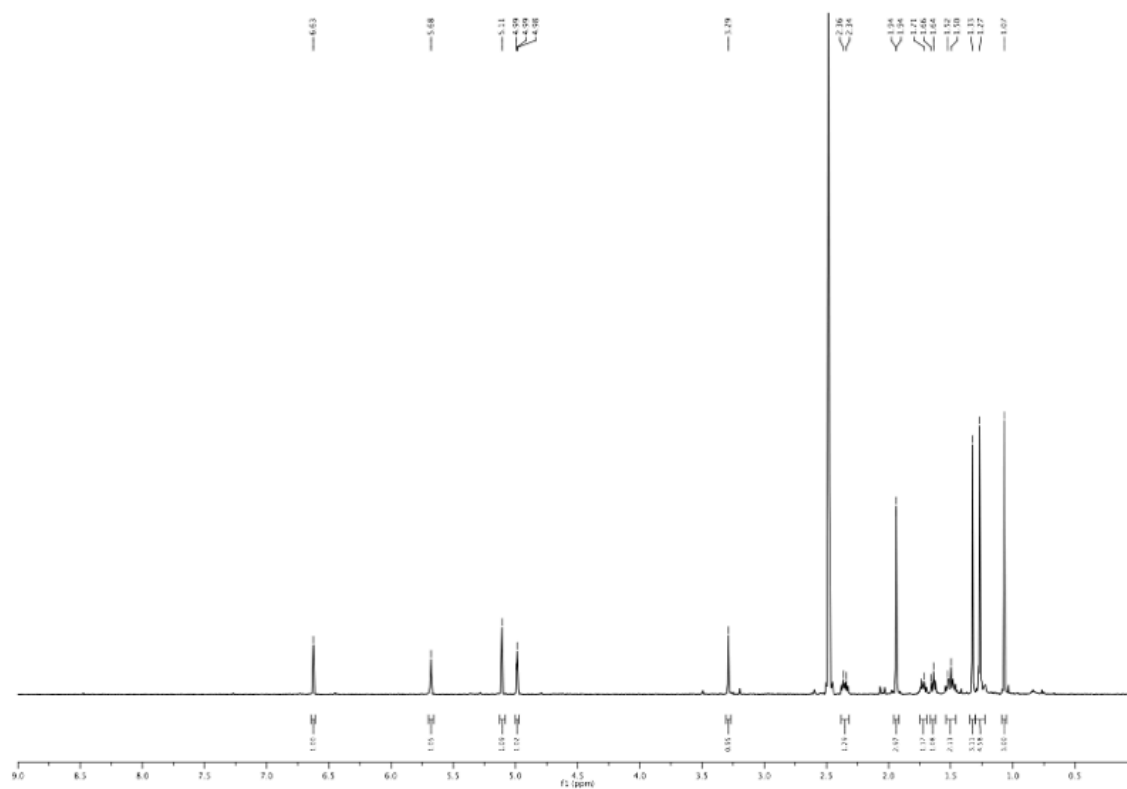
$^{13}\text{C}$  NMR,  $\text{CDCl}_3$ , 75 MHz



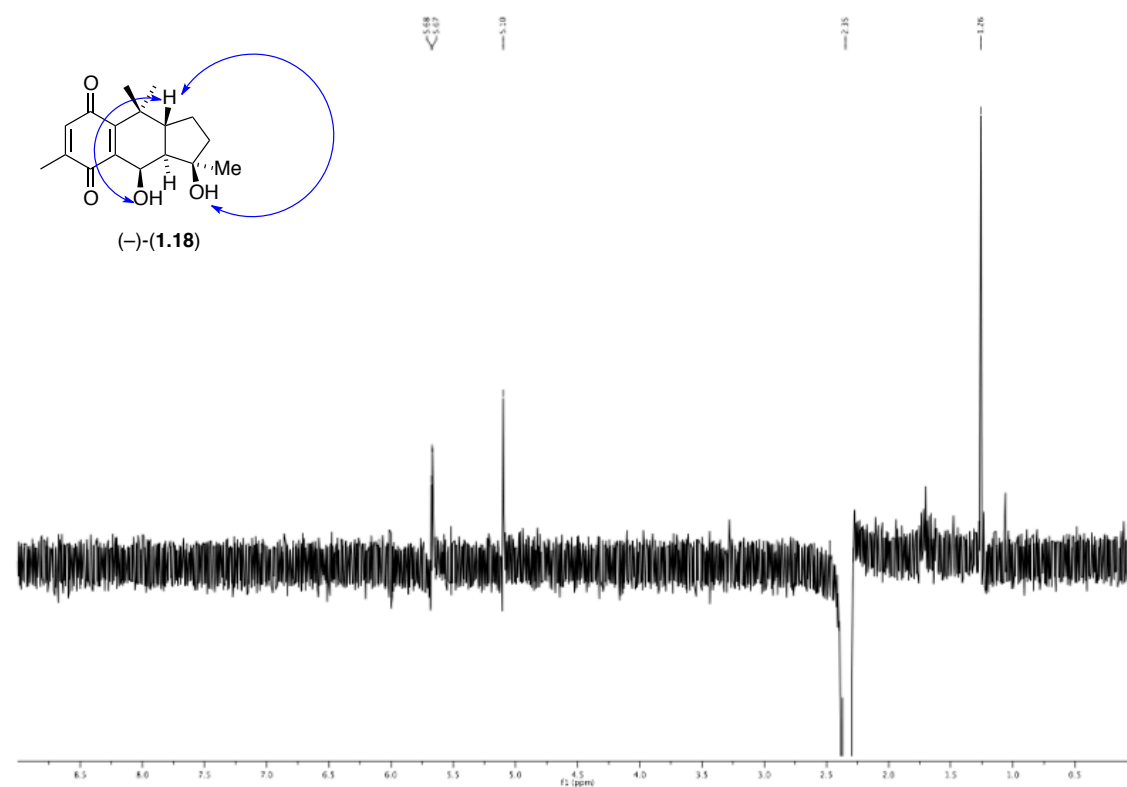
$^1\text{H}$  NMR,  $\text{CDCl}_3$ , 600 MHz $^{13}\text{C}$  NMR,  $\text{CDCl}_3$ , 150 MHz

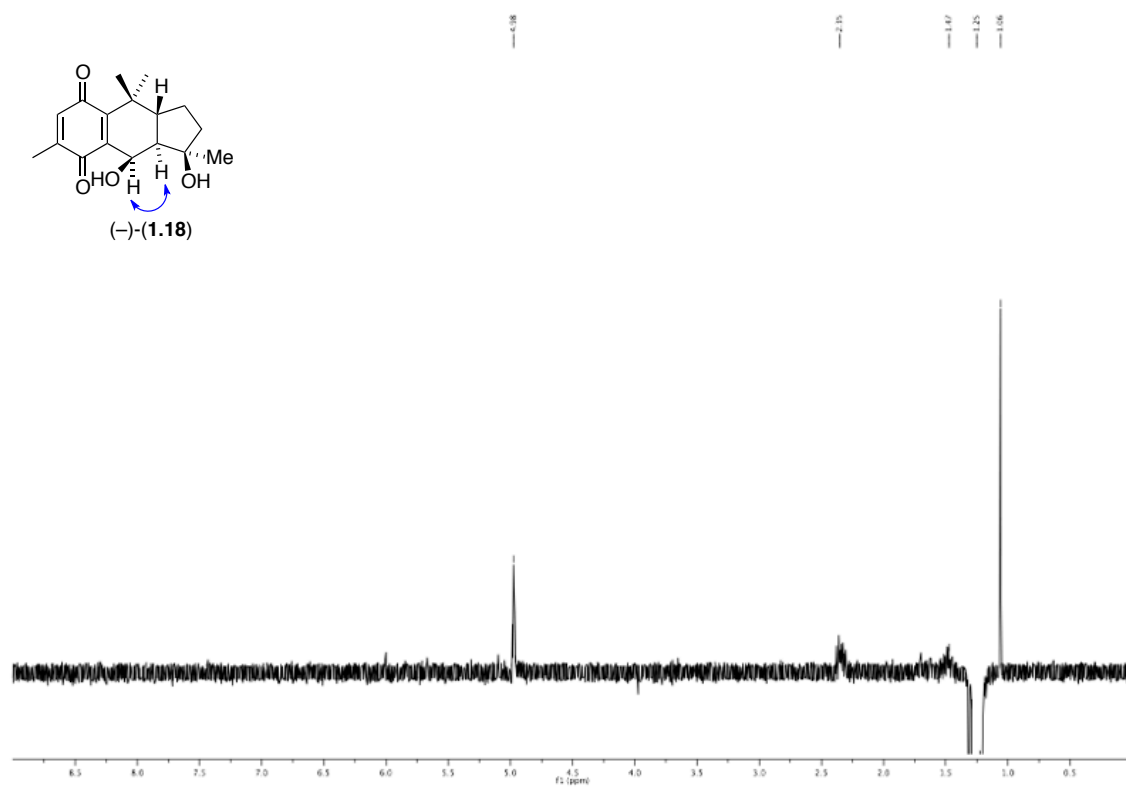
## 1.5. Experimental Section

$^1\text{H}$  NMR, DMSO, 600 MHz



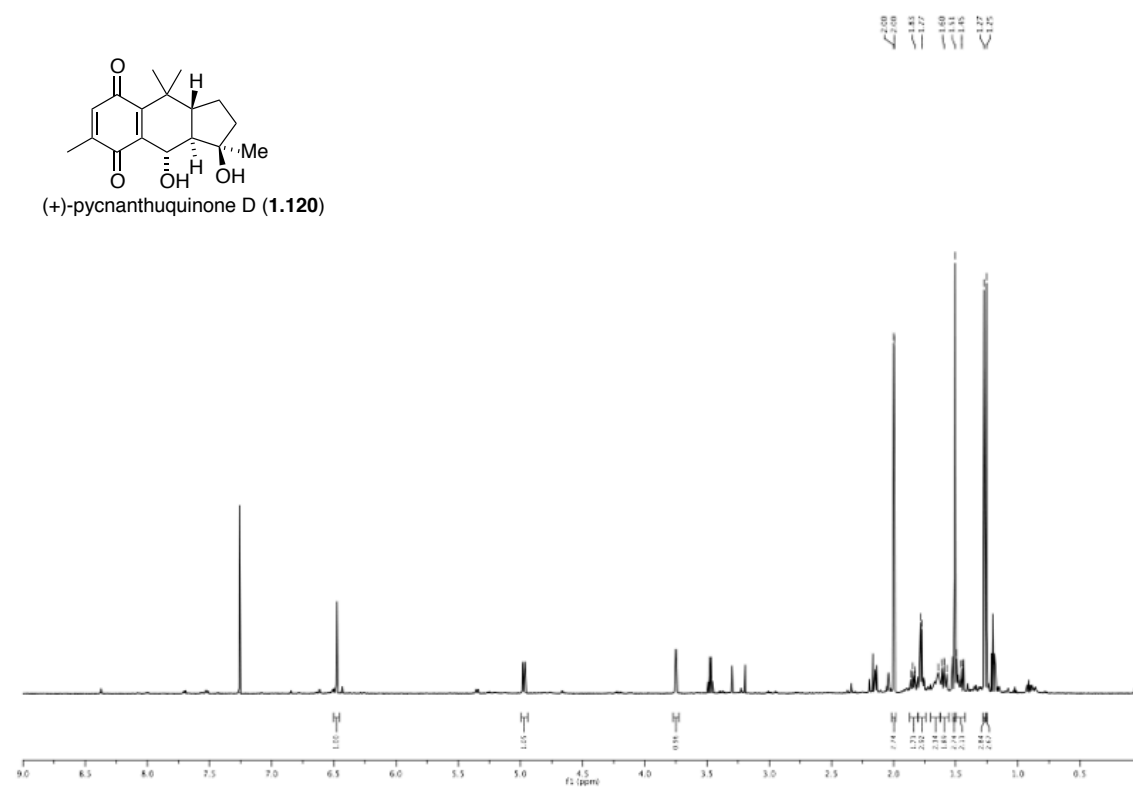
NOE for CH-6 in DMSO



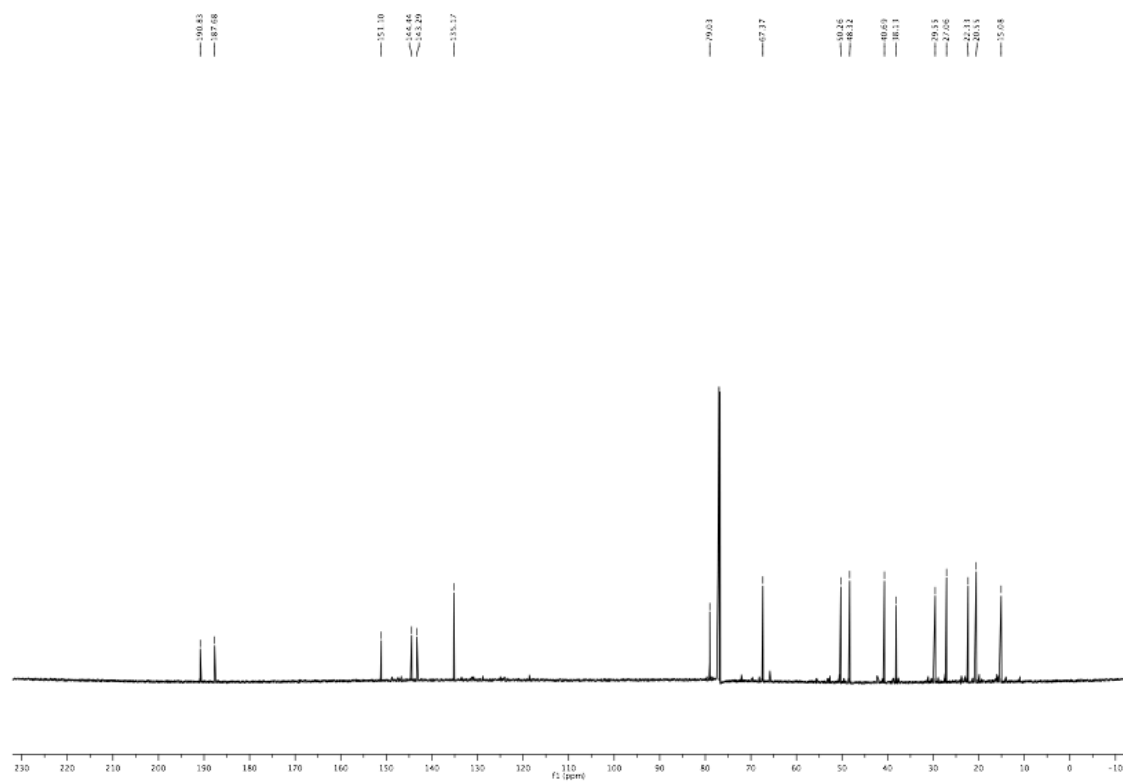
NOE for CH-2 (and CH<sub>3</sub>-9) in DMSO

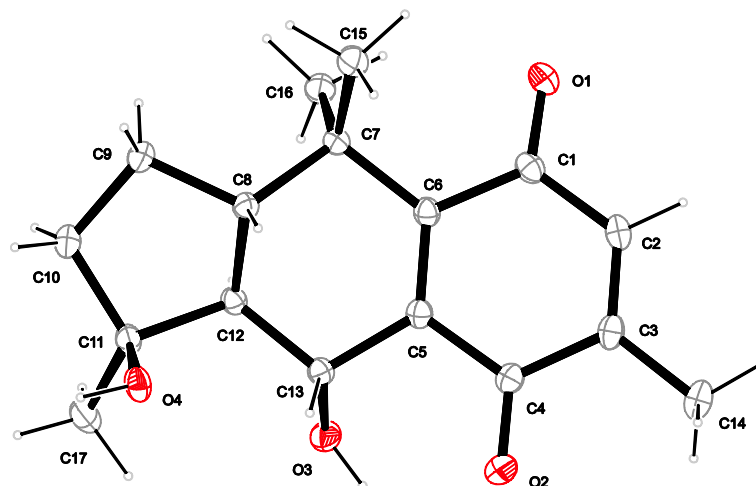
## 1.5. Experimental Section

$^1\text{H}$  NMR,  $\text{CDCl}_3$ , 600 MHz



$^{13}\text{C}$  NMR,  $\text{CDCl}_3$ , 150 MHz



**Figure S1.3:** X-ray crystal structure of pycnanthuquinone D (**1.120**).**Table S1.4:** Crystallographic data for pycnanthuquinone D (**1.120**).

net formula	$C_{17}H_{22}O_4$
$M_r/g\ mol^{-1}$	290.354
crystal size/mm	$0.09 \times 0.08 \times 0.03$
$T/K$	200(2)
radiation	MoK $\alpha$
diffractometer	'KappaCCD'
crystal system	monoclinic
space group	$P2_1/n$
$a/\text{\AA}$	10.1711(4)
$b/\text{\AA}$	8.2989(2)
$c/\text{\AA}$	18.1458(7)
$\alpha/^\circ$	90
$\beta/^\circ$	101.3682(18)
$\gamma/^\circ$	90
$V/\text{\AA}^3$	1501.62(9)
$Z$	4
calc. density/ $g\ cm^{-3}$	1.28435(8)
$\mu/mm^{-1}$	0.090
absorption correction	none

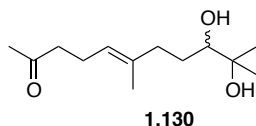
## 1.5. Experimental Section

---

refls. measured	9426
$R_{\text{int}}$	0.0352
mean $\sigma(I)/I$	0.0354
$\theta$ range	3.69–25.37
observed refls.	2161
$x, y$ (weighting scheme)	0.0503, 0.4358
hydrogen refinement	constr
refls in refinement	2728
parameters	196
restraints	0
$R(F_{\text{obs}})$	0.0416
$R_w(F^2)$	0.1110
$S$	1.053
shift/error <sub>max</sub>	0.001
max electron density/e $\text{\AA}^{-3}$	0.233
min electron density/e $\text{\AA}^{-3}$	-0.193

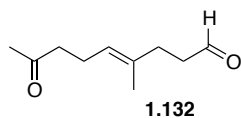


### 1.5.4 Towards the Total Synthesis of Pycnanthuquinones A and B



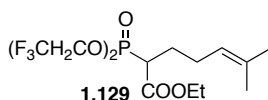
**(E)-9,10-Dihydroxy-6,10-dimethylundec-5-en-2-one (1.130).** To a solution of geranylacetone (**1.127**) (29.1 g, 150 mmol, 2.0 *eq.*) in acetone (200 mL) and H<sub>2</sub>O (50 mL) K<sub>2</sub>OsO<sub>4</sub> (0.276 g, 0.750 mmol, 0.01 *eq.*) and 4-methyl-4-oxide-morpholine (10.5 g, 90.0 mmol, 1.2 *eq.*) were added and the reaction mixture was stirred for 6 h at rt. Subsequently the reaction mixture was quenched with 10 % NaHSO<sub>4</sub> (30 mL), diluted with water and saturated with NaCl. After extraction with EtOAc (3 × 100 mL) combined organic phases were washed with brine and dried over Na<sub>2</sub>SO<sub>4</sub>. Solvents were removed *in vacuo*. Purification by silica gel chromatography (30% EtOAc in hexanes; then switch to 60% EtOAc in hexanes after first dihydroxylated regio-isomer) gave 10.7 g (31%) of diol **1.130** as a colourless oil. The double-bond isomers can be separated by HPLC.

**Data for 1.130:** IR (ATR):  $\tilde{\nu}$  = 3436, 2971, 1710, 1445, 1373, 1241, 1161, 1077, 1046, 935, 849 cm<sup>-1</sup>; <sup>1</sup>H NMR (300 MHz, CDCl<sub>3</sub>)  $\delta$  = 5.16 (t, *J* = 7.1, 1H), 3.34 (dt, *J* = 1.7, 10.3, 1H), 2.48 (t, *J* = 7.3, 2H), 2.37 – 2.00 (m, 9H), 1.64 (s, 3H), 1.63 – 1.32 (m, 2H), 1.21 (d, *J* = 1.1, 3H), 1.17 (d, *J* = 1.1, 3H); <sup>13</sup>C NMR (75 MHz, CDCl<sub>3</sub>)  $\delta$  = 208.9, 136.2, 123.3, 78.1, 73.0, 43.6, 36.7, 29.9, 29.6, 26.4, 23.3, 22.4, 15.9; HRMS (EI) calcd for C<sub>13</sub>H<sub>24</sub>O<sub>3</sub> (M<sup>+</sup>): 228.1725; found: 228.1711.



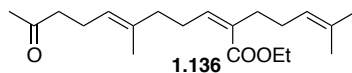
**(E)-4-Methyl-8-oxonon-4-enal (1.132).** To a solution of diol **1.130** (3.42 g, 15 mmol, 1.0 *eq.*) in THF/H<sub>2</sub>O (150 mL, 1:1) was added sodium periodate (9.63 g, 45 mmol, 3.0 *eq.*). The resulting suspension was stirred at rt and reaction progress monitored by TLC. After complete conversion, the reaction mixture was extracted with CH<sub>2</sub>Cl<sub>2</sub> (3 × 100 mL). The combined organic phases were washed with brine, dried over Na<sub>2</sub>SO<sub>4</sub> and concentrated. Purification by silica gel chromatography (17% EtOAc in hexanes) gave 2.50 g (99%) of aldehyde **1.132** as colourless oil.

**Data for 1.132:** IR (ATR):  $\tilde{\nu}$  = 2966, 2916, 2858, 1714, 1441, 1410, 1359, 1268, 1233, 1161, 916, 730, 648  $\text{cm}^{-1}$ ;  $^1\text{H}$  NMR (600 MHz,  $\text{CDCl}_3$ )  $\delta$  = 9.73 (d,  $J$  = 1.9, 1H), 5.10 (t,  $J$  = 7.1, 1H), 2.49 (tt,  $J$  = 1.7, 7.7, 2H), 2.44 (t,  $J$  = 7.4, 2H), 2.30 (t,  $J$  = 7.5, 2H), 2.25 (q,  $J$  = 7.2, 2H), 2.12 (dd,  $J$  = 0.6, 1.1, 3H), 1.62 (s, 3H);  $^{13}\text{C}$  NMR (150 MHz,  $\text{CDCl}_3$ )  $\delta$  = 208.4, 202.3, 134.3, 123.7, 43.4, 42.0, 31.7, 29.9, 22.3, 16.0; HRMS (EI) calcd for  $\text{C}_{10}\text{H}_{17}\text{O}_2$  ( $\text{M}+\text{H}^+$ ): 167.1070; found: 167.1078.



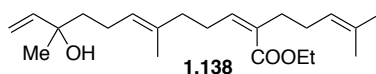
**Phosphonate (1.129).** To a suspension of pure NaH (0.226 g, 9.44 mmol, 1.5 *eq.*) in dry DMSO (8 mL) phosphonium acetate **1.133** (2.00 g, 6.29 mmol, 1.0 *eq.*) was added in small portions while cooling with a water bath to avoid excessive foaming. After stirring for 1 h at *rt*, a solution of bromine **1.134** (1.03 g, 6.29 mmol, 1.0 *eq.*) was added in one portion. The reaction mixture was kept under Ar-atmosphere and stirred for 1 day at *rt*. Subsequently the reaction mixture was poured onto a biphasic system of  $\text{H}_2\text{O}/\text{Et}_2\text{O}$  (100 mL, 1:1). The aqueous phase was extracted with  $\text{Et}_2\text{O}$  ( $3 \times 75$  mL). Combined organic phases were washed with brine, dried over  $\text{Na}_2\text{SO}_4$  and concentrated. Purification by silica gel chromatography (17% EtOAc in hexanes) gave 9.50 mg (38%) of phosphonate **1.129** as a colourless oil.

**Data for 1.129:**  $R_f$  = 0.2 (17 % EtOAc in hexanes); IR (ATR):  $\tilde{\nu}$  = 3350, 2969, 2932, 1721, 1454, 1418, 1378, 1290, 1248, 1167, 1103, 1065, 962, 844, 711, 660  $\text{cm}^{-1}$ ;  $^1\text{H}$  NMR (400 MHz,  $\text{CDCl}_3$ )  $\delta$  = 5.01 (t,  $J$ =6.5, 1H), 4.46 – 4.30 (m, 4H), 4.25 – 4.14 (m, 2H), 3.08 (ddd,  $J$  = 3.7, 10.0, 22.2, 1H), 2.14 – 1.94 (m, 3H), 1.94 – 1.78 (m, 1H), 1.67 (s, 3H), 1.56 (s, 3H), 1.27 (t,  $J$  = 7.1, 3H);  $^{13}\text{C}$  NMR (100 MHz,  $\text{CDCl}_3$ )  $\delta$  = 167.98, 167.94, 134.14, 121.74, 63.26 – 61.80 (m), 62.01, 45.49, 44.14, 26.83 (d,  $J^{\text{C-P}}$  = 67.4, 1C), 26.21 (d,  $J^{\text{C-P}}$  = 57.2, 1C), 25.61, 23.77, 17.54, 13.89; HRMS (EI) calcd for  $\text{C}_{14}\text{H}_{21}\text{F}_6\text{O}_5\text{P}$  ( $\text{M}-\text{H}^+$ ): 413.0950; found: 413.0951.



**(2Z,6E)-Ethyl 6-Methyl-2-(4-methylpent-3-enyl)-10-oxoundeca-2,6-dienoate (1.136).** To a solution of 18-crown-6 ether (4.32 g, 16.4 mmol, 5.0 *eq.*) in THF (30 mL) was added phosphonium acetate **1.129** (1.36 g, 3.27 mmol, 1.0 *eq.*). After cooling to  $-78$  °C, KHMDs (6.31 g, 3.6 mmol, 1.1 *eq.*) was added slowly and reaction stirred for 1 h. Subsequently aldehyde **1.132** (0.550 g, 3.27 mmol, 1.0 *eq.*) was added slowly over 10 min. The reaction mixture was stirred at  $-78$  °C for 3 h and then allowed to warm up to  $-10$  °C slowly until all starting material disappeared. The solution was poured onto a biphasic system of ice brine/Et<sub>2</sub>O (150 mL 1:1) and the aqueous phase extracted successively with Et<sub>2</sub>O (3 × 80 mL). The combined organic phases were washed with brine (1 × 50 mL), dried over Na<sub>2</sub>SO<sub>4</sub> and concentrated. Purification by silica gel chromatography (10% EtOAc in hexanes) gave 714 mg (68%) of title compound **1.136** as a colourless oil.

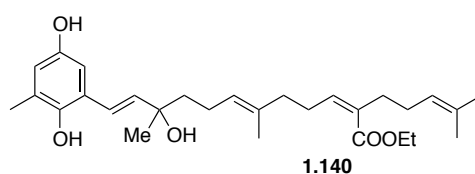
**Data for 1.136:** R<sub>f</sub> = 0.47 (17% EtOAc in hexanes); IR (ATR):  $\tilde{\nu}$  = 3507, 2968, 2923, 2857, 1704, 1642, 1446, 1377, 1208, 1184, 1153, 1121, 1029, 753, 667 cm<sup>-1</sup>; <sup>1</sup>H NMR (600 MHz, CDCl<sub>3</sub>)  $\delta$  = 5.83 – 5.76 (m, 1H), 5.11 – 5.03 (m, 2H), 4.18 (qd, *J* = 1.4, 7.1, 2H), 2.52 – 2.45 (m, 2H), 2.43 (t, *J* = 7.5, 2H), 2.21 – 2.27 (m, 4H), 2.11 (d, *J* = 2.2, 3H), 2.08 – 2.00 (m, 3H), 1.66 (d, *J* = 1.3, 3H), 1.28 (t, *J* = 7.1, 3H); <sup>13</sup>C NMR (150 MHz, CDCl<sub>3</sub>)  $\delta$  = 208.6, 168.0, 141.3, 135.8, 131.8, 124.5, 123.5, 60.0, 51.5, 44.6, 39.1, 34.8, 27.9, 24.3, 22.5, 17.6, 15.9, 14.3; HRMS (EI) calcd for C<sub>20</sub>H<sub>32</sub>O<sub>3</sub> (M<sup>+</sup>): 320.2351; found: 320.2340.



**(2Z,6E)-Ethyl 10-Hydroxy-6,10-dimethyl-2-(4-methylpent-3-enyl)dodeca-2,6,11-trienoate (1.138)** To a solution of keto ester **1.136** (1.65 g, 5.15 mmol, 1.0 *eq.*) in dry THF was slowly added vinylmagnesium bromide (7.57 g, 7.72 mmol, 1.5 *eq.*) at  $-78$  °C. The reaction mixture was stirred at  $-78$  °C for 5 h, then warmed to  $-40$  °C and stirred for 1.5 h. Subsequently the solution was allowed to warm to *rt* and stirring was continued over night. Purification by silica gel chromatography (10 % Et<sub>2</sub>O in hexanes) afforded 688 mg (38%) of vinyl alcohol **1.138** as colourless oil.

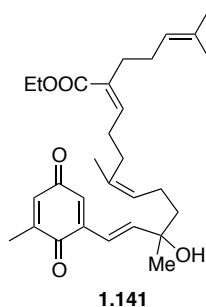
**Data for 1.138:** IR (ATR):  $\tilde{\nu}$  = 3494, 2971, 2925, 2857, 1704, 1641, 1447, 1377,

1207, 1183, 1154, 1112, 1029, 996, 829, 755, 690, 667;  $^1\text{H}$  NMR (600 MHz,  $\text{CDCl}_3$ )  $\delta$  = 5.90 (dd,  $J$  = 10.8, 17.3, 1H), 5.80 (t,  $J$  = 7.3, 1H), 5.20 (dd,  $J$  = 1.3, 17.3, 1H), 5.14 (t,  $J$  = 7.2, 1H), 5.08 (t,  $J$  = 7.2, 1H), 5.05 (dd,  $J$  = 1.3, 10.8, 1H), 4.19 (q,  $J$  = 7.1, 2H), 2.50 (dd,  $J$  = 7.4, 15.1, 2H), 2.25 – 2.20 (m, 2H), 2.16 (s, 1H, OH), 2.10 – 1.99 (m, 6H), 1.67 (d,  $J$  = 1.1, 3H), 1.61 – 1.54 (m, 8H), 1.29 (t,  $J$  = 7.1, 3H), 1.27 (s, 3H);  $^{13}\text{C}$  NMR (150 MHz,  $\text{CDCl}_3$ )  $\delta$  = 168.1, 145.0, 141.4, 134.8, 132.0, 131.8, 124.8, 123.5, 111.7, 73.4, 59.9, 42.0, 39.2, 34.7, 27.9, 27.9, 27.8, 25.6, 22.6, 17.6, 15.9, 14.3; HRMS (EI) calcd for  $\text{C}_{22}\text{H}_{36}\text{O}_3$  ( $\text{M}^+$ ): 348.2665; found: 348.2658.



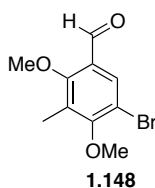
**(2Z,6E,11E)-Ethyl 12-(2,5-Dihydroxy-3-methylphenyl)-10-hydroxy-6,10-dimethyl-2-(4-methylpent-3-en-1-yl)dodeca-2,6,11-trienoate (1.140).** To a stirred solution of bromohydroquinone **1.118** (107 mg, 0.525 mmol, 1.5 *eq.*) in DMF (1.5 mL) was added finely ground  $\text{Na}_2\text{CO}_3$  (148 mg, 1.4 mmol, 4.0 *eq.*), tetrabutylammonium chloride (126 mg, 0.455 mmol, 1.3 *eq.*) and palladium(II)acetate (7.86 mg, 0.035 mmol, 0.1 *eq.*). The mixture was degassed with argon for 10 min. Subsequently allylic alcohol **1.138** (122 mg, 0.35 mmol, 1.0 *eq.*) was added and the reaction mixture heated to 80 °C for 2 h. The resulting mixture was filter over a pad of silica (EtOAc 200 mL) and the combined phases were concentrated using a rotary evaporator at rt. The resulting oil was submitted to silica gel chromatography (25%  $\text{Et}_2\text{O}$  in hexanes) yielding 70 mg (43%) of hydroquinone **1.140** as colourless solid.

**Data for 1.140:**  $^1\text{H}$  NMR (400 MHz,  $\text{CDCl}_3$ )  $\delta$  = 6.78 (d,  $J$  = 16.1, 1H), 6.68 (d,  $J$  = 3.0, 1H), 6.55 (d,  $J$  = 2.3, 1H), 6.17 (d,  $J$  = 16.1, 1H), 5.81 (t,  $J$  = 7.3, 1H), 5.15 (td,  $J$  = 1.1, 7.2, 1H), 5.11 – 5.05 (m, 1H), 4.20 (q,  $J$  = 7.1, 2H), 2.51 (dd,  $J$  = 7.3, 15.0, 2H), 2.39 – 2.15 (m, 6H), 2.14 – 1.97 (m, 6H), 1.74 – 1.54 (m, 11H), 1.37 (s, 3H), 1.30 (t,  $J$  = 7.1, 3H);  $^{13}\text{C}$  NMR (101 MHz,  $\text{cdcl}_3$ )  $\delta$  = 168.5, 149.1, 145.2, 141.7, 138.5, 135.0, 132.1, 131.8, 125.6, 124.76, 124.7, 123.5, 121.5, 116.9, 110.7, 73.8, 60.2, 42.4, 39.1, 34.7, 28.5, 28.0, 27.9, 25.7, 22.9, 17.7, 16.2, 16.1, 14.3; HRMS (EI) calcd for  $\text{C}_{29}\text{H}_{41}\text{O}_5$  ( $\text{M}-\text{H}^+$ ): 469.2950; found: 469.2954.



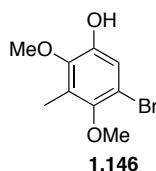
**(2Z,6Z,11E)-ethyl 10-hydroxy-6,10-dimethyl-12-(5-methyl-3,6-dioxocyclohexa-1,4-dien-1-yl)-2-(4-methylpent-3-en-1-yl)dodeca-2,6,11-trienoate (1.141).** To a solution of manganese(IV)oxide (332 mg, 3.82 mmol, 40 *eq.*) in CH<sub>2</sub>Cl<sub>2</sub> was added vinyl hydroquinone **1.140** (45.0 mg, 0.096 mmol, 1.0 *eq.*). The mixture was stirred at *rt* for 1 h and filtered over celite (CH<sub>2</sub>Cl<sub>2</sub>). The filtrate was concentrated using a rotary evaporator at *rt* and the resulting residue was submitted to preparative TLC (33% EtOAc in hexanes). Purification afforded 23 mg (51%, 0.049 mmol) of quinone **1.141** as orange oil.

**Data for 1.141:** <sup>1</sup>H NMR (600 MHz, CDCl<sub>3</sub>) δ = 6.46 (q, *J* = 1.5, 1H), 5.64 (t, *J* = 7.2, 1H), 5.03 (t, *J* = 7.2, 1H), 4.95 (dd, *J* = 2.1, 9.6, 1H), 4.11 (q, *J* = 7.1, 2H), 3.80 – 3.59 (m, 1H), 3.76 (d, *J* = 2.2, 1H), 3.67 (dd, *J* = 5.9, 7.9, 1H), 2.38 (m, 2H), 2.23 – 1.69 (m, 6H), 2.16 (s, 3H), 2.00 (d, *J* = 1.6, 3H), 1.66 (s, 3H), 1.64 – 1.40 (m, 4H), 1.49 (s, 3H), 1.25 (s, 3H), 1.24 (t, *J* = 7.1, 3H); HRMS (EI) calcd for C<sub>29</sub>H<sub>40</sub>O<sub>5</sub> (M<sup>+</sup>): 468.2876; found: 468.2881.



**5-Bromo-2,4-dimethoxy-3-methylbenzaldehyde (1.148).** To a solution of 2,4-dimethoxy-3-methylbenzaldehyde (3.60 g, 20.0 mmol, 1.0 *eq.*), NaOAc(6.89 g, 84 mmol, 4.2 *eq.*) in acetic acid (15 mL) was added a solution of Br<sub>2</sub> (6.71 g, 2.15 mL, 42.0 mmol, 2.1 *eq.*) in acetic acid (7 mL) at *rt*. The reaction mixture was heated to 80 °C for 1.5 h and the concentrated *in vacuo*. The resulting residue was treated with cold water H<sub>2</sub>O, upon which a colourless precipitate formed, which was then filtered off and washed with water and submitted to silica gel chromatography (10% EtOAc in hexanes) to give 4.57 g (88%) of title compound **1.148** as a colourless solid.

**Data for 1.148:**  $^1\text{H}$  NMR (600 MHz,  $\text{CDCl}_3$ )  $\delta$  = 10.22 (s, 1H), 7.90 (d,  $J$  = 0.6, 1H), 3.87 (s, 3H), 3.86 (s, 3H), 2.29 (d,  $J$  = 0.6, 3H);  $^{13}\text{C}$  NMR (150 MHz,  $\text{CDCl}_3$ )  $\delta$  = 188.1, 162.2, 161.4, 130.4, 128.0, 126.7, 113.5, 63.4, 60.5, 9.8; HRMS (EI) calcd for  $\text{C}_{10}\text{H}_{11}\text{BrO}_3$  ( $\text{M}^-$ ): 257.9892; found: 257.9891.

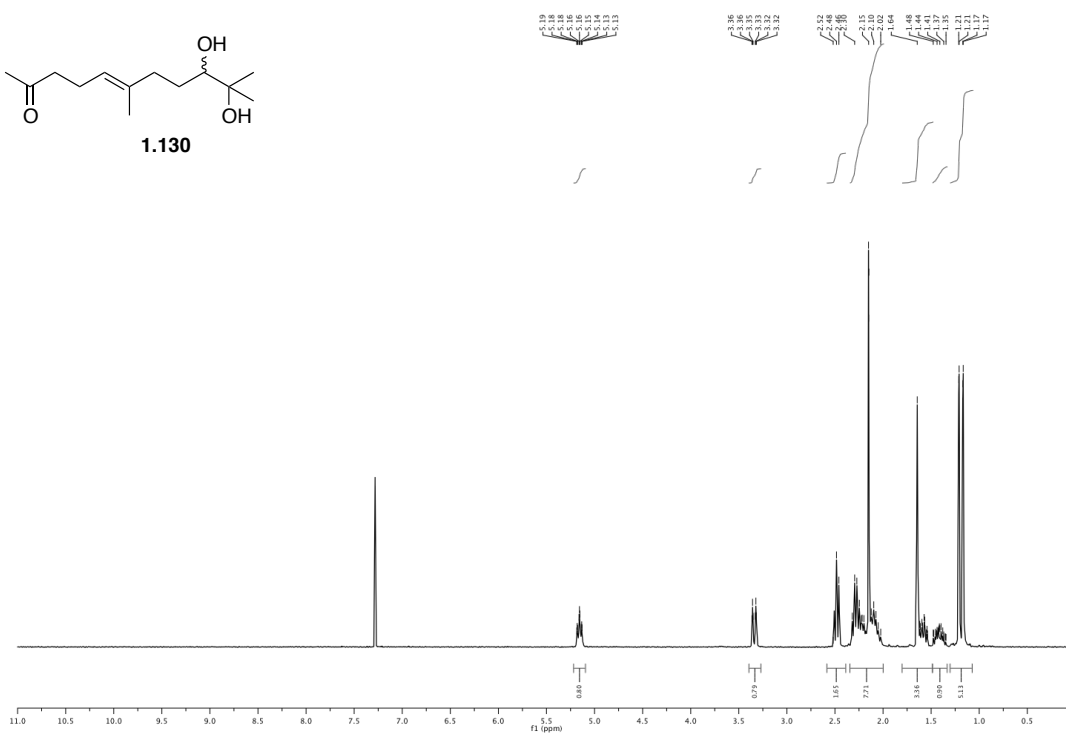
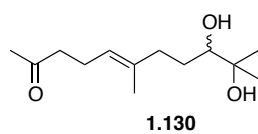


**5-Bromo-2,4-dimethoxy-3-methylphenol (1.146).** A solution of 5-bromo-2,4-dimethoxy-3-methylbenzaldehyde (**1.148**) (2.59 g, 10.0 mmol, 1.0 *eq.*) in  $\text{CH}_2\text{Cl}_2$  (5 mL) was added to a solution of *m*CPBA (2.96 g, 12.0 mmol, 1.2 *eq.*) at 0 °C. The mixture was continued to stir for 3 h at room temperature, upon which a colourless precipitate formed. The reaction mixture was washed with  $\text{NaHCO}_3$  sltn. (sat.  $3 \times 30$  mL). The organic phase was concentrated and the residue was taken up in MeOH (15 mL), which was added to a solution of KOH (0.84 g, 15 mmol, 1.5 *eq.*) in MeOH (20 mL) at 0 °C. After 20 min, the reaction mixture was neutralised with 2 N HCl and extracted with EtOAc ( $3 \times 50$  mL). Combined organic phases were washed with brine, dried over  $\text{Na}_2\text{SO}_4$  and concentrated. The resulting residue was purified by silica gel chromatography (16% EtOAc in hexanes) to furnish 1.43 g (58%) of title compound **1.146**.

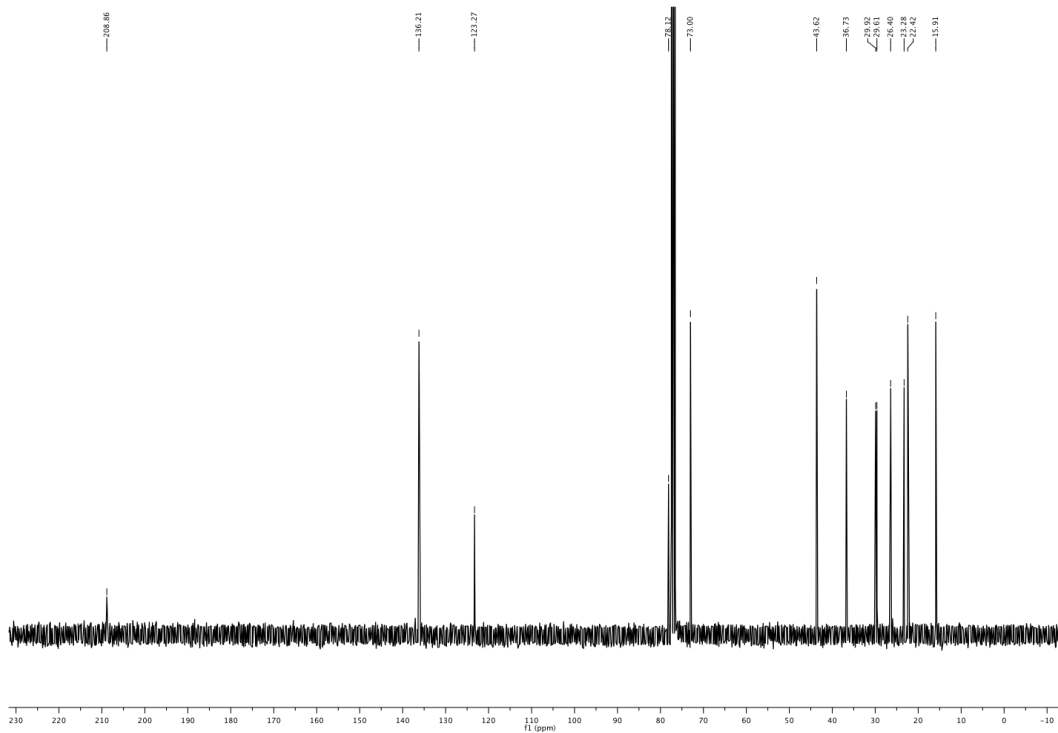
**Data for 1.146:** IR (ATR):  $\tilde{\nu}$  = 3374, 1659, 1592, 1473, 1451, 1410, 1342, 1280, 1231, 1194, 1158, 1087, 1029, 987, 891;  $^1\text{H}$  NMR (300 MHz,  $\text{CDCl}_3$ )  $\delta$  = 7.04 (s, 1H), 5.45 (s, 1H), 3.79 (d,  $J$  = 6.1, 6H), 2.30 (d,  $J$  = 0.6, 3H);  $^{13}\text{C}$  NMR (75 MHz,  $\text{CDCl}_3$ )  $\delta$  = 149.0, 145.8, 145.1, 126.0, 116.4, 112.0, 60.8, 60.5, 10.3; HRMS (EI) calcd for  $\text{C}_9\text{H}_{11}\text{BrO}_3$  ( $\text{M}^-$ ): 245.9892; found: 245.9894.

# 1. VINYL QUINONE DIELS-ALDER REACTIONS

$^1\text{H NMR}$ ,  $\text{CDCl}_3$ , 300 MHz

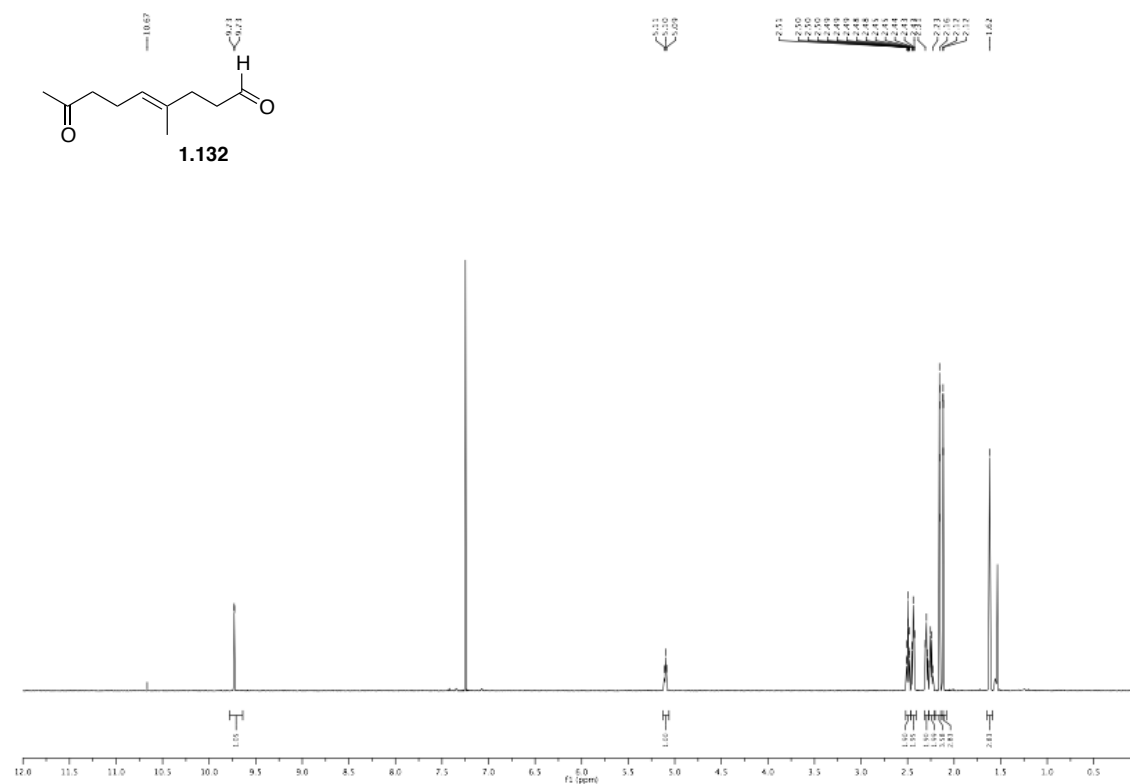


$^{13}\text{C NMR}$ ,  $\text{CDCl}_3$ , 150 MHz

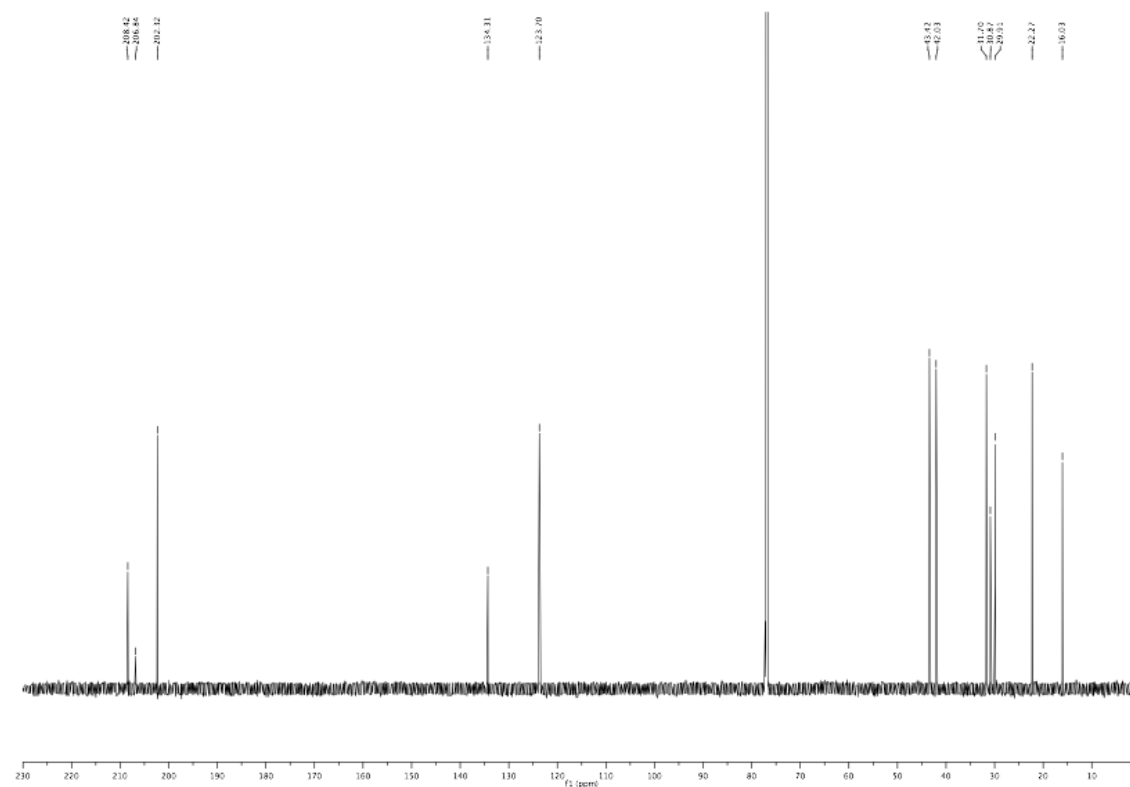


## 1.5. Experimental Section

$^1\text{H}$  NMR,  $\text{CDCl}_3$ , 300 MHz



$^{13}\text{C}$  NMR,  $\text{CDCl}_3$ , 150 MHz



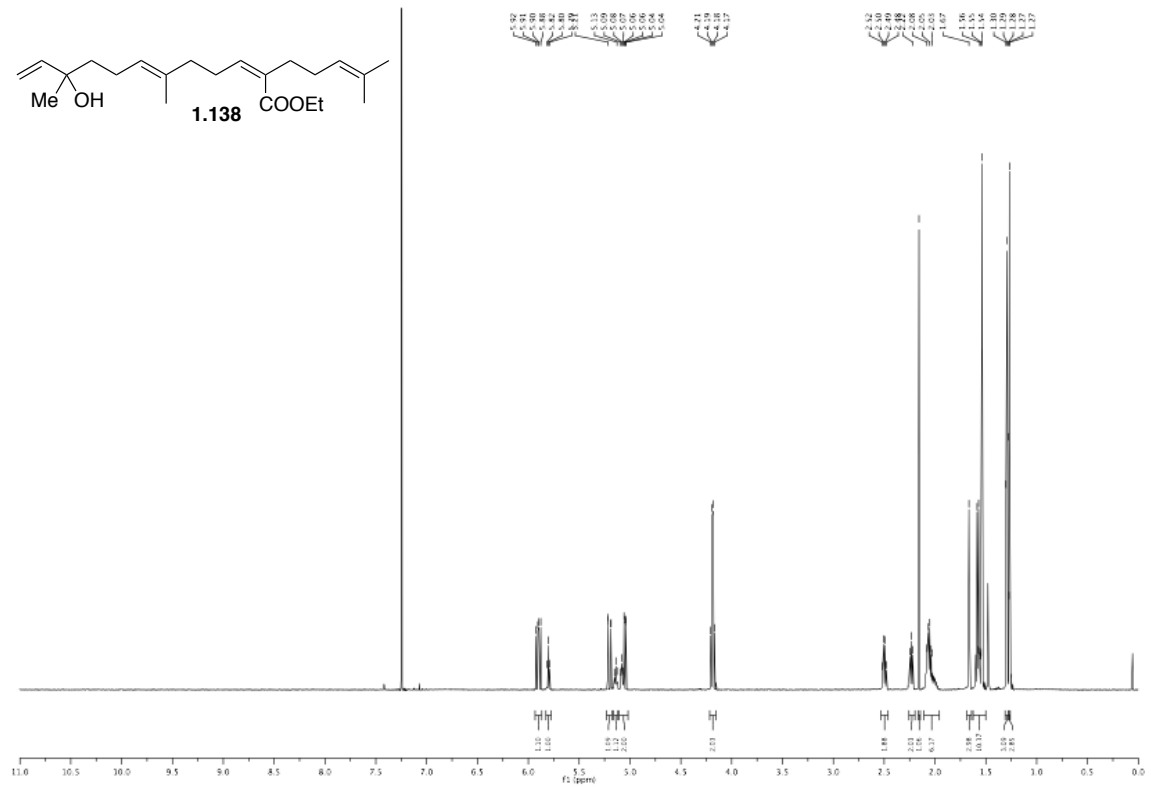




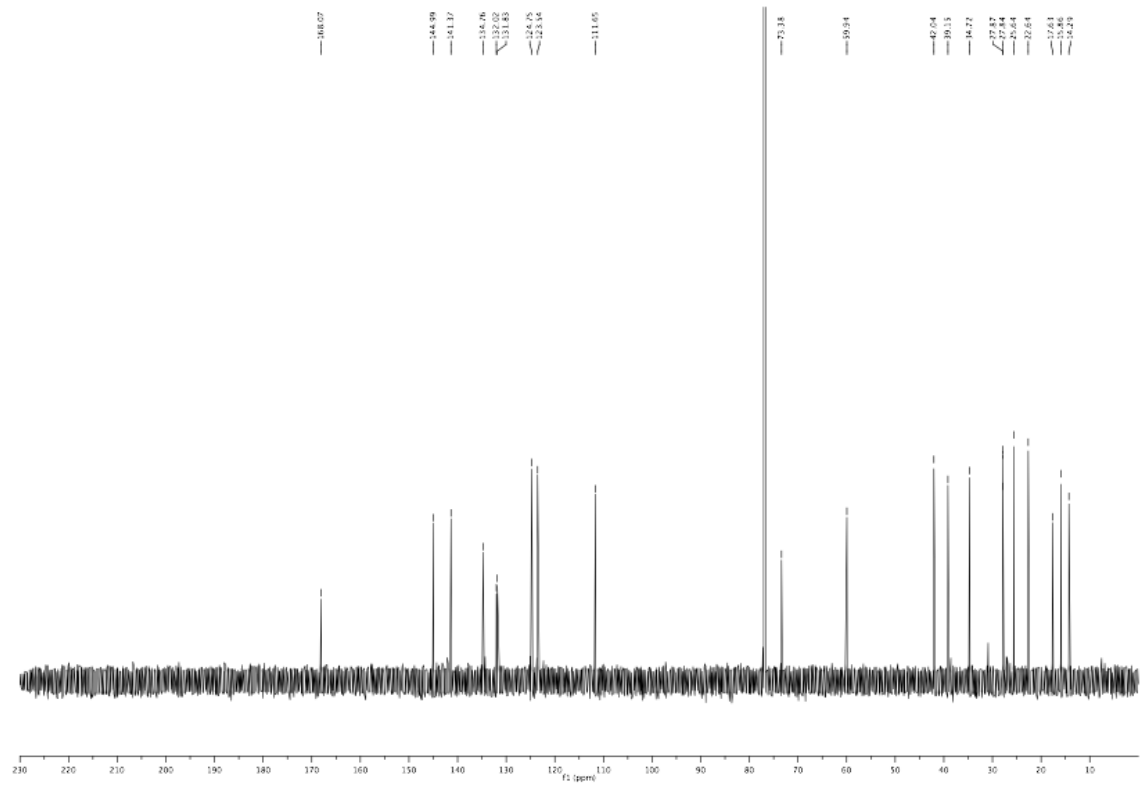


# 1. VINYL QUINONE DIELS-ALDER REACTIONS

$^1\text{H}$  NMR,  $\text{CDCl}_3$ , 300 MHz



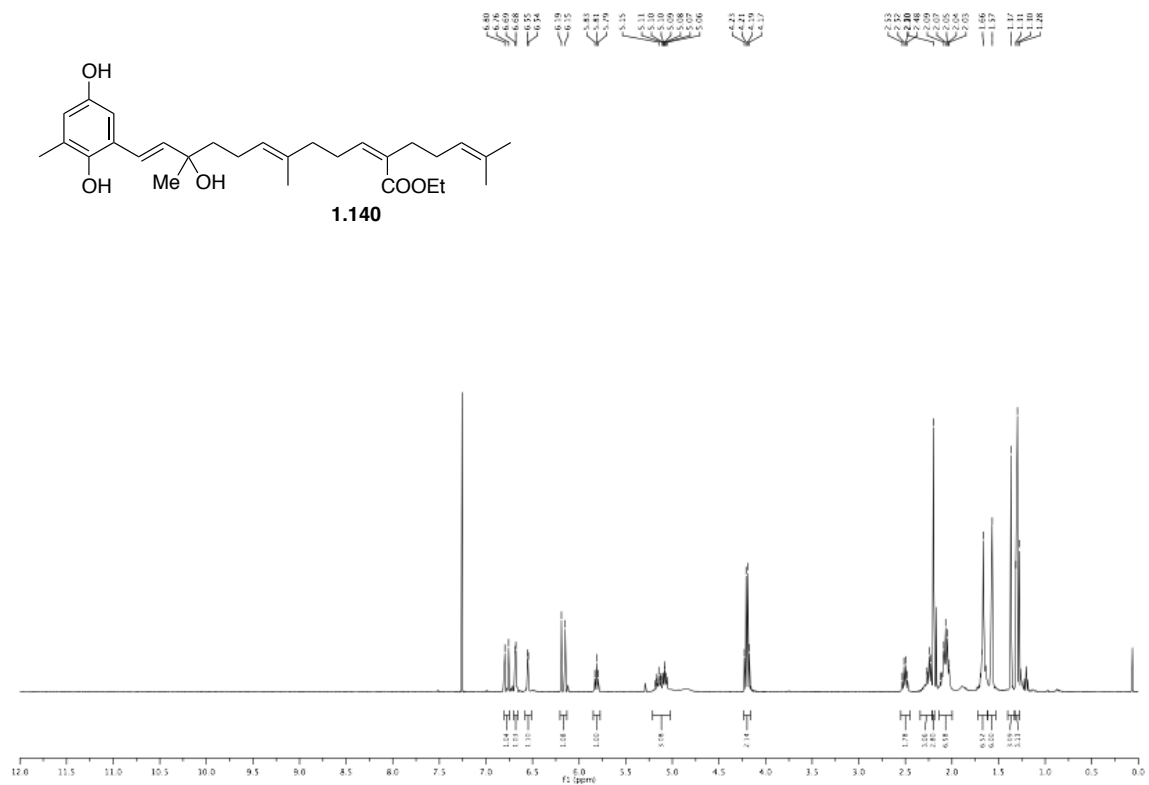
$^{13}\text{C}$  NMR,  $\text{CDCl}_3$ , 150 MHz



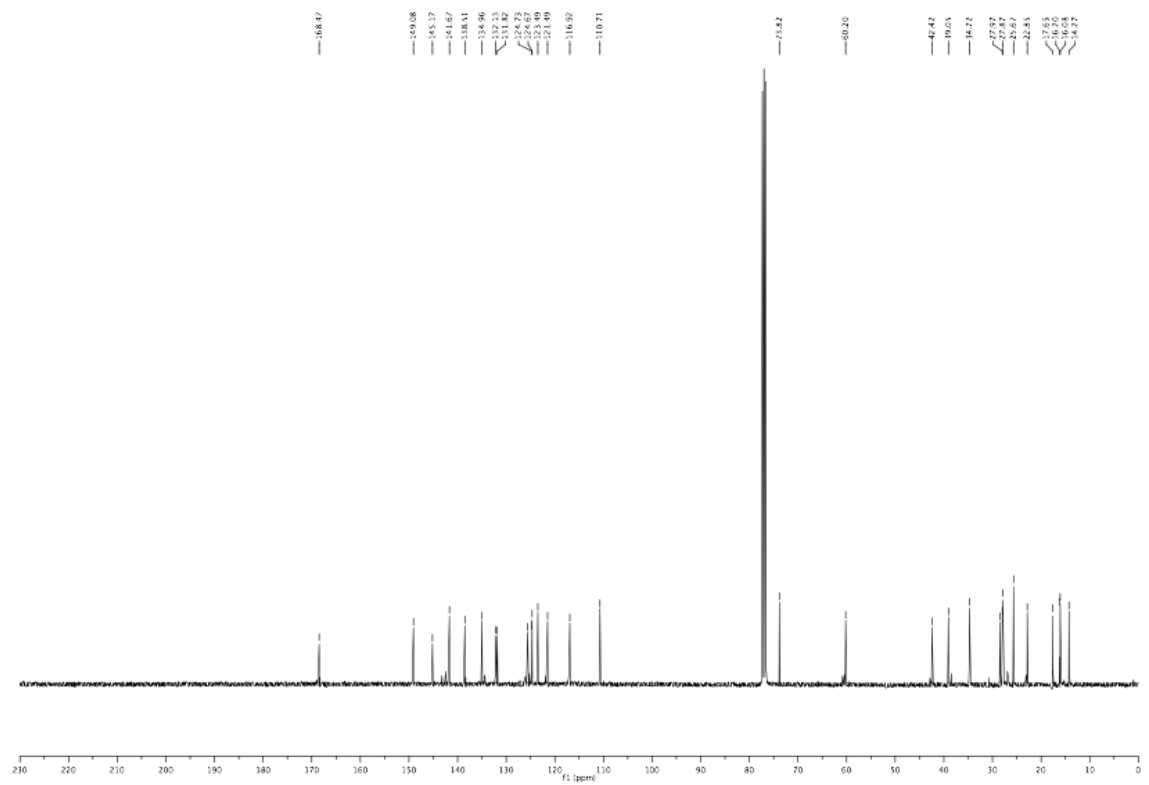


# 1. VINYL QUINONE DIELS-ALDER REACTIONS

$^1\text{H NMR}$ ,  $\text{CDCl}_3$ , 400 MHz

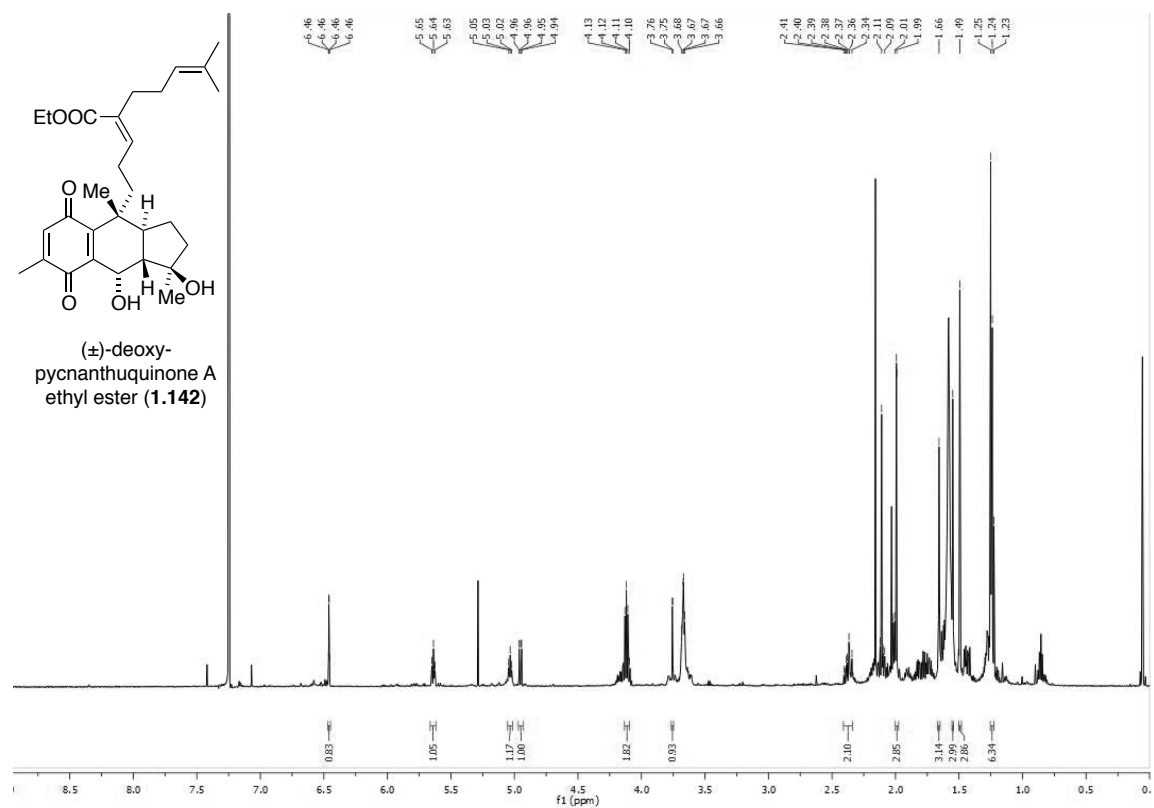


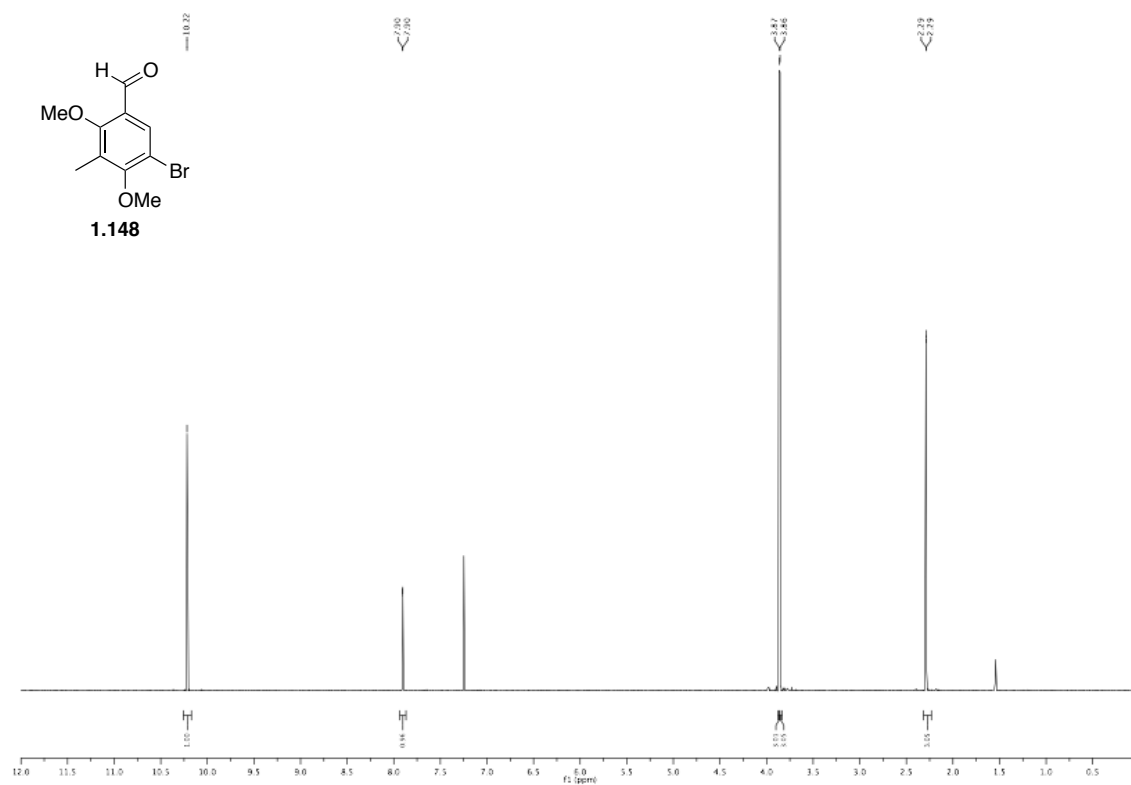
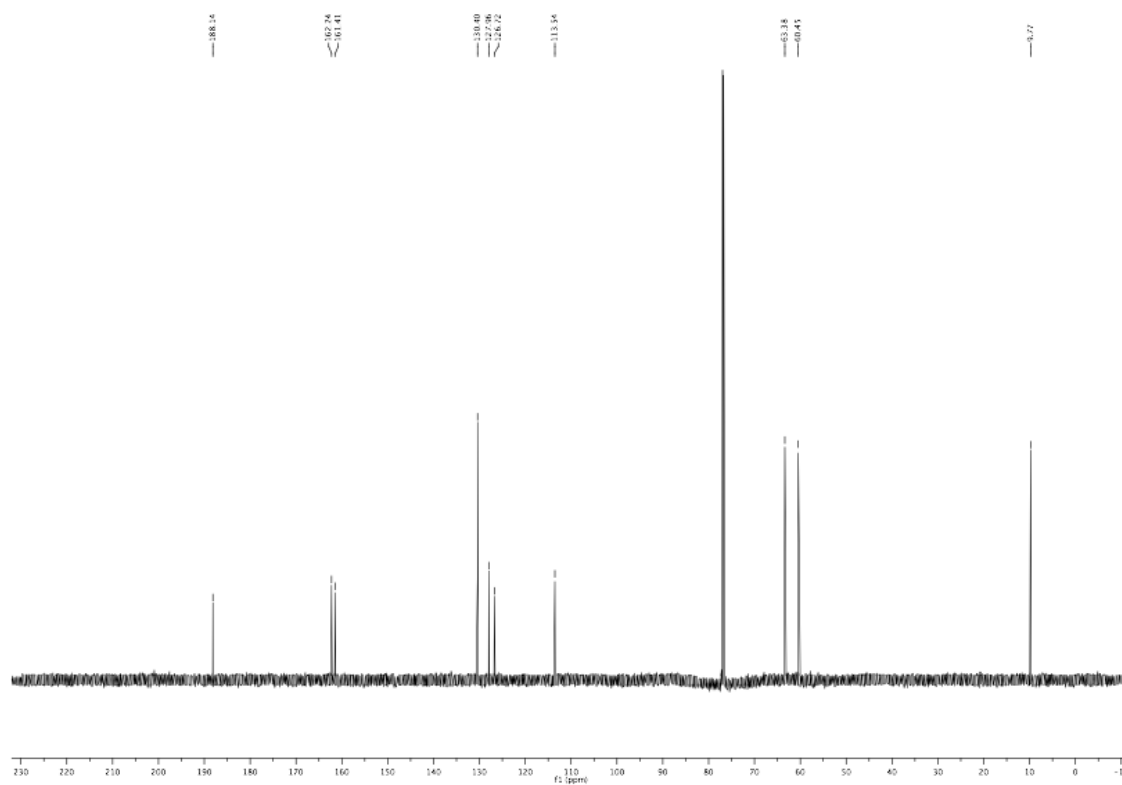
$^{13}\text{C NMR}$ ,  $\text{CDCl}_3$ , 100 MHz



## 1.5. Experimental Section

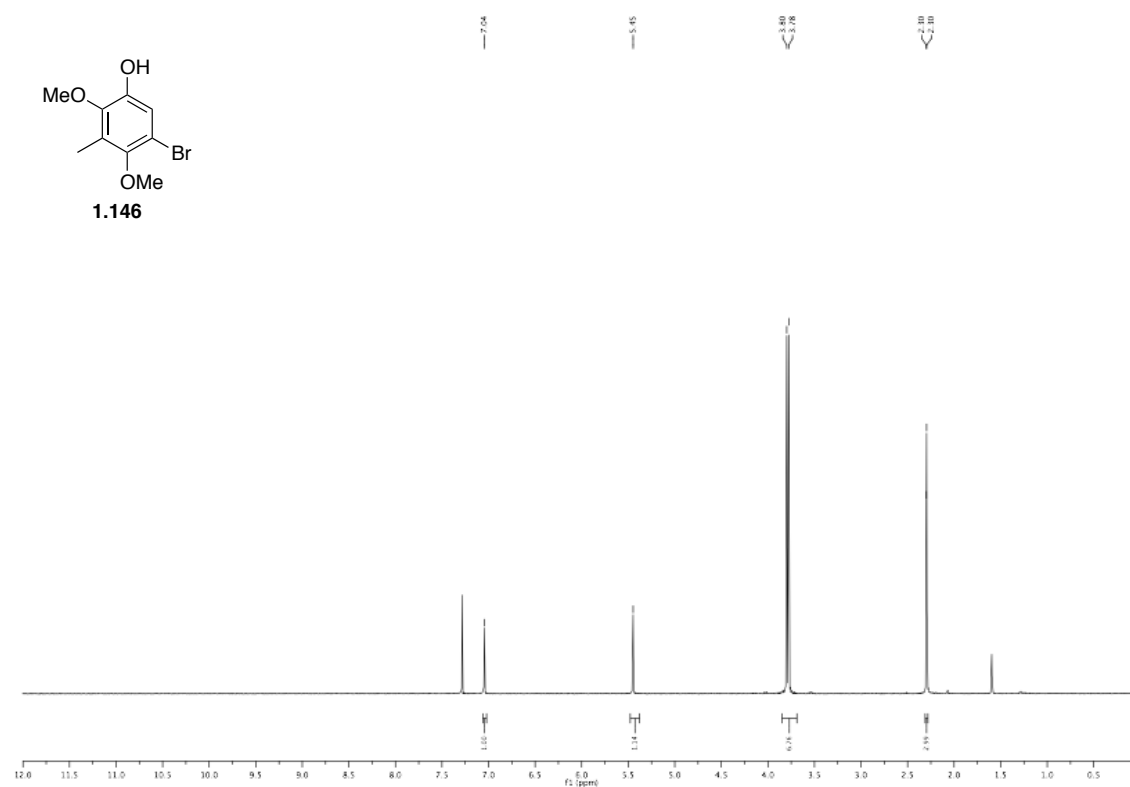
$^1\text{H}$  NMR,  $\text{CDCl}_3$ , 300 MHz



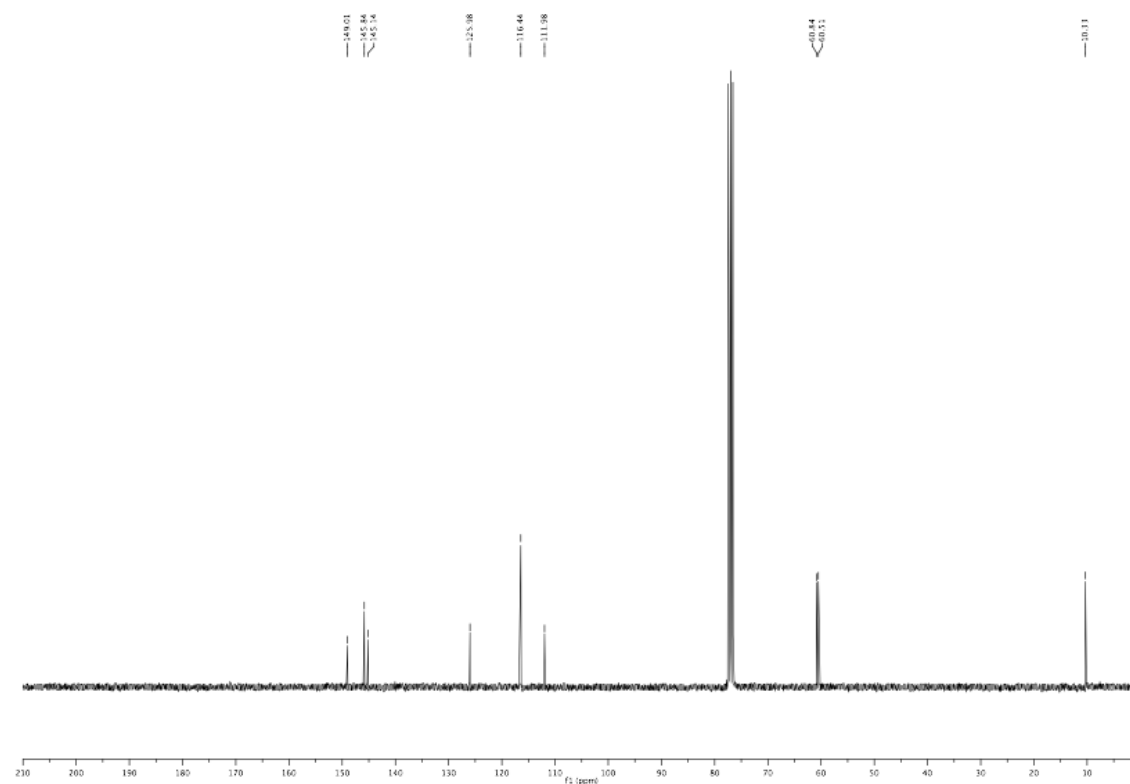
$^1\text{H}$  NMR,  $\text{CDCl}_3$ , 600 MHz $^{13}\text{C}$  NMR,  $\text{CDCl}_3$ , 150 MHz

## 1.5. Experimental Section

$^1\text{H}$  NMR,  $\text{CDCl}_3$ , 600 MHz

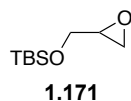


$^{13}\text{C}$  NMR,  $\text{CDCl}_3$ , 150 MHz



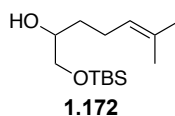


## 1.5.5 Towards the Total Synthesis of Glaziovianol



**Tert-butyldimethyl(oxiran-2-ylmethoxy)silane 1.171.** Glycidol (**1.170**) (5.36 g, 72.4 mmol, 1.0 *eq.*), TBSCl (16.8 g, 111 mmol, 1.5 *eq.*) and imidazole (7.59 g, 111 mmol, 1.5 *eq.*) were dissolved in THF (100 mL). The reaction mixture was stirred at room temperature over night. The resulting precipitate was filtered off over a plug of celite and the solution was concentrated. The resulting residue was purified by silica gel chromatography (10% EtOAc in hexanes) to yield 13.0 g (95%) of title compound **1.171** as colourless oil.

**Data for 1.171:** IR (ATR):  $\tilde{\nu}$  = 2929 (w), 2857 (w), 1737 (w), 1472 (w), 1252 (m), 1095 (m);  $^1\text{H NMR}$  (600 MHz,  $\text{CDCl}_3$ )  $\delta$  = 3.85 (dd,  $J$  = 3.3, 11.9, 1H), 3.66 (dd,  $J$  = 4.8, 11.9, 1H), 3.12 – 3.05 (m, 1H), 2.76 (dd,  $J$  = 4.0, 5.1, 1H), 2.63 (dd,  $J$  = 2.7, 5.2, 1H), 0.90 (s, 9H), 0.08 (d,  $J$  = 2.6, 6H);  $^{13}\text{C NMR}$  (75 MHz,  $\text{CDCl}_3$ )  $\delta$  = 63.7, 52.4, 44.4, 25.8, 18.3, -5.3, -5.4 (signal overlapping); MS (EI) calcd for  $\text{C}_8\text{H}_{17}\text{O}_2\text{Si}^-$  ( $\text{M}-\text{CH}_3^+$ ): 173.1003; found: 173.0975.



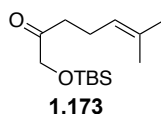
**Preparation of a Prenylmagnesium Chloride Solution.** Prenylchloride (13.5 mL, 0.12 mol, 1.0 *eq.*) was diluted with THF (30 mL). To a suspension of magnesium turnings (4.37 g, 180 mmol, 1.5 *eq.*) in THF (60 mL) was added one small  $\text{I}_2$  crystal and the mixture was briefly heated to etch the Mg. After the colour of  $\text{I}_2$  disappeared, prenylchloride solution (2 mL) was added at room temperature to initiate the reaction. The reaction mixture was then immediately cooled to  $-15\text{ }^\circ\text{C}$  and the remaining prenylchloride solution was added via a syringe pump over 2 h (injection rate: 20 mL/h) at  $-15\text{ }^\circ\text{C}$ . Upon completion of addition the reaction mixture was continued to stir for 30 min at  $-15\text{ }^\circ\text{C}$  and subsequently warmed to room temperature resulting in a grey suspension with slight precipitation was obtained. The GRIGNARD solution was separated from the precipitate by

cannulation into an appropriate SCHLENCK-flask. Titration usually gave a concentration in the range of 0.90 – 1.00 M. The GRIGNARD solution was used within 1 h after preparation.

**1-((*tert*-butyldimethylsilyl)oxy)-6-methylhept-5-en-2-ol (1.172).**

To a suspension of **1.171** (6.25 g, 33.2 mmol, 1.0 *eq.*) and CuI (0.63 g, 3.32 mmol, 0.1 *eq.*) in anhydrous THF (150 mL) was added a prenylmagnesium chloride solution (0.92 M, 43.3 mL, 39.8 mmol, 1.2 *eq.*) drop wise by a syringe pump at  $-60\text{ }^{\circ}\text{C}$  over 1 h. After warming to  $-40\text{ }^{\circ}\text{C}$  within 2 h, the reaction mixture was stirred at  $-20\text{ }^{\circ}\text{C}$  over night. Crushed ice was added and the mixture warmed to rt. The mixture was treated with sat.  $\text{NH}_4\text{Cl}$  solution (60 mL) and the aqueous phase was extracted with EtOAc ( $4 \times 50\text{ mL}$ ). Combined organic phases were washed with  $\text{NaHCO}_3$  solution (50 mL) and brine (50 mL), dried over  $\text{Na}_2\text{SO}_4$  and concentrated to yield 8.50 g (99%) of title compound (**1.172**).

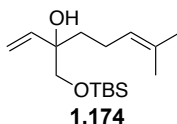
**Data for (1.172):**  $R_f = 0.17$  (1%  $\text{Et}_2\text{O}$  in hexanes); IR (ATR):  $\tilde{\nu} = 3452$  (w, br), 2955 (m), 2927 (m), 2856 (m), 1743 (w), 1472 (w), 1463 (w), 1376 (w), 1252 (m), 1106 (m), 1076 (m), 1005 (w), 939 (w)  $\text{cm}^{-1}$ ;  $^1\text{H NMR}$  (600 MHz,  $\text{CDCl}_3$ )  $\delta = 5.12$  (t,  $J = 7.1$ , 1H), 3.71 – 3.53 (m, 2H), 3.40 (dd,  $J = 8.2, 10.7$ , 1H), 2.38 (d,  $J = 3.3$ , 1H), 2.20 – 2.01 (m, 2H), 1.69 (s, 3H), 1.62 (s, 3H), 1.43 (dd,  $J = 6.9, 18.2$ , 2H), 0.90 (s, 9H), 0.07 (s, 6H);  $^{13}\text{C NMR}$  150 MHz,  $\text{CDCl}_3$ )  $\delta = 132.0, 124.0, 71.4, 67.2, 32.9, 25.9, 25.7, 24.1, 18.3, 17.6, -5.3, -5.4$  (two signals overlapping); MS (EI) calcd for  $\text{C}_{14}\text{H}_{30}\text{O}_2\text{Si}$  ( $\text{M}^+$ ): 258.2015; found: 258.2010.



**1-((*Tert*-butyldimethylsilyl)oxy)-6-methylhept-5-en-2-one (1.173).** In a 500 mL three necked round bottomed flask equipped with an internal thermometer oxalyl chloride (34.7 g, 52.0 mmol, 1.3 *eq.*) was dissolved in anhydrous  $\text{CH}_2\text{Cl}_2$  (200 mL) and cooled to  $-78\text{ }^{\circ}\text{C}$ . Now a solution of DMSO (7.67 mL, 108 mmol, 2.7 *eq.*) in anhydrous  $\text{CH}_2\text{Cl}_2$  (50 mL) was added drop wise, while keeping the internal temperature below  $-50\text{ }^{\circ}\text{C}$ . After 15 min alcohol **1.172** (10.3 g, 40.0 mmol, 1.0 *eq.*) was added drop wise at  $-78\text{ }^{\circ}\text{C}$  and the reaction mixture was continued to stir for 1 h. Now  $\text{NEt}_3$  (27.8 mL, 200 mmol, 5.0 *eq.*) was added in one go to afford a clear solution. The reaction mixture was slowly warmed to  $0\text{ }^{\circ}\text{C}$  over the course of 1 h and subsequently quenched with sat.  $\text{NaHCO}_3$  solution (100 mL). The aqueous phase was extracted with  $\text{CH}_2\text{Cl}_2$  ( $3 \times 150\text{ mL}$ ) and combined organic phases

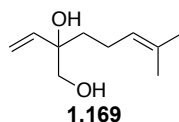
were dried over  $\text{Na}_2\text{SO}_4$  and concentrated. The resulting oil was purified by silica gel chromatography (1% EtOAc in hexanes) to yield 10.1 g (99%) of title compound **1.173**.

**Data for (1.173):**  $R_f = 0.26$  (1% Et<sub>2</sub>O in hexanes); IR (ATR):  $\tilde{\nu} = 2928$  (w), 2856 (w), 1721 (w), 1472 (w), 1252 (m), 1155 (w), 1099 (m), 1005 (w)  $\text{cm}^{-1}$ ; <sup>1</sup>H NMR (400 MHz, CDCl<sub>3</sub>)  $\delta = 5.06$  (t,  $J = 8.6$ , 1H), 4.15 (s, 2H), 2.50 (t,  $J = 7.4$ , 2H), 2.26 (d,  $J = 7.2$ , 2H), 1.67 (d,  $J = 1.1$ , 3H), 1.61 (s, 3H), 0.92 (s, 9H), 0.08 (s, 6H); <sup>13</sup>C NMR (150 MHz, CDCl<sub>3</sub>)  $\delta = 210.8$ , 132.8, 122.7, 69.4, 38.4, 25.8, 25.7, 22.1, 18.3, 17.6, -5.5 (three signals overlapping); MS (EI) calcd for C<sub>14</sub>H<sub>27</sub>O<sub>2</sub>Si (M-H<sup>+</sup>): 255.1786; found: 255.1768.



**3-(((Tert-butyldimethylsilyl)oxy)methyl)-7-methylocta-1,6-dien-3-ol (1.174).** Ketone **1.173** (2.90 g, 11.3 mmol, 1.0 *eq.*) was dissolved in anhydrous THF (25 mL). Now a vinylmagnesium bromide solution (1.0 M in Et<sub>2</sub>O, 13.6 mL, 13.6 mmol, 1.2 *eq.*) was added drop wise at  $-78$  °C. After 3 h of stirring at  $-78$  °C, the mixture was warmed to 0 °C and treated with sat. NH<sub>4</sub>Cl solution (40 mL). The aqueous phase was extracted with EtOAc (3 × 30 mL). Combined organic phases were dried over  $\text{Na}_2\text{SO}_4$  and concentrated. The resulting yellow oil was purified by silica gel chromatography (7% EtOAc in hexanes) to yield 3.14 g (98%) of title compound **1.174** as colourless oil.

**Data for 1.174:**  $R_f = 0.54$  (7% EtOAc in hexanes); IR (ATR):  $\tilde{\nu} = 2927$  (m), 2856 (m), 1472 (w), 1463 (w), 1361 (w), 1252 (m), 1093 (m), 1005 (m)  $\text{cm}^{-1}$ ; <sup>1</sup>H NMR (600 MHz, CDCl<sub>3</sub>)  $\delta = 5.77$  (dd,  $J = 10.8, 17.3$ , 1H), 5.29 (dd,  $J = 1.6, 17.3$ , 1H), 5.15 (dd,  $J = 1.6, 10.9$ , 1H), 5.09 (tdt,  $J = 1.4, 2.8, 7.1$ , 1H), 3.45 (s, 2H), 2.45 (s, 1H), 2.09 – 1.92 (m, 2H), 1.66 (d,  $J = 1.1$ , 3H), 1.62 – 1.55 (m, 1H), 1.58 (s, 3H), 1.44 (ddd,  $J = 5.2, 11.4, 13.7$ , 1H), 0.88 (s, 9H), 0.04 (d,  $J = 3.6$ , 6H); <sup>13</sup>C NMR (150 MHz, CDCl<sub>3</sub>)  $\delta = 141.0$ , 131.6, 124.5, 114.2, 75.2, 69.4, 37.0, 25.9, 25.82, 25.7, 22.1, 18.3, 17.6, -5.4, -5.5 (signal overlapping); HRMS (EI) calcd for C<sub>16</sub>H<sub>32</sub>O<sub>2</sub>Si (M<sup>+</sup>): 284.2170; found: 284.2171.

**3,10-Dihydroxymyrcene (1.169).**

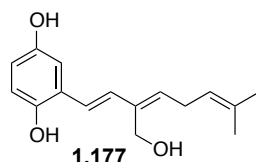
Procedure from **1.174**:

To a solution of **1.174** (10.2 g, 35.7 mmol, 1.0 *eq.*) in THF (90 mL) was added TBAF (1.0 M in THF, 31.8 mL, 107 mmol, 3.0 *eq.*) at 0 °C. The mixture was warmed to room temperature and stirred for 30 min. The reaction mixture was then diluted with EtOAc (200 mL) and washed with aqueous NaHCO<sub>3</sub>. The aqueous phases were extracted with EtOAc (3 × 200 mL). Combined organic phases were dried over Na<sub>2</sub>SO<sub>4</sub> and concentrated to yield 5.08 g (84%) of title compound **1.169** as colourless oil.

Procedure from myrcene (**1.168**):

A mixture of KMnO<sub>4</sub> (2.61 g, 16.5 mmol, 0.5 *eq.*) and benzyltributylammonium chloride (5.32 g, 16.5 mmol, 0.5 *eq.*) in anhydrous CH<sub>2</sub>Cl<sub>2</sub> (500 mL) was stirred for 3 h at room temperature. The solution was cooled to -5 °C. Myrcene (**1.168**) (5.00 g, 36.0 mmol, 1.0 *eq.*) was added and the mixture was stirred for 1 h. Aqueous NaOH (5.0 g in 80 mL H<sub>2</sub>O), sodium bisulphate (5.0 g in 80 mL H<sub>2</sub>O) and sulphuric acid (10 g in 100 mL H<sub>2</sub>O) were successively added. The aqueous phase was extracted with Et<sub>2</sub>O (3 × 150 mL) and the combined organic phases were washed with sat. NaHCO<sub>3</sub> solution (3 × 150 mL), H<sub>2</sub>O (150 mL) and brine (150 mL), dried over sodium sulfate and concentrated. The oily residue was purified by silica gel chromatography (33% EtOAc in hexanes) to yield 0.45 g (16%) of title compound **1.169** as colourless oil.

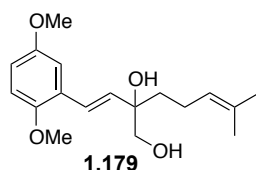
**Data for 1.169:** IR (ATR):  $\tilde{\nu}$  = 3384 (m, br), 2966 (m), 2916 (m), 2858 (m), 1643 (w), 1448 (m), 1376 (m), 1189 (m), 1042 (s), 993 (s), 920 (s) cm<sup>-1</sup>; <sup>1</sup>H NMR (600 MHz, CDCl<sub>3</sub>)  $\delta$  = 5.80 (dd, *J* = 10.8, 17.3, 1H), 5.35 (dd, *J* = 1.4, 17.3, 1H), 5.26 (dd, *J* = 1.4, 10.8, 1H), 5.14 – 5.06 (m, 1H), 3.53 – 3.41 (m, 2H), 2.04 (dd, *J* = 16.2, 23.5, 4H), 1.67 (d, *J* = 1.2, 3H), 1.63 (ddd, *J* = 6.3, 10.3, 13.8, 1H), 1.59 (s, 3H), 1.50 (ddd, *J* = 5.4, 10.4, 13.8, 1H); <sup>13</sup>C NMR (150 MHz, CDCl<sub>3</sub>)  $\delta$  = 140.6, 132.3, 124.1, 115.3, 76.2, 68.9, 36.7, 25.7, 22.0, 17.7; HRMS (EI) calcd for C<sub>10</sub>H<sub>18</sub>O<sub>2</sub> (M<sup>+</sup>): 170.1307; found: 170.1298.



**2-((1E,3Z)-3-(Hydroxymethyl)-7-methylocta-1,3,6-trien-1-yl)benzene-1,4-diol**

**(1.177).** A mixture of dihydroxymyrceene (**1.169**) (300 mg, 1.76 mmol, 1.0 *eq.*), 2-bromobenzene-1,4-diol (**1.175**) (500 mg, 2.64 mmol, 1.5 *eq.*), Pd(OAc)<sub>2</sub> (40 mg, 1.76 mmol, 0.1 *eq.*), TBACl (636 mg, 2.29 mmol, 1.3 *eq.*), NaHCO<sub>3</sub> (429 mg, 4.05 mmol, 2.3 *eq.*) in anhydrous DMF (6 mL) was degassed for 20 min with N<sub>2</sub>. After sealing the pressure tube with a teflon screw-cap, the mixture was heated to 100 °C for 2 h. The reaction mixture was filtered over a plug of silica and washed with EtOAc (150 mL). All volatiles were removed *in vacuo* and the resulting dark oil was purified by silica gel chromatography (25% EtOAc in hexanes) to give 345 mg (75%) of the title compound **1.177** as a colourless solid.

**Data for 1.177:** IR (ATR):  $\tilde{\nu}$  = 3391 (m); 3116 (m) 2924 (w), 1607 (w), 1513 (w), 1485 (vs), 1371 (w), 1348 (m), 1257 (w), 1228 (2), 1197 (vs) 1159 (w), 1050 (vs), 983 (s); <sup>1</sup>H NMR (400 MHz, DMSO-*d*<sub>6</sub>)  $\delta$  = 8.70 (s, 1H), 8.53 (s, 1H), 6.72 (dd, *J* = 6.7, 9.6, 2H), 6.57 (d, *J* = 8.6, 1H), 6.41 (dd, *J* = 2.9, 8.6, 1H), 6.10 (d, *J* = 16.3, 1H), 5.07 (s, 1H), 4.54 (s, 1H), 4.33 (s, 1H), 3.27 (dd, *J* = 4.1, 9.3, 2H), 2.03 – 1.82 (m, 2H), 1.60 (s, 3H), 1.51 (s, 3H); <sup>13</sup>C NMR (100 MHz, DMSO-*d*<sub>6</sub>)  $\delta$  = 150.2, 147.5, 141.4, 133.9, 130.6, 125.6, 124.9, 123.0, 116.7, 115.2, 112.3, 75.2, 69.1, 37.9, 25.9, 17.9; HRMS (EI): calcd for C<sub>16</sub>H<sub>20</sub>O<sub>3</sub> (M<sup>+</sup>) 260.1412; found: 260.1425.

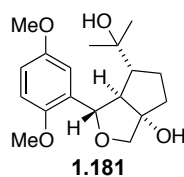


**(E)-2-(2,5-Dimethoxystyryl)-6-methylhept-5-ene-1,2-diol (1.179).**\* In a pressure tube PdCl<sub>2</sub>(PPh<sub>3</sub>)<sub>2</sub> (84.0 mg, 0.120 mmol, 0.1 *eq.*), dppp (97.0 mg, 0.236 mmol, 0.2 *eq.*) and NaHCO<sub>3</sub> (200.0 mg, 2.4 mmol, 2.0 *eq.*) were dissolved in dry DMF (3 ml). After addition of dihydroxymyrceene **1.169** (200 mg, 1.18 mmol, 1.0 *eq.*) and 2-bromo-1,4-dimethoxybenzene (**1.178**) (308.0 mg, 1.42 mmol, 1.2 *eq.*) the mixture was heated to 130 °C and stirred for 16 h. Subsequently, it was diluted with EtOAc (9 ml) and the organic layer was washed

\* For this compound also see: F. Löbermann, Diploma Thesis, 2009 Ludwig-Maximilians-Universität-München.

with water (25 ml), followed by brine (25 ml), dried over Na<sub>2</sub>SO<sub>4</sub>, filtered and concentrated. The product was purified by column chromatography (50 % Et<sub>2</sub>O in hexanes) to afford 220 mg (60 %) of **1.179** as a oil, which solidifies over night at -30 °C.

**Data for 1.179:** R<sub>f</sub> 0.13 (50 % Et<sub>2</sub>O in hexanes); IR (ATR):  $\tilde{\nu}$  = 3410 (br), 2926 (vs), 2856 (w), 2834 (w), 1607 (m), 1582 (m), 1495 (vs), 1463 (s), 1427 (w), 1376 (w), 1321 (w), 1284 (m), 1216 (vs), 1178 (m), 1162, (w), 1121 (w), 1045 (s), 1026 (m), 977 (s); <sup>1</sup>H NMR (300 MHz, CDCl<sub>3</sub>):  $\delta$  = 7.00 (dd, *J* = 9.5, 6.7, 1H), 6.98 (d, *J* = 11.3, 1H), 6.86 – 6.76 (m, 2H), 6.18 (d, *J* = 16.3, 1H), 5.15 (t, *J* = 7.2, 1H), 3.78 (s, 3H), 3.77 (s, 3H), 3.59 (q, *J* = 11.0, 2H), 2.58 (br, 1H), 2.46 – 2.05 (m, 2H), 1.67 (s, 3H), 1.85 – 1.63 (m, 2H), 1.69 (s, 3H); <sup>13</sup>C NMR (300 MHz, CDCl<sub>3</sub>):  $\delta$  = 153.6, 151.2, 133.0, 132.3, 126.5, 124.9, 124.3, 113.6, 112.3, 112.2, 76.4, 69.2, 56.1, 55.8, 37.3, 25.7, 22.2, 17.8. HRMS (EI) calcd for C<sub>18</sub>H<sub>26</sub>O<sub>4</sub> (M<sup>+</sup>): 306.1831; found: 306.1823.

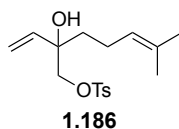


#### 1-(2,5-Dimethoxyphenyl)-6-(2-hydroxypropan-2-yl)hexahydro-1H-

**cyclopenta[ε]furan-3a-ol (1.181).** To a solution of **1.179** (24 mg, 0.078 mmol, 1.0 *eq.*) in acetonitrile (4 mL) was added a mixture of CAN (128 mg, 0.234 mmol, 3.0 *eq.*) and NaHCO<sub>3</sub> (35 mg, 0.421 mmol, 5.4 *eq.*) in H<sub>2</sub>O (1 mL) at 0 °C. The reaction mixture was diluted with EtOAc (50 mL) and NaHCO<sub>3</sub> sltn. (sat. 30 mL) after vigorous stirring for 30 min. The aqueous phase was extracted with EtOAc (3 × 30 mL) and the combined organic phases washed with brine (30 mL), dried over Na<sub>2</sub>SO<sub>4</sub> and concentrated under reduced pressure. The resulting oil was purified by silica gel chromatography (40% EtOAc in hexanes) to yield 14 mg (56%) of the title compound **1.181** as colourless oil.

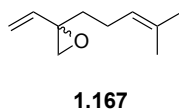
**Data for 1.181:** IR (ATR):  $\tilde{\nu}$  = 3361 (br), 1493 (vs), 1464 (s), 1365 (vs), 1277 (s), 1212 (vs), 1178 (w), 1161 (vw), 1045 (s), 1021 (s), 855 (s); <sup>1</sup>H NMR (600 MHz, CDCl<sub>3</sub>)  $\delta$  = 7.09 (d, *J*=3.1, 1H), 6.77 (d, *J*=8.9, 1H), 6.72 (dd, *J*=3.1, 8.9, 1H), 5.11 (d, *J*=9.9, 1H), 3.80 (s, 3H), 3.77 (s, 3H), 3.23 (d, *J*=11.1, 1H), 3.16 (d, *J*=11.1, 1H), 2.89 (td, *J*=5.8, 12.8, 1H), 2.30 (ddd, *J* = 1.3, 9.5, 14.6, 1H), 2.10 (dt, *J* = 8.9, 14.6, 1H), 1.92 (dd, *J*=9.9, 13.4, 1H), 1.68 (dddd, *J* = 1.3, 5.8, 8.2, 11.7, 1H), 1.41 (s, 3H), 1.29 (s, 3H), 1.27 – 1.24 (m, 1H); <sup>13</sup>C NMR (150 MHz, CDCl<sub>3</sub>)  $\delta$  = 154.5, 149.4, 131.6, 112.5, 111.8, 111.8, 77.4, 76.4, 70.5,

69.8, 65.0, 58.9, 56.3, 55.6, 42.2, 29.0, 24.1, 21.9; HRMS (ESI) calcd for  $C_{18}H_{26}O_5$  ( $M^+$ ): 322,1780; found: 322,1783.



**2-Hydroxy-6-methyl-2-vinylhept-5-en-1-yl 4-Methylbenzenesulfonate (1.186).** To a solution of **1.169** (1.40 g, 8.22 mmol, 1.0 *eq.*) in anhydrous pyridine (7 mL) was added 4-toluenesulfonyl chloride (1.88 g, 6.96 mmol, 1.2 *eq.*) at 0 °C. The reaction mixture was stirred for 3 h, while letting the ice bath warm to room temperature. The mixture was hydrolysed with 10% HCl (40 mL) and extracted with  $Et_2O$  ( $3 \times 30$  mL). The combined organic phases were washed with aqueous  $NaHCO_3$  and brine, dried over  $Na_2SO_4$  and concentrated to yield 2.00 g (75%) of title compound **1.186** as colourless oil.

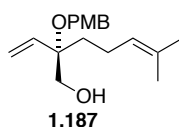
**Data for 1.186:** IR (ATR):  $\tilde{\nu} = 3526$  (w, br), 2968 (w), 2923 (w), 1644 (w), 1598 (w), 1451 (w), 1357 (s), 1308 (w), 1189 (s), 1174 (vs), 1097 (m), 968 (s)  $cm^{-1}$ ;  $^1H$  NMR (600 MHz,  $CDCl_3$ )  $\delta = 7.74$  (d, 2H,  $J = 9.1$ ), 7.30 (d, 2H,  $J = 9.1$ ), 7.69 (dd, 1H,  $J = 17.3, 11.0$ ), 5.29 (d, 1H,  $J = 17.3$ ), 5.18 (d, 1H,  $J = 11.0$ ), 5.00 (t, 1H,  $J = 7.2$ ), 3.85 (s, 2H), 2.40 (s, 3H), 2.26 (brs, 1H), 2.00 – 1.87 (m, 2H), 1.61 (s, 3H), 1.59 – 1.55 (m, 1H), 1.51 (s, 3H) 1.48 – 1.43 (m, 1H);  $^{13}C$  NMR (150 MHz,  $CDCl_3$ )  $\delta = 145.1, 138.9, 132.7, 132.5, 130.0, 128.0, 123.8, 116.0, 75.27, 74.4, 36.7, 25.8, 21.9, 21.8, 17.8$  (two signals overlapping); HRMS (EI) calcd for  $C_{17}H_{23}O_4S$  ( $M+H^+$ ): 323.1323; found: 323.1314.



**2-(4-Methylpent-3-en-1-yl)-2-vinyloxirane 1.167.** To a solution of **1.186** (3.35 g, 10.3 mmol, 1.0 *eq.*) in anhydrous  $Et_2O$  (30 mL) was added finely ground potassium hydroxide (1.16 g, 20.7 mmol, 2.0 *eq.*) in small portions at 0 °C for 3h. The colourless precipitate was filtered off over a plug of celite and was washed excessively with  $Et_2O$ . The solution was careful concentrated on a rotary evaporator at 40 °C and min. 300 mbar, to yield 1.38 g (91%) of title compound **1.167** as colourless oil.

**Data for 1.167:** IR (ATR):  $\tilde{\nu} = 3386$  (w, br), 2966 (m), 2915 (s), 2857 (m), 1641 (w), 1451 (s), 1376 (s), 1235 (w), 1105 (m), 987 (s), 920 (vs)  $cm^{-1}$ ;  $^1H$  NMR (600 MHz,  $CDCl_3$ )  $\delta = 5.75$  (dd, 1H,  $J = 17.4, J = 11.2$ ), 5.32 (dd, 1H,  $J = 17.3, 1.2$ ), 5.18 (dd, 1H,

$J = 11.3, J = 1.2$ ), 5.08 (t, 1H,  $J = 7.8$ ), 2.79 (d, 1H,  $J = 5.3$ ), 2.64 (d, 1H,  $J = 5.4$ ), 2.07 (q, 2H,  $J = 8.0$ ), 1.74 – 1.67 (m, 2H), 1.65 (s, 3H), 1.57 (s, 3H);  $^{13}\text{C}$  NMR (150 MHz,  $\text{CDCl}_3$ )  $\delta = 137.7, 132.3, 132.8, 116.6, 58.7, 55.2, 33.8, 25.9, 23.9, 17.9$ ; HRMS (EI) calcd for  $\text{C}_{10}\text{H}_{16}\text{O}$  ( $\text{M}^+$ ): 152.1201; found: 152.1189.



**(*S*)-2-((4-Methoxybenzyl)oxy)-6-methyl-2-vinylhept-5-en-1-ol (1.187).**

Preparation of a 0.345 M stock solution of triethylborane:

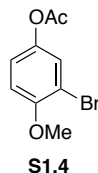
Neat triethylborane (0.5 mL) was diluted with degassed, anhydrous  $\text{CH}_2\text{Cl}_2$  (10 mL, degassed through three freeze-pump-thaw cycles).

A Schlenk flask, filled with 4-methoxybenzyl alcohol (546  $\mu\text{L}$ , 4.40 mmol, 1.1 *eq.*),  $\text{Pd}_2(\text{dba})_3$  (36.6 mg, 0.04 mmol, 0.01 *eq.*) and (*S,S*)-DACH-Phenyl TROST Ligand (41.4 mg, 0.06 mmol, 0.015 *eq.*), was evacuated and flushed with  $\text{N}_2$  inert gas five times. Subsequently anhydrous  $\text{CH}_2\text{Cl}_2$  (30 mL, degassed through three freeze-pump-thaw cycles) was added and the mixture was stirred at room temperature for 15 min, upon which the purple colour of the solution turned to a dirty yellow. Now, triethylborane (232  $\mu\text{L}$ , 0.345 M in  $\text{CH}_2\text{Cl}_2$ , 0.08 mmol, 0.02 *eq.*) was added through the septum via a syringe. Addition of vinyl epoxide **1.167** (609 mg, 4.00 mmol, 1.0 *eq.*) immediately resulted in a colour change from yellow to a pale green. The reaction vessel was carefully sealed with a yellow-cap and the reaction mixture stirred at rt over night, upon which the solution changed colour to a dark orange. The reaction mixture was filtered over a plug of silica gel (EtOAc) and concentrated. The resulting green oil was purified by silica gel chromatography (11% EtOAc in hexanes) to yield 0.94 g (81%) of title compound **1.187** as colourless oil.

**Data for 1.187:**  $[\alpha]_{\text{D}}^{20} -1.6$  ( $c$  1.00,  $\text{CHCl}_3$ ); 93% *ee*; IR (ATR):  $\tilde{\nu} = 3432$  (w, br), 2926 (m), 2871 (m), 1614 (m), 1587 (w), 1514 (vs), 1464 (m), 1377 (m), 1302 (m), 1248 (vs), 1173 (m), 1248 (vs), 1037 (s)  $\text{cm}^{-1}$ ;  $^1\text{H}$  NMR (600 MHz,  $\text{CDCl}_3$ )  $\delta = 7.28 - 7.26$  (m, 2H), 6.90 – 6.85 (m, 2H), 5.87 (dd,  $J = 11.1, 17.8$ , 1H), 5.34 (ddd,  $J = 1.3, 14.5, 19.0$ , 2H), 5.16 – 5.09 (m, 1H), 4.39 – 4.31 (m, 2H), 3.80 (s, 3H), 3.64 (dd,  $J = 11.4, 44.8$ , 2H), 2.05 (dt,  $J = 5.3, 10.8$ , 2H), 1.80 – 1.65 (m, 5H), 1.61 (s, 3H);  $^{13}\text{C}$  NMR (150 MHz,  $\text{CDCl}_3$ )  $\delta = 159.0$ ,

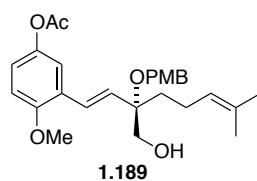


139.1, 131.8, 131.0, 128.9, 124.1, 117.1, 113.8, 79.9, 65.2, 63.9, 55.3, 33.0, 25.7, 22.0, 17.7 (two signals overlapping); HRMS (EI) calcd for  $C_{18}H_{26}O_3$  ( $M^+$ ): 290.1882; found: 290.1894.



**3-Bromo-4-methoxy Phenyl Acetate S1.4.** To a solution of 4-methoxyphenol (6.21 g, 50.0 mmol, 1.0 *eq.*) in anhydrous THF (50 mL) was added  $Ac_2O$  (10.2 g, 0.10 mol, 2.0 *eq.*), DMAP (12.9 mg, 10.5 mmol, 0.1 *eq.*) and TEA (7 mL). The reaction mixture was stirred at rt for 2 h. All volatiles were removed *in vacuo* and the resulting residue was taken up in glacial acetic acid (25 mL). NaOAc (8.20 g, 100 mmol, 2.0 *eq.*) was added at 0 °C, followed by slow addition of  $Br_2$  (2.82 mL, 55.0 mmol, 1.1 *eq.*) in acetic acid (35 mL). After 1 h the ice bath was removed and the reaction was stirred at room temperature over night. After further addition of  $Br_2$  (1.00 mL, 19.5 mmol, 0.4 *eq.*) the reaction mixture was continued to stir for 5 h. The mixture was treated with aqueous  $NaHCO_3$  (150 mL), and extracted with  $Et_2O$  (3 × 200 mL). The combined organic phases were washed with dilute  $Na_2S_2O_3$  solution (100 mL) and brine (100 mL), dried over  $Na_2SO_4$ , concentrated and purified by silica gel chromatography (9% EtOAc in hexanes) to yield 12.2 g (99%) of title compound **S1.4** as a beige solid.

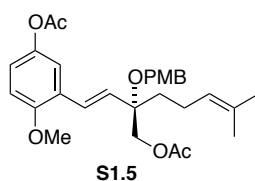
**Data for S1.4:**  $R_f$ : 0.20 (9% EtOAc in hexanes); IR (ATR):  $\tilde{\nu}$  = 2948 (w), 1746 (vs), 1598 (m), 1583 (m), 1490 (s), 1439 (s), 1365 (s), 1265 (s), 1215 (vs), 1179 (vs), 1047 (s), 1009 (s), 928 (s)  $cm^{-1}$ ;  $^1H$  NMR (400 MHz,  $CDCl_3$ )  $\delta$  = 7.31 (d,  $J$  = 2.8, 1H), 7.01 (dd,  $J$  = 2.8, 8.9, 1H), 6.87 (d,  $J$  = 8.9, 1H), 3.87 (s, 3H), 2.27 (s, 3H);  $^{13}C$  NMR (100 MHz,  $CDCl_3$ )  $\delta$  = 169.5, 153.8, 144.1, 126.6, 121.3, 111.8, 111.4, 56.5, 21.0; HRMS (EI) calcd for  $C_9H_9O_3Br$  ( $M^+$ ): 243.9735; found: 243.9735.



**(*S,E*)-3-(3-(Hydroxymethyl)-3-((4-methoxybenzyl)oxy)-7-methylocta-1,6-dien-1-yl)-4-methoxyphenyl Acetate 1.189.** Compound **S1.4** (0.92 g, 3.75 mmol, 1.5 *eq.*), **1.187**

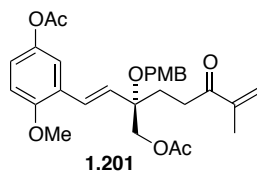
(0.73 g, 2.50 mmol, 1.0 *eq.*), Tri(*o*-tolyl)phosphine (0.30 g, 0.1 mmol, 0.4 *eq.*) and Pd(OAc)<sub>2</sub> (56.1 mg, 0.25 mmol, 0.1 *eq.*) was dissolved in TEA (10 mL) and anhydrous toluene (25 mL). The reaction mixture was degassed and then heated to 110 °C for 7 h. Note: palladium black might precipitate from the reaction mixture very easily. If this is the case, try reducing the stirring speed and use a flask with homogeneous surface. If precipitation of palladium occurs in the course of the reaction, portion wise addition of further catalyst can push this reaction to completion. The resulting black mixture was filtered off over a short plug of silica gel and washed with EtOAc (100 mL). The dark solution was concentrated and the resulting brown oil was purified by silica gel chromatography (25% EtOAc in hexanes) to yield 0.85 g (74%) of title compound **1.189** as yellow oil.

**Data for 1.189:** R<sub>f</sub>: 0.18 (25% EtOAc in hexanes); IR (ATR):  $\tilde{\nu}$  = 3480 (w, br), 2927 (m), 1758 (s), 1612 (m), 1513 (s), 1490 (s), 1368 (m), 1245 (s), 1199 (vs), 1176 (vs), 1030 (vs), 980 (s) cm<sup>-1</sup>; <sup>1</sup>H NMR (600 MHz, CDCl<sub>3</sub>)  $\delta$  = 7.32 – 7.26 (m, 2H), 7.14 (d, *J* = 2.8, 1H), 6.97 – 6.91 (m, 2H), 6.91 – 6.87 (m, 2H), 6.85 (d, *J* = 8.9, 1H), 6.20 (d, *J* = 16.7, 1H), 5.19 – 5.13 (m, 1H), 4.43 – 4.36 (m, 2H), 3.84 (s, 3H), 3.81 (d, *J* = 3.1, 3H), 3.71 (dd, *J* = 14.3, 25.7, 2H), 2.29 (s, 3H), 2.11 (d, *J* = 7.2, 2H), 1.92 (s, 1H), 1.89 – 1.79 (m, 2H), 1.70 (d, *J* = 1.0, 3H), 1.62 (s, 3H); <sup>13</sup>C NMR (150 MHz, CDCl<sub>3</sub>)  $\delta$  = 169.9, 159.0, 154.4, 144.1, 131.8, 131.7, 131.2, 129.1, 126.7, 125.8, 124.2, 121.4, 119.4, 113.8, 111.4, 80.2, 65.7, 64.2, 55.8, 55.3, 33.6, 25.7, 22.2, 21.0, 17.7 (two signals overlapping); HRMS (EI) calcd for C<sub>27</sub>H<sub>34</sub>O<sub>6</sub> (M<sup>+</sup>): 454.2355; found: 454.2340.



**(*S,E*)-2-(5-Acetoxy-2-methoxystyryl)-2-((4-methoxybenzyl)oxy)-6-methylhept-5-en-1-yl Acetate S1.5.** To a solution of **1.189** (433 mg, 1.05 mmol, 1.0 *eq.*) in anhydrous CH<sub>2</sub>Cl<sub>2</sub> (5 mL) was added acetic anhydride (0.39 mL, 4.2 mmol, 4.0 *eq.*), DMAP (25.7 mg, 0.21 mmol, 0.2 *eq.*) and pyridine (0.34 mL, 4.2 mmol, 4 *eq.*). The reaction mixture was stirred at room temperature for 2 h. Subsequently the reaction was diluted with water (50 mL) and the aqueous phase was extracted with EtOAc (3 × 50 mL) and combined organic phases were dried over Na<sub>2</sub>SO<sub>4</sub> and concentrated to yield 516 mg (99%) of title compound **S1.5** as a colourless oil.

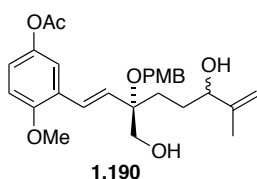
**Data for S1.5:**  $R_f$ : 0.33 (25% EtOAc in hexanes); IR (ATR):  $\tilde{\nu}$  = 2930 (m), 1738 (s), 1612 (m), 1513 (s), 1490 (s), 1368 (s), 1243 (vs), 1199 (vs), 1176 (vs), 1030 (vs), 980 (s);  $^1\text{H NMR}$  (600 MHz,  $\text{CDCl}_3$ )  $\delta$  = 7.28 (d,  $J$  = 8.8, 2H), 7.10 (d,  $J$  = 2.8, 1H), 6.95 (dd,  $J$  = 2.8, 8.8, 1H), 6.91 (d,  $J$  = 16.7, 1H), 6.89 – 6.86 (m, 2H), 6.85 (d,  $J$  = 8.9, 1H), 6.13 (d,  $J$  = 16.7, 1H), 5.16 – 5.10 (m, 1H), 4.46 – 4.38 (m, 2H), 4.31 (dd,  $J$  = 11.6, 47.0, 2H), 3.82 (d,  $J$  = 17.2, 6H), 2.29 (s, 3H), 2.12 – 2.06 (m, 2H), 2.08 (s, 3H), 1.84 (ddd,  $J$  = 3.1, 5.7, 11.1, 2H), 1.68 (s, 3H), 1.60 (s, 3H);  $^{13}\text{C NMR}$  (150 MHz,  $\text{CDCl}_3$ )  $\delta$  = 170.9, 169.9, 158.9, 154.4, 144.1, 131.9, 131.8, 131.3, 128.9, 126.8, 125.6, 124.1, 121.4, 119.4, 113.7, 111.4, 78.5, 66.1, 64.4, 55.8, 55.3, 34.8, 25.7, 21.9, 21.0, 21.0, 17.7 (two signals overlapping); HRMS (EI): calcd for  $\text{C}_{29}\text{H}_{36}\text{O}_7$  ( $\text{M}^+$ ): 496.2461; found: 496.2442.



**(*S,E*)-2-(5-Acetoxy-2-methoxystyryl)-2-((4-methoxybenzyl)oxy)-6-methyl-5-oxohept-6-en-1-yl Acetate 1.201.** To a solution of **S1.5** (0.47 g, 1.0 mmol, 1.0 *eq.*) (alternatively compound **1.201** can also be prepared from **1.189** in one pot after this procedure) in anhydrous  $\text{CH}_2\text{Cl}_2$  (120 mL) was added acetic anhydride (0.49 mL, 5.15 mmol, 5.0 *eq.*), pyridine (0.33 mL), DMAP (25.2 mg, 0.21 mmol, 0.2 *eq.*) and a spatula tip of TPP. The reaction mixture was stirred at room temperature for 15 min. After cooling to 0 °C, oxygen was bubbled through for 5 min and then the *Reflux UV Heat D3* lamp (160 W,  $\nu_{\text{min}}$  = 280 nm) was switched on and the mixture was irradiated for 1 h at 0 °C. All volatiles were removed *in vacuo*. The resulting oil was purified by silica gel (inactivated with 1v%  $\text{Et}_3\text{N}$ ) chromatography (25% EtOAc in hexanes) to yield 0.30 g (56%) of title compound **1.201** as colourless oil.

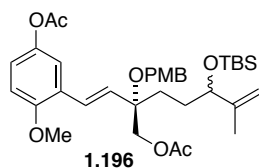
**Data for 2.302:**  $[\alpha]_{\text{D}}^{20}$  +100.4 ( $c$  5.0, EtOAc);  $R_f$  = 0.24 (25% EtOAc in hexanes); IR (ATR):  $\tilde{\nu}$  = 2956 (m), 1738 (s), 1674 (m), 1513 (s), 1491 (s), 1368 (s), 1244 (vs), 1199 (vs), 1177 (vs), 1030 (vs), 982 (m);  $^1\text{H NMR}$  (600 MHz,  $\text{CDCl}_3$ )  $\delta$  = 7.29 – 7.22 (m, 2H), 7.08 (d,  $J$  = 2.8, 1H), 6.96 – 6.90 (m, 2H), 6.88 – 6.82 (m, 3H), 6.08 (d,  $J$  = 16.6, 1H), 5.93 (s, 1H), 5.72 (d,  $J$  = 0.8, 1H), 4.45 – 4.35 (m, 2H), 4.32 (d,  $J$  = 11.7, 1H), 4.25 (d,  $J$  = 11.7, 1H), 3.82 (s, 3H), 3.79 (s, 3H), 2.87 – 2.73 (m, 2H), 2.28 (s, 3H), 2.18 (ddd,  $J$  = 6.1, 9.3, 15.7, 1H), 2.14 – 2.07 (m, 1H), 2.07 (s, 3H), 1.83 (s, 3H);  $^{13}\text{C NMR}$  (150 MHz,  $\text{CDCl}_3$ )  $\delta$  = 201.5, 170.8, 169.9, 159.0, 154.5, 144.4, 144.1, 131.1, 131.0, 128.8, 126.5, 126.1, 124.6,

121.6, 119.5, 113.7, 111.4, 78.2, 66.2, 64.5, 55.8, 55.3, 31.2, 28.9, 21.0, 21.0, 17.6 (two signals overlapping); HRMS (EI): calcd for C<sub>29</sub>H<sub>34</sub>O<sub>8</sub> (M<sup>+</sup>): 510.2254; found: 510.2243.



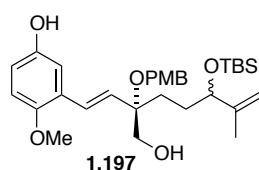
**3-((3*S*,*E*)-6-Hydroxy-3-(hydroxymethyl)-3-((4-methoxybenzyl)oxy)-7-methylocta-1,7-dien-1-yl)-4-methoxyphenyl Acetate 1.190.** To a solution of **1.189** (150 mg, 0.33 mmol, 1.0 *eq.*) in anhydrous CH<sub>2</sub>Cl<sub>2</sub> (250 mL) was added a spatula tip of TPP. The reaction mixture was stirred at room temperature for 15 min. After cooling to 0 °C, the mixture was saturated with oxygen for five minutes. The reaction mixture was irradiated with a reptile lamp while continuously bubbling oxygen through for 1 h at 0 °C. After completion *t*-Bu<sub>3</sub>P (1.0 M in toluene, 1.32 mL, 1.32 mmol, 4.0 *eq.*) was added and the mixture continued to stir at rt for 1 h. All volatiles were removed *in vacuo*. The resulting oil was purified by silica gel chromatography (40% EtOAc in hexanes) to yield 60 mg (38%) of title compound **1.190** as colourless oil.

**Data for 1.190:** IR (ATR):  $\tilde{\nu}$  = 3453 (br), 1612 (w), 1513 (s), 1490 (s), 1455 (w), 1441 (w), 1424 (w), 1365 (vs), 1301 (w), 1200 (vs), 1176 (s), 1156 (w), 1029 (vs), 902 (vs); <sup>1</sup>H NMR (600 MHz, CDCl<sub>3</sub>); mixture of two diastereoisomers  $\delta$  = 7.28 (d, *J* = 8.3, 2H), 7.12 (dd, *J* = 2.8, 13.4, 1H), 7.02 – 6.93 (m, 1H), 6.93 – 6.85 (m, 3H), 6.82 (dd, *J* = 3.3, 8.8, 1H), 6.19 (t, *J* = 16.5, 1H), 5.07 (d, *J* = 39.7, 1H), 4.85 (d, *J* = 10.5, 1H), 4.61 (s, 2H), 4.50 – 4.42 (m, 1H), 3.84 – 3.77 (m, 6H), 3.64 (dd, *J* = 11.4, 21.6, 1H), 3.54 (d, *J* = 11.4, 1H), 2.27 (s, 3H), 2.21 – 2.06 (m, 2H), 1.99 – 1.87 (m, 2H), 1.80 – 1.73 (m, 3H); <sup>13</sup>C NMR (150 MHz, CDCl<sub>3</sub>)  $\delta$  = 171.12, 169.90, 159.19, 154.44, 154.41, 145.27, 145.05, 144.11, 144.09, 133.58, 133.08, 133.05, 128.61, 126.88, 126.66, 123.90, 123.63, 121.06, 121.02, 119.69, 119.44, 113.93, 111.51, 111.43, 111.14, 110.60, 86.31, 86.22, 84.06, 81.97, 67.96, 67.60, 65.03, 60.36, 55.86, 55.80, 55.27, 33.02, 32.53, 30.93, 30.86, 21.03, 21.02, 21.02, 18.23, 14.17; HRMS (EI): calcd for C<sub>27</sub>H<sub>34</sub>O<sub>7</sub> (M<sup>+</sup>): 470.2305; found: 470.2312.



**(2*S*)-2-((*E*)-5-Acetoxy-2-methoxystyryl)-5-((*tert*-butyldimethylsilyl)oxy)-2-((4-methoxybenzyl)oxy)-6-methylhept-6-en-1-yl Acetate **1.196**.** A solution of **S1.5** (256 mg, 0.5 mmol, 1.0 *eq.*), TBSCl (113 mg, 0.75 mmol, 1.5 *eq.*) imidazole (51 mg, 0.75 mmol, 1.5 *eq.*) and DMAP (6 mg, 0.05 mmol, 0.1 *eq.*) in CH<sub>2</sub>Cl<sub>2</sub> (1.5 mL) was stirred at room temperature for 36 h. The precipitate was filtered off, washed with CH<sub>2</sub>Cl<sub>2</sub> (50 mL) and all volatiles were removed *in vacuo*. The resulting oil was purified by silica gel chromatography (14% EtOAc in hexanes) to yield 312 mg (99%) of title compound **1.196** as colourless oil.

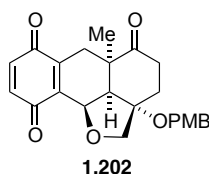
**Data for 1.196:** <sup>1</sup>H NMR (600 MHz, CDCl<sub>3</sub>); mixture of two diastereoisomers δ = 7.27 (d, *J* = 7.4, 2H), 7.09 (dd, *J* = 2.8, 5.8, 1H), 6.99 – 6.81 (m, 5H), 6.10 (d, *J* = 16.7, 1H), 4.89 (s, 1H), 4.78 (s, 1H), 4.44 – 4.36 (m, 2H), 4.26 (dd, *J* = 8.9, 22.8, 2H), 4.08 – 4.01 (m, 1H), 3.86 – 3.77 (m, 6H), 2.29 (d, *J* = 0.5, 3H), 2.06 (s, 3H), 1.77 – 1.49 (m, 4H), 1.66 (s, 3H) 0.90 (s, 9H), 0.03 (dd, *J* = 2.5, 25.7, 6H); <sup>13</sup>C NMR (150 MHz, CDCl<sub>3</sub>) δ = 170.9, 170.8, 169.9, 158.9, 158.9, 154.5, 147.4, 147.3, 144.1, 131.9, 131.8, 131.3, 131.3, 128.9, 128.9, 126.8, 126.8, 125.7, 125.7, 121.4, 121.4, 119.4, 119.4, 113.7, 111.4, 110.9, 110.8, 78.4, 78.3, 76.6, 76.5, 66.3, 66.3, 64.3, 64.3, 55.8, 55.3, 30.2, 30.0, 29.4, 29.4, 25.9, 21.0, 21.0, 18.2, 17.3, -4.8, -5.1; HRMS (EI) calcd for C<sub>35</sub>H<sub>50</sub>O<sub>8</sub>Si (M<sup>+</sup>): 626.3275; found: 626.3268



**(2*S*)-2-((*E*)-5-Acetoxy-2-methoxystyryl)-5-hydroxy-2-((4-methoxybenzyl)oxy)-6-methylhept-6-en-1-yl acetate **1.197**.** To a solution of **1.196** (339 mg, 0.54 mmol, 1.0 *eq.*) in anhydrous MeOH (2 mL) was added K<sub>2</sub>CO<sub>3</sub> (149 mg, 1.1 mmol, 2.0 *eq.*). The reaction mixture was stirred at room temperature for 1.5 h. The reaction mixture was diluted with EtOAc (50 mL) and brine (25 mL), extracted with EtOAc (3 × 50 mL), dried over Na<sub>2</sub>SO<sub>4</sub> and concentrated to yield 290 mg (99%) of title compound **1.197** as colourless oil.

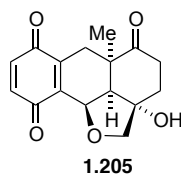
**Data for 1.197.** R<sub>f</sub> = 0.15 (25% EtOAc in hexanes); IR (ATR):  $\tilde{\nu}$  = 3351 (br), 2951 (w), 2927 (w), 1855 (w), 1611 (w), 1513 (s), 1496 (vs), 1462 (s), 1438 (w), 1247 (vs), 1217 (s), 1178 (s), 1068 (w), 1032 (vs); <sup>1</sup>H NMR (600 MHz, CDCl<sub>3</sub>); mixture of two

diastereoisomers  $\delta = 7.29$  (dd,  $J = 5.7, 12.4, 2\text{H}$ ),  $6.90$  (ddd,  $J = 9.3, 12.4, 20.0, 4\text{H}$ ),  $6.77 - 6.69$  (m,  $2\text{H}$ ),  $6.16$  (dd,  $J = 10.6, 16.7, 1\text{H}$ ),  $4.90$  (s,  $1\text{H}$ ),  $4.79$  (s,  $1\text{H}$ ),  $4.43 - 4.33$  (m,  $2\text{H}$ ),  $4.05$  (s,  $1\text{H}$ ),  $3.85 - 3.76$  (m,  $6\text{H}$ ),  $3.70$  (s,  $2\text{H}$ ),  $1.73 - 1.56$  (m,  $4\text{H}$ ),  $1.68$  (s,  $3\text{H}$ )  $0.90$  (t,  $J = 2.5, 9\text{H}$ ),  $0.08 - 0.01$  (m,  $6\text{H}$ );  $^{13}\text{C}$  NMR (150 MHz,  $\text{CDCl}_3$ )  $\delta = 159.0, 151.2, 149.4, 147.40, 147.3, 131.3, 131.2, 131.2, 131.1, 129.2, 129.1, 128.6, 126.7, 126.3, 126.2, 115.2, 114.0, 113.8, 113.2, 113.2, 112.4, 110.9, 80.1, 79.9, 66.1, 66.0, 65.1, 64.1, 56.2, 55.3, 29.8, 29.7, 29.1, 28.8, 25.9, 18.3, 18.2, 17.4, 17.3, -4.8, -5.0, -5.0$ ; HRMS (EI) calcd for  $\text{C}_{31}\text{H}_{46}\text{O}_6\text{Si}$  ( $\text{M}^+$ ): 542.3064; found: 542.3050.



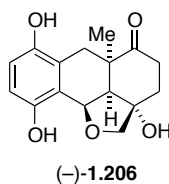
**(2a*S*, 2a'*R*, 5a*R*, 10b*R*)-2a-((4-Methoxybenzyl)oxy)-5a-methyl-3,4,5a,6-tetrahydro-2*H*-anthra[9,1-*bc*]furan-5,7,10(2a*H*, 2a'*H*, 10b*H*)-trione 1.202.** To a solution of **1.201** (10 mg, 0.024 mmol, 1.0 *eq.*) in THF/ $\text{H}_2\text{O}$  (2:1, 1 mL) was added a solution of [bis(trifluoroacetoxy)iodo]benzene (10 mg, 0.024 mmol, 1.0 *eq.*) in THF/ $\text{H}_2\text{O}$  (2:1, 100  $\mu\text{L}$ ) at  $0^\circ\text{C}$  for 20 min. The reaction mixture was diluted with EtOAc (50 mL), quenched with  $\text{NaHCO}_3$ , washed with aqueous  $\text{NaHCO}_3$  ( $2 \times 50$  mL) and brine (50 mL), dried over  $\text{Na}_2\text{SO}_4$  and concentrated to obtain a yellow oil, which was purified by silica gel chromatography (25% EtOAc in hexanes) to yield 3.8 mg (39%) of title compound **1.202**.

**Data for 1.202:**  $[\alpha]_{\text{D}}^{20} -27.2$  ( $c$  0.80,  $\text{CHCl}_3$ ); IR (ATR):  $\tilde{\nu} = 2934$  (w, br), 1709 (s), 1657 (s), 1611 (m), 1513 (s), 1464 (m), 1297 (m), 1245 (s), 1172 (m), 1050 (s), 920 (m);  $^1\text{H}$  NMR (600 MHz,  $\text{CDCl}_3$ )  $\delta = 7.27-7.25$  (m,  $2\text{H}$ ),  $6.90-6.86$  (m,  $2\text{H}$ ),  $6.78-6.72$  (m,  $2\text{H}$ ),  $5.07$  (d,  $J = 7.9, 1\text{H}$ ),  $4.52$  (d,  $J = 10.7, 1\text{H}$ ),  $4.42$  (d,  $J = 10.7, 1\text{H}$ ),  $4.14$  (dd,  $J = 1.1, 9.7, 1\text{H}$ ),  $3.85$  (d,  $J = 9.7, 1\text{H}$ ),  $3.79$  (s,  $3\text{H}$ ),  $3.08$  (d,  $J = 18.6, 1\text{H}$ ),  $2.71$  (d,  $J = 7.9, 1\text{H}$ ),  $2.61$  (ddd,  $J = 7.6, 14.9, 20.9, 2\text{H}$ ),  $2.43$  (ddd,  $J = 5.5, 9.8, 16.3, 1\text{H}$ ),  $2.18$  (dd,  $J = 7.9, 13.4, 1\text{H}$ ),  $2.07$  (dd,  $J = 1.4, 18.5, 1\text{H}$ ),  $1.31$  (s,  $3\text{H}$ );  $^{13}\text{C}$  NMR (150 MHz,  $\text{CDCl}_3$ )  $\delta = 211.3, 186.1, 185.6, 159.3, 143.5, 142.3, 136.8, 136.1, 130.1, 128.9, 114.0, 83.9, 77.3, 72.1, 65.7, 55.3, 52.7, 44.5, 33.4, 30.1, 28.5, 25.4$ , (two signals overlapping); HRMS (EI) calcd for  $\text{C}_{24}\text{H}_{26}\text{O}_6$  ( $\text{M}^+$ ): 410.1729; found: 410.1726.



**(2a*S*,2a<sup>1</sup>*R*,5a*R*,10b*R*)-2a-Hydroxy-5a-methyl-3,4,5a,6-tetrahydro-2*H*-anthra[9,1-*bc*]furan-5,7,10(2a*H*,2a<sup>1</sup>*H*,10b*H*)-trione 1.205.** To a solution of **1.202** (3.8 mg, 0.007 mmol, 1.0 *eq.*) in CH<sub>2</sub>Cl<sub>2</sub>/H<sub>2</sub>O (100 μL, 18:1) was added DDQ (2.1 mg, 0.00924 mmol, 1.2 *eq.*) at rt. The reaction mixture was stirred vigorously for 2.5 h and then treated with sat. NaHCO<sub>3</sub> solution (10 mL). The aqueous phase was extracted with CH<sub>2</sub>Cl<sub>2</sub> (3 × 15 mL) and combined organic phases were dried over Na<sub>2</sub>SO<sub>4</sub> and concentrated. The resulting brown oil was purified by preparative TLC (20% EtOAc in hexanes) to give 1.5 mg (68%) of the title compound **1.205** as a yellow oil.

**Data for 1.205:** [α]<sub>D</sub><sup>20</sup> -63.0 (*c* 0.40, CHCl<sub>3</sub>); IR (ATR):  $\tilde{\nu}$  = 3469 (br), 2929 (w), 1709 (s), 1657 (vs), 1604 (w), 1464 (w), 1412 (w), 1300 (s), 1274 (w), 1247 (w), 1222 (w), 1107 (w), 998 (w); <sup>1</sup>H NMR (600 MHz, CDCl<sub>3</sub>) δ = 6.80 – 6.73 (m, 2H), 5.20 (d, *J* = 8.1, 1H), 3.86 (d, *J* = 9.7, 1H), 3.71 (d, *J* = 9.8, 1H), 2.89 (d, *J* = 18.6, 1H), 2.68 – 2.62 (m, 1H), 2.59 (d, *J* = 8.1, 1H), 2.50 – 2.43 (m, 1H), 2.37 (ddd, *J* = 5.6, 8.1, 13.9, 1H), 2.20 – 2.15 (m, 2H), 2.12 (ddd, *J* = 5.2, 8.6, 14.0, 1H), 1.27 (s, 3H); <sup>13</sup>C NMR (150 MHz, CDCl<sub>3</sub>) δ = 211.5, 186.0, 185.5, 142.1, 136.8, 136.3, 136.1, 79.6, 79.1, 71.9, 54.9, 44.6, 33.8, 31.5, 29.7, 24.9; HRMS (EI) calcd for C<sub>16</sub>H<sub>16</sub>O<sub>5</sub> (M<sup>+</sup>): 288.0998; found: 288.0982.



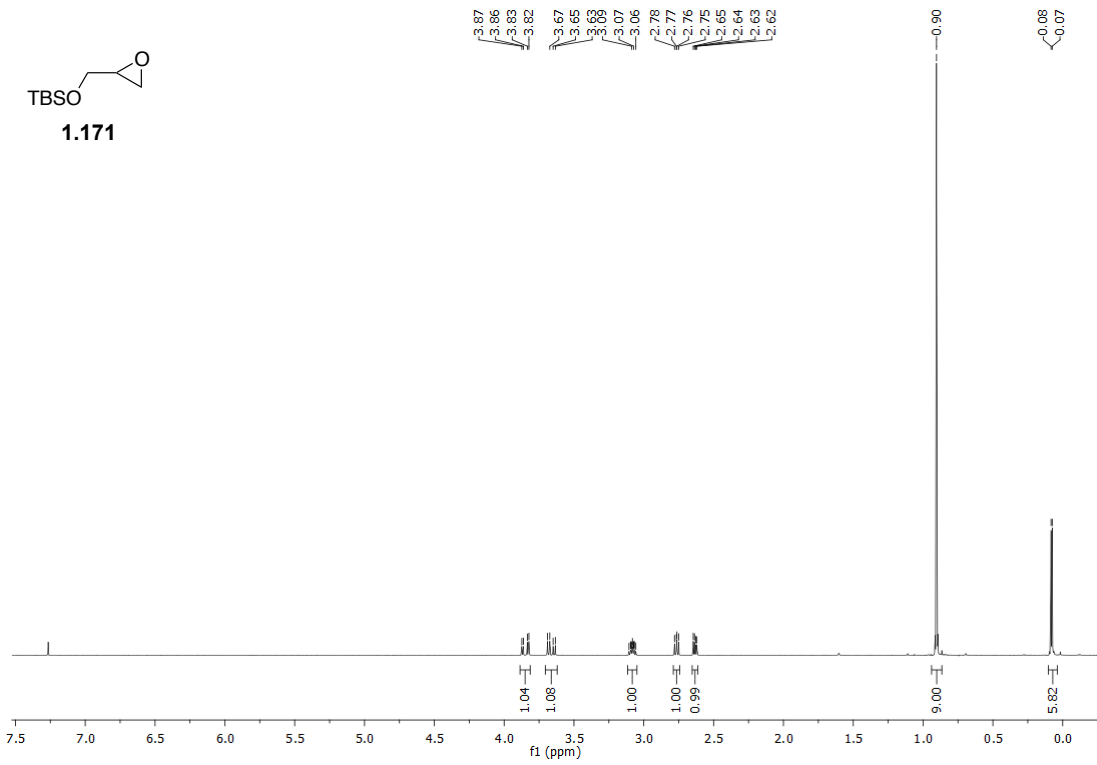
***Iso*-Glaziovianol (1.206).** To a solution of **1.205** (7.5 mg, 0.026 mmol, 1.0 *eq.*) in acetone (8 mL) was added a solution of Na<sub>2</sub>S<sub>2</sub>O<sub>4</sub> (90.5 mg, 0.52 mmol, 20.0 *eq.*) in H<sub>2</sub>O (800 μL) at 0 °C. The reaction mixture was diluted with brine (15 mL) and extracted with EtOAc (3 × 15 mL). Combined organic phases were dried over Na<sub>2</sub>SO<sub>4</sub> and concentrated to give 7.0 mg (93%) of title compound **1.206** as a colourless oil.

**Data for 1.206:**  $[\alpha]_{\text{D}}^{20} -44.4$  ( $c$  0.27, EtOAc); IR (ATR):  $\tilde{\nu} = 3382$  (vs, br), 2957 (w), 2924 (vs), 2853 (s), 1701 (vs), 1658 (s), 1468 (vs), 1375 (w), 1355 (w), 1250 (vs), 1108 (w), 1046 (vs);  $^1\text{H}$  NMR (600 MHz, acetone- $d_6$ )  $\delta = 7.60$  (s, 1H), 7.52 (s, 1H), 6.62 (d,  $J = 8.6$ , 1H), 6.46 (d,  $J = 8.6$ , 1H), 5.38 (d,  $J = 9.2$ , 1H), 4.49 (s, 1H), 3.90 (q,  $J = 8.8$ , 2H), 3.36 (d,  $J = 15.3$ , 1H), 2.74 (d,  $J = 9.2$ , 1H), 2.54 (ddd,  $J = 4.4, 8.9, 16.5$ , 1H), 2.26 – 2.07 (m, 4H), 1.27 (d,  $J = 1.9$ , 3H);  $^{13}\text{C}$  NMR (100 MHz, acetone- $d_6$ )  $\delta = 212.0, 148.9, 147.1, 123.3, 120.6, 114.9, 113.4, 78.7, 77.3, 76.2, 55.6, 44.9, 34.1, 32.7, 31.2, 26.4$ ; HRMS (EI) calcd for  $\text{C}_{16}\text{H}_{18}\text{O}_5$  ( $\text{M}^+$ ): 290.1154; found: 290.1147.

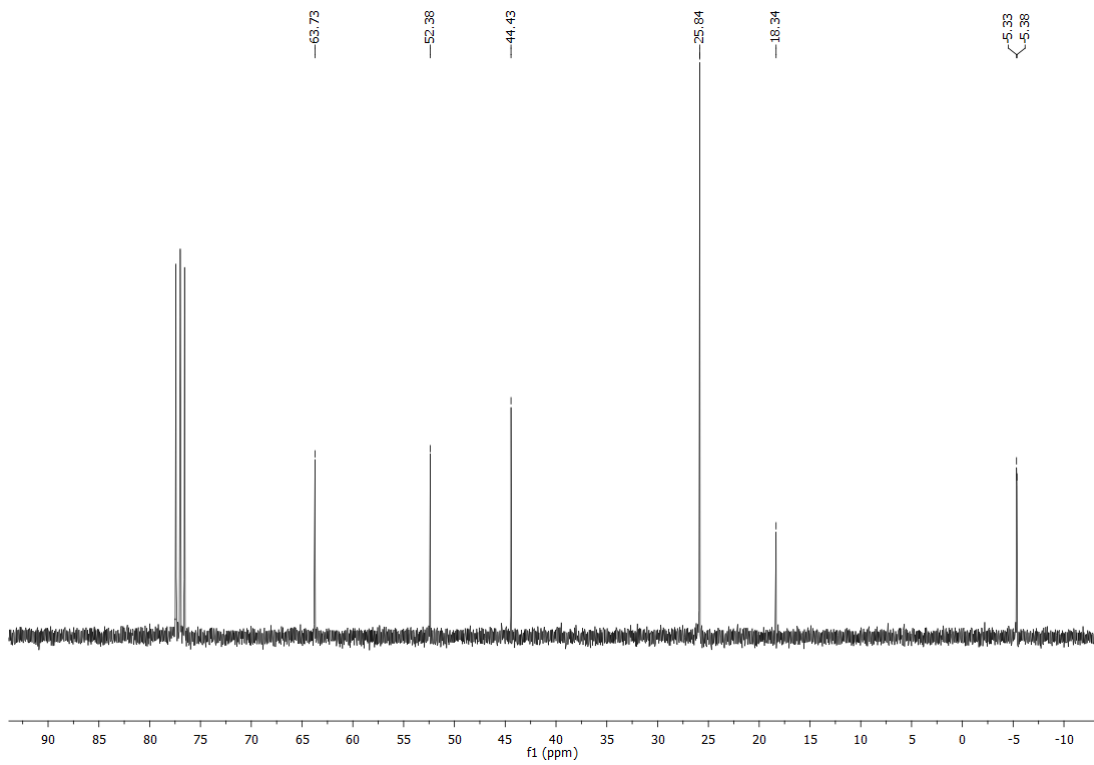


# 1. VINYL QUINONE DIELS-ALDER REACTIONS

$^1\text{H}$  NMR,  $\text{CDCl}_3$ , 600 MHz

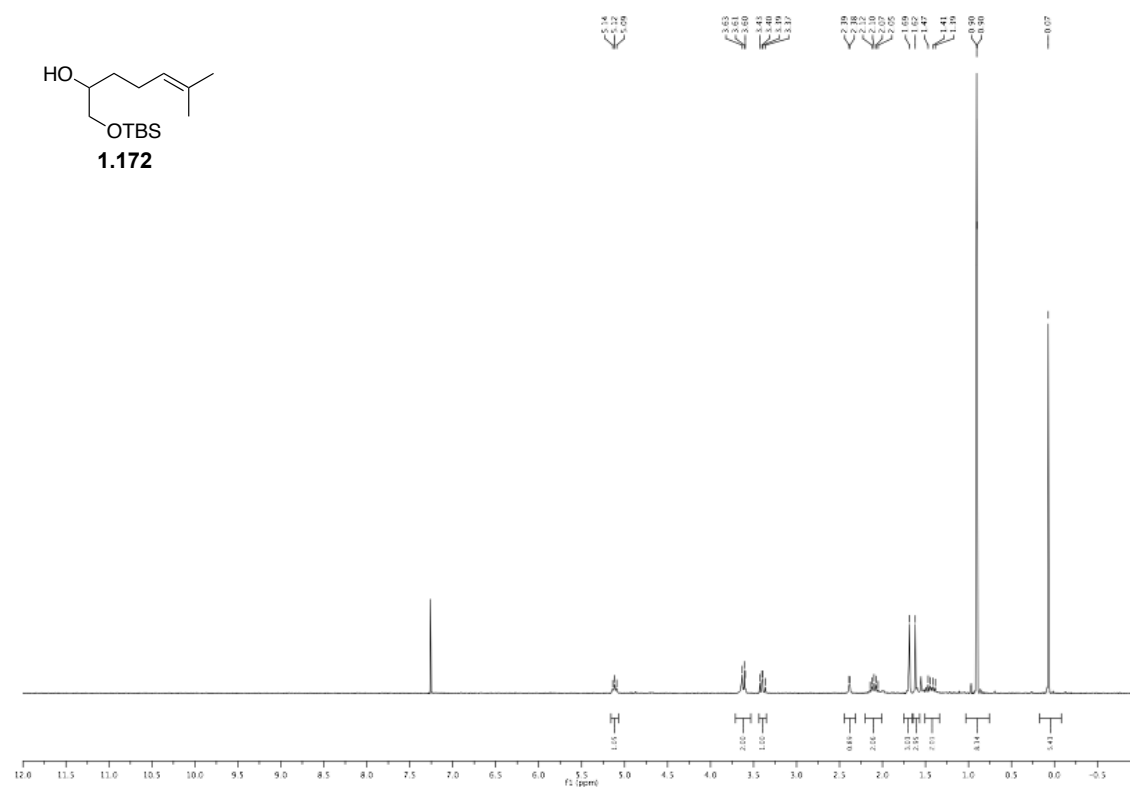


$^{13}\text{C}$  NMR,  $\text{CDCl}_3$ , 150 MHz

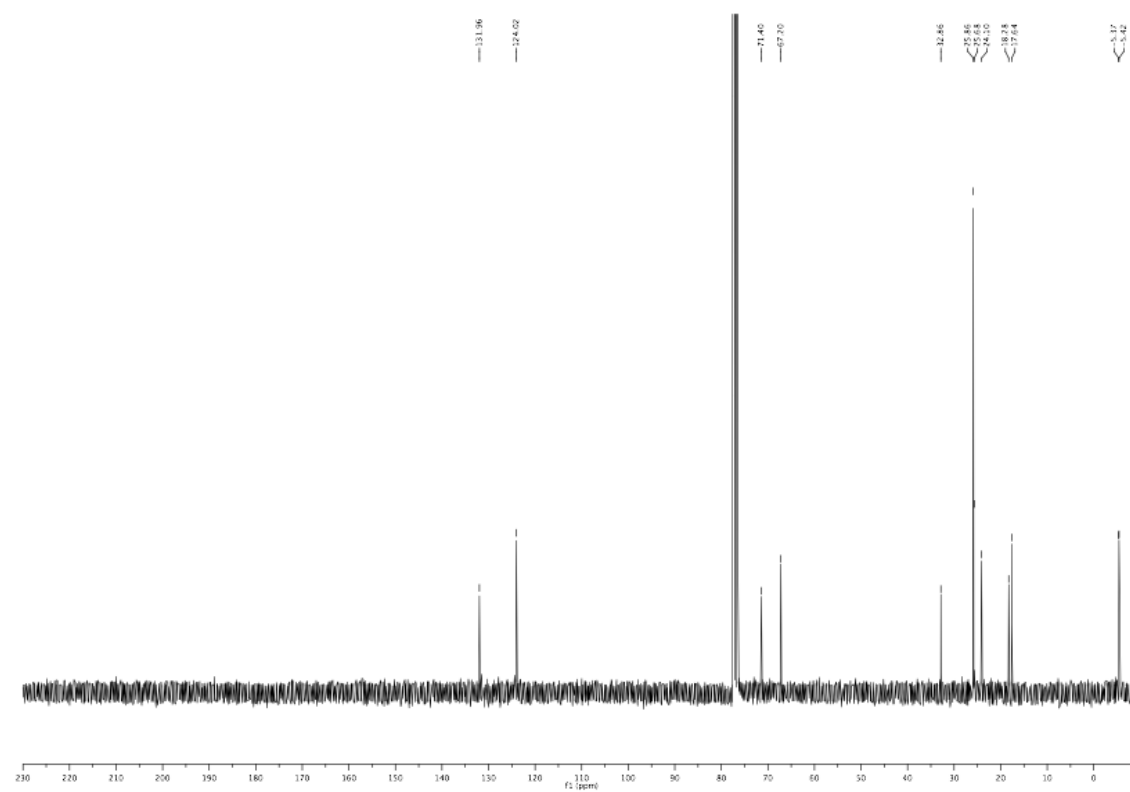


## 1.5. Experimental Section

$^1\text{H}$  NMR,  $\text{CDCl}_3$ , 300 MHz

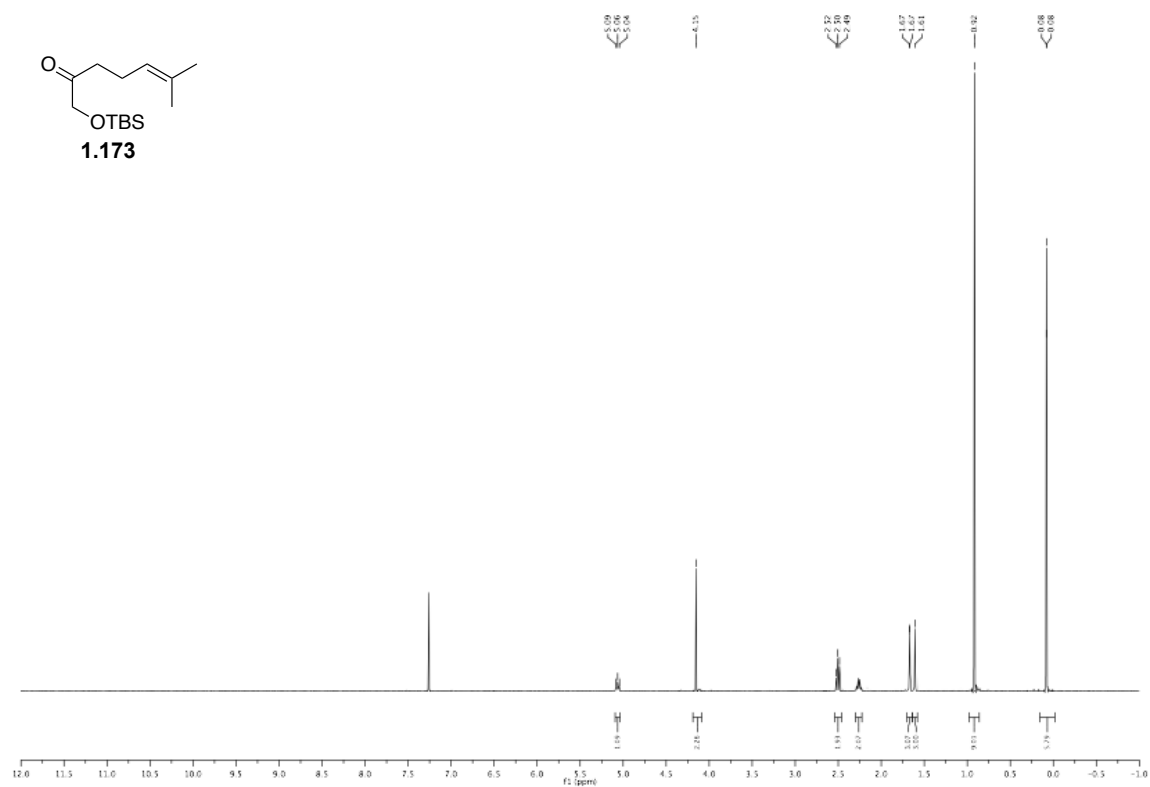


$^{13}\text{C}$  NMR,  $\text{CDCl}_3$ , 75 MHz

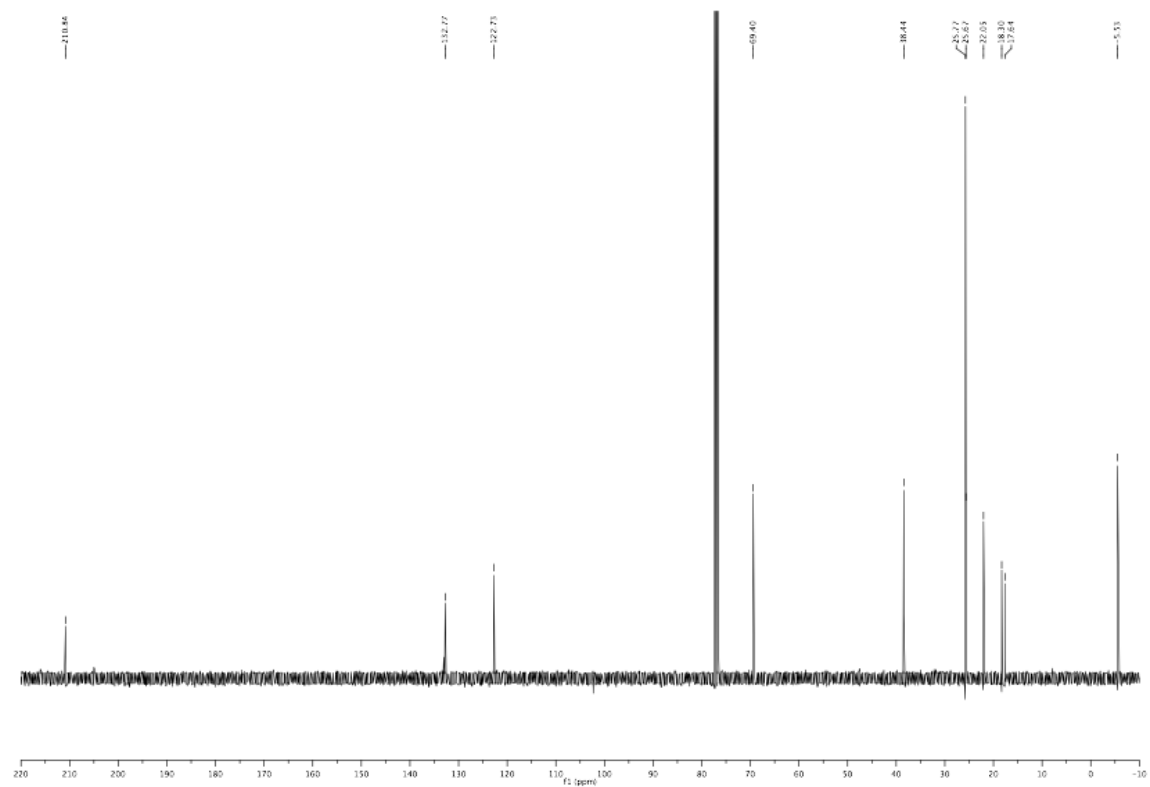


# 1. VINYL QUINONE DIELS-ALDER REACTIONS

$^1\text{H}$  NMR,  $\text{CDCl}_3$ , 600 MHz

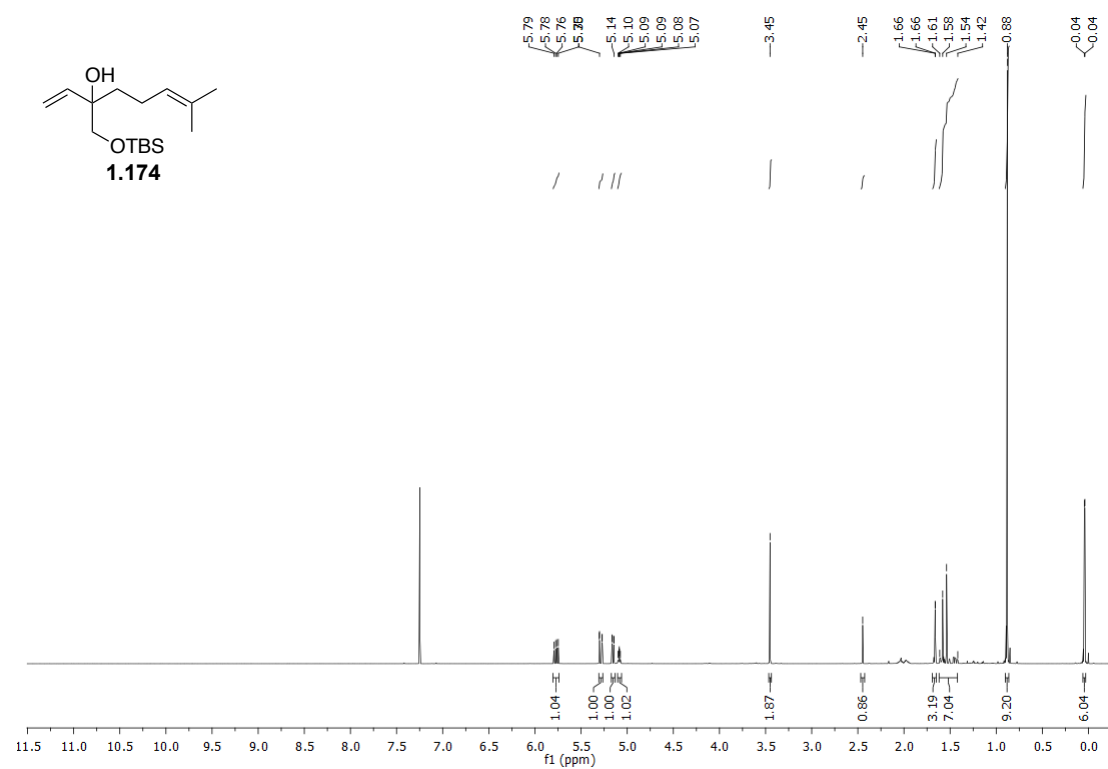


$^{13}\text{C}$  NMR,  $\text{CDCl}_3$ , 150 MHz

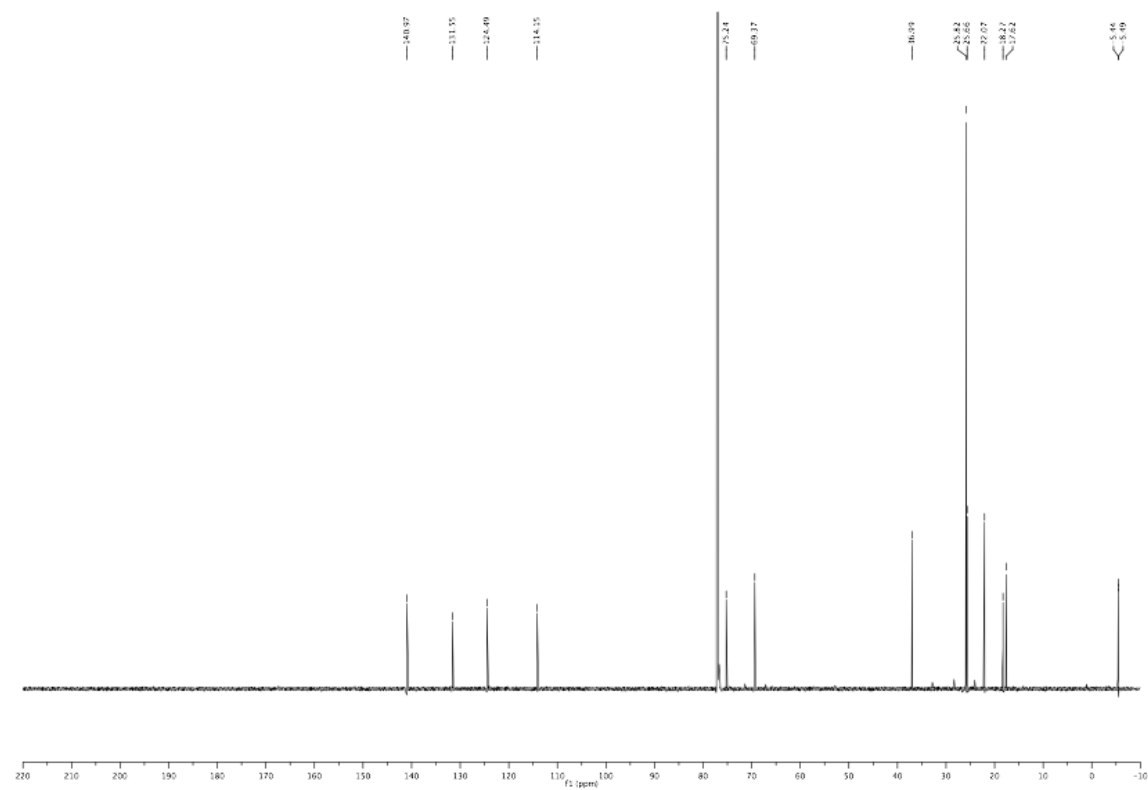


# 1.5. Experimental Section

$^1\text{H}$  NMR,  $\text{CDCl}_3$ , 600 MHz

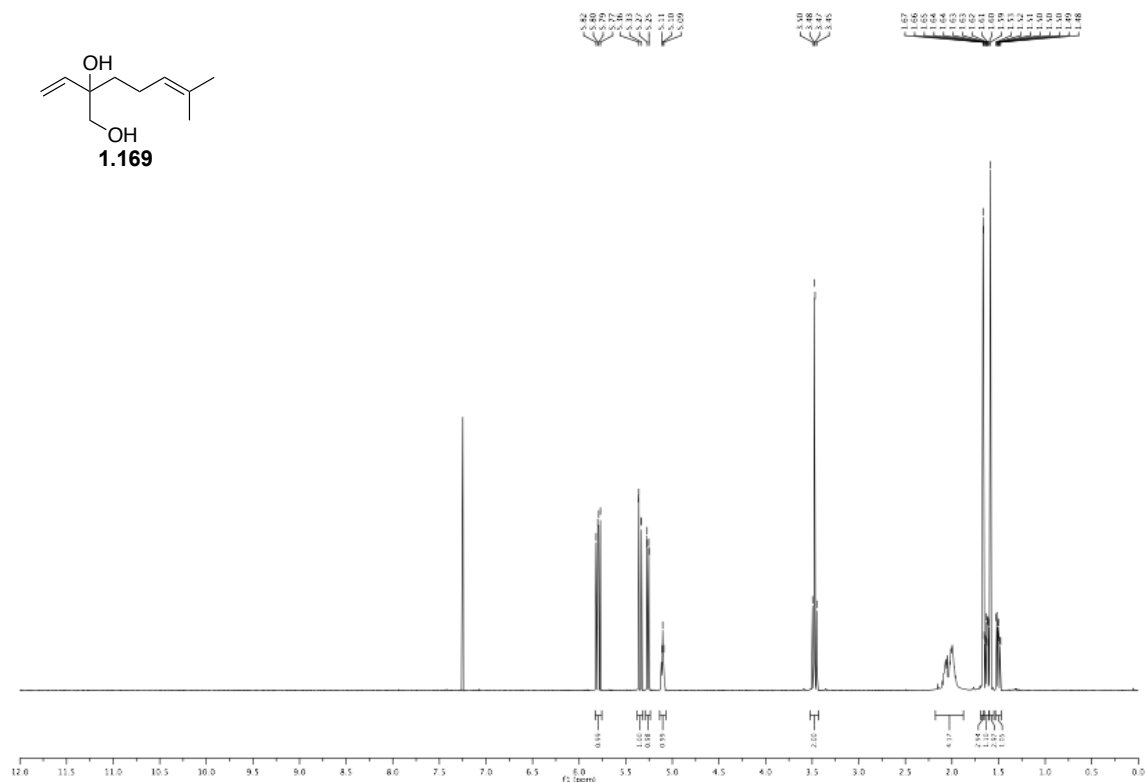


$^{13}\text{C}$  NMR,  $\text{CDCl}_3$ , 150 MHz

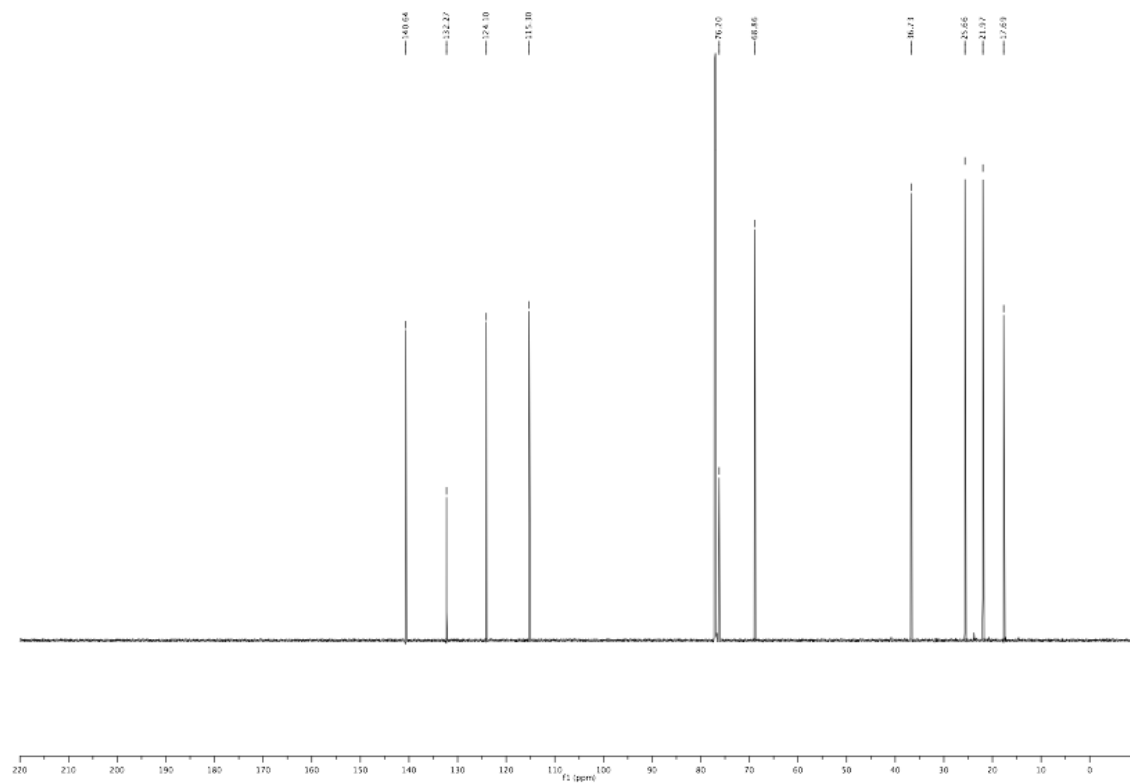


# 1. VINYL QUINONE DIELS-ALDER REACTIONS

$^1\text{H}$  NMR,  $\text{CDCl}_3$ , 600 MHz

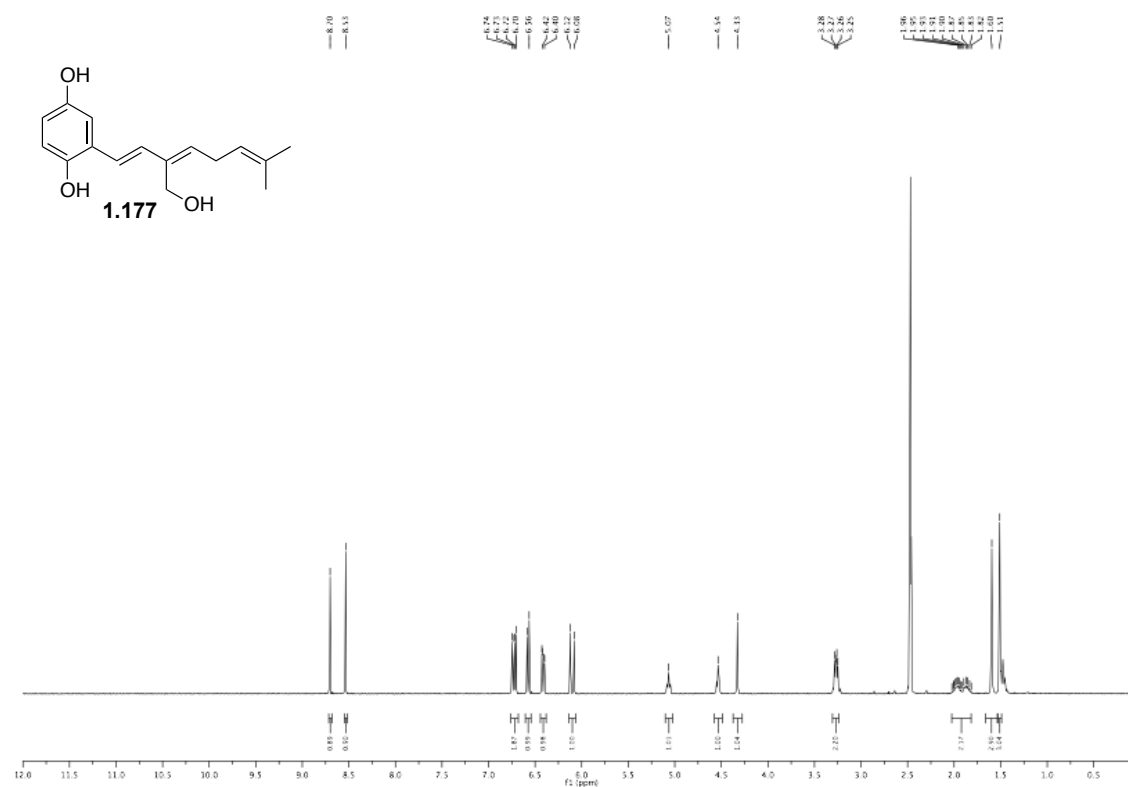


$^{13}\text{C}$  NMR,  $\text{CDCl}_3$ , 150 MHz

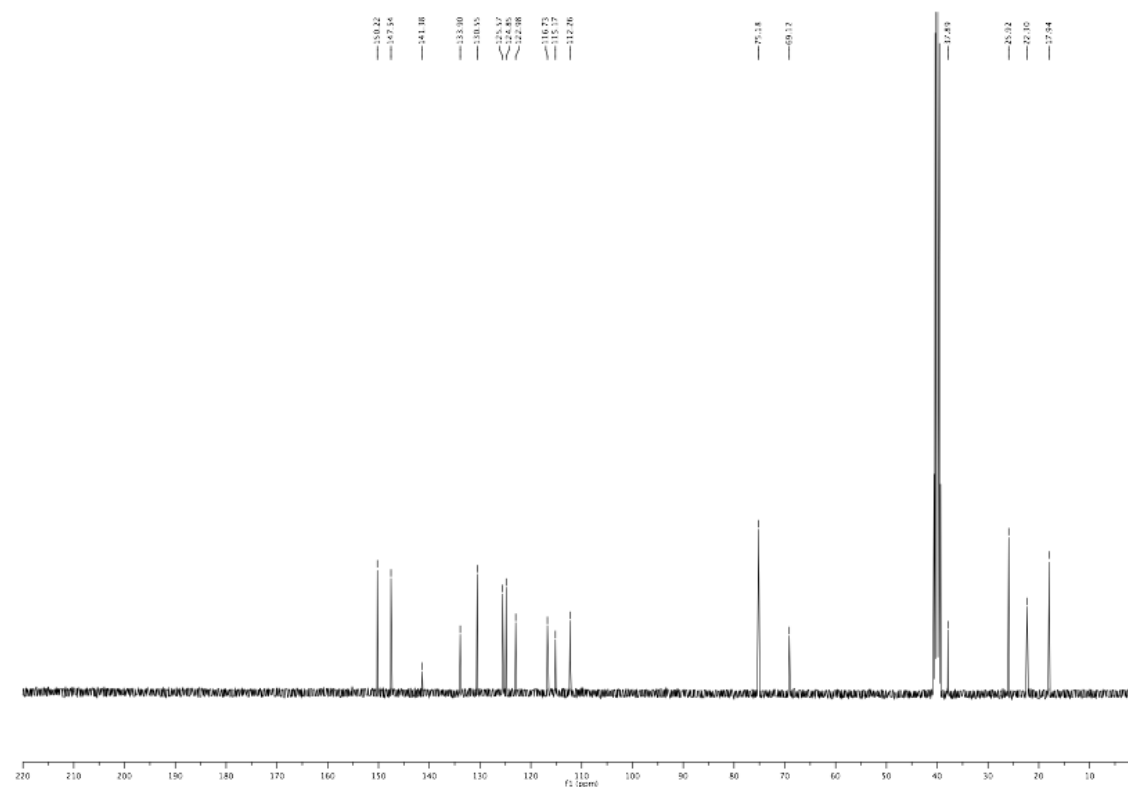


## 1.5. Experimental Section

$^1\text{H}$  NMR,  $\text{DMSO-}d_6$ , 600 MHz

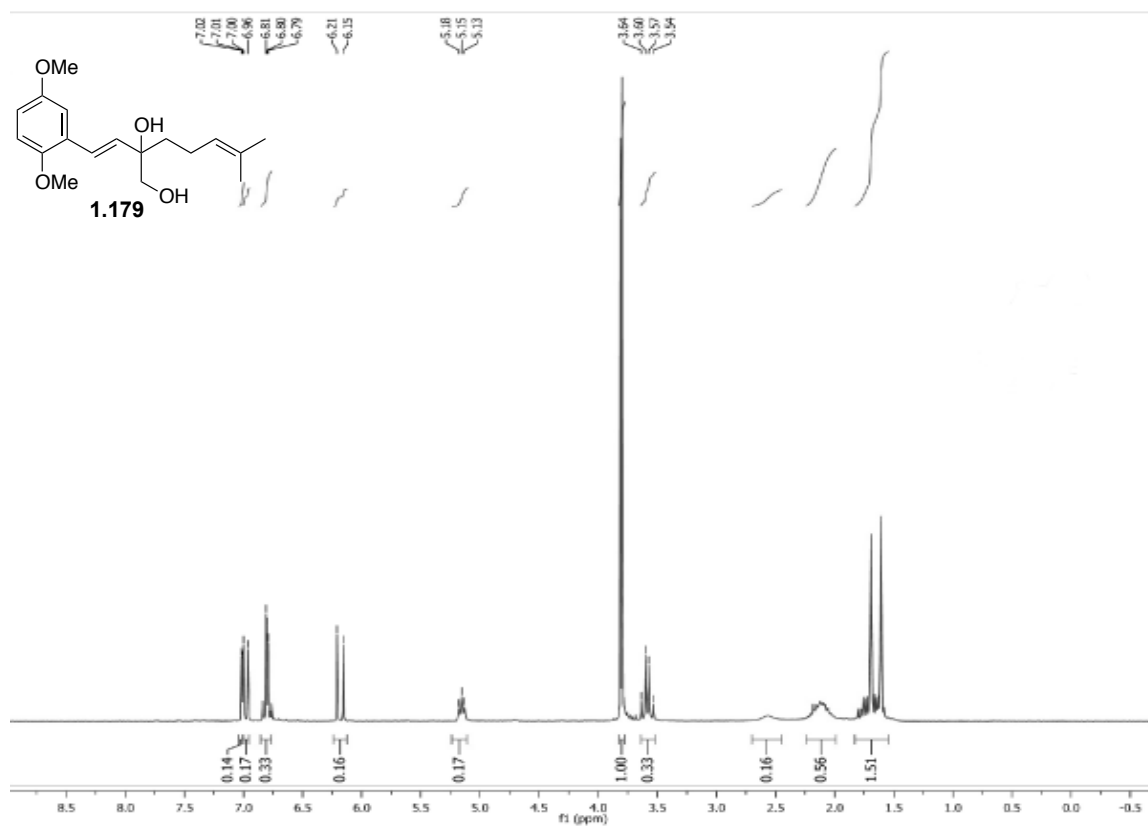


$^{13}\text{C}$  NMR,  $\text{DMSO-}d_6$ , 150 MHz

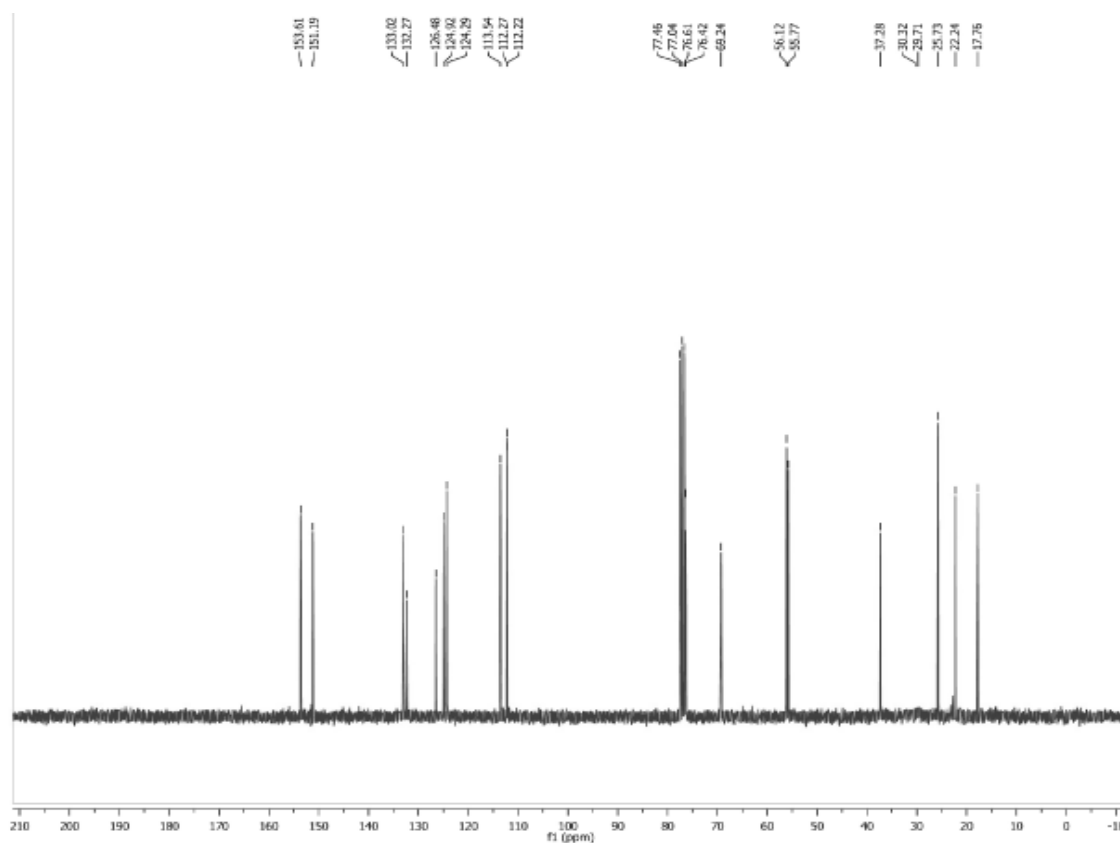


# 1. VINYL QUINONE DIELS-ALDER REACTIONS

$^1\text{H NMR}$ ,  $\text{CDCl}_3$ , 400 MHz

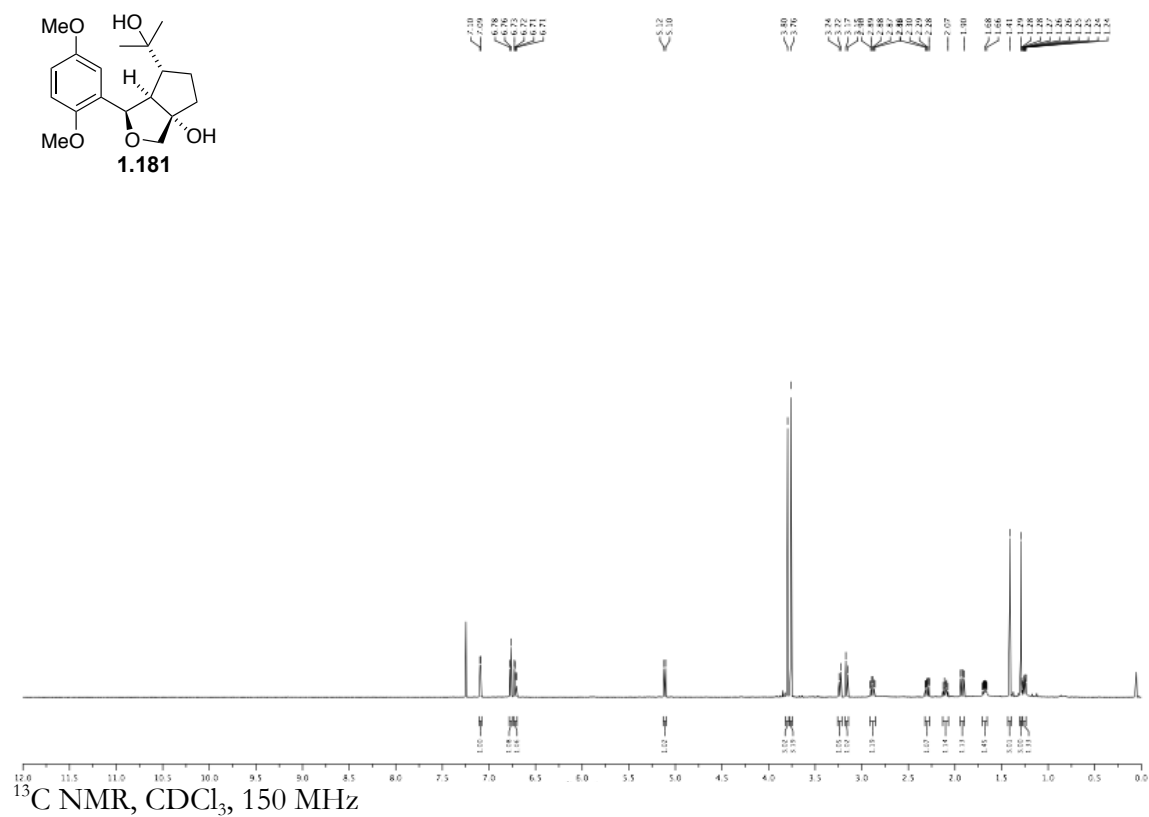
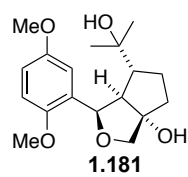


$^{13}\text{C NMR}$ ,  $\text{CDCl}_3$ , 100 MHz

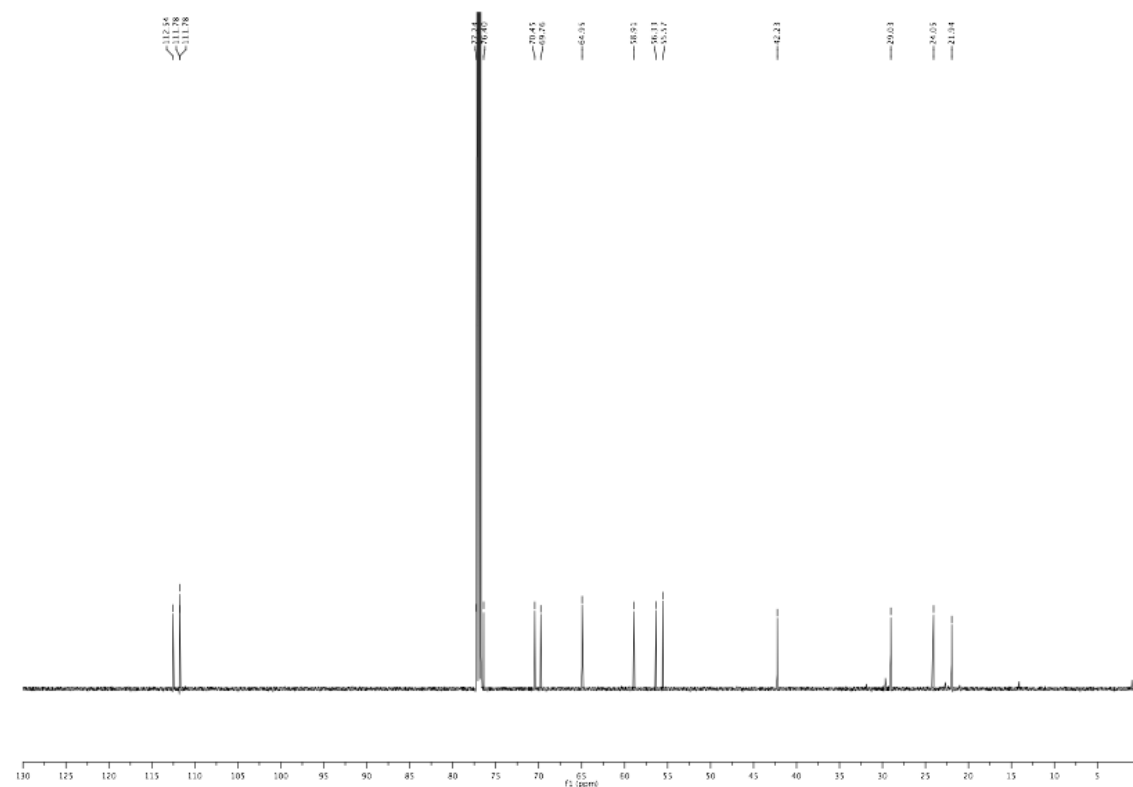


# 1.5. Experimental Section

$^1\text{H}$  NMR,  $\text{CDCl}_3$ , 600 MHz



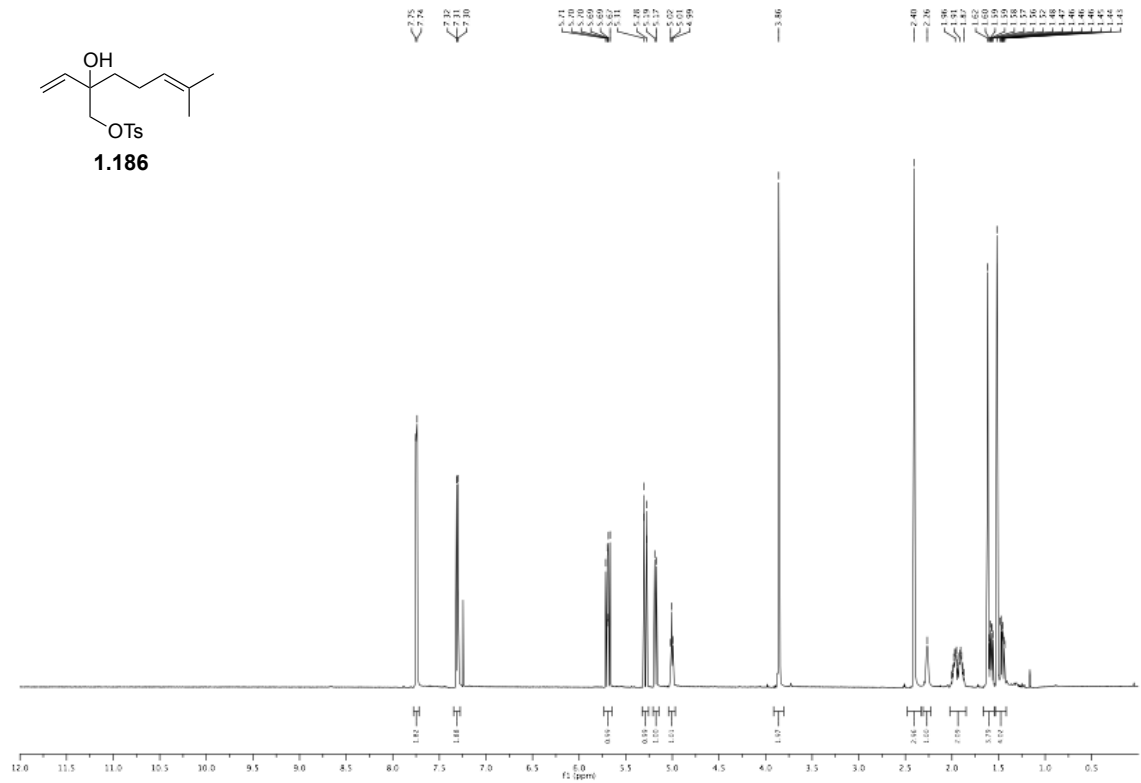
$^{13}\text{C}$  NMR,  $\text{CDCl}_3$ , 150 MHz



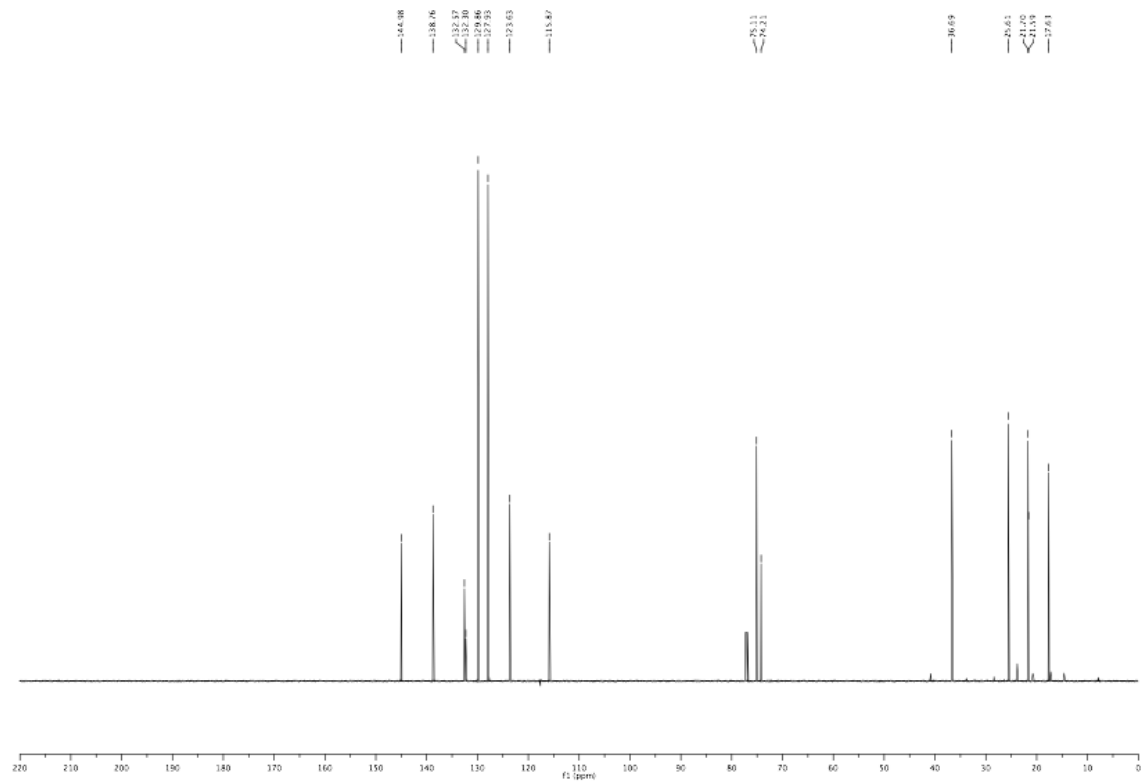


# 1. VINYL QUINONE DIELS-ALDER REACTIONS

$^1\text{H}$  NMR,  $\text{CDCl}_3$ , 600 MHz

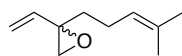


$^{13}\text{C}$  NMR,  $\text{CDCl}_3$ , 150 MHz

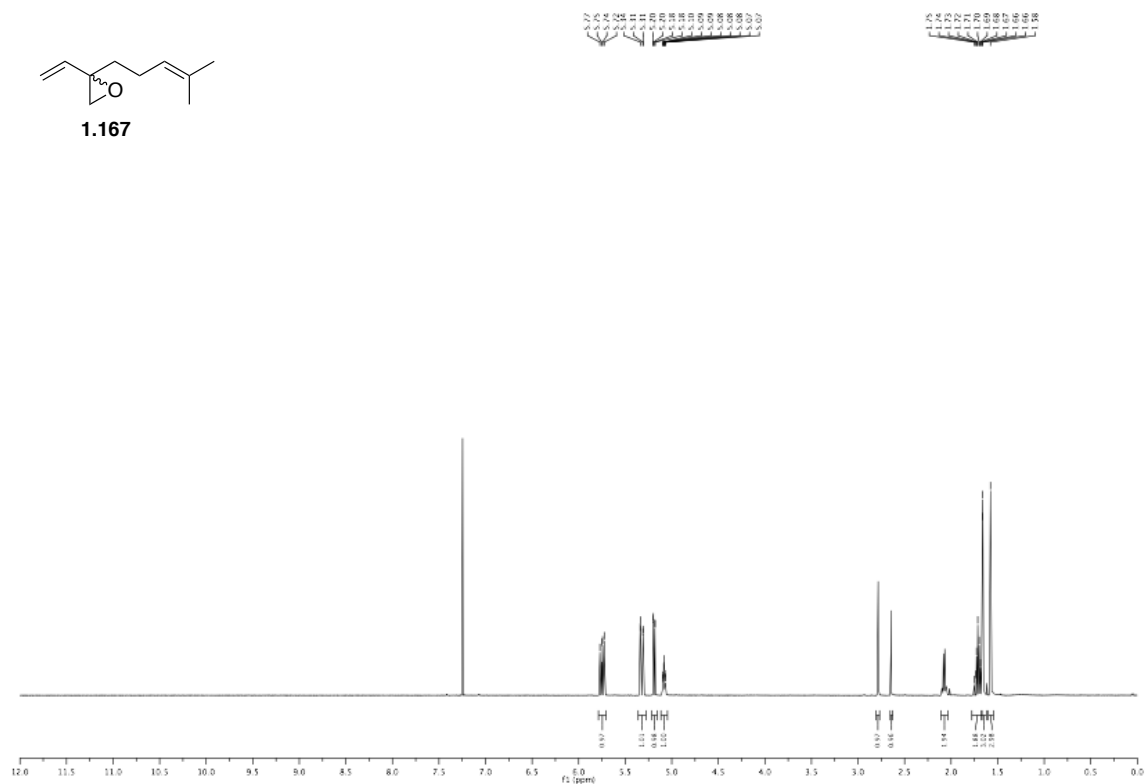


## 1.5. Experimental Section

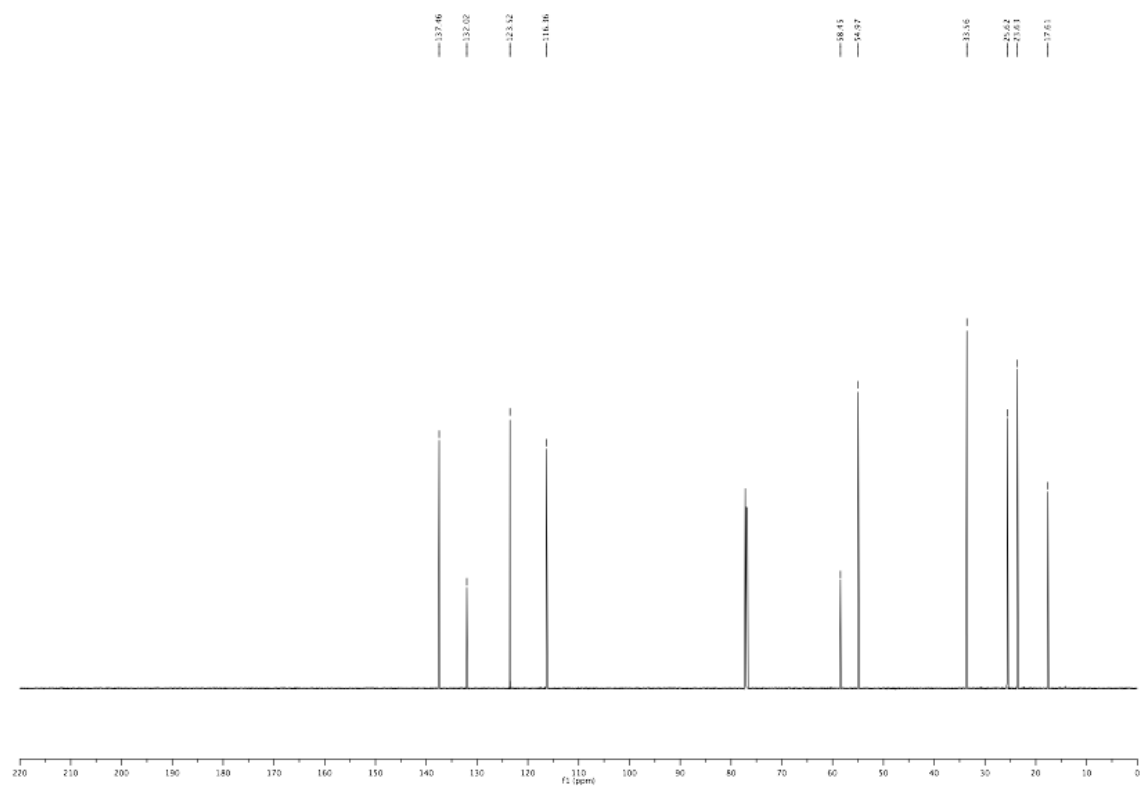
$^1\text{H}$  NMR,  $\text{CDCl}_3$ , 600 MHz



**1.167**

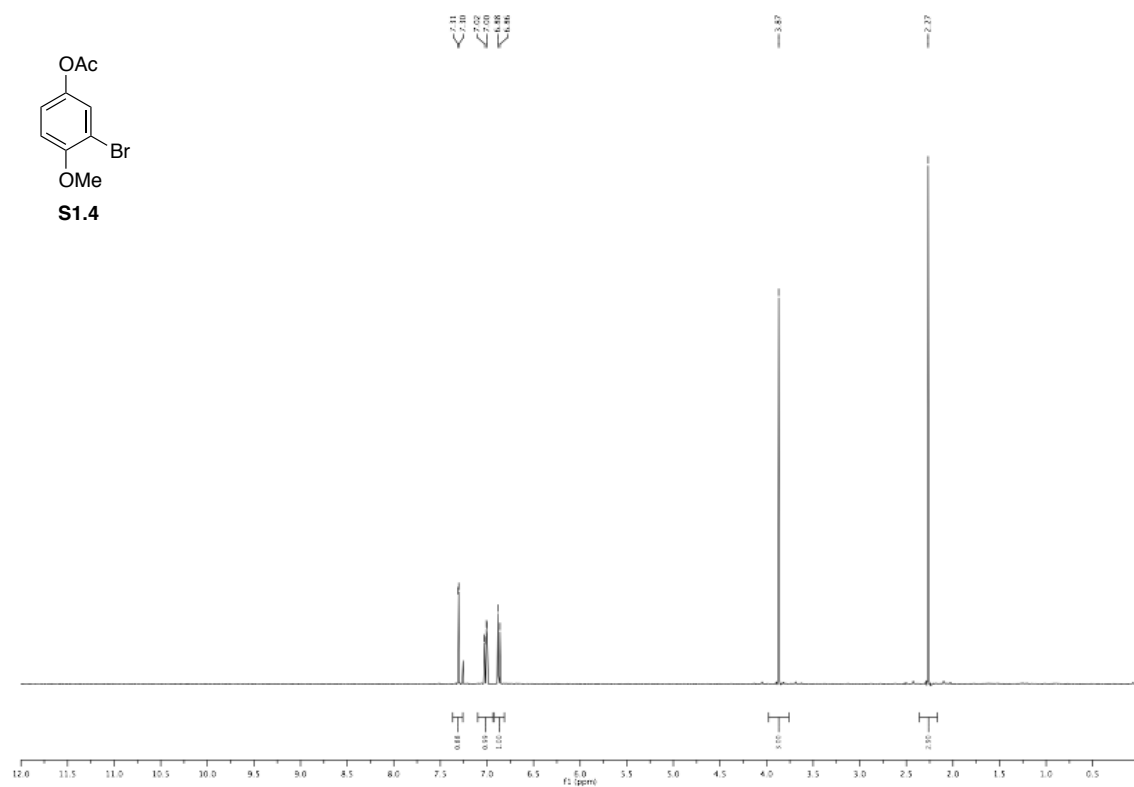
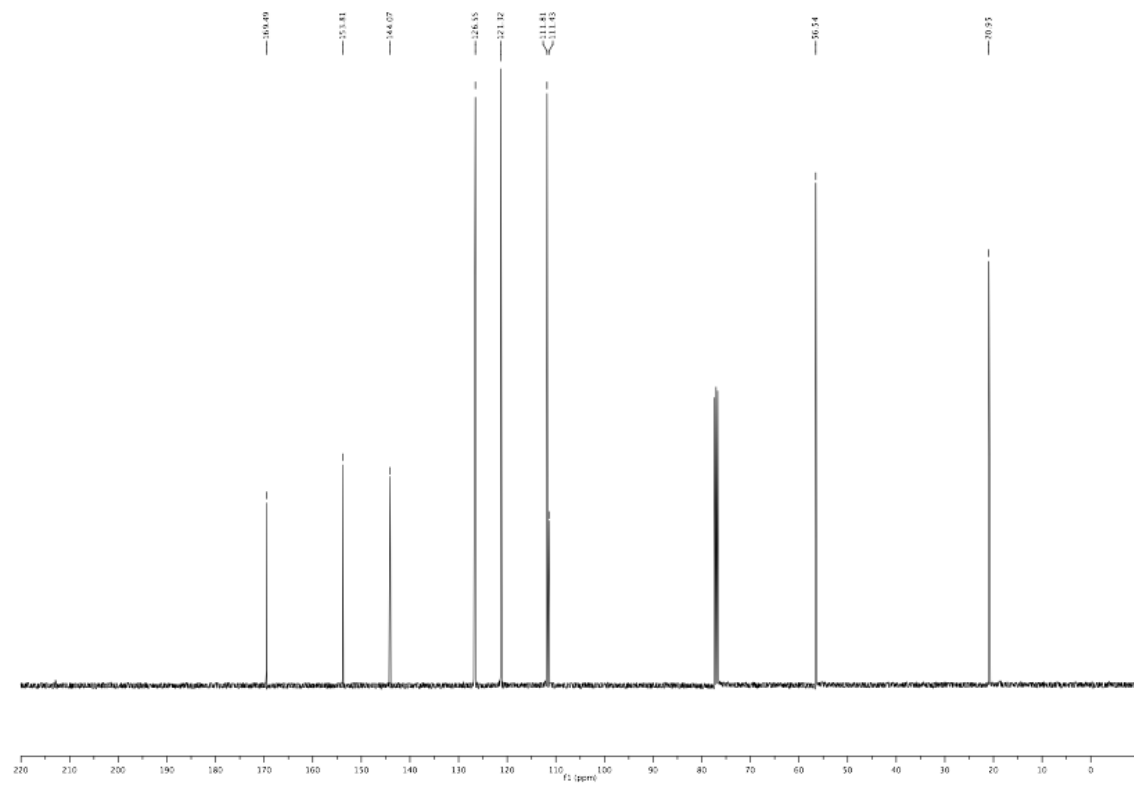


$^{13}\text{C}$  NMR,  $\text{CDCl}_3$ , 150 MHz



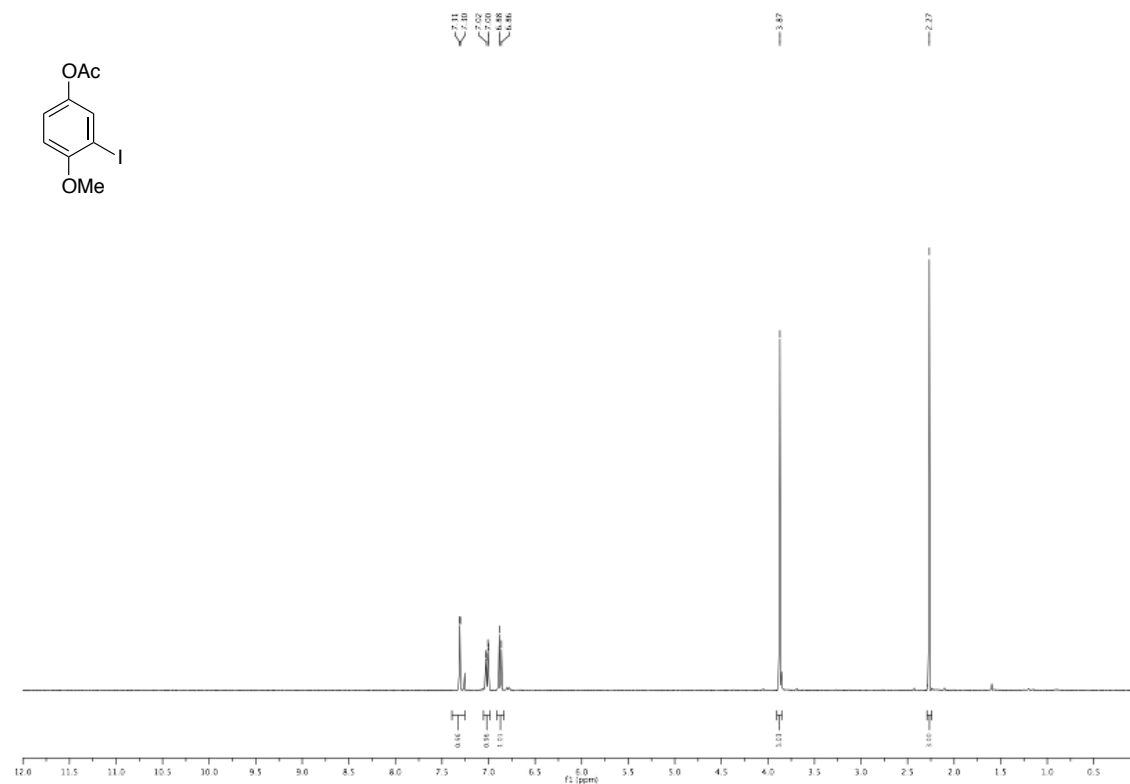




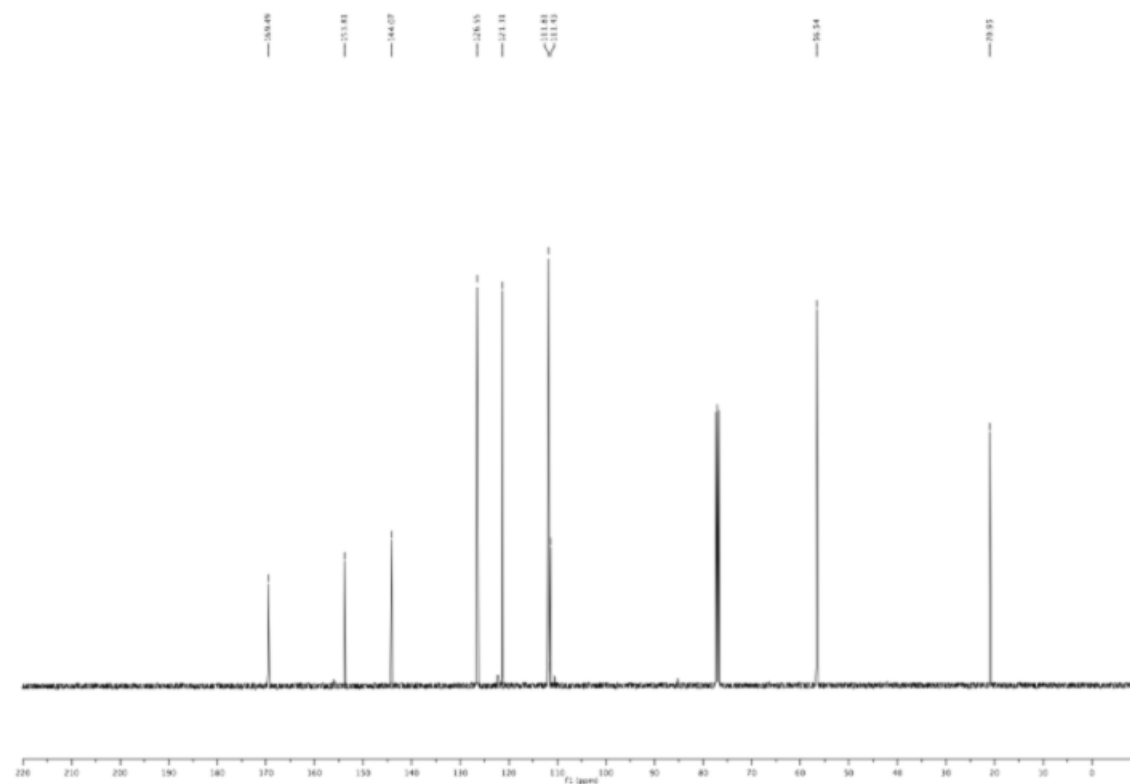
$^1\text{H}$  NMR,  $\text{CDCl}_3$ , 600 MHz $^{13}\text{C}$  NMR,  $\text{CDCl}_3$ , 150 MHz

## 1.5. Experimental Section

$^1\text{H}$  NMR,  $\text{CDCl}_3$ , 600 MHz

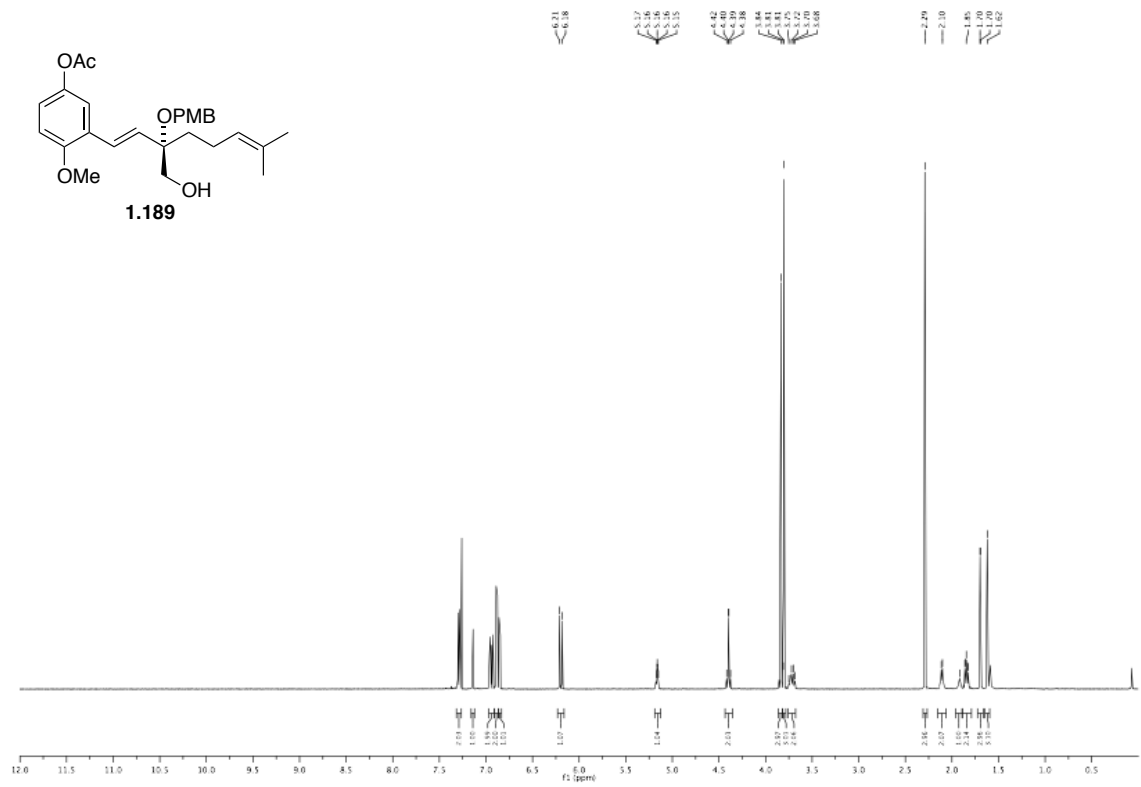


$^{13}\text{C}$  NMR,  $\text{CDCl}_3$ , 150 MHz

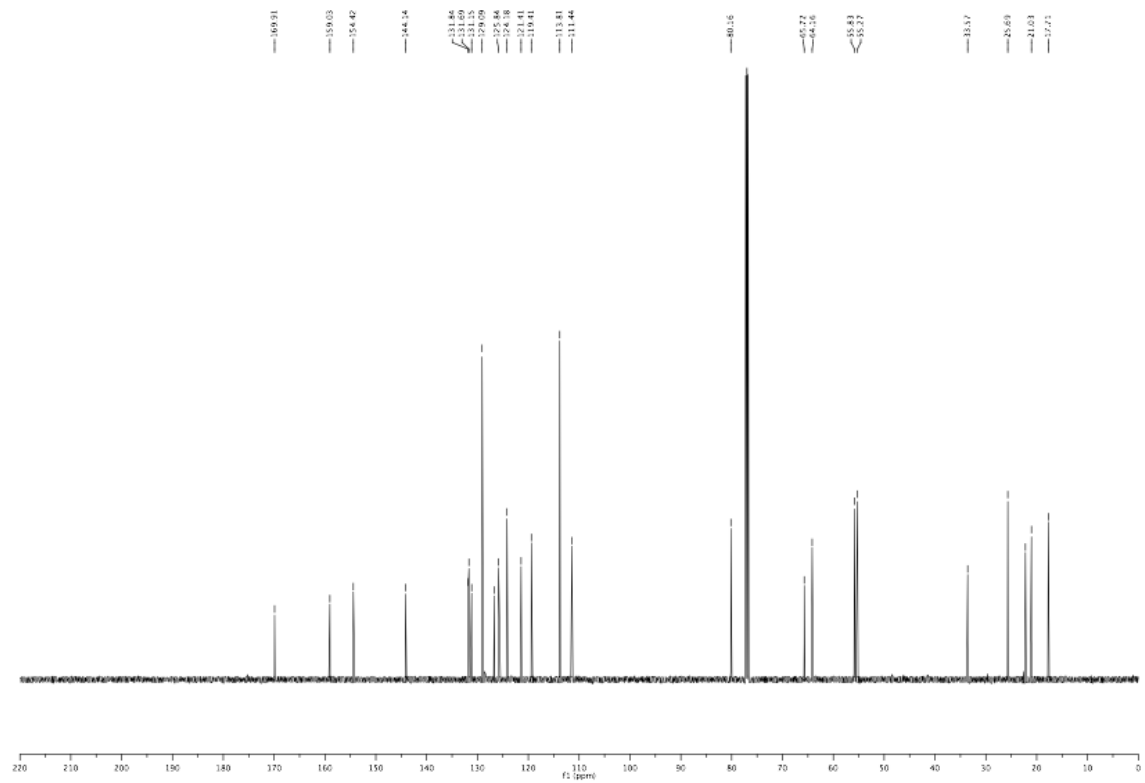


# 1. VINYL QUINONE DIELS-ALDER REACTIONS

$^1\text{H NMR}$ ,  $\text{CDCl}_3$ , 600 MHz

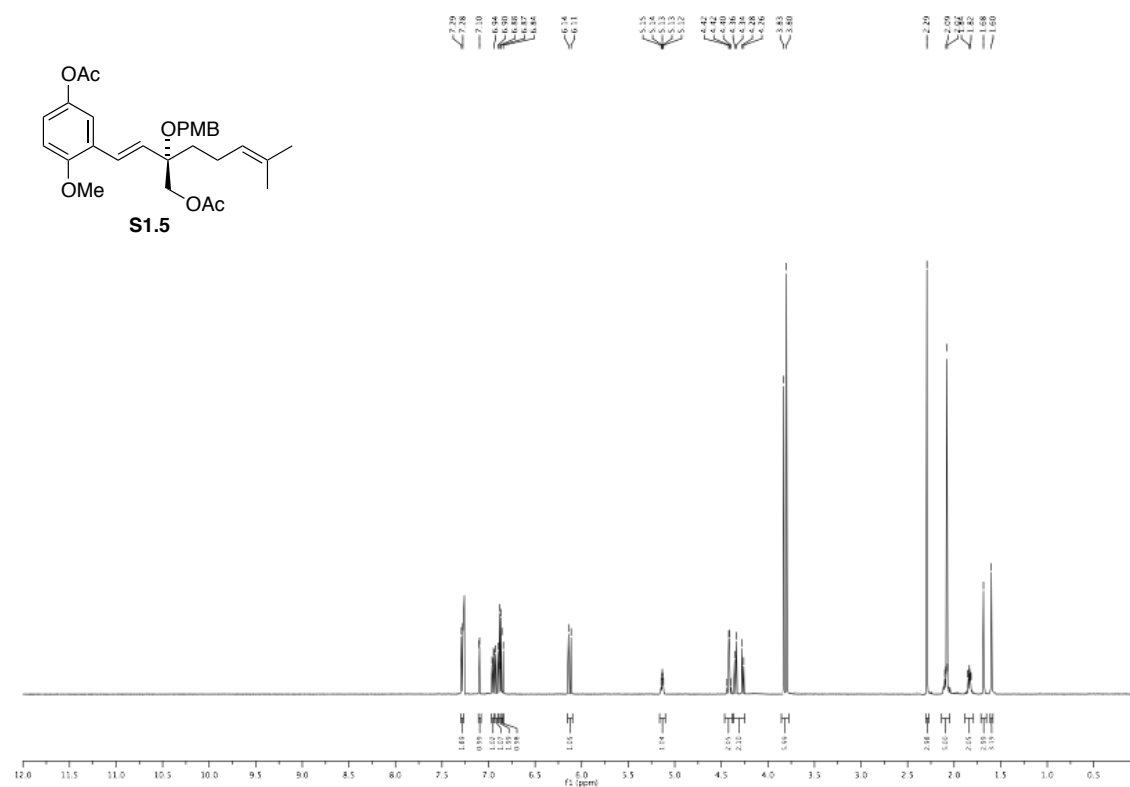


$^{13}\text{C NMR}$ ,  $\text{CDCl}_3$ , 150 MHz

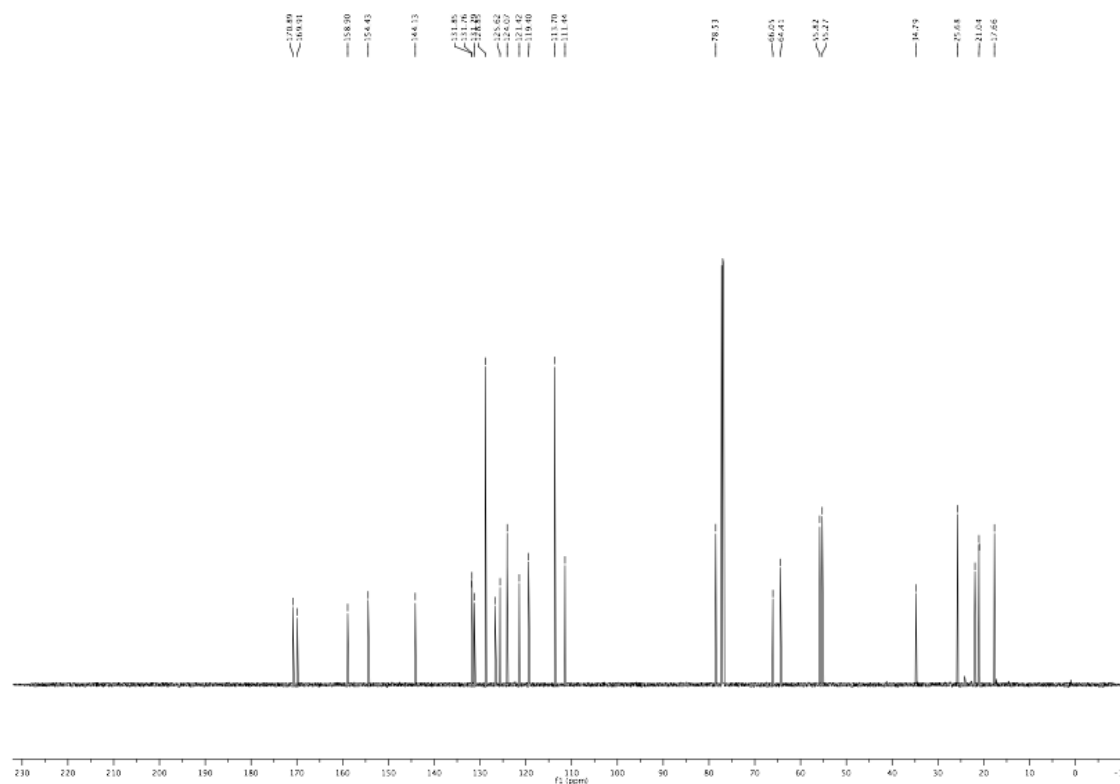


## 1.5. Experimental Section

$^1\text{H}$  NMR,  $\text{CDCl}_3$ , 600 MHz



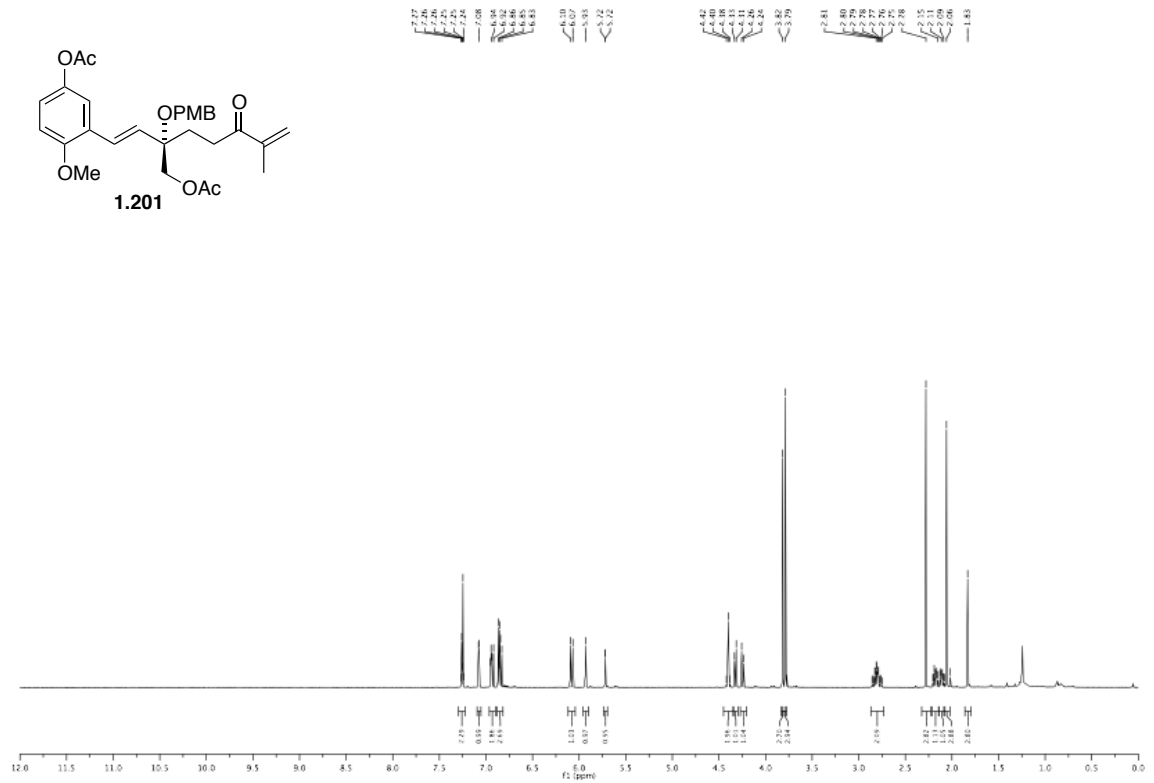
$^{13}\text{C}$  NMR,  $\text{CDCl}_3$ , 150 MHz



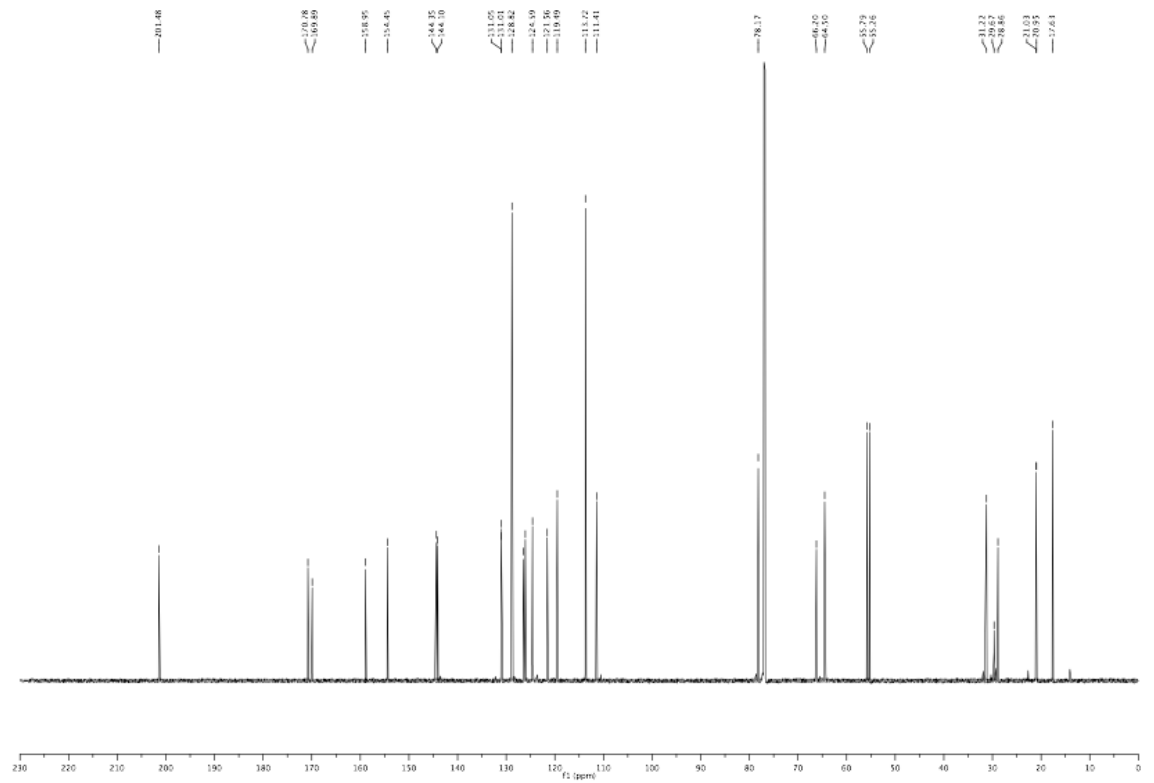


# 1. VINYL QUINONE DIELS-ALDER REACTIONS

$^1\text{H NMR}$ ,  $\text{CDCl}_3$ , 600 MHz



$^{13}\text{C NMR}$ ,  $\text{CDCl}_3$ , 150 MHz

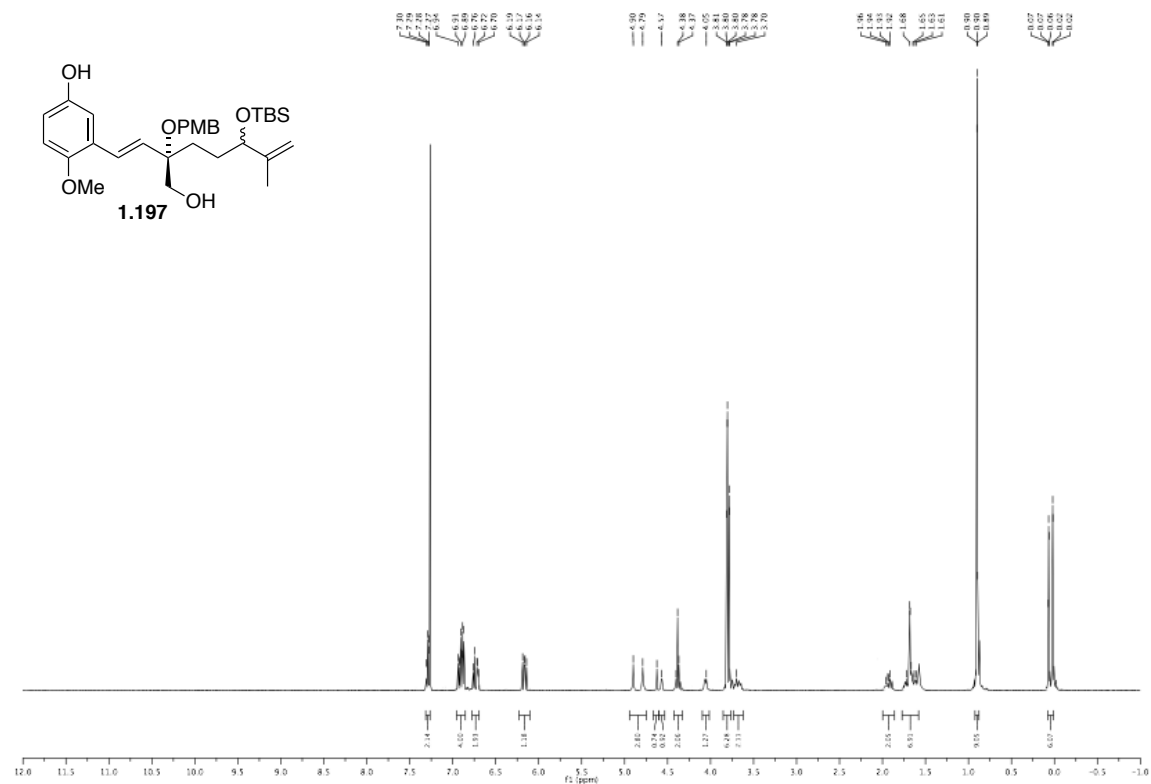




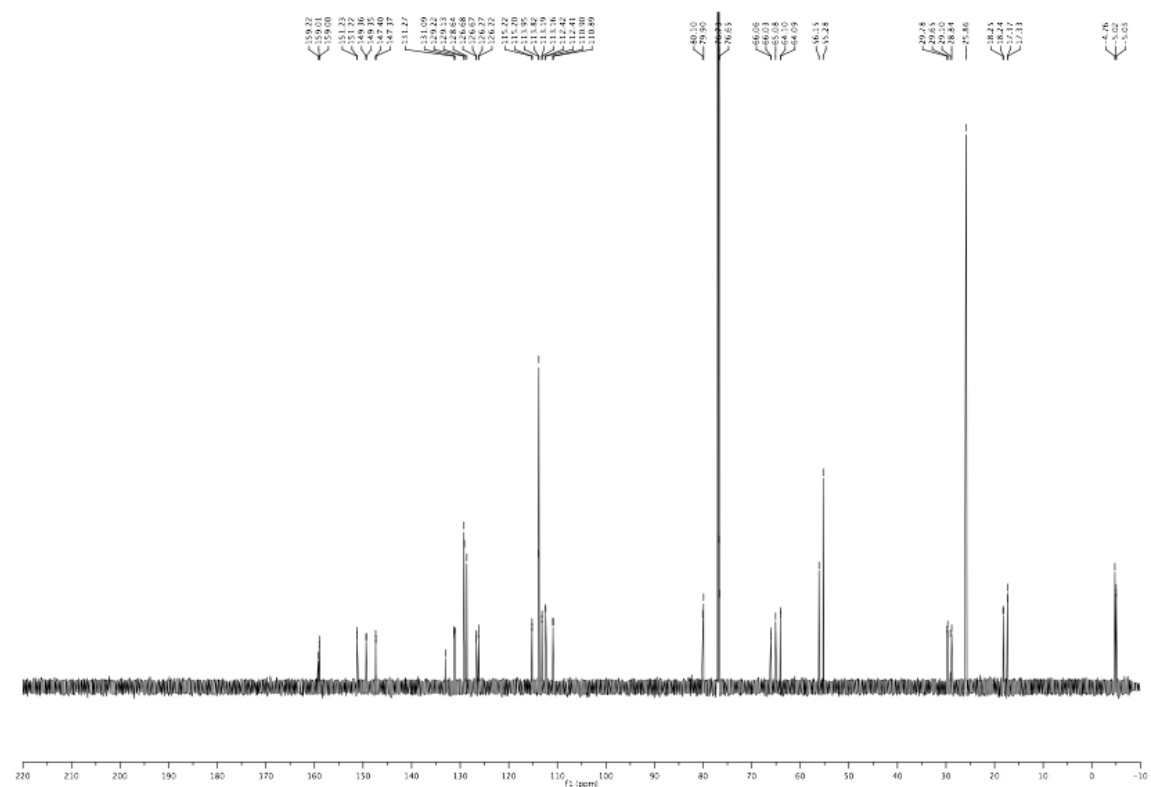


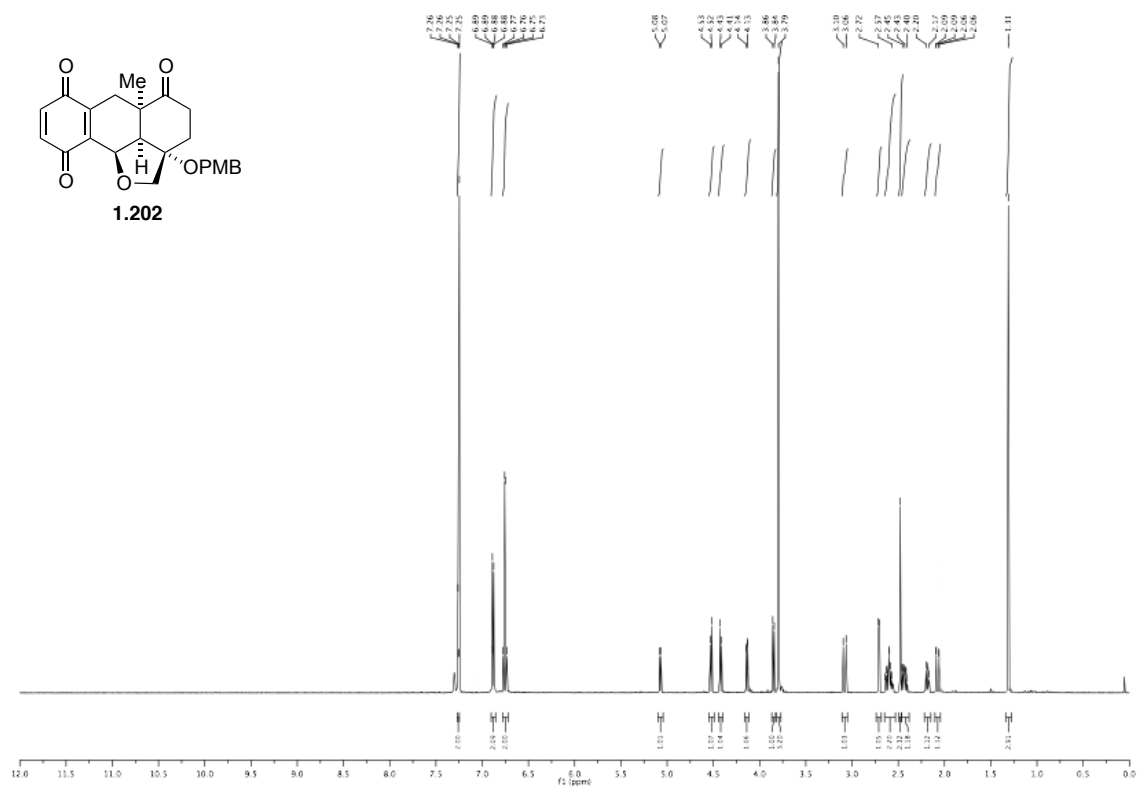
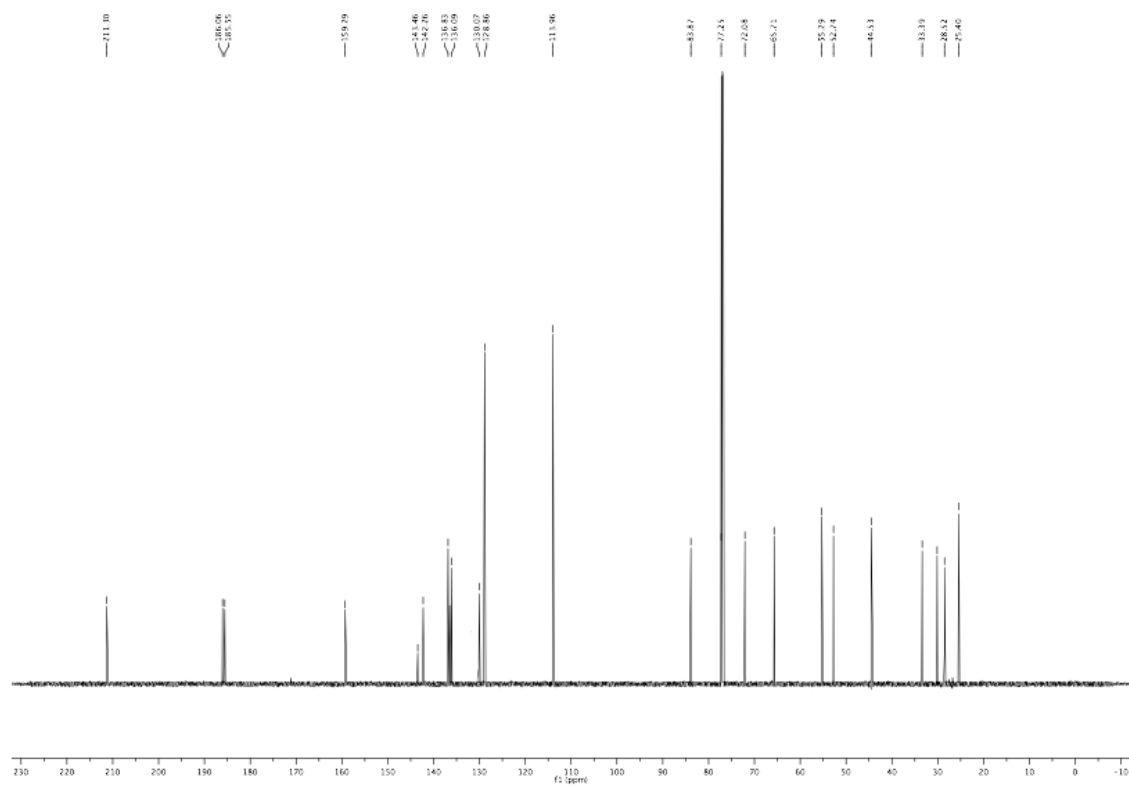
## 1.5. Experimental Section

$^1\text{H}$  NMR,  $\text{CDCl}_3$ , 600 MHz



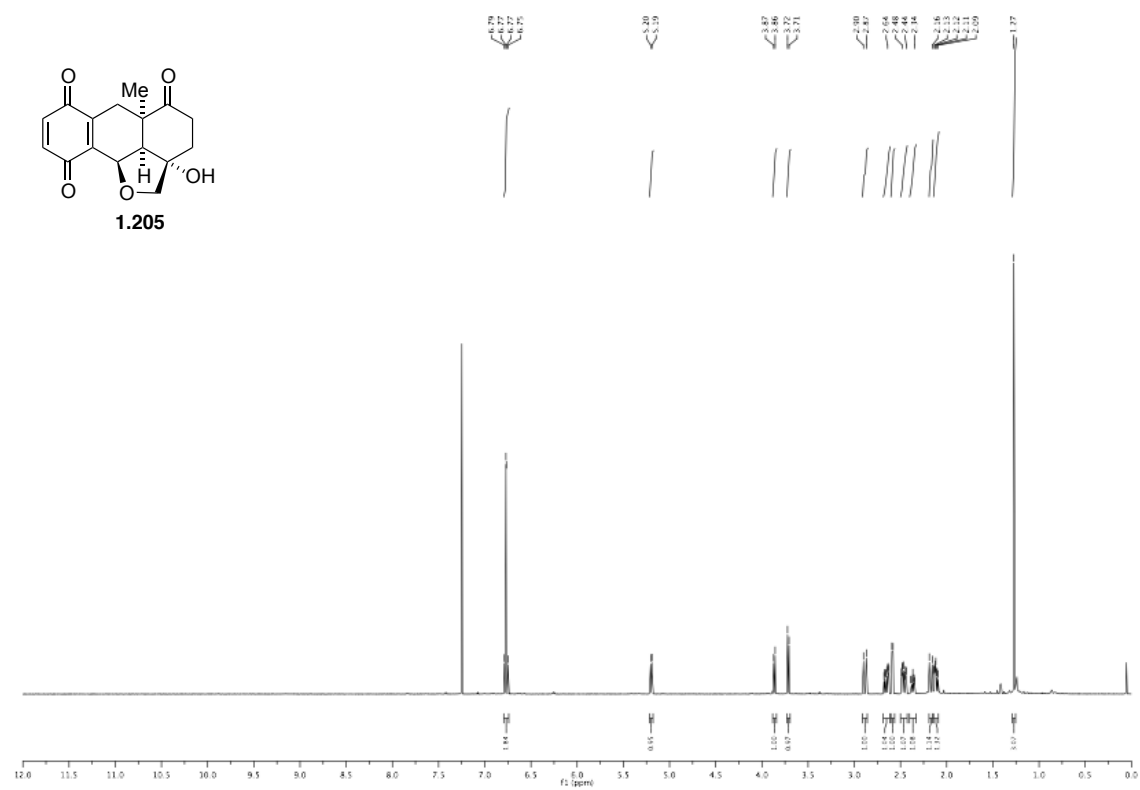
$^{13}\text{C}$  NMR,  $\text{CDCl}_3$ , 150 MHz



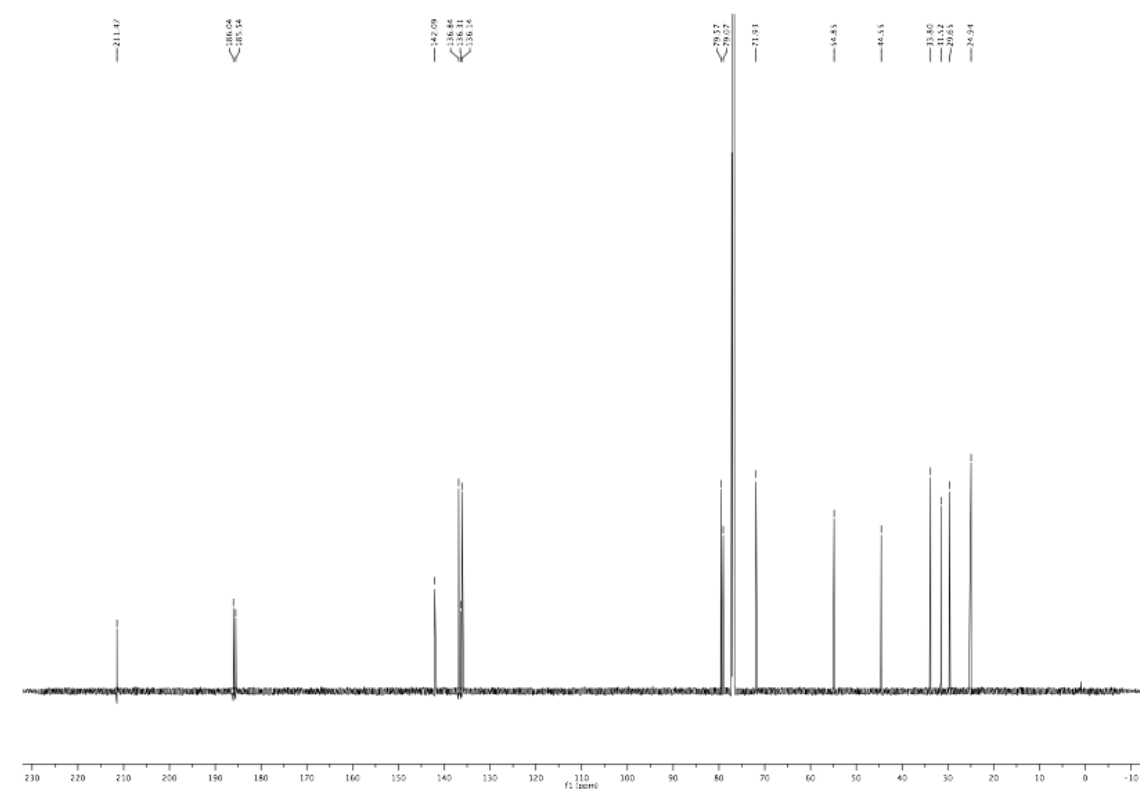
$^1\text{H}$  NMR,  $\text{CDCl}_3$ , 600 MHz $^{13}\text{C}$  NMR,  $\text{CDCl}_3$ , 150 MHz

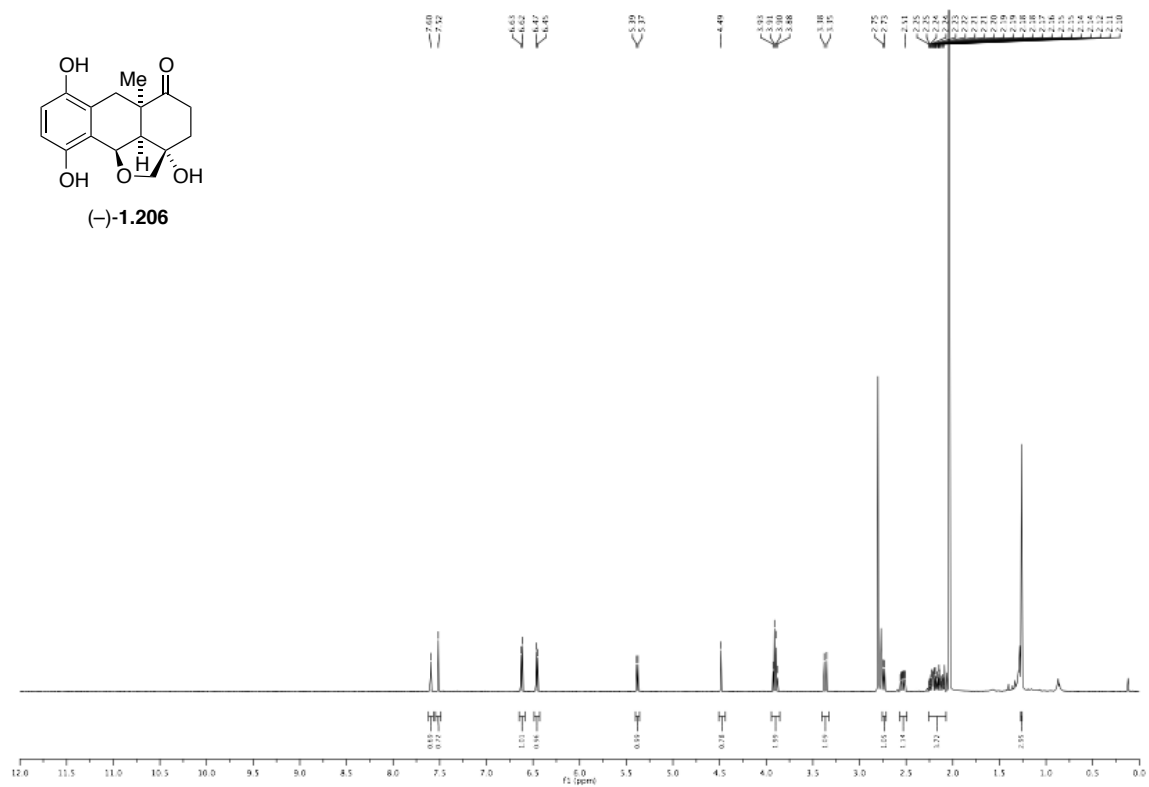
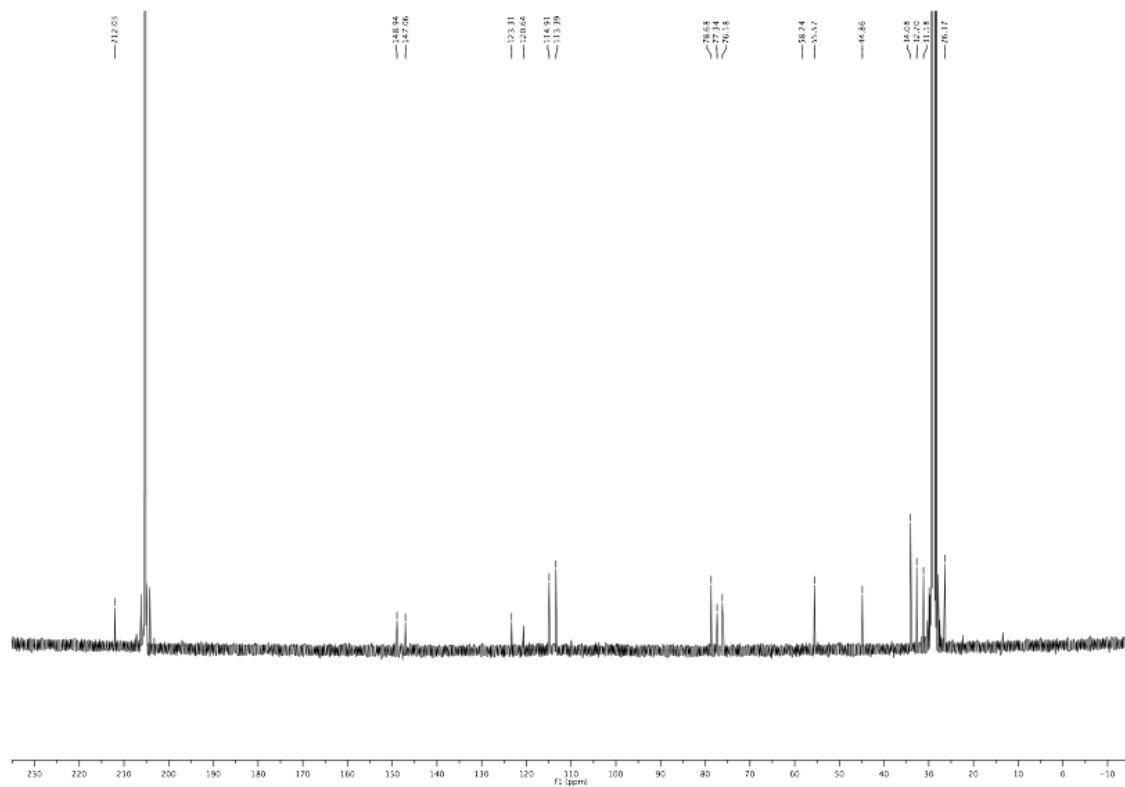
## 1.5. Experimental Section

$^1\text{H}$  NMR,  $\text{CDCl}_3$ , 600 MHz



$^{13}\text{C}$  NMR,  $\text{CDCl}_3$ , 150 MHz



$^1\text{H}$  NMR, acetone- $d_6$ , 600 MHz $^{13}\text{C}$  NMR, acetone- $d_6$ , 150 MHz

## 1.6 Bibliography

- [1] O. Diels, K. Alder, *Liebigs Ann. Chem.* **1928**, *460*, 98–122.
- [2] K. C. Nicolaou, S. a Snyder, T. Montagnon, G. Vassilikogiannakis, *Angewandte Chemie (Int. Ed. Engl.)* **2002**, *41*, 1668–1698.
- [3] M. Juhl, D. Tanner, *Chemical Society Reviews* **2009**, *38*, 2983–2992.
- [4] H. Irngartinger, B. Stadler, *European Journal of Organic Chemistry* **1998**, 605–626.
- [5] H. Iwamoto, A. Takuwa, K. Hamada, R. Fujiwara, *Journal of the Chemical Society, Perkin Transactions 1* **1999**, 575–582.
- [6] W. E. Noland, B. L. Kedrowski, *Journal of Organic Chemistry* **2002**, *67*, 8366–8373.
- [7] W. E. Noland, B. L. Kedrowski, *Journal of Organic Chemistry* **1999**, *64*, 596–603.
- [8] M. a Kienzler, S. Suseno, D. Trauner, *Journal of the American Chemical Society* **2008**, *130*, 8604–8605.
- [9] D. M. Roll, P. J. Scheuer, G. K. Matsumoto, J. Clardy, *Journal of the American Chemical Society* **1983**, *105*, 6177–6178.
- [10] P. Wipf, R. J. Halter, *Organic & Biomolecular Chemistry* **2005**, *36*, 2053–2061.
- [11] D. M. Fort, R. P. Ubillas, C. D. Mendez, S. D. Jolad, W. D. Inman, J. R. Carney, J. L. Chen, T. T. Ianiro, C. Hasbun, R. C. Bruening, et al., *Journal of Organic Chemistry* **2000**, *65*, 6534–6539.
- [12] D. W. Laird, R. Poole, M. Wikström, I. A. van Altena, *J. Nat. Prod.* **2007**, *70*, 671–674.
- [13] G. M. da Costa, T. L. G. de Lemos, O. D. L. Pessoa, F. J. Q. Monte, R. Braz-Filho, *Journal of Natural Products* **1999**, *62*, 1044–1045.
- [14] F. Kavanagh, W. J. Robbins, A. Hervey, *PNAS* **1947**, *33*, 171–176.



- [15] D. R. Appleton, C. S. Chuen, M. V Berridge, V. L. Webb, B. R. Copp, *Journal of Organic Chemistry* **2009**, *74*, 9195–9198.
- [16] F. Löbermann, P. Mayer, D. Trauner, *Angewandte Chemie (Int. Ed. Engl.)* **2010**, *49*, 6199–6202.
- [17] Z. Zhang, J. Chen, Z. Yang, Y. Tang, *Organic Letters* **2010**, *12*, 5554–5557.
- [18] J. Lee, H. S. Mei, J. K. Snyder, *Journal of Organic Chemistry* **1990**, *237*, 5013–5016.
- [19] M. Mathew, S. Jacobson, A. J. Carty, G. J. Palenik, *Journal of the American Chemical Society* **1974**, *237*, 4332–4334.
- [20] B. J. Sauer, R. Sustmann, *Angewandte Chemie (Int. Ed. Engl.)* **1980**, *19*, 779–807.
- [21] M. Karplus, *Journal of the American Chemical Society* **1962**, *85*, 1962–1963.
- [22] R. W. Van De Water, T. R. R. Pettus, *Tetrahedron* **2002**, *58*, 5367–5405.
- [23] P. A. Grieco, J. K. Walker, *Tetrahedron* **1997**, *53*, 8975–8996.
- [24] J. L. Collins, P. A. Grieco, J. K. Walker, *Tetrahedron Letters* **1997**, *38*, 1321–1324.
- [25] T. Dohi, Y. Hu, T. Kamitanaka, N. Washimi, Y. Kita, *Organic Letters* **2011**, *13*, 4814–4817.
- [26] D. M. Gelman, C. M. Forsyth, P. Perlmutter, *Organic Letters* **2009**, *11*, 4958–4960.
- [27] K. N. Houk, R. W. Strozier, *Journal of the American Chemical Society* **1973**, *94*, 4094–4096.
- [28] P. Li, H. Yamamoto, S. E. Ave, *Journal of the American Chemical Society* **2009**, *131*, 16628–16629.
- [29] D. M. Birney, K. N. Houk, *Journal of the American Chemical Society* **1990**, *112*, 4127–4133.
- [30] D. a. Evans, J. S. Johnson, E. J. Olhava, *Journal of the American Chemical Society* **2000**, *122*, 1635–1649.

- [31] K. N. Houk, *Journal of the American Chemical Society* **1973**, *95*, 4092–4094.
- [32] I. Suzuki, H. Kin, H. Yamamoto, *Journal of the American Chemical Society* **1993**, *115*, 10139–10146.
- [33] K. Ishihara, H. Yamamoto, *Journal of the American Chemical Society* **1994**, *116*, 1561–1562.
- [34] T. E. Shubina, M. Freund, S. Schenker, T. Clark, S. B. Tsogoeva, *Beilstein Journal of Organic Chemistry* **2012**, *8*, 1485–1498.
- [35] A. Wittkopp, P. R. Schreiner, *Chemistry - A European Journal* **2003**, *9*, 407–414.
- [36] W. Wang, M. Namikoshi, *Heterocycles* **2007**, *74*, 53–88.
- [37] R. Capon, E. Ghisalberti, P. Jefferies, *Phytochemistry* **1981**, *20*, 2598–2600.
- [38] C. Nieto-Oberhuber, S. López, A. M. Echavarren, *Journal of the American Chemical Society* **2005**, *127*, 6178–6179.
- [39] C. Nieto-Oberhuber, P. Pérez-Galan, E. Herrero-Gómez, T. Lauterbach, C. Rodríguez, S. López, C. Bour, A. Rosellón, D. J. Cardenas, A. M. Echavarren, *Journal of the American Chemical Society* **2008**, *130*, 269–279.
- [40] V. López-Carrillo, N. Huguet, Á. Mosquera, A. M. Echavarren, *Chemistry - A European Journal* **2011**, *17*, 10972–10978.
- [41] T. Jeffery, *Tetrahedron* **1996**, *52*, 10113–10130.
- [42] U. Schädel, W. D. Habicher, *Heterocycles* **2002**, *57*, 1049–1055.
- [43] Y. R. Lee, L. Xia, *Tetrahedron Letters* **2008**, *49*, 3283–3287.
- [44] L.-F. Tietze, G. von Kiedrowski, B. Berger, *Angewandte Chemie (Int. Ed. Engl.)* **1982**, *21*, 221–222.
- [45] N. J. Willis, C. D. Bray, *Chemistry* **2012**, *18*, 9160–9173.
- [46] D. J. Maloney, S. M. Hecht, *Organic Letters* **2005**, *7*, 4297–4300.

- [47] J. F. Arteaga, V. Domingo, J. F. Quílez del Moral, A. F. Barrero, *Organic Letters* **2008**, *10*, 540–554.
- [48] V. L. Mizyuk, M. I. Struchkov, A. P. Kharchevnikov, *Russian Journal of Organic Chemistry* **1987**, *23*, 1093 – 1097.
- [49] M. Ceruti, F. Rocco, F. Viola, G. Balliano, P. Milla, S. Arpicco, L. Cattel, *Journal of Medicinal Chemistry* **1998**, *41*, 540–554.
- [50] F. Farina, R. Martinez-Utrilla, C. Paredes, *Synthesis* **1981**, *4*, 300–301.
- [51] M. De Min, M. T. Maurette, E. Oliveros, *Tetrahedron* **1986**, *42*, 4953–4962.
- [52] N. Pradidphol, N. Kongkathip, P. Sittikul, N. Boonyalai, B. Kongkathip, *European Journal of Medicinal Chemistry* **2012**, *49*, 253–270.
- [53] B. M. Moir, O. Aberdeen, *Journal of the Chemical Society, Perkin Transactions 1* **1973**, 1556–1561.
- [54] B. M. Moir, R. H. Thomson, *Journal of the Chemical Society, Chemical Communications* **1972**, *14*, 363–364.
- [55] O. D. L. Pessoa, T. L. G. Lemos, E. R. Silveira, B. F. Raimundo, *Natural Product Letters* **1993**, *2*, 145–150.
- [56] M. a D. Ferreira, O. D. R. H. Nunes, J. B. Fontenele, O. D. L. Pessoa, T. L. G. Lemos, G. S. B. Viana, *Phytomedicine: International Journal of Phytotherapy and Phytopharmacology* **2004**, *11*, 315–322.
- [57] T. L. G. de Lemos, G. Mario, O. D. L. Pessoa, R. Braz-Filho, *Phytochemistry* **1995**, *40*, 1777–1786.
- [58] R. Braga, *Plantas Do Nordeste, Especialmente Do Ceara*, Imprensa Oficial, Fortaleza, Ceará, Brasil, **1960**.
- [59] J. R. Ioset, A. Marston, M. P. Gupta, K. Hostettmann, *Journal of Natural Products* **2000**, *63*, 424–426.

- [60] G. D. Manners, L. Jurd, *Journal of the Chemical Society, Perkin Transactions 1* **1977**, 405–410.
- [61] V. Fauchet, B. A. Miguel, M. Taran, B. Delmond, *Synthetic Communications* **1993**, *23*, 2503–2510.
- [62] T. R. Hoye, H. Zhao, *Organic Letters* **1999**, *1*, 169–171.
- [63] B. V. S. Reddy, P. Borkar, J. S. Yadav, P. P. Reddy, a C. Kunwar, B. Sridhar, R. Grée, *Organic & Biomolecular Chemistry* **2012**, *10*, 1349–1358.
- [64] C. Chen, P. S. Mariano, *Journal of Organic Chemistry* **2000**, *65*, 3252–3254.
- [65] X. Han, G. Peh, P. E. Floreancig, *European Journal of Organic Chemistry* **2013**, *2013*, 1193–1208.
- [66] B. M. Trost, E. J. McEachern, F. D. Toste, *Journal of the American Chemical Society* **1998**, *120*, 12702–12703.
- [67] H. Tohma, H. Morioka, Y. Harayama, M. Hashizume, Y. Kita, *Tetrahedron Letters* **2001**, *42*, 253–270.
- [68] J.-J. Helesbeux, O. Duval, D. Guilet, D. Séraphin, D. Rondeau, P. Richomme, *Tetrahedron* **2003**, *59*, 5091–5104.
- [69] W. Adam, M. Braun, A. Griesbeck, V. Lucchini, I. E. Staab, *Journal of the American Chemical Society* **1989**, *111*, 203–212.
- [70] M. K. Gurjar, K. Maheshwar, *Journal of Organic Chemistry* **2001**, 7552–7554.
- [71] A. G. M. Barrett, F. Blaney, A. D. Campbell, D. Hamprecht, T. Meyer, A. J. P. White, D. Witty, D. J. Williams, *Journal of Organic Chemistry* **2002**, *67*, 2735–2750.

Chapter 2 

Mushroom Metabolites:

Crocipodin, a Benzotropolone Pigment from  
the Mushroom *Leccinum Crocipodium*  
(Boletales)

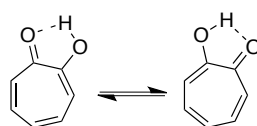


## 2.1 Project Aims

The goal of this project was to confirm the chemical structure of crocipodin through total synthesis. This natural product has been isolated from the fruit bodies of the mushroom *Leccinum crocipodium* by Lydia KERSCHENSTEINER in the group of Prof. Dr. W. STEGLICH.

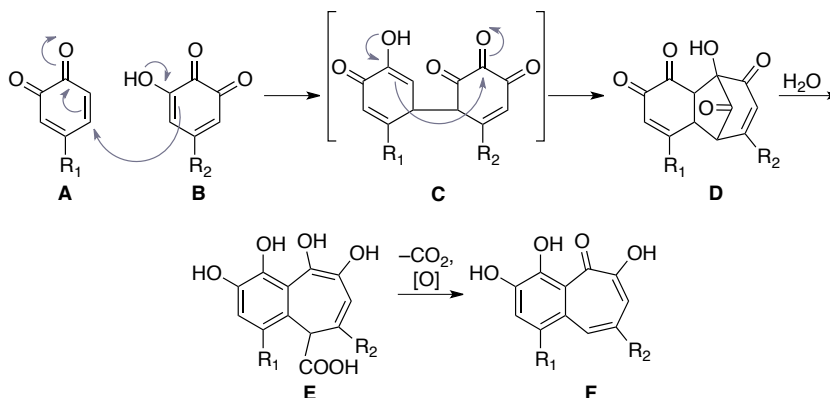
## 2.2 Benzotropolones

The chemical structure of tropolone was first elucidated by DEWAR in 1945, when he determined that the natural products colchicine, stipitatic acid and puberulic acid contain a seven membered carbocyclic ring featuring a carbonyl and hydroxyl functionality together with three conjugated  $\pi$ -bonds.<sup>[1]</sup> Tropolones are hydroxylated derivatives of tropone and are like benzene  $6\pi$  aromatic compounds.



**Scheme 2.1.** Mesomeric structure of tropolone.

Benzotropolones often occur as metabolites in the pigments of fermented tea,<sup>[2]</sup> but can also be found in other natural sources, such as mushrooms.<sup>[3]</sup> The biosynthetic pathway of the usually highly coloured benzotropolones involves the coupling of *ortho*-quinones, which commences with a tandem MICHAEL-Aldol addition between quinone (**A**) and hydroxyquinone (**B**) involving intermediate (**C**) (Scheme 2.2).



**Scheme 2.2.** Biosynthetic pathway for the formation of benzotropolones.<sup>[4]</sup>

This reaction gives the highly reactive tetracyclic intermediate (**D**), which can only be isolated in rare cases, when substituted appropriately.<sup>[5]</sup> Hydrolysis of the bridgehead carbonyl moiety with water results in bicyclic system (**E**). Decarboxylation followed by oxidation finally yields benzotropolone (**F**).

## 2.3 Isolation and Structure Determination\*

*Leccinum crocipodium* (= *L. nigrescens*) (German: Gelber Rauhuß) is a rare thermophilic bolete, found on loamy soil in association with oak and hornbeam trees (Figure 2.1). The mushroom is easily recognized by its bright yellow pores and the darkening of its flesh where cut or bruised.

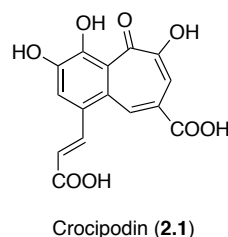


**Figure 2.1.** Representation of *Leccinum crocipodium* and the structure of crocipodin (**2.1**).<sup>†</sup>

For an investigation of the pigments, the lyophilized and defatted fruit bodies of *L. crocipodium* were extracted with acidified acetone. Chromatography of the concentrated extract with acetone on Sephadex LH-20 furnished a brownish orange fraction, which on repeated chromatography yielded almost pure crocipodin (**2.1**, 0.14% of dry weight). The orange-red pigment showed intense UV–vis maxima at 282 and 400 nm. In the IR spectrum (KBr), a carbonyl band at 1701 cm<sup>-1</sup> and aromatic vibrations at 1634 and 1602 cm<sup>-1</sup> could be recognized, in addition to a broad OH absorption at 3433 cm<sup>-1</sup>.

\* Isolation and structure elucidation was conducted by L. KERSCHENSTEINER; synthesis of the natural product was carried out by F. L.

† Photography by R. MARKONES, (www.pilzseite.de). Image used with permission of the author. Accessed on Friday, 25 January 2013.



Croicipodin (**2.1**) exhibited a rather simple  $^1\text{H}$  NMR spectrum (Figure 2.2). The spectrum displayed two doublets at  $\delta_{\text{H}}$  6.33 and 8.16 in  $\text{DMSO}-d_6$ , which could be assigned to a *trans* double bond ( $^3J_{\text{H,H}} = 15.5$  Hz). In addition, three signals for aromatic protons were present, a singlet at  $\delta_{\text{H}}$  7.69 and two broadened singlets at 7.68 and 8.60, which were resolved into two 1.5 Hz doublets in acetone- $d_6$ . The  $^{13}\text{C}$  NMR spectrum exhibited 15 resonances, which, according to DEPT measurements, could be assigned to five methine carbons at  $\delta_{\text{C}}$  115.8 ( $\delta_{\text{H}}$  7.68), 121.8 ( $\delta_{\text{H}}$  7.69), 123.5 ( $\delta_{\text{H}}$  6.33), 131.8 ( $\delta_{\text{H}}$  8.60), and 141.8 ( $\delta_{\text{H}}$  8.16), and ten quaternary carbons at  $\delta_{\text{C}}$  121.5, 125.0, 126.8, 129.3, 148.2, 153.1, 154.3, 167.2, 167.8, and 185.6.

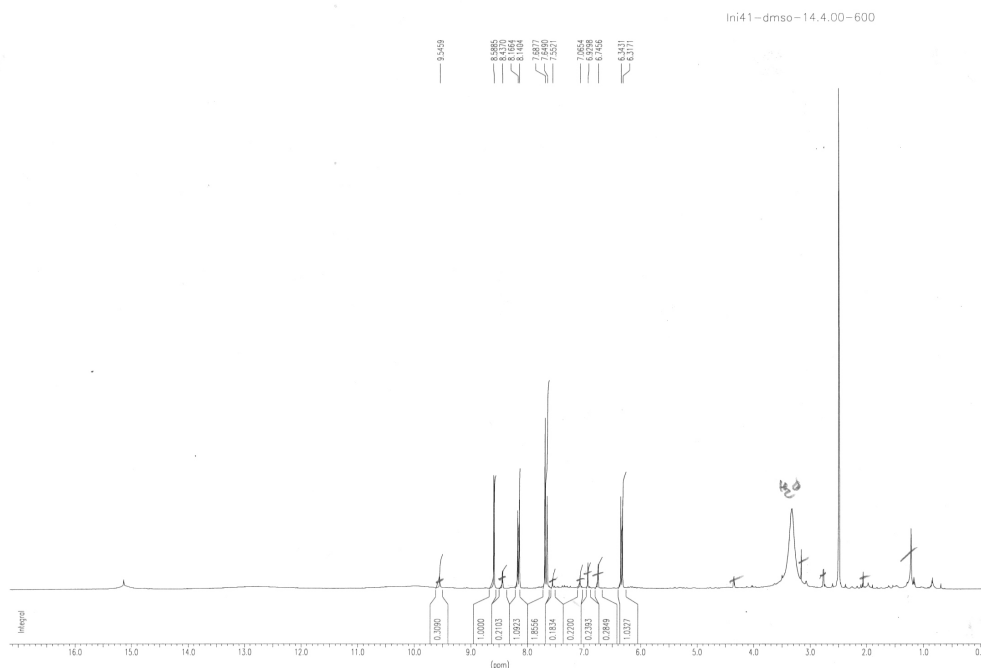


**Figure 2.2.**  $^1\text{H}$  NMR spectrum of natural croicipodin (**2.1**).\*

The EI mass spectrum of croicipodin (**2.1**) showed a molecular ion at  $m/z$  318. After silylation with *N*-methyl-*N*-(trimethylsilyl)trifluoroacetamide (MSTFA), a weak molecular peak at  $m/z$  678 was visible, indicating the formation of a pentakis(trimethylsilyl) derivative. Unfortunately, no high-resolution mass spectra could be obtained, probably due to impurities in the samples. Assuming that croicipodin contains only oxygen as heteroatoms,

\* Data by L. KERSCHENSTEINER.

the molecular formula  $C_{15}H_{10}O_8$  was proposed, incorporating five methine carbons, seven quaternary carbons, three CO moieties, and five hydroxy groups.

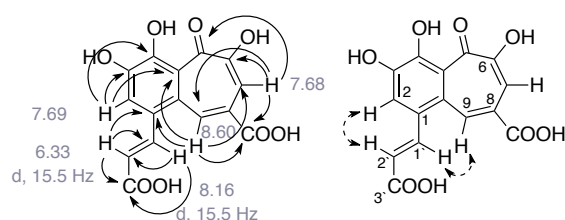


**Figure 2.3.** Selected HMBC (left) and NOESY correlations (right) for **2.1** in  $DMSO-d_6$ .

From the HMBC and NOESY correlations (Figure 2.3) structure **2.1** could be assigned to crocipodin. Especially informative were the nuclear Overhauser effects between the side-chain proton H-1' and H-9, and between H-2' and H-2. From the HMBC correlations of H-2, the substitution of the benzene ring could be determined, and the correlations of the *meta*-coupled protons H-7 and H-9 allowed the assignment of the carbons of the tropolone ring. A comparison of the  $^1H$  and  $^{13}C$  NMR signals of crocipodin (**2.1**) with the corresponding resonances of the tea pigment neotheaflavate B (**2.2**)<sup>[6-8]</sup> shows excellent agreement (Figure 2.4).

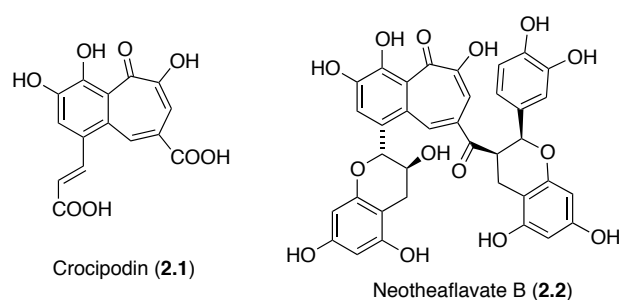
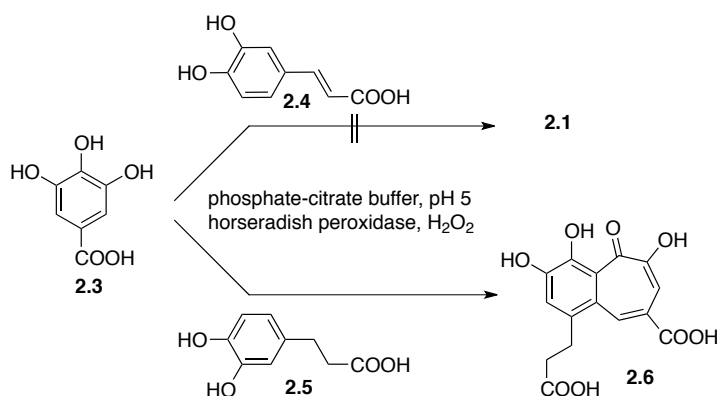


**Figure 2.4.** Comparison of the chemical structure of Crocipodin (**2.1**) with the tea pigment neotheaflavate B (**2.2**).

## 2.4 Total synthesis of Crocipodin\*

The structure of crocipodin (**2.1**) points to a simple biosynthesis via oxidative condensation of gallic acid (**2.3**) and caffeic acid (**2.4**) (Scheme 2.1), analogous to the formation of 3,4,6-trihydroxybenzotropolones from catechols and pyrogallol.<sup>[6,8]</sup> However, neither the oxidation with potassium iodate<sup>[9]</sup> nor the enzymatic conditions previously described by Sang *et al.*<sup>[6]</sup> were successful when applied to this system. This may be attributed to<sup>[10]</sup> the electron-withdrawing effect of the conjugated carboxyl group in caffeic acid.<sup>[11]</sup> In accordance with this proposal, dihydrocrocipodin (**2.6**) was formed from dihydrocaffeic acid (**2.5**) and gallic acid (**2.3**) upon treatment with horseradish peroxidase and H<sub>2</sub>O<sub>2</sub> in buffer solution at pH 5 (Scheme 2.2).<sup>[7]</sup>



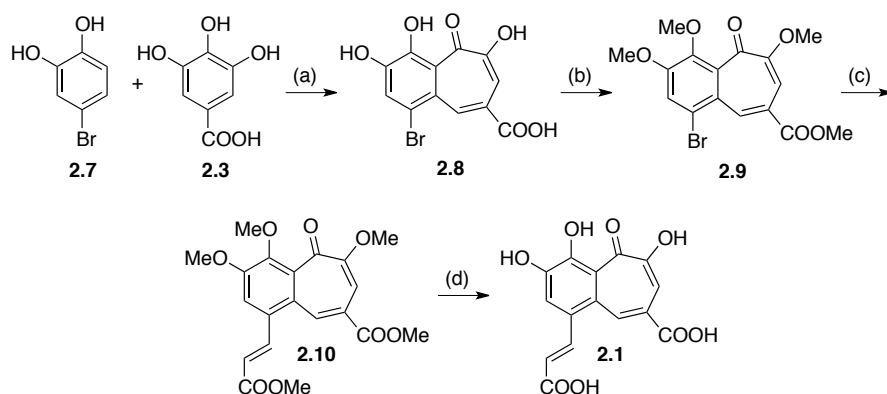
Reagents and conditions: (a) 3% aq. H<sub>2</sub>O<sub>2</sub>, horseradish peroxidase, acetone/phosphate-citrate buffer pH 5, 32% of **2.6**.

**Scheme 2.2.** Attempted synthesis of crocipodin (**2.1**) and synthesis of dihydrocrocipodin (**2.6**).

In order to overcome the issues with the one-step protocol starting with **2.4**, a three-step synthesis of crocipodin (**2.1**) was envisaged. Oxidative condensation of 4-bromocatechol (**2.7**) with gallic acid (**2.3**) in the presence of H<sub>2</sub>O<sub>2</sub> and horseradish gave known bromo-compound **2.8** (Scheme 2.3).<sup>[7]</sup> Methylation of compound **2.8** afforded the permethyl derivative **2.9**, which then submitted to Heck conditions with methyl acrylate to produce the desired *E*-propenoate **2.10** in high yield. It was possible to obtain X-ray quality crystals of **2.9** and **2.10** by slow evaporation of chloroform (Figure 2.3).

\* The experimental work in this chapter was performed together with R. GREINER, an undergraduate researcher in the Trauner laboratories supervised by F. L.

## 2.4. Total Synthesis of Crocipodin



Reagents and conditions: (a) 3% aq.  $\text{H}_2\text{O}_2$ , horseradish peroxidase, acetone/phosphate-citrate buffer pH 5, 75% of **2.8**; (b) MeI,  $\text{K}_2\text{CO}_3$  (anhyd), DMF, 98% of **2.9**; (c)  $\text{H}_2\text{C}=\text{CHCOOMe}$ ,  $\text{Pd}(\text{OAc})_2$ ,  $\text{K}_2\text{CO}_3$  (anhyd),  $n\text{-Bu}_4\text{NCl}$ , DMF,  $100^\circ\text{C}$ , 2h, 91% of **2.10**; (d)  $\text{BBr}_3$ ,  $\text{CH}_2\text{Cl}_2$ , 75% of **2.1**.

**Scheme 2.3.** Synthesis of crocipodin (**2.1**).

In the final step, the methoxy groups were cleaved with  $\text{BBr}_3$  to provide crocipodin (**2.1**). The synthetic product was identical with natural crocipodin by comparison of the IR, NMR, and mass spectra as well as co-chromatography in the HPLC.

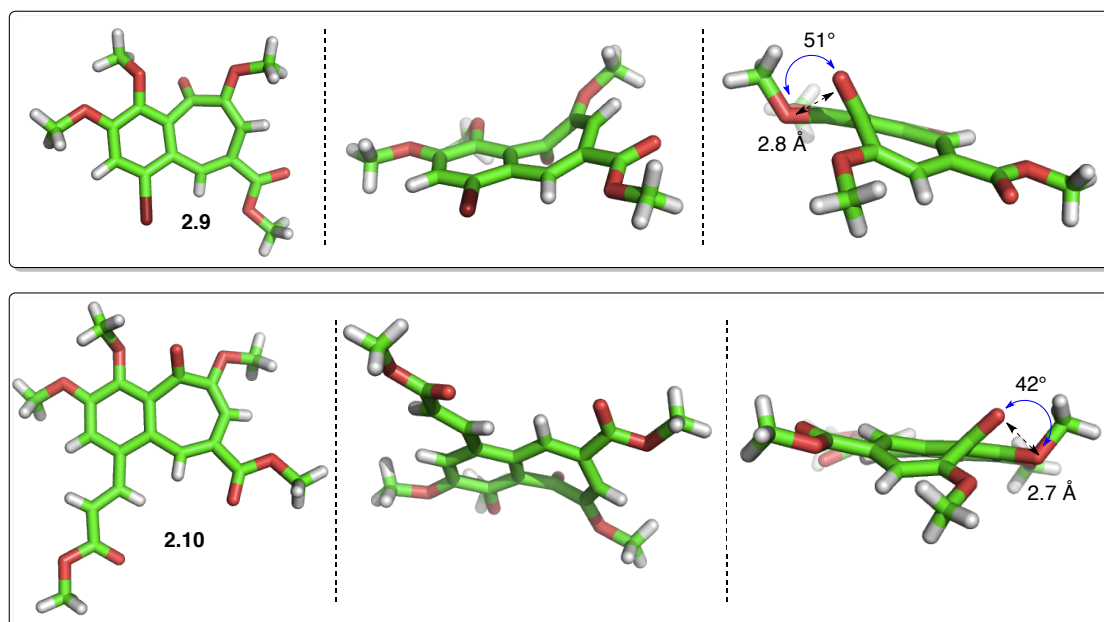


**Figure 2.5.** X-ray structures of **2.9** and **2.10** showing a distorted benzotropolone scaffold.

Although benzotropolones are aromatic compounds and hence known to adopt a planar conformation, both derivatives **2.9** and **2.10** are clearly distorted.<sup>[10,12]</sup> Especially the carbonyl moiety within the seven-membered ring is bent out of plane with six carbon atoms of the seven-membered ring approaching planarity (Figure 2.5). This effect can be explained by the repulsive electrostatic and steric effects of the neighbouring methoxy moieties and the absence of intramolecular hydrogen bonding. The distance between the oxygen atoms are 2.8 Å and 2.7 Å in the case of **2.9** and **2.10** respectively. In compound **2.9** the carbonyl moiety is bent out of plane by 51° and the distance, whereas in permethylcrocipodin (**2.10**) it is only distorted by 42°, which is congruent with the shorter oxygen–oxygen distance in compound **2.10**. Similar observations were reported in literature for permethylated purpurogallin, where a dihedral angle of 36° was found within the seven-membered ring.<sup>[12]</sup>

In conclusion the structure of crocipodin (**2.1**) has been elucidated from spectroscopic evidence and confirmed by total synthesis. The occurrence of a benzotropolone pigment in *Leccinum* is exceptional. Other yellow species, such as the North American *L. rugosiceps* ssp. *corrugis* and *L. rubropunctum* owe their colour to polyhydroxypulvinic acids.<sup>[13]</sup> Benzotropolones have not been isolated from boletes previously, however, they are known from the agaric *Tricholoma aurantium*<sup>[14]</sup> and the polypore *Fomes fomentarius*.<sup>[15]</sup>

## 2.5 Experimental Section

### 2.5.1 General Experimental Details

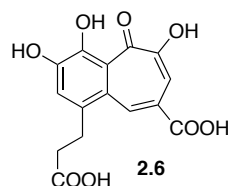
**Chemicals and chromatography.** Unless otherwise noted, all reagents were purchased from commercial suppliers and used without further purification. Unless otherwise noted, all reaction mixtures were magnetically stirred in oven-dried glassware under a blanket of argon. External bath temperatures were used to record all reaction mixture temperatures. Analytical thin layer chromatography (TLC) was carried out on Merck silica gel 60 F<sub>254</sub> TLC plates. TLC visualisation was accomplished using 254 nm UV light or charring solutions of KMnO<sub>4</sub> and ceric ammonium molybdenate. All organic extracts were washed with brine, dried over sodium sulfate and filtered; solvents were then removed with a rotary evaporator at aspirator pressure. Flash chromatography was performed on Merck KGaA Geduran<sup>®</sup> Silica Gel (40–63 μm particle size) using a forced flow of eluent at 1.3–1.5 bar pressure. Yields refer to chromatographically and spectroscopically (<sup>1</sup>H NMR and <sup>13</sup>C NMR) homogenous material.

**NMR spectroscopy.** NMR spectra were recorded on Bruker AC 300, WH 400, or AMX 600 instruments (operating at 300 MHz, 400 MHz and 600 MHz for proton nuclei and 75 MHz, 100 MHz, 150 MHz for carbon nuclei, respectively). Chemical shifts are reported in ppm with the solvent resonance employed as the internal standard (CDCl<sub>3</sub> at 7.26 and 77.0 ppm; DMSO at 2.50 and 39.5 ppm). Additional to standard <sup>1</sup>H and <sup>13</sup>C NMR measurements, 2D NMR techniques such as homonuclear correlation spectroscopy (COSY), heteronuclear single quantum coherence (HSQC) and heteronuclear multiple bond coherence (HMBC) were used to assign signals. The following abbreviations are used to explain the multiplicities: s = singlet, d = doublet, t = triplet, q = quartet, m = multiplet, br = broad.

**IR spectroscopy.** IR spectra were recorded 4000–400 cm<sup>-1</sup> on a Perkin Elmer Spectrometer BY FT-IR-System with a Smith Dura sample IR II ATR-unit. Samples were measured as neat materials (neat). The absorption bands are reported in wave numbers (cm<sup>-1</sup>). Abbreviations: ss, very strong; s, strong; m, medium; w, weak; br, broad.

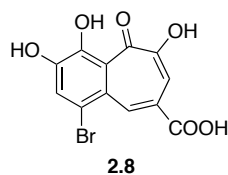
**Mass spectroscopy.** MS (EI, ESI): Finnigan MAT 90, Finnigan MAT 95 Q, and Varian MAT 711 spectrometer.

## 2.5.2 Synthesis of Crocipodin



**Dihydrocrocipodin (2.6).** Gallic acid (**2.3**) (1.87 g, 11.0 mmol) and dihydrocaffeic acid **2.5** (3.01 g, 16.5 mmol) were dissolved in acetone/pH 5.0 phosphate-citrate buffer (1:10 v/v, 50 mL). Then, horseradish peroxidase type I (25 ku) was added in three portions, 4 mg each time. Additionally, every 15 min and four times per period, 3% aq H<sub>2</sub>O<sub>2</sub> (1.2 mL) was added to the reaction mixture, which was occasionally shaken by hand. The resulting precipitate was collected by filtration and dried under high vacuum overnight to yield compound **6** (0.74 g, 21%) as a red solid.

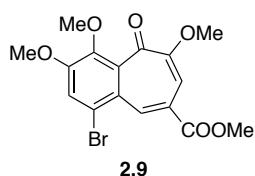
**Data for 2.6.** mp > 290 °C (dec). IR (ATR):  $\tilde{\nu}$  = 3674 (br), 3392 (br), 3220 (w), 1740 (ss), 1646 (s), 1517 (s), 1454 (m), 1401 (m), 1362 (ss), 1290 (ss), 1150 (m), 1089 (m), 972 (ss), 891 (m), 855 (m) cm<sup>-1</sup>; <sup>1</sup>H NMR (400 MHz, DMSO-*d*<sub>6</sub>)  $\delta$  = 2.55 (t, *J* = 7.7 Hz, 2H), 3.18 (t, *J* = 7.7 Hz, 2H), 7.43 (s, 1H), 7.61 (d, *J* = 1.3 Hz, 1H), 8.57 (d, *J* = 1.3 Hz, 1H), 9.73 (s, 1H), 10.26 (s, 1H), 12.71 (br, 2H), 14.70 (s, 1H); <sup>13</sup>C NMR (100 MHz, DMSO-*d*<sub>6</sub>)  $\delta$  = 30.3, 35.5, 115.7, 122.2, 123.6, 124.6, 126.1, 132.5, 135.2, 148.5, 150.4, 153.9, 168.3, 173.7, 185.9; MS (ESI): calcd for C<sub>15</sub>H<sub>11</sub>O<sub>8</sub> (M-H<sup>+</sup>): 319.0459, found: 319.0456.



**1-Bromo-3,4,6-trihydroxy-5-oxo-5H-benzocycloheptene-8-carboxylic Acid (2.8).** Gallic acid **2.3** (0.6 g, 3.53 mmol) and 4-bromocatechol (**2.7**) (0.96 g, 5.08 mmol) were dissolved in acetone/pH 5.0 phosphate-citrate buffer (1:10 v/v, 50 mL). Horseradish peroxidase type I (25 ku) was added in three portions, 2 mg each time. Additionally, every 15 min and four times per period, 3 % H<sub>2</sub>O<sub>2</sub> (0.6 mL) was added to the reaction mixture, which was occasionally shaken by hand. The dark red precipitate was collected by filtration

and washed with water. After drying under high vacuum overnight, title compound **2.8** (860 mg, 75%) was obtained as a red powder.

**Data for 2.8.** mp > 300 °C (dec) (lit. mp 303–305 °C); IR (ATR):  $\tilde{\nu}$  = 3674 (br), 3385 (br), 3220 (w), 1648 (s), 1520 (s), 1487 (w), 1456 (w), 1401 (w), 1361 (s), 1288 (s), 1150 (w), 1088 (w), 969 (m)  $\text{cm}^{-1}$ ;  $^1\text{H}$  NMR (400 MHz,  $\text{DMSO}-d_6$ )  $\delta$  = 7.57 (d,  $J$  = 1.4 Hz, 1H), 7.82 (s, 1H), 8.86 (d,  $J$  = 1.4 Hz, 1H), 9.96 (s, 1H), 10.72 (s, 1H), 12.53 (br, 1H), 14.79 (s, 1H);  $^{13}\text{C}$  NMR (100 MHz,  $\text{DMSO}-d_6$ )  $\delta$  = 115.6, 118.8, 122.1, 125.3, 126.0, 126.8, 135.9, 149.1, 152.0, 154.5, 168.0, 185.7; MS (ESI): calcd for  $\text{C}_{12}\text{H}_8\text{BrO}_6$  ( $\text{M}-\text{H}^+$ ): 324.9353, found: 324.9349.

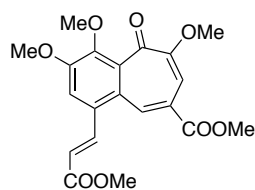


**Methyl 1-Bromo-3,4,6-trimethoxy-5-oxo-5H-benzocycloheptene-8-carboxylate (2.9).**

To a suspension of compound **2.8** (0.10 g, 0.31 mmol) and  $\text{K}_2\text{CO}_3$  (0.51 g, 3.67 mmol) in anhydrous DMF (4 mL), maintained at 0 °C under argon, was added drop wise iodomethane (0.15 mL, 2.45 mmol), and the mixture was stirred overnight at room temperature. Subsequently, the reaction mixture was diluted with water (10 mL) and stirred for 20 min at room temperature. After addition of EtOAc (100 mL), the organic phase was washed with water ( $3 \times 100$  mL), and the combined aqueous phases were extracted with EtOAc (200 mL). Then, the combined organic phases were washed with brine, dried over  $\text{Na}_2\text{SO}_4$  and concentrated under reduced pressure. The crude yellow product was purified via column chromatography (33%  $\text{Et}_2\text{O}$  in hexanes) to afford **2.9** (115 mg, 98%) as a yellow solid.

**Data for 2.9.** mp 179–180 °C; IR (ATR):  $\tilde{\nu}$  = 3392 (br), 3225 (w), 2939 (w), 1715 (s), 1658 (w), 1620 (w), 1448 (m), 1364 (s), 1289 (s), 1219 (m), 1150 (m), 1091 (m), 1031 (m), 968 (m), 858 (w), 709 (m)  $\text{cm}^{-1}$ ;  $^1\text{H}$  NMR (300 MHz,  $\text{CDCl}_3$ )  $\delta$  = 3.86 (s, 3H), 3.94 (s, 3H), 3.97 (s, 6H), 6.71 (s, 1H), 7.50 (s, 1H), 8.44 (d,  $J$ =1.0 Hz, 1H);  $^{13}\text{C}$  NMR (75 MHz,  $\text{CDCl}_3$ )  $\delta$  = 52.9, 56.5, 62.7, 65.2, 102.1, 120.1, 120.6, 124.9, 125.4, 132.3, 134.1, 145.9, 154.4, 156.7, 167.5, 185.9; MS (EI): calcd for  $\text{C}_{16}\text{H}_{15}\text{BrO}_6$  ( $\text{M}^+$ ): 382.0052, found: 382.0030.

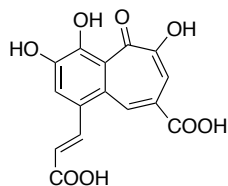




2.10

**Methyl (*E*)-3-(3,4,6-Trimethoxy-8-methoxycarbonyl-5-oxo-5*H*-benzocyclohepten-1-yl)-2-propenoate (2.10).** A mixture of compound **2.9** (50 mg, 0.13 mmol), methyl acrylate (60 mg, 0.65 mmol), Pd(OAc)<sub>2</sub> (3 mg, 0.01 mmol), anh. K<sub>2</sub>CO<sub>3</sub> (30 mg, 0.22 mmol), and tetrabutylammonium chloride (50 mg, 0.17 mmol) in anhydrous DMF (4 mL) was placed in a scintillation vial and purged with nitrogen for 5 min. Subsequently, the mixture was heated to 100 °C for 2 h in the sealed vial. After cooling to room temperature, the reaction mixture was diluted with CH<sub>2</sub>Cl<sub>2</sub> (30 mL) and washed with water (3×30 mL). The combined aqueous phases were re-extracted with CH<sub>2</sub>Cl<sub>2</sub> (2 × 50 mL). Combined organic phases were dried over Na<sub>2</sub>SO<sub>4</sub> and concentrated under reduced pressure. The resulting yellow oil was submitted to column chromatography (50% Et<sub>2</sub>O in hexanes) to yield **2.10** (46 mg, 91%) as a yellow solid.

**Data for 2.10.** mp 152 °C; IR (ATR):  $\tilde{\nu}$  = 3394 (br), 2955 (m), 1698 (ss), 1665 (ss), 1621 (ss), 1584 (m), 1567 (m), 1451 (w), 1426 (m), 1310 (s), 1273 (s), 1219 (ss), 1187 (w), 1150 (w), 1093 (ss), 1033 (ss), 1007 (s), 976 (s), 900 (w), 859 (w), 759 (w) cm<sup>-1</sup>; <sup>1</sup>H NMR (600 MHz, CDCl<sub>3</sub>)  $\delta$  = 3.85 (s, 6H), 3.92 (s, 3H), 3.98 (s, 6H), 6.34 (d, *J* = 15.7 Hz, 1H), 6.68 (s, 1H), 7.30 (s, 1H), 8.21 (m, 2H); <sup>13</sup>C NMR (150 MHz, CDCl<sub>3</sub>)  $\delta$  = 52.0, 52.9, 56.2, 56.3, 62.7, 101.8, 114.4, 122.5, 125.0, 125.4, 128.7, 131.0, 134.3, 141.9, 147.8, 154.3, 157.0, 166.6, 167.5, 186.6; MS (ED): calcd for C<sub>20</sub>H<sub>20</sub>O<sub>8</sub> (M<sup>+</sup>): 388.1158, found: 388.1140.



Crocipodin (2.1)

**Crocipodin (2.1).** To a stirred solution of **2.10** (58 mg, 0.15 mmol) in anhydrous CH<sub>2</sub>Cl<sub>2</sub> (1 mL), was added drop wise a 1M solution of BBr<sub>3</sub> in CH<sub>2</sub>Cl<sub>2</sub> (3 mL, 3.0 mmol). The reaction mixture was stirred at room temperature for 18 h. Subsequently it was carefully

quenched upon drop wise addition of aq. sat.  $\text{NaHCO}_3$  (30 mL). The biphasic mixture was stirred for 10 min at room temperature and then washed with EtOAc ( $2 \times 20$  mL). After phase separation, the aqueous phase was acidified with 1N HCl and extracted with EtOAc ( $3 \times 30$  mL). Combined organic phases were washed with brine (50 mL), dried over  $\text{Na}_2\text{SO}_4$  and concentrated. The resulting red solid was purified via HPLC:  $t_{\text{R}}=23.8$  min (RP-18; solvent system A: water + 0.5% TFA; solvent system B: MeOH; gradient start: 55% A, within 25 min to 80% B, then 10 min 80% B; flow rate:  $1 \text{ mL min}^{-1}$ ); to obtain crocipodin (**2.1**) (35 mg, 73%) as a brown-orange solid.

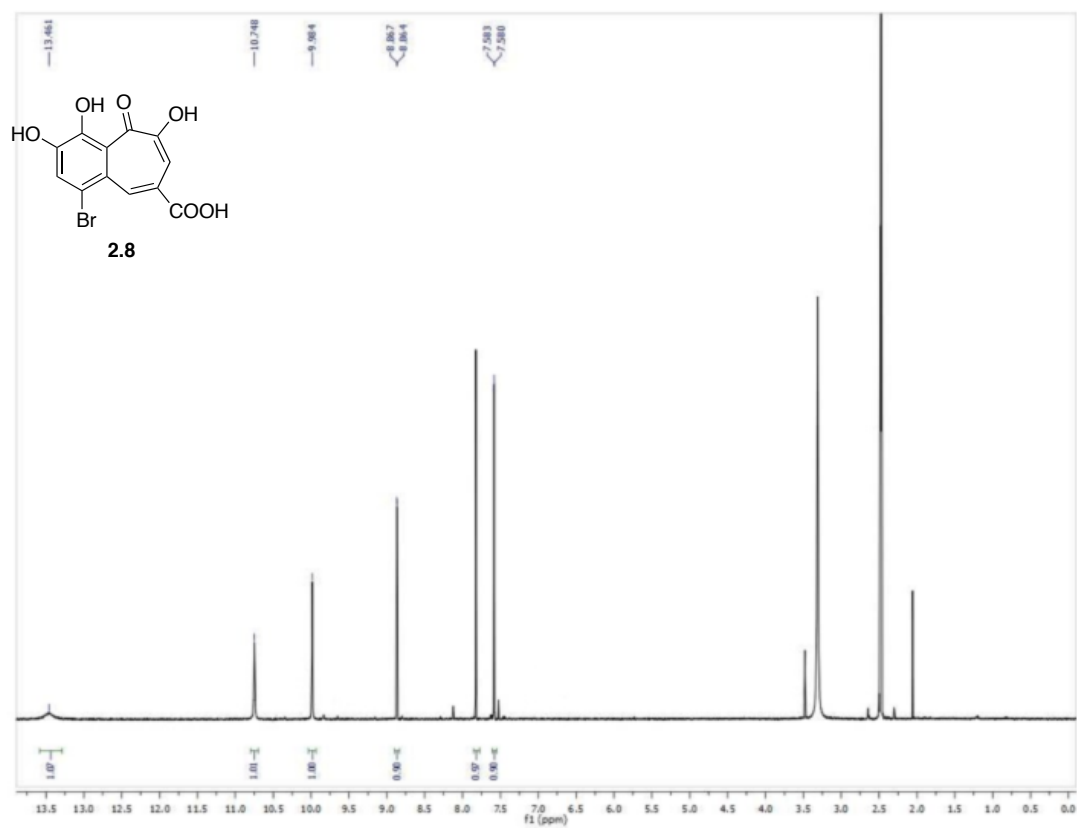
**Data for 2.1.** mp  $> 300$  °C (dec); UV-vis (MeOH):  $\lambda_{\text{max}}$  (e) 280 (3.67), 400 (2.95), 460 (sh, 2.49); IR (ATR):  $\tilde{\nu} = 3381$  (ss), 3250 – 2875 (br), 2644 (w), 1704 (ss), 1633 (s), 1590 (s), 1512 (w), 1448 (s), 1419 (s), 1334 (s), 1260 (s), 1244 (s), 1191 (s), 1080 (m), 1000 (w), 948 (w), 861 (m), 769 (w), 696 (m)  $\text{cm}^{-1}$ ;  $^1\text{H}$  NMR (400 MHz,  $\text{DMSO-}d_6$ )  $\delta = 6.31$  (d,  $J = 15.4$  Hz, 1H), 6.99 (s, 1H), 10.51 (br, 1H), 9.97 (br, 1H), 8.56 (s, 1H), 8.13 (d,  $J = 15.4$ , 1H), 7.12 (s, 1H), 7.24 (s, 1H), 7.61 (s, 1H), 7.68 (s, 1H);  $^{13}\text{C}$  NMR (100 MHz,  $\text{DMSO-}d_6$ )  $\delta = 115.8, 121.8, 122.0, 123.8, 124.6, 126.9, 129.7, 132.2, 142.0, 148.6, 153.4, 154.6, 167.5, 168.0, 185.9$ ; HRMS (ESI):  $m/z$ : calcd for  $\text{C}_{15}\text{H}_{10}\text{O}_8$  ( $\text{M-H}^+$ ): 317.0303, found: 317.0298; MS (ESI):  $m/z$  (%) = 339 [ $\text{M+Na}$ ] $^-$  (30), 317 [ $\text{M}$ ] $^-$  (41), 315 (6), 273 (6), 194 (7).

**Table S1.** Comparison of NMR data for crocipodin (**2.1**)isolation: 600 MHz, DMSO- $d_6$  mp 235 °C (dec)synthetic: 400 MHz, DMSO- $d_6$  mp >300 °C (dec)

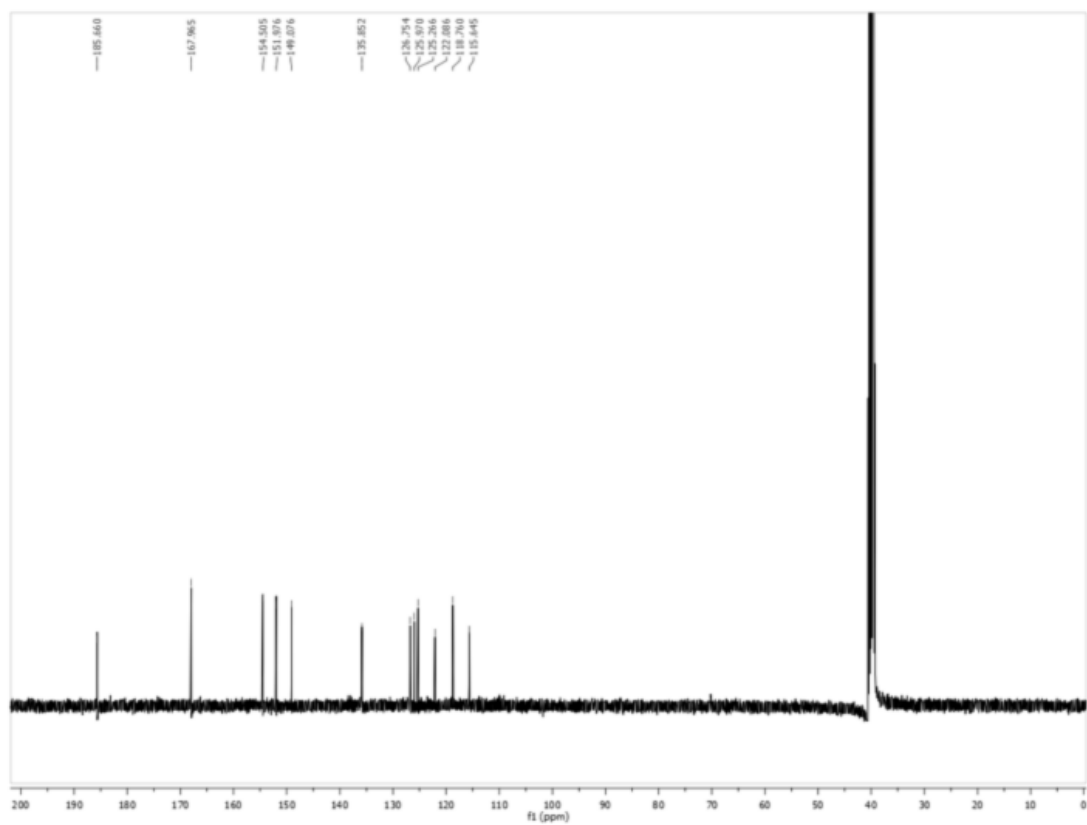
$\delta$ C		$\delta$ H	
isolation	synthetic	isolation	synthetic
185.6	185.9	8.60 s	8.56 s
167.8	167.9	8.16 d	8.13 d
167.2	167.4	7.69 s	7.67 s
154.3	154.5	7.68 s	7.61 s
153.1	153.4	-	7.24 s
148.2	148.6	-	7.11 s
141.8	142.0	-	6.99 s
131.8	132.2	6.33 d	6.31 d
129.3	129.7		
126.8	126.9		
125.0	124.6		
123.5	123.8		
121.8	122.0		
121.5	121.7		
115.8	115.8		

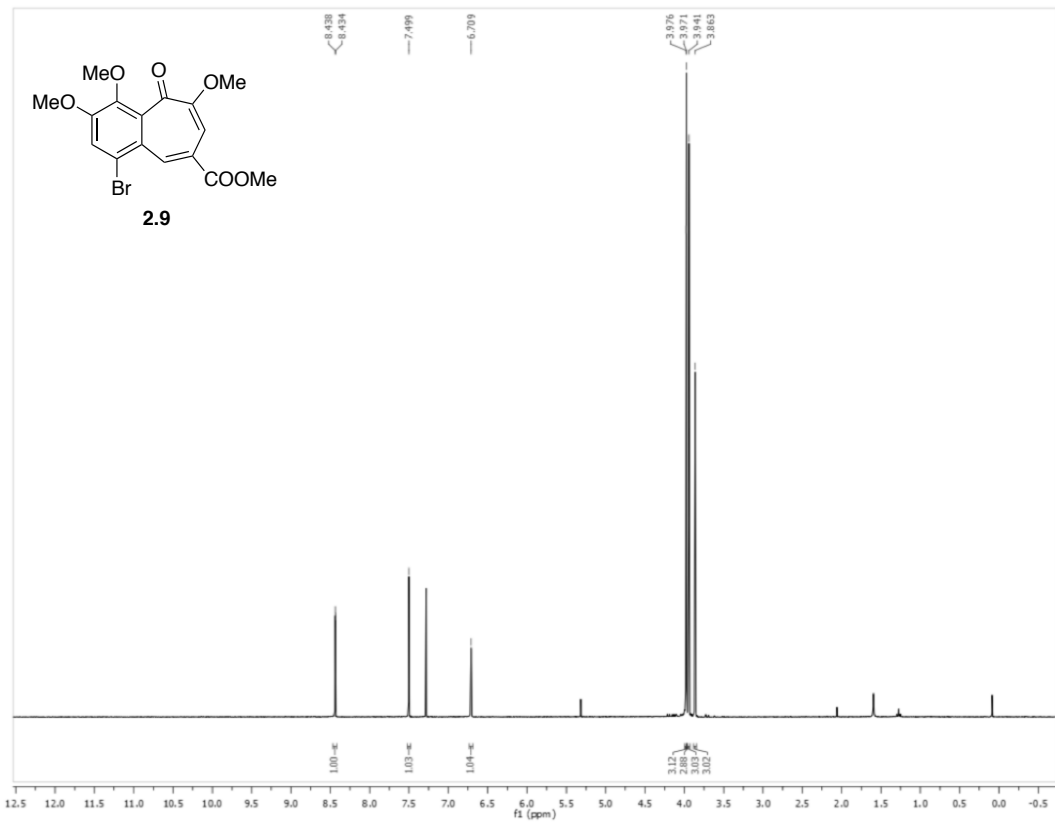
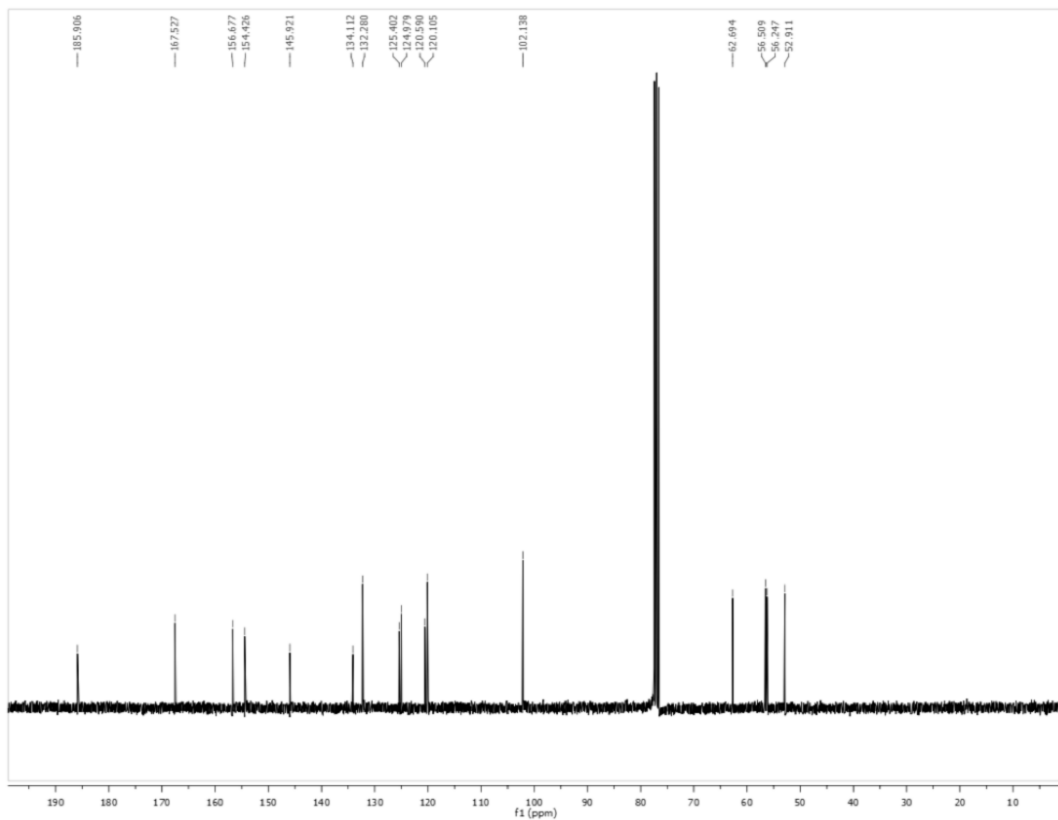
## 2.5. Experimental Section

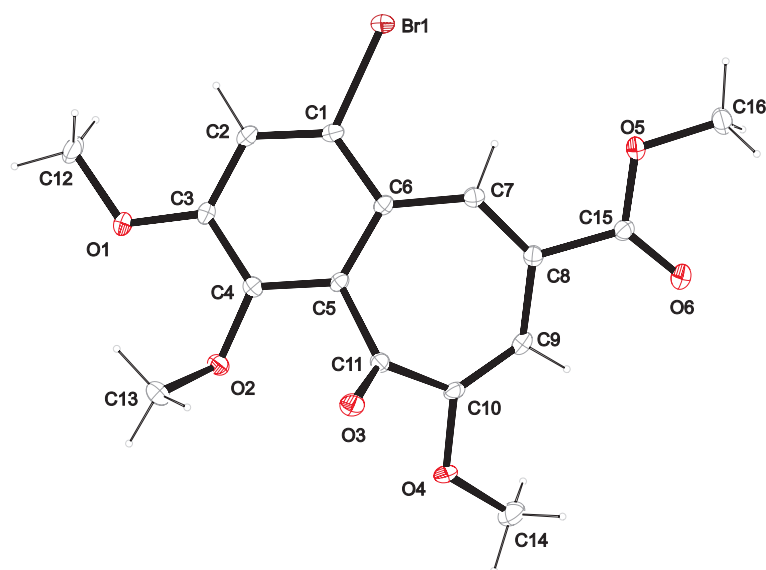
$^1\text{H}$  NMR,  $\text{DMSO-}d_6$ , 400 MHz



$^{13}\text{C}$  NMR,  $\text{DMSO-}d_6$ , 100 MHz



$^1\text{H}$  NMR,  $\text{CDCl}_3$ , 300 MHz $^{13}\text{C}$  NMR,  $\text{CDCl}_3$ , 75 MHz

**Figure S1:** X-ray crystal structure of benzotropolone **2.9**.**Table S2:** Crystallographic data for benzotropolone **2.9**.

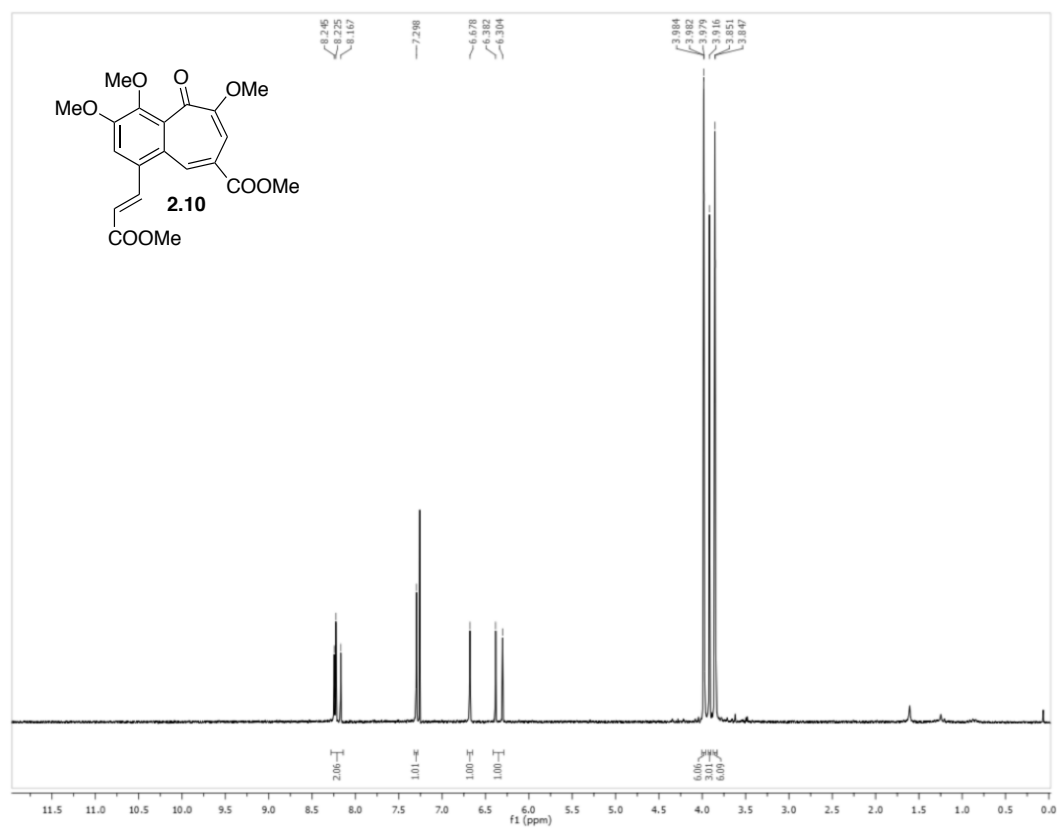
net formula	$C_{16}H_{15}BrO_6$
$M_r/g\ mol^{-1}$	383.191
crystal size/mm	$0.39 \times 0.24 \times 0.19$
$T/K$	173(2)
radiation	MoK $\alpha$
diffractometer	'Oxford XCalibur'
crystal system	triclinic
space group	$P1bar$
$a/\text{\AA}$	7.5741(5)
$b/\text{\AA}$	8.4391(3)
$c/\text{\AA}$	12.9838(8)
$\alpha/^\circ$	100.443(4)
$\beta/^\circ$	99.258(5)
$\gamma/^\circ$	102.612(4)
$V/\text{\AA}^3$	778.90(8)
$Z$	2
calc. density/ $g\ cm^{-3}$	1.63387(17)
$\mu/mm^{-1}$	2.667
absorption correction	'multi-scan'
transmission factor range	0.76401–1.00000

---

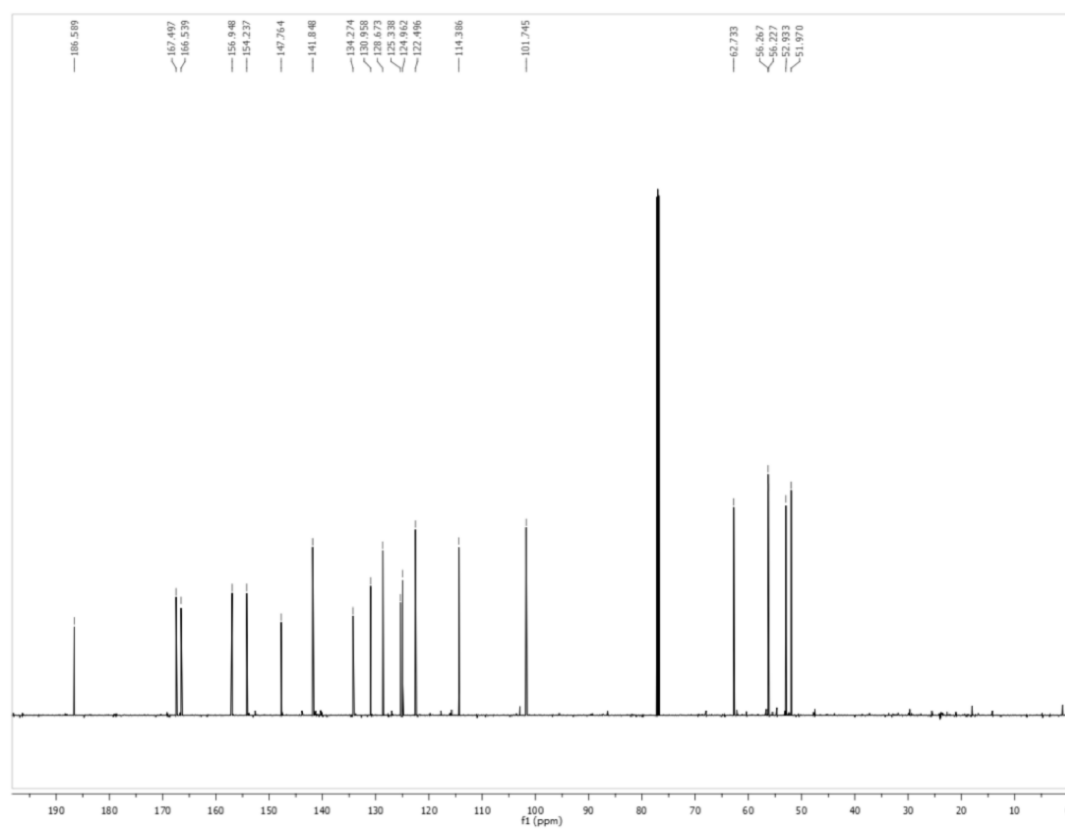
refls. measured	5382
$R_{\text{int}}$	0.0217
mean $\sigma(I)/I$	0.0432
$\theta$ range	4.25–26.31
observed refls.	2578
$x, y$ (weighting scheme)	0.0457, 1.5278
hydrogen refinement	Constr
refls in refinement	3140
parameters	212
restraints	0
$R(F_{\text{obs}})$	0.0400
$R_w(F^2)$	0.1077
$S$	1.064
shift/error <sub>max</sub>	0.001
max electron density/e $\text{\AA}^{-3}$	1.073
min electron density/e $\text{\AA}^{-3}$	–0.398

## 2.5. Experimental Section

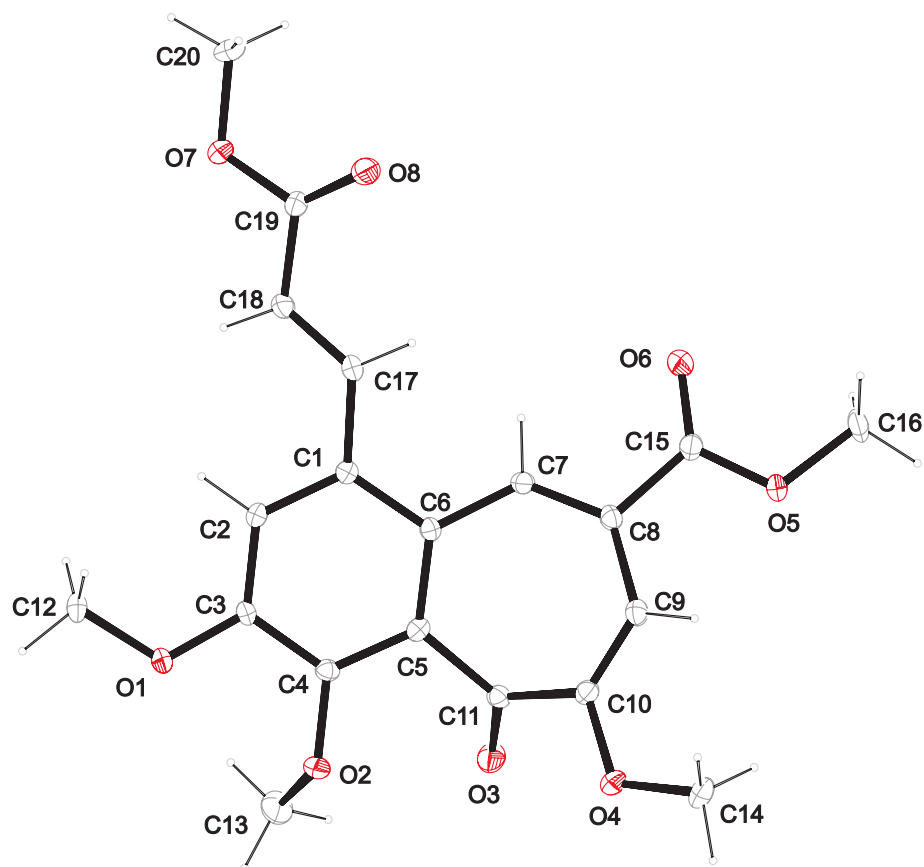
$^1\text{H}$  NMR,  $\text{CDCl}_3$ , 600 MHz



$^{13}\text{C}$  NMR,  $\text{CDCl}_3$ , 150 MHz





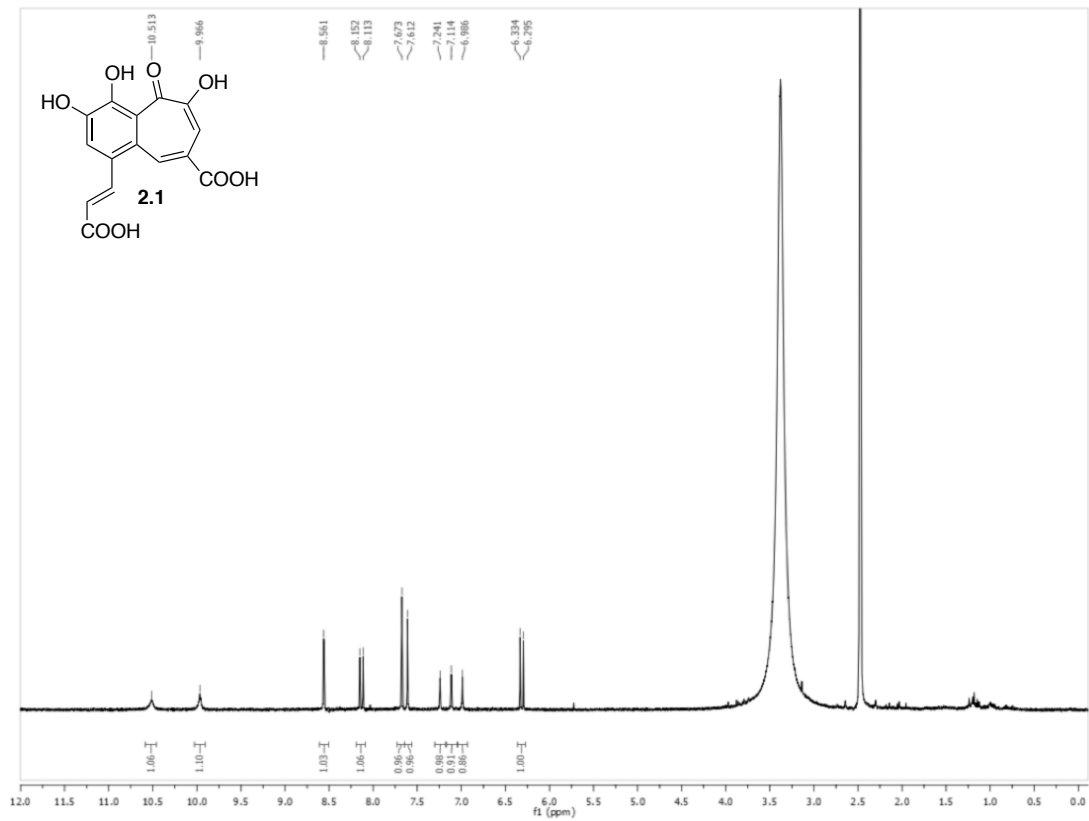
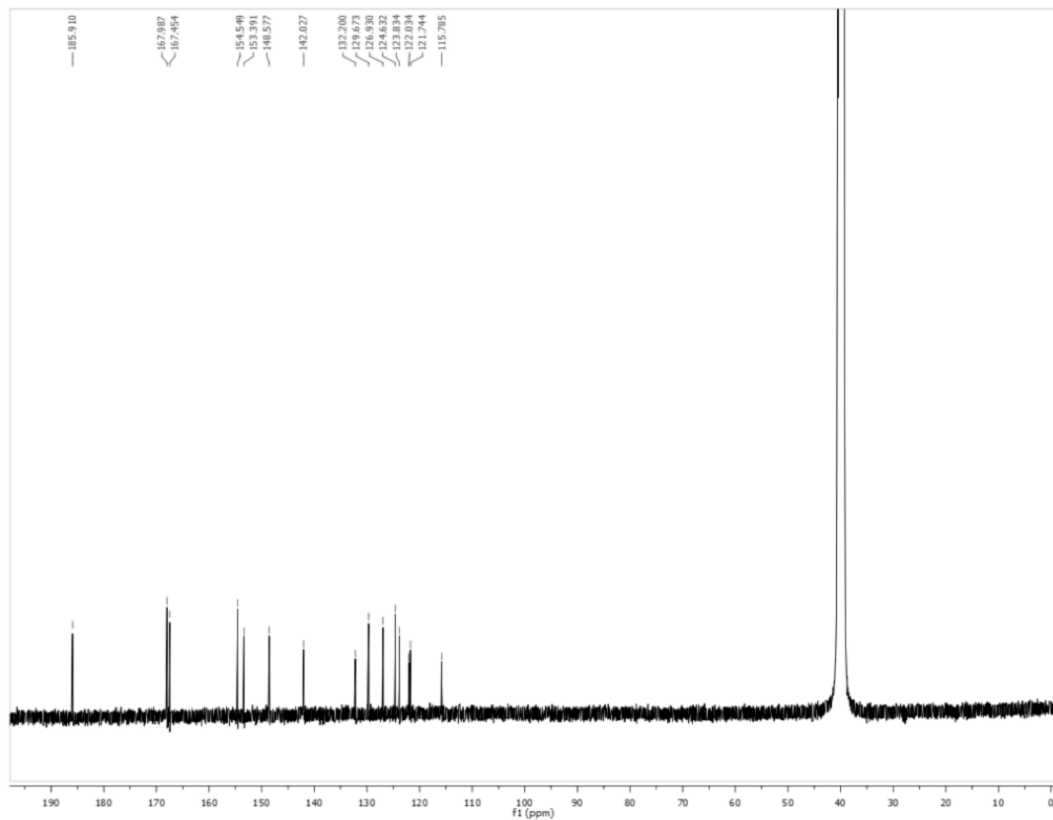
**Figure S2:** X-ray crystal structure of permethoxy-crocipodin (**2.10**).**Table S2:** Crystallographic data for permethoxy-crocipodin (**2.10**).

	<b>2.10</b>
net formula	C <sub>20</sub> H <sub>20</sub> O <sub>8</sub>
<i>M<sub>r</sub></i> /g mol <sup>-1</sup>	388.368
crystal size/mm	0.37 × 0.28 × 0.14
<i>T</i> /K	173(2)
radiation	MoKα
diffractometer	'Oxford XCalibur'
crystal system	monoclinic
space group	<i>P</i> 2 <sub>1</sub> / <i>c</i>
<i>a</i> /Å	21.5854(9)
<i>b</i> /Å	7.2867(5)
<i>c</i> /Å	11.7130(5)
α/°	90
β/°	93.489(4)
γ/°	90
<i>V</i> /Å <sup>3</sup>	1838.88(17)
<i>Z</i>	4

## 2.5. Experimental Section

---

calc. density/g cm <sup>-3</sup>	1.40283(13)
$\mu$ /mm <sup>-1</sup>	0.109
absorption correction	'multi-scan'
transmission factor range	0.90603–1.00000
refls. measured	4355
$R_{\text{int}}$	0.0000
mean $\sigma(I)/I$	0.0693
$\theta$ range	4.28–26.25
observed refls.	3213
$x, y$ (weighting scheme)	0.0326, 0
hydrogen refinement	constr
refls in refinement	4355
parameters	259
restraints	0
$R(F_{\text{obs}})$	0.0365
$R_w(F^2)$	0.0800
$S$	0.906
shift/error <sub>max</sub>	0.001
max electron density/e Å <sup>-3</sup>	0.171
min electron density/e Å <sup>-3</sup>	-0.171

$^1\text{H}$  NMR,  $\text{DMSO-}d_6$ , 400 MHz $^{13}\text{C}$  NMR,  $\text{DMSO-}d_6$ , 100 MHz

## 2.6 Bibliography

- [1] M. J. S. Dewar, *Nature* **1945**, *155*, 141–142.
- [2] M.-C. Menet, S. Sang, C. S. Yang, C.-T. Ho, R. T. Rosen, *Journal of Agricultural and Food Chemistry* **2004**, *52*, 2455–61.
- [3] J. Velišek, K. Cejpek, *Czech Journal of Food Sciences* **2011**, *29*, 87–102.
- [4] N. Fukui, K. Ohmori, K. Suzuki, *Helvetica Chimica Acta* **2012**, *95*, 2194–2217.
- [5] D. Horner L., *Zeitschrift für Naturforschung* **1959**, *14b*, 741.
- [6] H. C.-T. J. Jhoo J.-W., Sang S., Wei G.-J., Lee T. C., Rosen R. T., *Food Lipids* **2004**, *11*, 89–103.
- [7] H. C.-T. Sang S., Lambert J.D., Tian S., Hong J., Hou Z., Ryu J.-H., Stark R.E., Rosen R. T., Huang M.-T., Yang C. S., *Bioorg. Med. Chem.* **2004**, *12*, 459–467.
- [8] V. M. Takino Y., Ferretti A., Flanagan V., Gianturco M. A., *Can. J. Chem.* **1967**, *45*, 1949–1956.
- [9] D. K. Horner L., Dürckheimer W., Weber K. H., *Chem. Ber.* **1964**, *97*, 312–324.
- [10] A. J. Charlton, A. L. Davis, D. P. Jones, J. R. Lewis, A. P. Davies, E. Haslam, M. P. Williamson, *Journal of the Chemical Society, Perkin Transactions 2* **2000**, 317–322.
- [11] K. Suzuki, *Nippon Kagaku Zasshi* **1956**, *77*, 305–308.
- [12] T. W. Wu, L. H. Zeng, J. Wu, K. P. Fung, R. D. Weisel, a Hempel, N. Camerman, *Biochemical Pharmacology* **1996**, *52*, 1073–80.
- [13] A. Bresinsky, H. Z. Besl, *Mykol.* **1979**, *45*, 247–274.
- [14] D. Klostermeyer, L. Knops, T. Sindlinger, K. Polborn, W. Steglich, *European Journal of Organic Chemistry* **2000**, 603–609.
- [15] N. Arpin, J. Favre-Bonvin, W. Steglich, *Phytochemistry* **1974**, *13*, 1949–1952.



# Organic Photovoltaics:<sup>\*</sup>

## Porphyrin- and Phthalocyanine-based Periodic Porous Frameworks

Y. Li, F. Löbermann, F. Auras, M. Döblinger, J. Schuster, L. Peters, D. Trauner, T. Bein  
*manuscript in preparation.*

Y. Li, F. Auras, F. Löbermann, M. Döblinger, J. Schuster, L. Peters, D. Trauner, T. Bein  
*manuscript in preparation.*

---

<sup>\*</sup> This project was conducted in collaboration with the group of Prof. Dr. THOMAS BEIN at the LMU München.  
The corresponding collaboration partners are documented in each sub-chapter.



### 3.1 Project Aims

The economy and development of mankind is currently still mostly powered by harvesting the chemical energy stored within fossil fuels through combustion and conversion of the thus obtained heat into electricity or kinetic energy. Fossil fuels are easy to store and available in large quantities. However, they are geologically limited and the production of oil is believed to have peaked in 2006.<sup>[1]</sup> Another drawback is the release of large amounts of greenhouse gases, such as CO<sub>2</sub>. Hence, great efforts have been taken to replace fossil fuel-based energy generation with renewable energy sources, which are in principle available in unlimited amounts and are mostly CO<sub>2</sub> neutral.

Photovoltaic cells based on mono- or polycrystalline silicon convert solar light directly into electricity by exploiting the photo effect.<sup>[2]</sup> While those cells are already reaching high degrees of effectiveness, there is still a huge potential for improvement of so-called organic solar cells. Organic photovoltaics (OPVs) hold several advantages over their silicon-based counterparts. Organic semiconductors with very high absorption coefficients allow the design of thin and flexible cells, while established production techniques like roll-to-roll processing enable at the same time the fabrication of large area devices.<sup>[3]</sup>

The aim of this project was to explore the potential of increased efficiency of novel heterojunction architectures and to provide organic precursors for the bottom-up synthesis of highly ordered nanometre scale structures. Ordered structures with tailor-made heterojunctions should facilitate charge separation within the electroactive layer and hence increase the efficiency of the organic solar cell. In principal two different types of materials could exhibit the desired properties. One part of this work focussed on the development of novel, photoactive periodic-mesoporous organosilica and the fabrication of photovoltaic devices. The second part of this research was geared towards the synthesis and design of covalent organic frameworks (COFs). The highly ordered 2D polymeric structures are a relatively new class of functional materials and hold great promise for the application in electronic devices.

## 3.2 Introduction

### 3.2.1 The Working Principle and General Architectures of Organic Photovoltaic Cells

An organic photovoltaic cell consists of at least one photoactive layer, which is embedded between two electrodes. One of the electrodes must be transparent to allow the absorption of light within the photoactive layer. Usually indium tin oxide (ITO) coated glass substrates are employed as the transparent anode.<sup>[4]</sup> Currently there are three different device architectures for the construction of OPVs.

The first OPVs were based on a single layer of a photoactive organic semiconductor (Figure 3.1). Within these SCHOTTKY cells (A), charge separation only occurs at the heterojunction of one electrode, which at the same time is the greatest disadvantage of this design: positive and negative charge carriers have to diffuse through the same material, automatically resulting in high recombination loss.<sup>[5]</sup> The built-in potential of single-layer solar cells is either derived from the difference in work function of the dissimilar electrodes or from a SCHOTTKY potential barrier at the metal/organic interface of the electrode contact.<sup>[6]</sup>

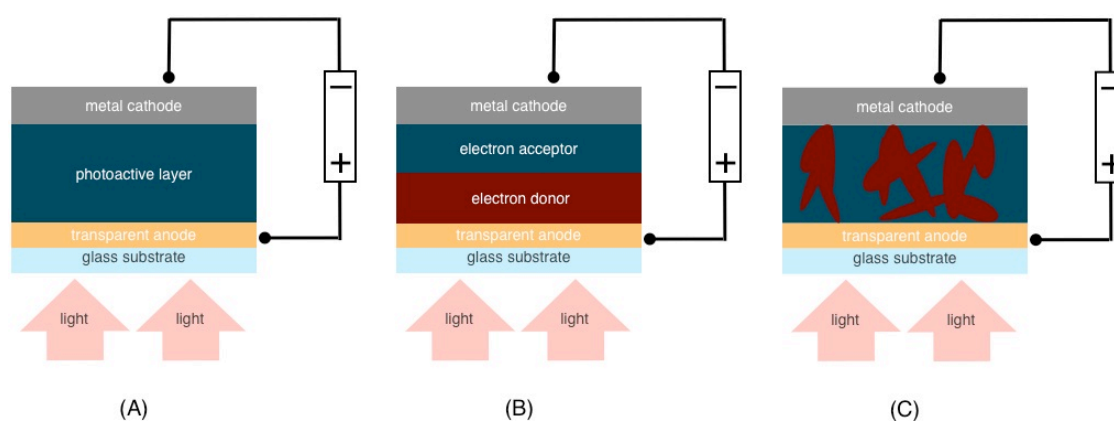


**Figure 3.1.** Schematic representation of a single layer (A), a bilayer (B) and a bulk heterojunction organic photovoltaic cell.

The development of heterojunction bilayer photovoltaic devices (B), first reported by TANG, overcame the limitations of single-layer cell architectures, because the performance of these cells highly depends on the nature of the organic–organic interface.<sup>[7]</sup> Because charge separation now occurs at the heterojunction, recombination of excitons is a less



likely process, resulting in a higher overall efficiency. Nonetheless, exciton recombination remains a problem, still limiting the efficiency of cells with such architectures. This is mainly due to the relatively short exciton diffusion length of 5–20 nm within organic semiconductors before recombination takes place.<sup>[8]</sup> Therefore, bilayer devices usually have a very thin photoactive layer.

The introduction of bulk heterojunctions (BHJ) into OPVs (C) tackles the issue of relatively short exciton diffusion lengths. For the construction of BHJ solar cells, donor and acceptor materials are blended so that phase separation results in an disordered 3D interpenetrating network. This significantly reduces the exciton diffusion distance to the heterojunction, where charge separation can occur. Hence, with this type of device architecture a much larger amount of generated excitons can be harvested.<sup>[5]</sup>

The next step to further develop the structural properties of OPVs and facilitate charge separation would be the construction of highly ordered 3D nanoscale interfaces (Figure 3.2). It would be highly desirable to create an ordered structural platform, which would allow studying the impact of electronic properties, nanostructure and morphology on exciton generation, separation and charge carrier diffusion.

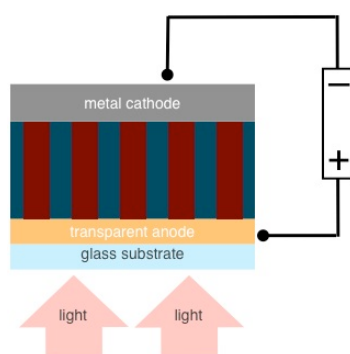


**Figure 3.2.** Schematic representation of an OPV, featuring a periodic nanoscale interpenetrating donor–acceptor system.

### 3.2.2 Molecular Self-Assembly

Within silicon-based materials nanoscale structures can be introduced through top down approaches, such as electrochemical etching.<sup>[9]</sup> On the other hand, structures in materials based on organic precursors have to be designed in a bottom-up fashion through molecular self-assembly. Molecular self-assembly can be defined as the spontaneous conglomeration of molecules or particles under equilibrium conditions into stable, structurally well-defined aggregates.<sup>[10,11]</sup> The principles of molecular self-assembly have, amongst others, been summarized by WHITESIDES and co-workers.<sup>[10]</sup> A self-assembly system consists of molecules or sections of macromolecules that interact with each another through short ranged forces. Single or multi component systems are possible, where the assembly partners can be of the same or different nature. Through interactions between the components within the self-assembly process, a less ordered state is transformed into a stable, more ordered state. This can, for example result, in the formation of a crystal or the folding of a protein. Well-balanced attractive and repulsive forces drive the self-assembly process. However, it is important that the interactions between the components must be reversible under the self-assembly conditions. Crystalline materials can only be obtained, when the components are able to adjust their position within a formed aggregate, otherwise amorphous structures will form. The self-assembly process of given components can itself be influenced through the choice of the environment. Changes of the constitution of the solution or interface at which the process occurs can greatly influence the outcome of the process.

For novel heterojunction architectures in OPVs, a self-assembly process must yield porous systems with dimensions in the order of the diffusion length of an exciton to maximize charge separation and minimize recombination losses. At the same time, the obtained pores need to be large enough to accommodate guest molecules, as electron acceptor materials. In principal, these prerequisites can be fulfilled by so called covalent organic frameworks (COFs) and periodic-mesoporous organosilicas (PMOs). The nanoscale structures in both types of materials are obtained through a molecular self-assembly process of organic precursor molecules.<sup>[12,13]</sup>

### 3.2.3 Optical Properties of Porphyrins and Phthalocyanines

Porphyrin and its derivatives, such as phthalocyanines contain a macrocyclic, conjugated, aromatic 18  $\pi$ -system with high photostability.<sup>[14]</sup> Due to this extended  $\pi$ -system, all porphyrins and phthalocyanines absorb light the strongest in the visible region of the solar light spectrum between 350 and 750 nm (Figure 3.3). Porphyrins are of red to purple colour and usually exhibit their absorption maximum between 400 and 450 nm. Phthalocyanines are typically green to blue with a maximum absorption in the region of 650 to 700 nm.

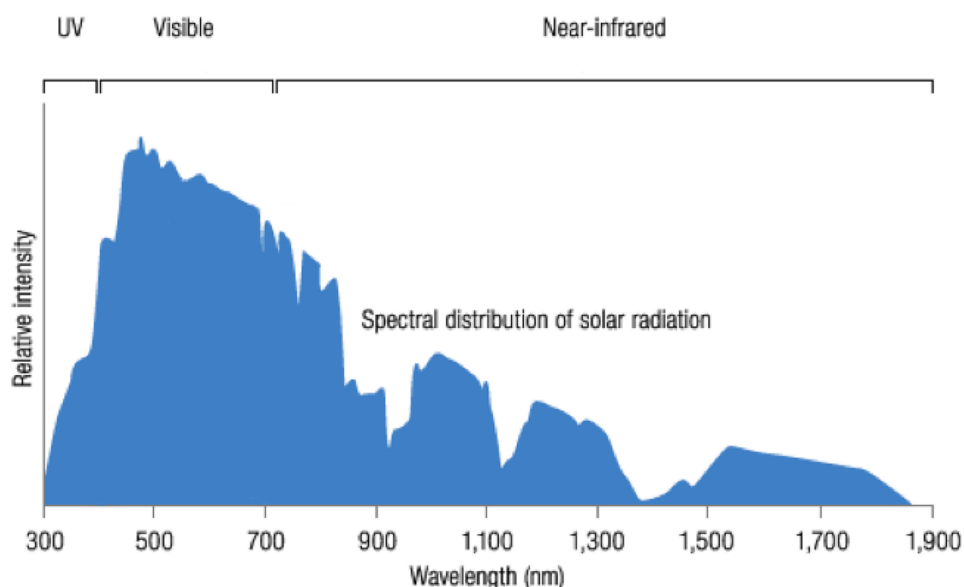


**Figure 3.3.** Solar spectrum reaching the Earth's surface after being filtered by the different gases in the atmosphere.\*

Porphyrins feature two types of characteristic bands in their absorption spectrum: an intensive Soret band ( $n \rightarrow \pi^*$  transition) in the near UV region at 390 – 420 nm and additionally up to four weaker Q-bands ( $\pi \rightarrow \pi^*$  transition) at approximately 480 – 700 nm.<sup>[15,16]</sup> The HOMO/LUMO energy difference decreases from porphyrins to phthalocyanines, which leads to a bathochromic shift of the Q-band to longer wavelengths with increasing intensity for phthalocyanines. The absorption spectrum of phthalocyanines

---

\*Original graphics by E Source Companies LLC. Used with permission, © 2013 E Source.

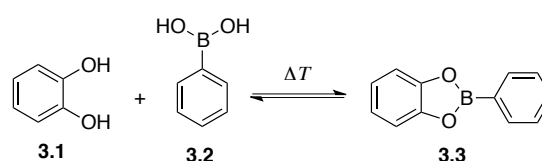
([http://www.esource.com/BEA1/OMA/OMA\\_BuildingEnvelope/OMA-20](http://www.esource.com/BEA1/OMA/OMA_BuildingEnvelope/OMA-20)). Accessed on Thursday, 31 January 2013.

shows a strong Q-band in a range of 660 – 740 nm and a weaker Soret band around 350 nm.<sup>[17]</sup> Metal-free phthalocyanines exhibit a split Q-band, which is attributed to the non-degenerated LUMOs and can be rationalized on GOUTERMAN`S four-orbital model for the spectra of porphyrins.<sup>[18]</sup> Insertion of a metal ion maintains the planarity of the macrocycle and increases the symmetry from D<sub>2h</sub> to D<sub>4h</sub>. This change in symmetry leads to degeneration of the orbitals, as a result of which splitting of the Q-bands is not observed anymore. In addition to the dimension of the aromatic system, the position and intensity of the absorption bands also strongly depend on the type and position of substituents. Electron-donating groups lead to a red-shift (longer wavelength) and electron-withdrawing groups to a blue-shift (shorter wavelength).

## 3.3 Towards Novel Electroactive Covalent Organic Frameworks\*

### 3.3.1 Introduction to Covalent Organic Frameworks

Covalent organic frameworks (COFs) are a new class of porous materials that recently have attracted much attention. COFs are crystalline polymers with a well-defined porous 2D or 3D structure. In order to obtain the polymer with the required crystallinity, the bond-forming event needs to be reversible, which allows self-healing of defects within the lattice in the course of the self-assembly process. The condensation reaction of catechol (**3.1**) and benzenboronic acid (**3.2**) reversibly gives boronate ester **3.3** and two water molecules (Scheme 3.1). Hence, this type of reaction is suitable for the formation of COF structures.



**Scheme 3.1.** Condensation reaction of catechol (**3.1**) and benzenboronic acid (**3.2**) to a boronate ester.

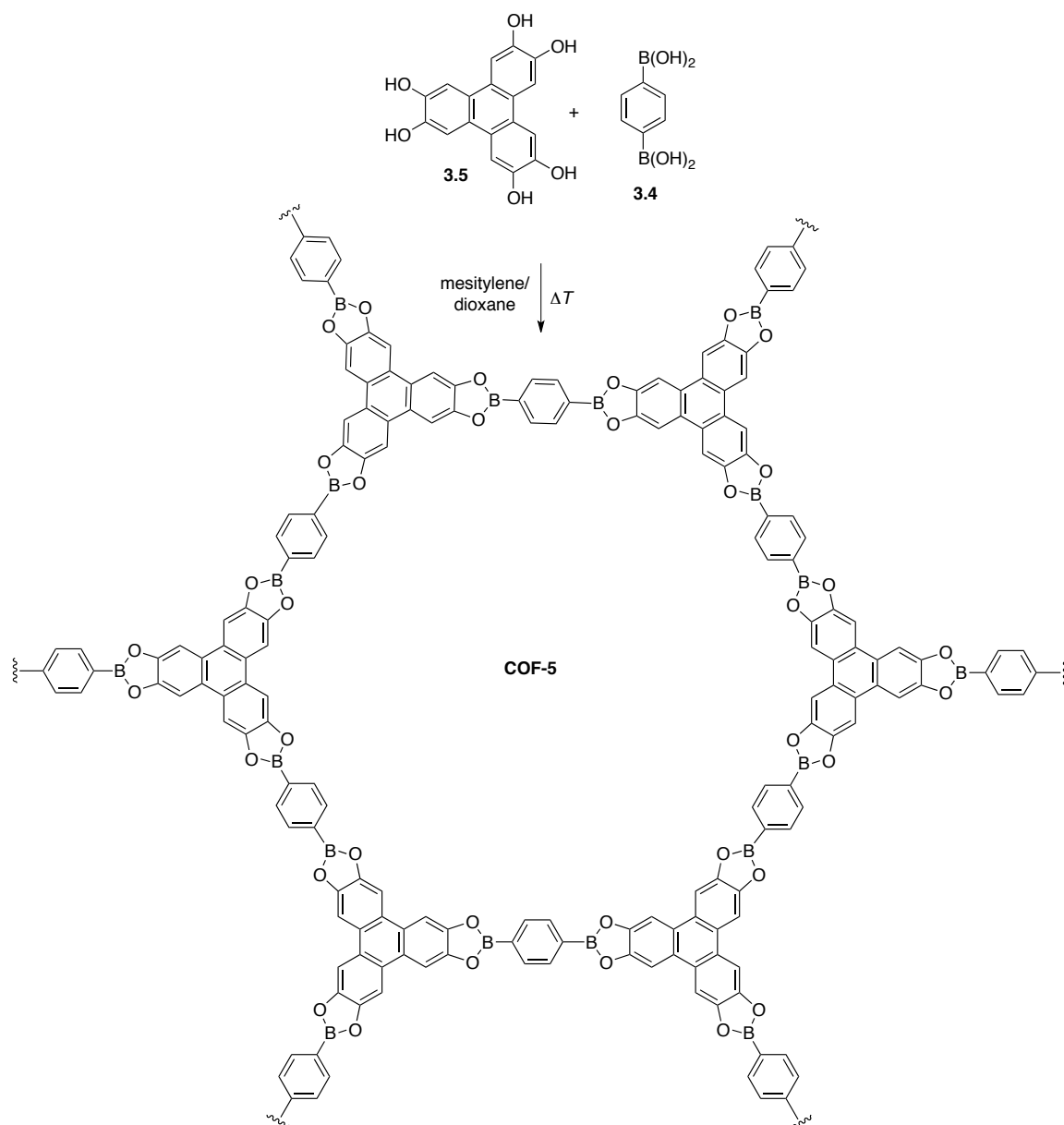
First, the group of O. YAGHI reported the poly-condensation reaction of 1,4-phenyldiboronic acid (**3.4**) (PDBA) with 2,3,6,7,10,11-hexahydroxytriphenylene (HHTP) (**3.5**), which resulted in the formation of COF-5 as a crystalline powder (Scheme 3.2).<sup>[12]</sup> This two-dimensional, highly ordered polymer features pores with a diameter of 2.7 nm. Usually the 2D layers of COF materials are stacking in an eclipsed fashion, although also COFs exhibiting a staggered conformation have been reported in literature.<sup>[12]</sup> Based on the work by YAGHI, COF materials relying on either the formation of boronate esters,<sup>[19]</sup> boroxin anhydrides<sup>[20]</sup> or imines<sup>[21]</sup> have been synthesised. However, the exact mechanism of COF formation is still unknown and the synthesis of new frameworks remains a challenge.

---

\* This work was performed in collaboration with Dr. MIRJAM DOGRU, MONA CALIK and Dr. DANA MEDINA - researchers in the group of Prof. Dr. THOMAS BEIN – as well as with Dr. LAURA SALONEN researcher in the group of Prof. Dr. DIRK TRAUNER).

F. L. and L. S. were equally responsible for the synthesis of COF precursors. M. D, M. C and D. M were in charge of the synthesis and characterisation of the COF materials.

The properties of the COFs can be fine-tuned towards specific applications through the modular assembly of those structures, because the length and relative orientation of the linking groups determine the lattice structure. This is in contrast to the unpredictable packing of traditional semiconductors.<sup>[22]</sup> The conjugated  $\pi$ -system in combination with the permanent porosity and high thermal stability renders COFs suitable candidates for the development of electronic devices, gas storage or other applications taking advantage of host-guest interactions, such as catalysis.



**Scheme 3.2.** Condensation reaction of HHTP with PDBA to 2D polymer COF-5.<sup>[12]</sup>

The pore size of the COF material is determined by the choice of organic building blocks employed in the synthesis. The group of T. Bein has reported a hexagonal boronate ester-based COF with a free pore size of 4 nm.<sup>[23]</sup>

## CONTRIBUTIONS TO THE CHEMISTRY OF POLYHYDROXYLATED AROMATIC COMPOUNDS

At the outset of this project, no tetragonal or porphyrin/phthalocyanine-based COF material has been reported. However, in the course of this project on the development of novel COF frameworks, DICHTTEL and co-workers were the first to report a tetragonal, phthalocyanine-based COF with 2.3 nm pore size (Figure 3.5).<sup>[19]</sup> Shortly after, the first porphyrin-containing tetragonal COF was prepared with a pore size of 2.5 nm.<sup>[24]</sup> It was also shown that porphyrin COFs allow close intermolecular interactions through  $\pi$ -stacking, which results in materials with high charge carrier mobility.<sup>[25]</sup>

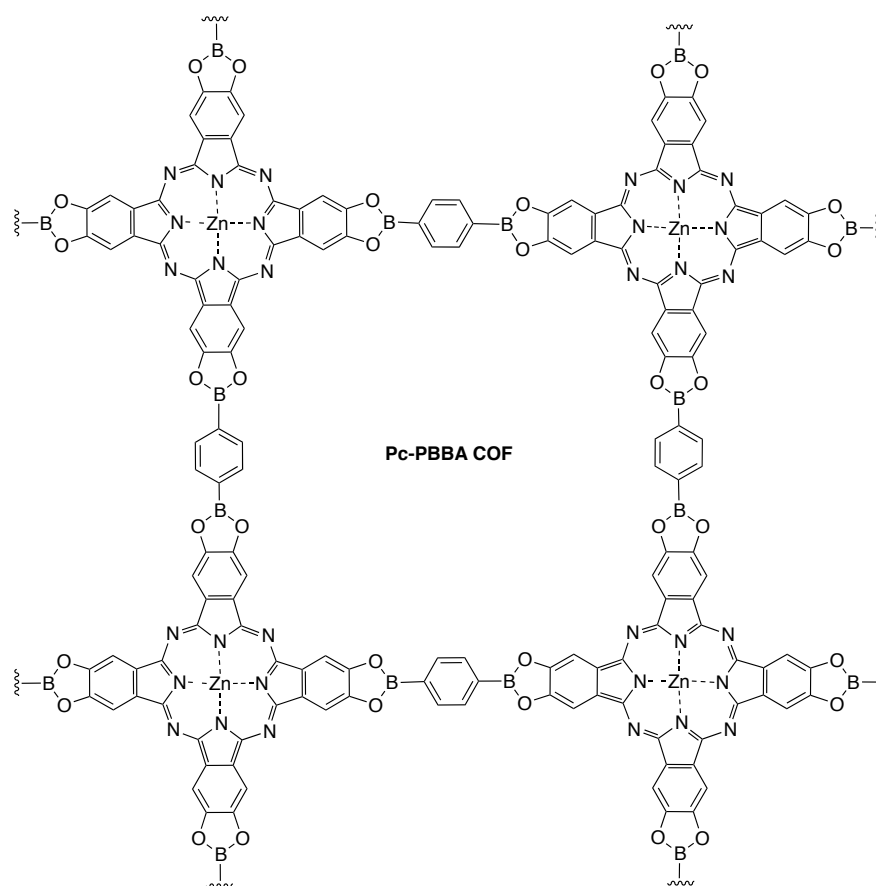


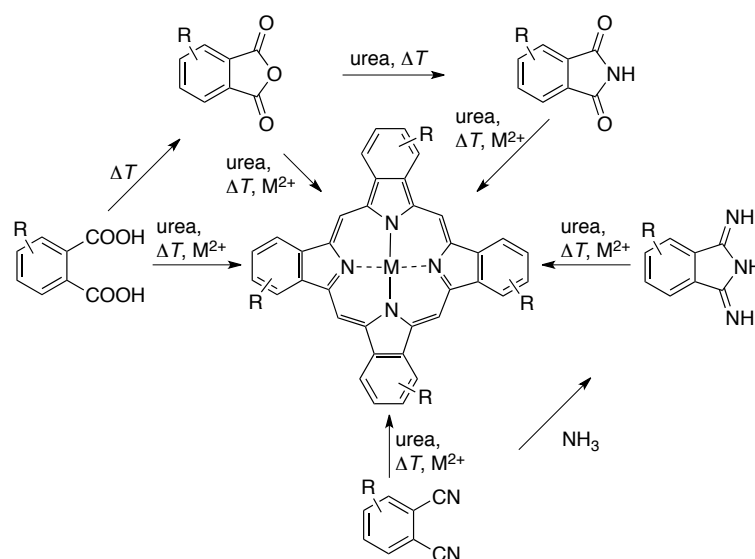
**Figure 3.5.** Representation of Pc-PBBA COF.<sup>[19]</sup>

In order to fabricate opto-electronic devices, such as OPVs, it is important that the nano-structured material can be obtained as thin films. The synthesis of COF thin films is a challenge, because they are usually isolated as crystalline powders. However, it was possible to obtain oriented 2D COF thin films of COF-5 through catalysed growth on a graphene surface.<sup>[26]</sup>

The group of JIANG were the first to report the post-synthesis functionalisation of COF pore walls through click-chemistry. This approach is the first example for the engineering of the COF pore walls.<sup>[27]</sup>

### 3.3.2 Towards the Synthesis of Phthalocyanine and Porphyrin Containing COFs

Phthalocyanines can be obtained through the tetramerisation of phthalic acid derivatives (Scheme 3.3). Most of the established syntheses for symmetric phthalocyanines (Pc) rely on the presence of metal ions, such as  $\text{Cu}^{2+}$  or  $\text{Zn}^{2+}$ . These ions promote the tetramerisation process, serving as a template for the coordination of four precursor molecules. Consequently, the corresponding metal-containing phthalocyanines (PcM) are obtained.<sup>[28]</sup> Metal-free phthalocyanines can be prepared by treatment of phthalic dinitriles with e.g. alcoholates.<sup>[29]</sup>



**Scheme 3.3.** Formation of PcM from phthalic acid derivatives.

Since PcM can be prepared with  $D_{4h}$  symmetry, they are ideal building blocks for tetragonal COF structures, as is illustrated in Figure 3.6.

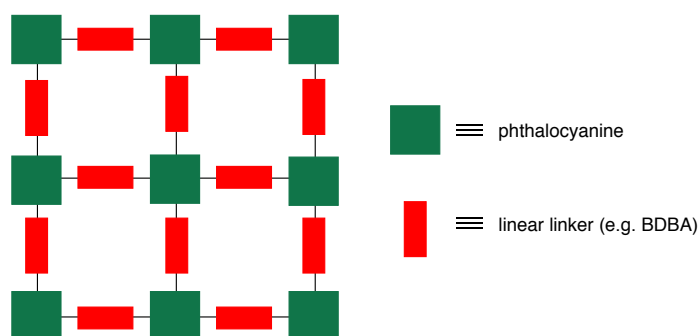


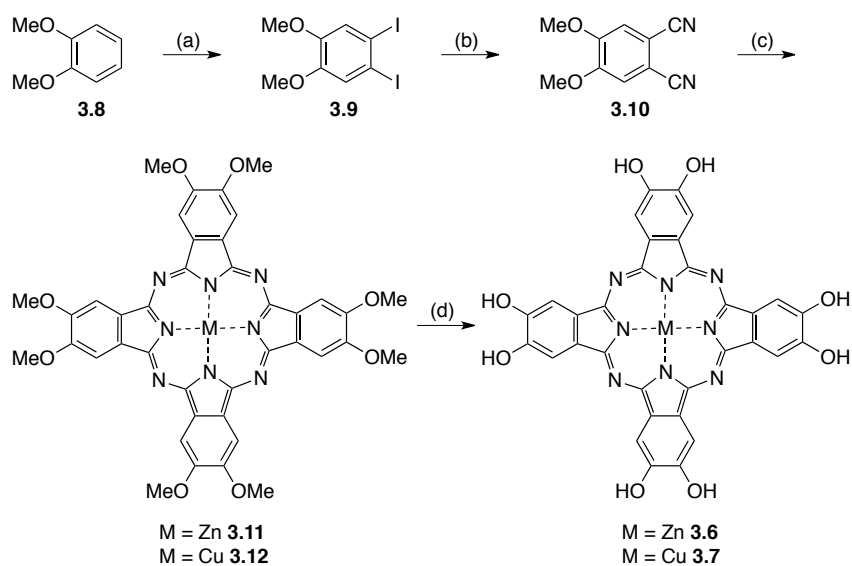
**Figure 3.6.** Schematic representation of the connectivity within a Pc-based COF.



## CONTRIBUTIONS TO THE CHEMISTRY OF POLYHYDROXYLATED AROMATIC COMPOUNDS

Because the synthesis of COFs featuring boronate ester linkage was proven by DICHTEL and JIANG to be reliable,<sup>[22,27]</sup> it was chosen to first approach Pc containing organic frameworks through the condensation of boronic acids with catechols. For this purpose phthalocyanine octaols (Pc-OH<sub>8</sub>) were prepared.

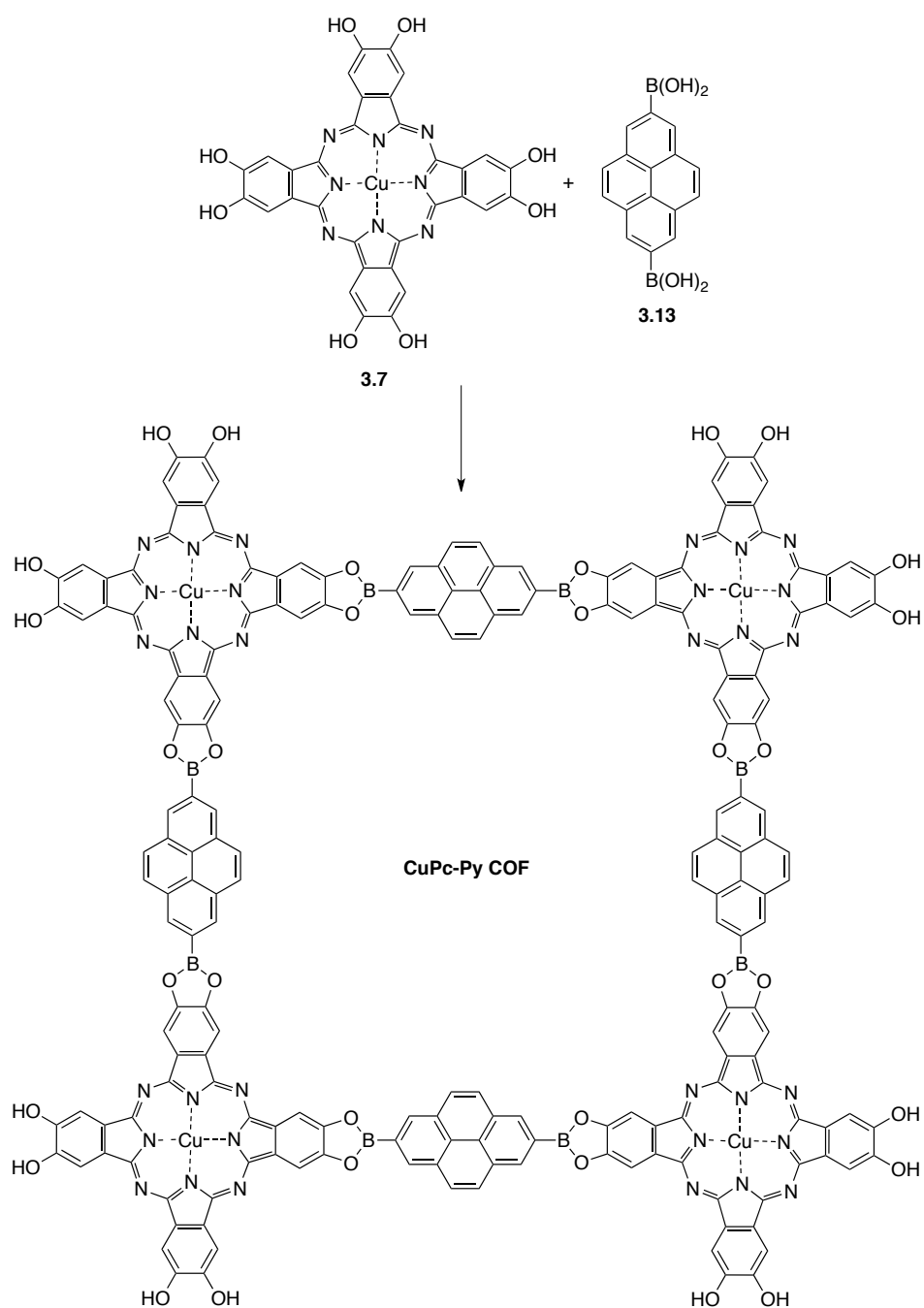
The synthesis of literature known Pc-OH<sub>8</sub> **3.6** and **3.7**<sup>[22]</sup> began with the iodination of veratrole (**3.8**) (Scheme 3.4). Refluxing **3.8** with iodine and periodic acid in methanol gave diiodide **3.9** in excellent yield.<sup>[30]</sup> A palladium-catalysed ROSENMUND-VON BRAUN reaction of **3.9** with Zn(CN)<sub>2</sub> resulted in dinitrile **3.10**. The reaction was much more sluggish, when employing the commercial dibromoveratrole. Tetramerisation of phthalonitrile **3.10** with zinc(II)acetate or copper(II)chloride with catalytic amounts of ammonium molybdate in ethylene glycol gave the corresponding metallated Pcs **3.11** and **3.12** as insoluble, dark green solids.



Reagents and conditions: (a) I<sub>2</sub>, H<sub>5</sub>IO<sub>6</sub>, reflux, 95% of **3.9**; (b) Pd(PPh<sub>3</sub>)<sub>4</sub>, Zn(CN)<sub>2</sub>, DMF, 74% of **3.10**; (c) Zn(OAc)<sub>2</sub> or CuCl<sub>2</sub>, urea, DBU, ammonium molybdate ethylene glycol, heat, 74% of **3.11** or 87% of **3.12**; (d) BBr<sub>3</sub>, CH<sub>2</sub>Cl<sub>2</sub>, 5 d, 75% of **3.6** or 65% of **3.7**.

**Scheme 3.4.** Synthesis of metallated Pc-OH<sub>8</sub>.

Demethylation of the corresponding protected Pc with excess boron tribromide finally resulted in zinc or copper Pc-OH<sub>8</sub> **3.6** and **3.7** as dark powders. The material was purified by washing excessively with methanol and CH<sub>2</sub>Cl<sub>2</sub>. The thus obtained (Pc-OH<sub>8</sub>) was then submitted to COF synthesis with pyrene-2,7-diboronic acid (**3.13**), to obtain a tetragonal COF with large pores (Scheme 3.5).



**Scheme 3.5.** Synthesis of ZnPc-Py COF.

When subjecting pyrene-2,7-diboronic acid (PDBA) (3.13) and CuPC-OH<sub>8</sub> 3.7 to highly optimised solvothermal reaction conditions, CuPc-Py COF, with a pore size of 2.7 nm, was obtained as a dark powder. For the formation of a COF the fine-tuning of reaction conditions is crucial. Especially the polarity of the solvents, as well as reaction time and temperature seem to have huge impact on the outcome of a COF synthesis.

Simulation of the X-ray diffraction patterns revealed that the 2D sheets of the COF undergo  $\pi$ - $\pi$  stacking in a highly symmetric eclipsed fashion (Figure 3.7). The obtained

characterisation data is congruent with that reported by DICHTEL and co-workers shortly after this successful synthesis.<sup>[22]</sup>

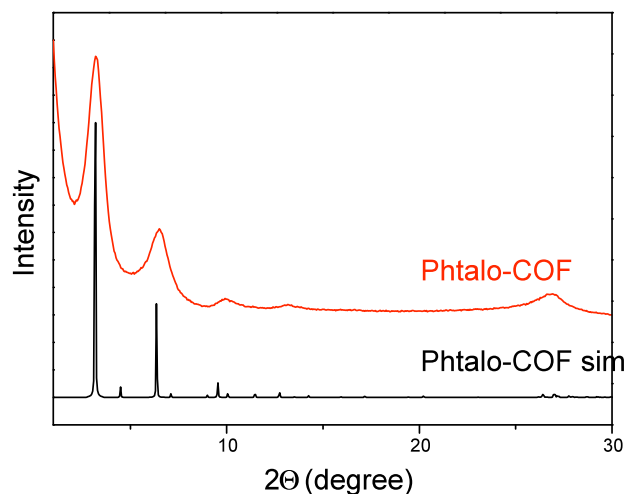


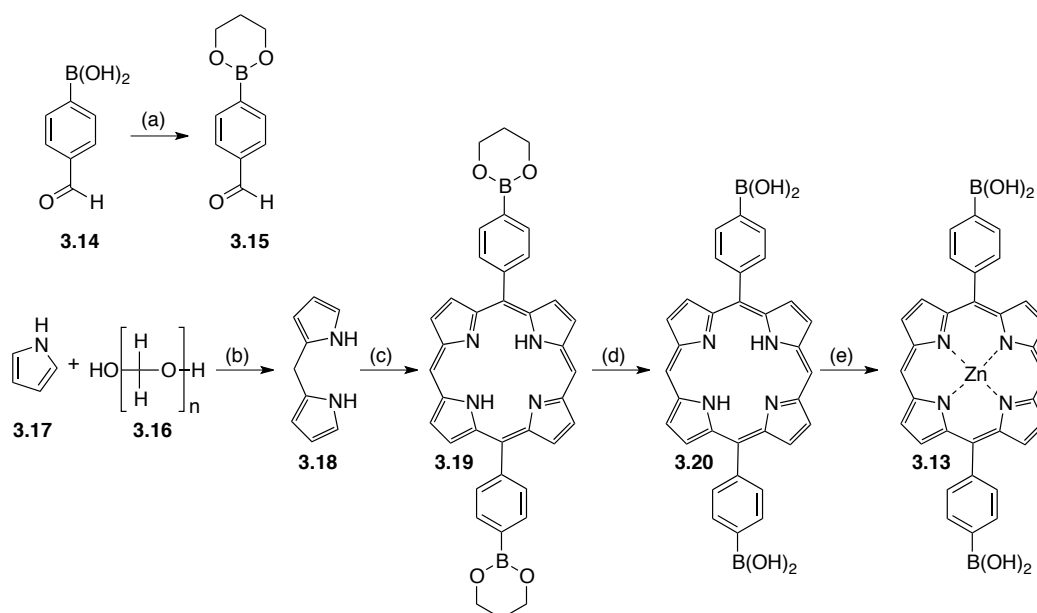
**Figure 3.7.** Powder X-ray diffraction pattern of ZnPc-Py COF; experimental (red) vs. predicted (black).\*

Having successfully incorporated phthalocyanine macrocycles into a COF, the focus was then turned on expanding the pore size and enhancing the optical properties of the porous materials. Because porphyrins have different absorption maxima from phthalocyanines, the additional integration of porphyrin linkers would allow harvesting light from a broader area of the solar spectrum. In addition to large tetragonal COF systems, a linear, porphyrin-based boronic acid linker in combination with HHTP (**3.5**) would also allow the synthesis of very large hexagonal pores.

Synthesis of literature-known linear porphyrin bis-boronic acid **3.13** commenced with the protection of commercial (4-formylphenyl)boronic acid (**3.14**) with propane-1,3-diol to give aldehyde **3.15** (Scheme 3.6).<sup>[31,32]</sup> The condensation reaction of paraformaldehyde (**3.16**) and pyrrole (**3.17**), mediated by  $\text{InCl}_3$  as a very mild LA, to furnish dipyrromethane (**3.18**) in good yield. The sensitive product was stable for months, if recrystallized and stored under Ar at  $-20\text{ }^\circ\text{C}$ . The porphyrin synthesis from dipyrromethane (**3.18**) with aldehyde **3.15** under the mild conditions first developed by LINDSEY,<sup>[33]</sup> resulted in the formation of linearly substituted porphyrin **3.19** in 37% yield. Deprotection to the free boronic acid (**3.19**→**3.20**) with aq. HCl in THF, followed by metallation with  $\text{Zn}(\text{OAc})_2$  resulted in the smooth formation of zincated porphyrin **3.13**.

---

\* COF synthesis and characterisation by M. DOGRU from the group of Prof. Dr. T. BEIN.



Reagents and conditions: (a) propane-1,3-diol, toluene, reflux, 99% of **3.15**; (b)  $\text{InCl}_3$ , pyrrole, 50 °C, 75% of **3.18**; (c)  $\text{BF}_3 \cdot \text{OEt}_2$ ,  $\text{CHCl}_3$ , rt, 3 h, then DDQ over night, 37% of **3.19**; (d)  $\text{HCl}$ , THF, over night, 87% of **3.20**; (e)  $\text{Zn}(\text{OAc})_2$ , THF/MeOH, over night, 88% of **3.13**.

**Scheme 3.6.** Synthesis of zincated porphyrin boronic acid linker **3.13**.

Multiple grams of  $\text{Pc-OH}_8$  (**3.7**) and porphyrin **3.13** have been prepared and submitted to hydrothermal reaction conditions. Despite considerable efforts and screening of numerous solvent systems and ratios, until now it was not possible to obtain the desired  $\text{CuPc-ZnPor}$  COF, as depicted in Scheme 3.7. One possible explanation might be, that the aryl ring in the meso position is twisted (mean = 73°) out of the porphyrin plane (Figure 3.8).<sup>[34]</sup> This effect could prevent stacking of the 2D sheets and thus hinder the formation of a crystalline COF structure. Hence, finding the optimum conditions is much more challenging for this type of system.

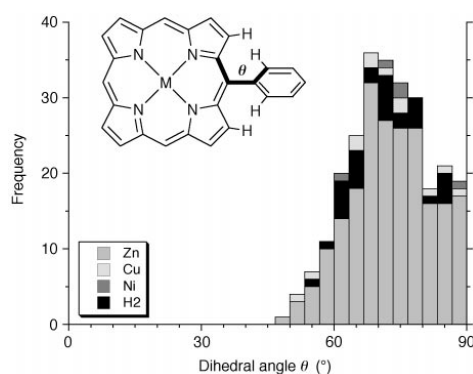
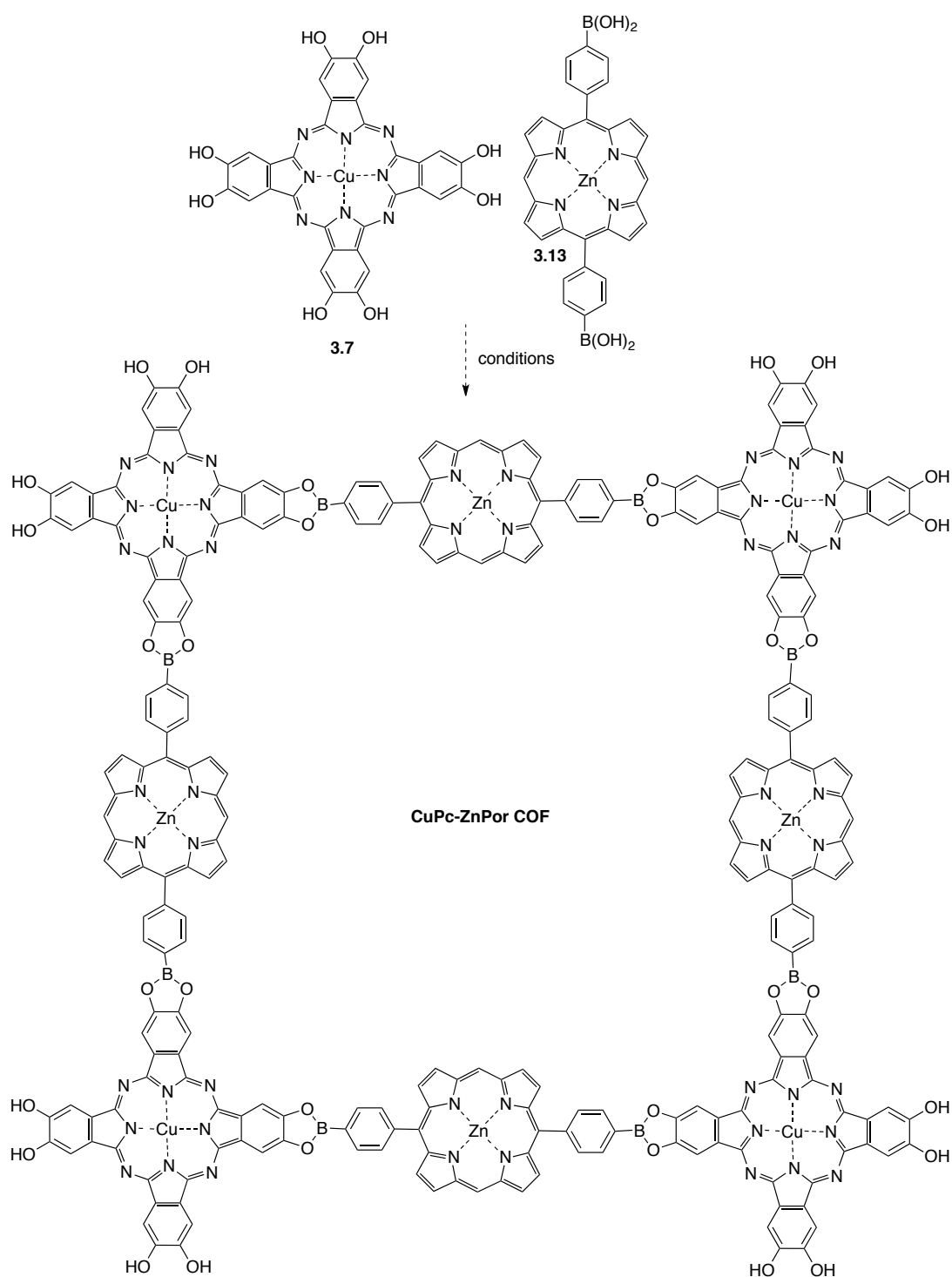


**Figure 3.8.** Distribution of dihedral angles in *meso*-aryl  $\text{Zn}^{\text{II}}$ ,  $\text{Cu}^{\text{II}}$ ,  $\text{Ni}^{\text{II}}$  and free-base porphyrins from the Cambridge Crystallographic Database.<sup>[34]</sup>



**Scheme 3.7.** Envisaged synthesis of ZnPc-Por COF.

Although it was not yet possible to obtain a novel COF material based on the co-condensation of phthalocyanine and porphyrins, a robust synthetic route for the synthesis of the necessary precursor molecules has been developed. Especially the dipyrromethane-

based approach to the porphyrin linkers allows the access of many different potential porphyrin-based COF precursors.

Reacting porphyrin linker **3.13** with HHTP (**3.5**) would result in a ZnPor-HHTP COF with an unprecedented pore-sizes (Figure 3.9). Currently efforts towards the synthesis of this framework are underway.

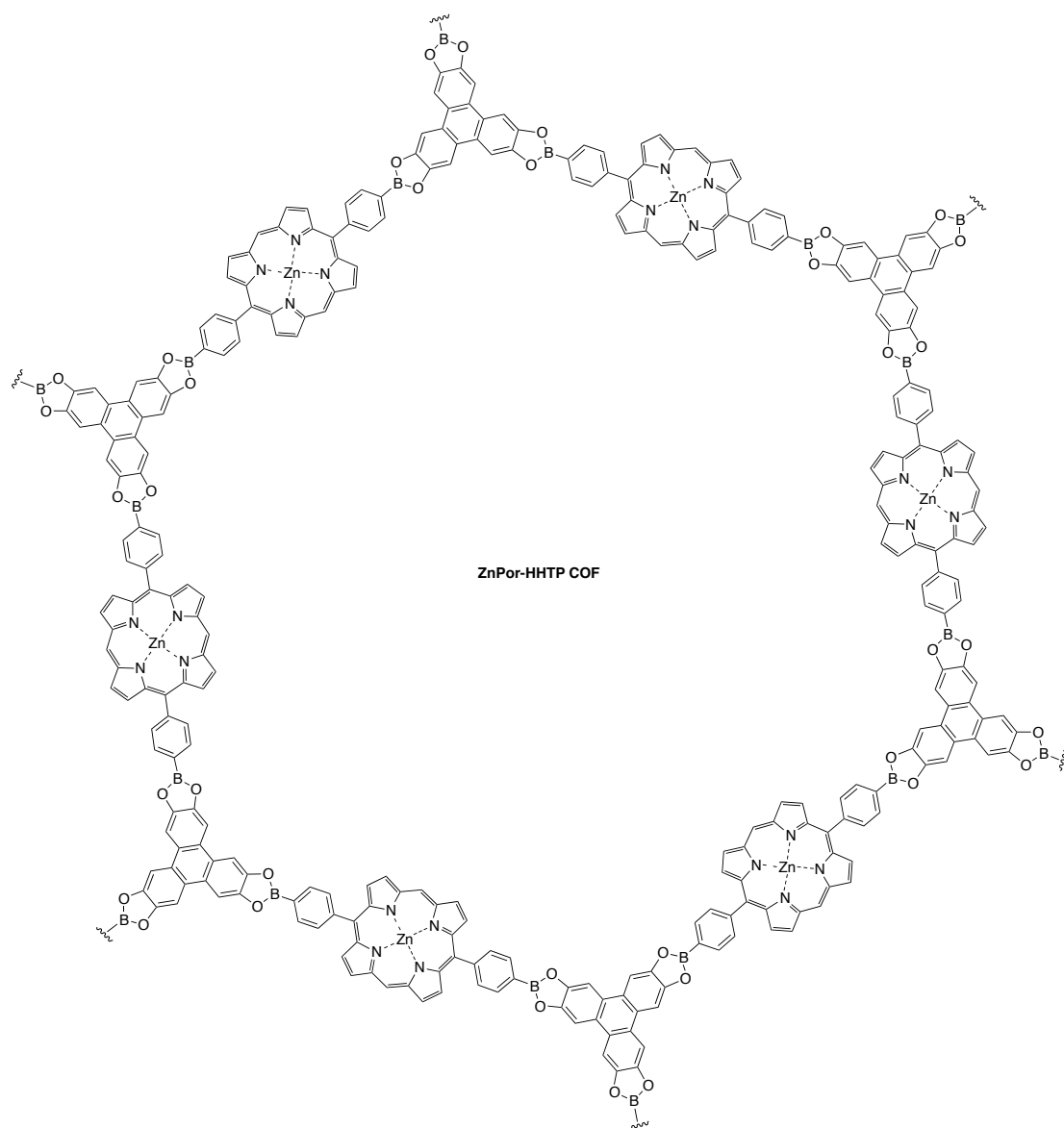


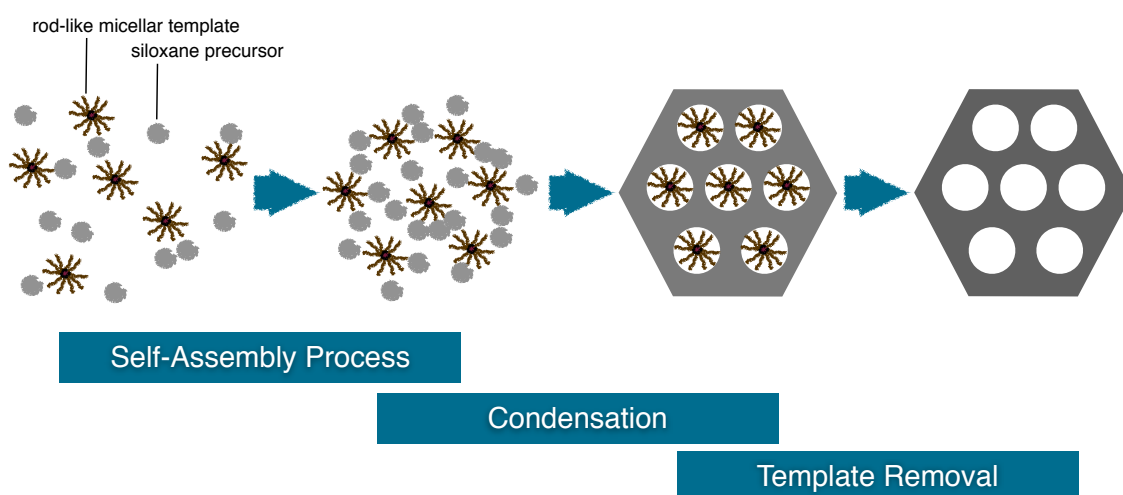
**Figure 3.9.** Illustration of ZnPor-HHTP COF.

In summary several building blocks for the synthesis of novel COF frameworks have been prepared on a multi-gram scale. However, the formation of COF materials has proven to be very capricious. Thus, very thorough screenings and the preparation of more material is required.

## 3.4 Opto-Electronically Active Periodic Mesoporous Organosilica\*

### 3.4.1 Introduction to Periodic Mesoporous Organosilica

The synthesis of novel mesoporous organic–inorganic hybrid materials has opened up new avenues in the field of materials science. They allow the tailor-made design of materials for the application in areas such as gas adsorption and storage,<sup>[35]</sup> chemical sensors,<sup>[36]</sup> catalysis<sup>[37,38]</sup> as well as photovoltaics.<sup>[39]</sup> Mesoporous materials feature nanoscale architectures with pore diameters between 2 and 50 nm.<sup>[40]</sup> Periodic mesoporous silica were discovered in 1992 and are formed through a sol-gel process in the presence of self-assembled aggregates of structure-directing agents (Scheme 3.8).<sup>[41]</sup> The structure-directing agent, such as surfactants or block co-polymers, forms rod-like micelles in the reaction medium. These micelles self-assemble to highly ordered aggregates upon slow evaporation of the solvent due to an increase of the concentration. Additionally the slow evaporation triggers the condensation of the siloxane precursors to form solid pore walls. Finally, extraction of the template then results in accessible mesopores.




---

\* This work was performed together with YAN LI, a PhD student in the group of Prof. Dr. THOMAS BEIN, Ludwigs-Maximilians-Universität München. Y. L. was responsible for the synthesis and characterisation of the PMO materials from the corresponding precursors; F. L. was responsible for the synthesis and characterisation of the alkoxy silane precursors. The results presented herein can also be found in: Y. Li, PhD Thesis, Ludwigs-Maximilians-Universität München, 2012.

**Scheme 3.8.** Illustration of the mechanism involved in the self-assembly process during thin film liquid deposition techniques, resulting in mesoporous silica structures.<sup>[42]</sup>

This discovery triggered many studies on the synthesis and application of novel mesoporous silica. The key features of this class of materials are tuneable pore sizes and high specific surface areas. Modification of the surface with organic molecules containing functional groups allows the tailor-made design of novel functional materials. Those functional groups can be introduced into the porous system through post-synthesis grafting of the silica surface within the pores. However, this approach automatically leads to reduced pore sizes and surface areas.

If the mesoporous silica is synthesised from bis(trialkoxysilyl) precursors bridged by an organic molecule, the periodic mesoporous organosilica (PMO) is obtained. This new class of organic–inorganic hybrid materials was first reported in 1999.<sup>[13,43,44]</sup> Periodic mesoporous organosilica (PMO) is a class of porous materials possessing accessible mesopores as well as tuneable organic functional pore walls. In the presence of a surfactant template, the condensation of alkoxysilyl precursor  $R'[Si(OR)]_n$  ( $n \geq 2$ ) can lead to a PMO framework with organic linker groups  $R'$  uniformly distributed within the pore walls.<sup>[13,43,44]</sup> The covalent incorporation of organic molecules within the pore walls leaves the pores accessible and thus leads to larger surface areas. However, the synthesis of PMO materials involving large organic linker groups, such as phthalocyanines (Pc), poses challenges.<sup>[45,46]</sup> This issue is due to the fact that alkoxysilane precursors with bulky organic linkers often exhibit low solubility and high hydrolysis rates, thus leading to almost instant precipitation of amorphous material under standard polycondensation conditions.

#### 3.4.2 Synthesis of Functional Phthalocyanine PMO\*

Previously attempts to introduce Pc dyes into a silica matrix exhibiting large mesopores have been reported in literature.<sup>[47,48]</sup> However, in these reported silica matrices, the Pc molecules were either blocking the mesopores or were covalently attached as a layer on the inner surface of the pore channels. In both cases, this resulted in a significantly reduced porosity. Due to these limitations, to date no Pc-based nano structured material has been

---

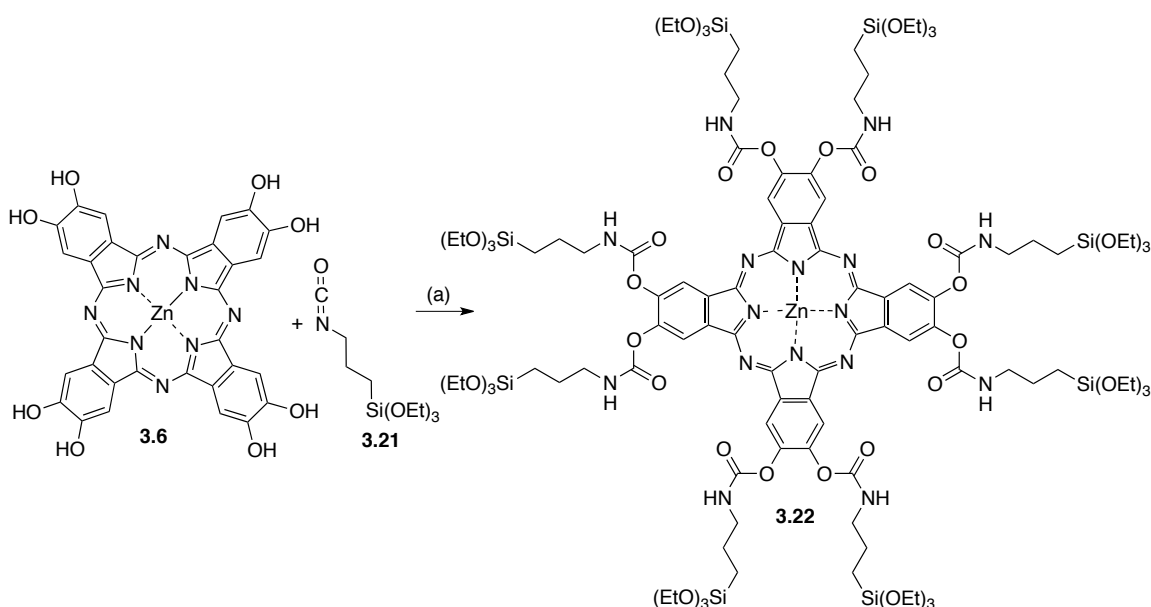
\* Y. Li, F. Löbermann, F. Auras, M. Döblinger, J. Schuster, L. Peters, D. Trauner, T. Bein *manuscript in preparation*.



## CONTRIBUTIONS TO THE CHEMISTRY OF POLYHYDROXYLATED AROMATIC COMPOUNDS

employed in the fabrication of an opto-electronic device. Hence, the goal of this work was to develop a Pc-based organosiloxane precursor that can be employed to synthesise novel PMO materials and apply the obtained nanoscale architecture in the fabrication of photovoltaic devices.

Zincated Pc-OH<sub>8</sub> **3.6** (also see Chapter 3.3.2) was reacted with commercially available isocyanate **3.21** to give Pc-Si precursor **3.22** with eight polar and flexible alkoxysilyl side-chains (Scheme 3.9).



Reagents and conditions: (a) NEt<sub>3</sub>, THF, 18 h, 47% of **3.22**.

**Scheme 3.9.** Synthesis of Pc-Si **3.22** from Pc-OH<sub>8</sub> **3.6** and alkoxysilyl isocyanate **3.21**.

Precursor **3.22** was unstable in solution and polymerisation was observed after a short period of time in various solvents. However, compound **3.22** could be stored as neat material under argon at -20 °C for several days and still give structured material when employed in the PMO synthesis.

The mesostructured Pc-based hybrid material was obtained as a thin film after spin-coating an acidic solution of **3.22**, F108 and 50 wt% solution of tetraethoxysilane in EtOH/THF on flat substrates, followed by slow evaporation of the solvent. Figure 3.10 shows small angle X-ray diffraction (XRD) patterns of the films as prepared containing surfactant (denoted as Pc-Si\_PMO\_ap), films after thermal annealing at 120 °C (denoted as Pc-Si\_PMO\_ta) and after extraction with supercritical CO<sub>2</sub> (denoted as Pc-Si\_PMO\_ex). The reflection observed for Pc-Si\_PMO\_ap material at  $2\theta = 0.76^\circ$  indicates formation of a

periodic mesoporous structure with a d-spacing of 11.6 nm. After annealing at 120 °C for 5 h the d-spacing decreases to 9.2 nm. Removal of the template results in a further contraction of the structure, now featuring a d-spacing of 8.7 nm. The films remained crack-free after these treatments, implying that significant shrinkage only occurred along the substrate normal. This uniaxial shrinking behaviour is commonly observed for mesoporous thin films after template removal.<sup>[45]</sup>

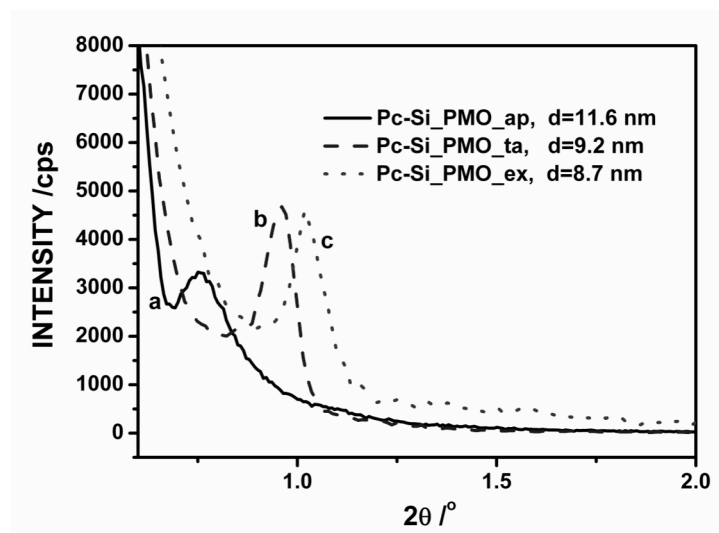


**Figure 3.10.** X-ray diffraction patterns of the Pc-Si-PMO films, (a) as-prepared, (b) after thermal annealing at 120 °C and (c) after extraction with supercritical CO<sub>2</sub>.

Transmission electron microscopy (TEM) cross-sections of the Pc-Si\_PMO\_ex film (Figure 3.11) show the highly ordered structure throughout the film thickness of about 160 nm. The porosity of the extracted material was examined by a nitrogen sorption measurement of films removed from the glass substrate. The Brunauer-Emmett-Teller (BET) surface area calculated from its nitrogen sorption isotherms is 379 m<sup>2</sup> g<sup>-1</sup> and the pore size calculated with non-local density functional theory (NLDFT) indicate mesopores of 17 nm in diameter. Such large diameters allow the incorporation of a broad variety of guest molecules into the PMO mesopores.

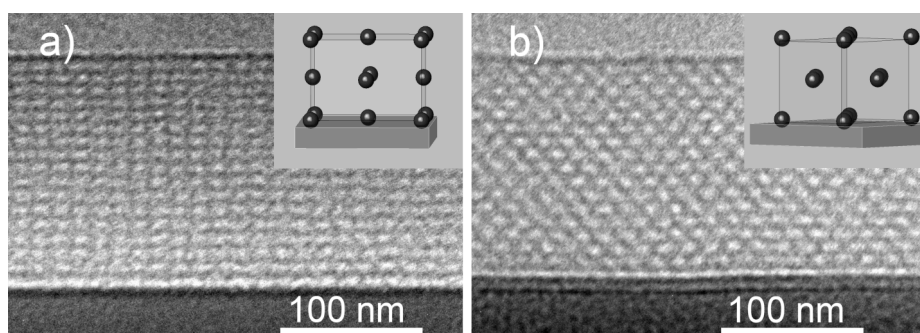


**Figure 3.11.** Cross-section TEM images of Pc-Si\_PMO\_ex film. The insets show the corresponding orientations of the structure model.

To obtain detailed information about the architecture of the PMO framework, the extracted Pc-Si\_PMO material was examined with energy dispersive X-ray spectroscopy (EDXS), electron energy loss spectroscopy (EELS), as well as solid-state NMR spectroscopy of both  $^{13}\text{C}$  and  $^{29}\text{Si}$  nuclei. All these data consistently demonstrate the covalent integration of Pc molecules into the condensed silica walls of the PMO material.\*

With this novel phthalocyanine-based PMO material in hand, its photoactive and electronic properties were investigated by preparing Pc-Si\_PMO\_ex films on indium tin-oxide (ITO) coated glass substrates. In a two-electrode configuration, the sample was connected as working electrode to a Pt counter-electrode in an aqueous electrolyte solution (Figure 3.12).

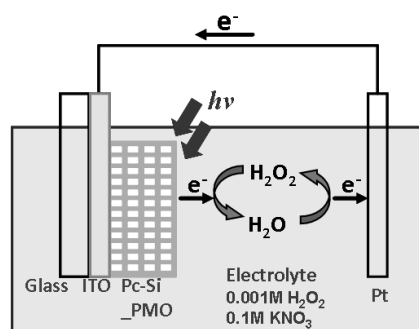


**Figure 3.12.** Illustration of the set-up for photoelectrochemical experiments in aqueous electrolyte solution containing the supporting electrolyte  $\text{KNO}_3$  (100 mM) and the redox-active species  $\text{H}_2\text{O}_2$  (1 mM).

Upon illumination with simulated solar light a current pulse was generated, which quickly decayed to a lower steady-state current (Figure 3.12). Switching off the light resulted in a pulse of similar amplitude, but with opposite sign. The sign of the photocurrent denotes that the Pc-Si\_PMO\_ex is a hole-conducting (p-type) semiconductor. The observed anodic and cathodic current spikes are well known for Pc films in electrolytes and presumably originate from charging and discharging of surface states.<sup>[49,50]</sup> However, such current transient behaviour could also originate from limitations in charge transport within the film. To analyse whether charge transport was restricted in the films, current transients were recorded at various light intensities and subsequently normalized to an intensity of

---

\* For detailed film characterisation data see: Y. Li, PhD Thesis, Ludwig-Maximilians-Universität München, 2012.

100 mW/cm<sup>2</sup> as can be seen in inset of Figure 3.13. These normalized current response curves are congruent with each other, which means that the current response correlates linearly with the light intensity. Hence, it can be deduced that the observed initial decay is a capacitive effect rather than indicative for a current-dependent resistance.

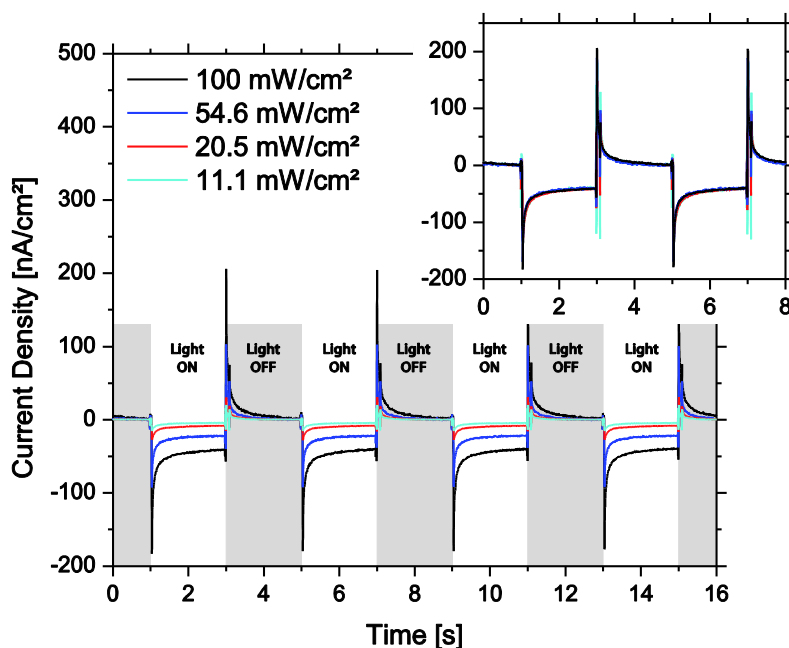


**Figure 3.13.** Time-resolved photocurrent response of the extracted Pc-Si\_PMO\_ex film deposited on ITO in aqueous electrolyte (active surface-area = 1 cm<sup>2</sup>). The experiment was carried out using simulated AM1.5G solar light of different light intensity.

Inset: Photocurrent transients normalized to 100 mW/cm<sup>2</sup> irradiance.

To examine whether the highly ordered PMO architecture can be employed for the construction of a heterojunction enabling light-induced charge separation, an electron-acceptor material was introduced into the mesopores by soaking the Pc-Si\_PMO\_ex film in a [6,6]-phenyl-C<sub>61</sub>-butyric acid methyl ester (PCBM) solution to obtain Pc-Si\_PMO\_PCMBM films. The behaviour of the resulting device was compared to a bilayer set-up, in which the structured PMO film on a ITO substrate was replaced by an amorphous layer of condensed Pc-Si precursor **3.22**, which was subsequently coated with PCBM (Figure 3.14).

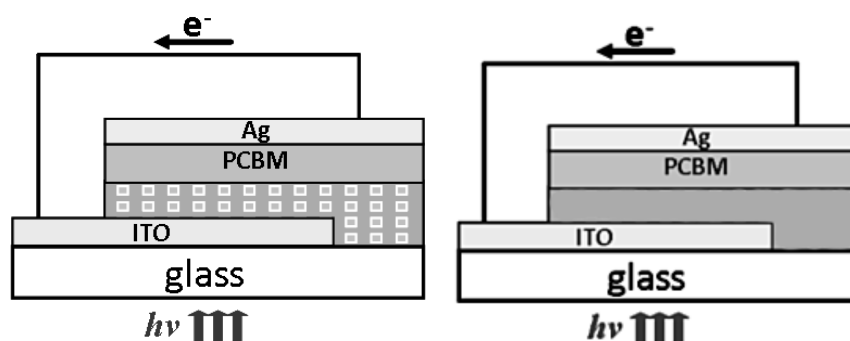


**Figure 3.14.** Illustration of the configuration of the solid-state devices with mesostructured Pc-Si\_PMO\_PCBM film (left) and the bi-layer device with amorphous Pc-Si film (right).

The two devices were irradiated with simulated solar light and the external quantum efficiency (EQE), which is defined as the ratio of collected electrons to incident photons, was measured. The resulting curves for both the mesostructured Pc-Si\_PMO\_PCBM and the amorphous bilayer devices are illustrated in Figure 3.15. The obtained EQE spectrum of the structured device closely resembles the absorption features of the Pc-Si\_PMO film between 550 nm and 750 nm. However, the photocurrent response in the blue and UV part of the spectrum is much higher, which might be due to a contribution of the PCBM to the measured EQE. The observed photocurrent seems to be a superposition of (i) excitons generated in the Pc-Si\_PMO film followed by electron injection into the PCBM, and (ii) excitons generated upon light absorption by the PCBM followed by hole injection into the Pc-Si\_PMO. Interestingly, the EQE of the mesostructured, but otherwise identical device is more than one order of magnitude higher than that of the amorphous counterpart (note that in Figure 3.14 the response of the amorphous device was multiplied by factor ten for clarity). This data suggests that only excitons generated in the vicinity of the heterojunction can diffuse to the interface and get separated. In case of the amorphous device, the heterojunction is flat and only allows charge separation on a small surface area, resulting in a relatively low measured current. The mesoporous architecture exhibits a much larger surface area due to its 3D heterojunction. Hence, photo-generated excitons from a larger volume can be harvested. Consequently the mesostructured device generates a much higher photocurrent than its amorphous counterpart.

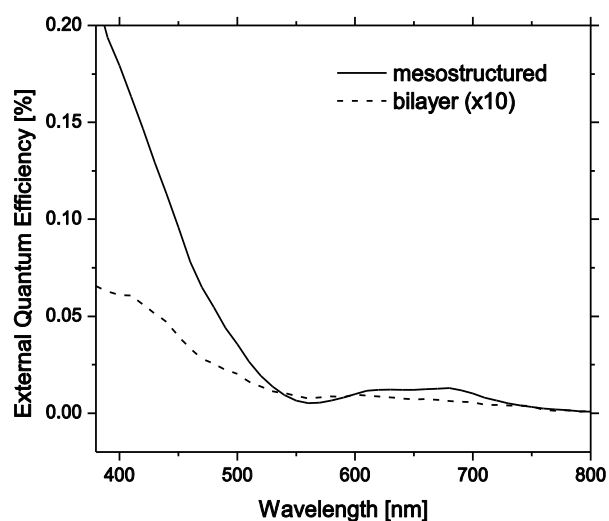


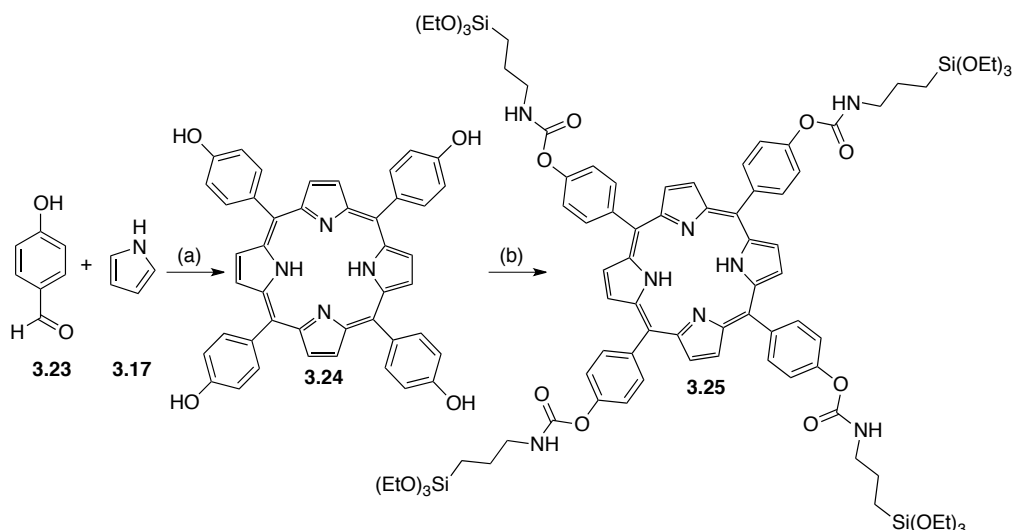
**Figure 3.15.** External quantum efficiency of the mesostructured Pc-Si\_PMO/PCBM device in comparison to that of a non-porous bilayer counterpart. The EQE of the bilayer device was multiplied by a factor of ten for better visibility.

In conclusion, the first periodic mesoporous organosilica film material with phthalocyanine dyes incorporated into the silica pore walls was successfully synthesized. Moreover, the Pc-Si\_PMO\_ex film showed light-induced charge generation and p-type semiconducting properties. These experiments showed that phthalocyanine-based PMO frameworks could serve as a platform to further explore the new field of ordered device architectures in organic photovoltaics. The photovoltaic devices obtained from the mesostructured thin films were shown to exhibit much higher external quantum efficiencies in comparison to their bilayer counterparts. Hence, a three-dimensional interpenetrating heterojunction based on the mesoporous Pc-Si\_PMO framework and PCBM can collect charges from a much larger volume and consequently produce a more than ten-fold increased photocurrent. However, overall efficiency and measured EQE is still relatively low, when compared to state of the art OPVs. This might be due to the fact that a large amount of TEOS had to be added to precursor **3.22** to obtain a mesostructured material. The auxiliary TEOS required in this case for the formation of a porous structure presumably gave rise to insulating silica domains and thus decreased the conductivity. The Pc-PMO precursor needs to be redesigned in a way that a PMO structure can be obtained without the addition of auxiliary silica sources. This would enable a better  $\pi$ - $\pi$  stacking of the Pc macrocycles and result in an improved semicrystallinity of the material and thus enhance the opto-electronic properties.

### 3.4.3 Synthesis of a Porphyrin-based 3D Donor-Acceptor Interpenetrating System\*

Porphyrin molecules are well known to possess suitable electrical and optical properties, the integration of porphyrin units into organosilica frameworks should lead to novel PMO materials with promising optoelectronic activities. However, as it was shown in Chapter 3.4.2, alkoxy-silyl precursors with large organic bridges are not easily incorporated into periodic mesostructures. The introduction of a large phthalocyanine-based organosilica precursor into a PMO framework was only achieved upon the addition of an auxiliary silica source, in this case TEOS, which ultimately resulted in relatively low measured EQE. This challenge might be overcome by designing a less flexible organic linker, which can undergo  $\pi$ - $\pi$  stacking within the pore walls to give a material with improved charge carrier conductivity. Reducing the amount of linkers attached to the core from eight to four could very well result in an improved PMO material.

When refluxing a mixture of 4-hydroxybenzaldehyde (**3.23**) and pyrrole (**3.17**) in propionic acid *meso*-tetra(*p*-hydroxy)phenyl porphyrin (**3.24**) was obtained as a purple solid in good yield.<sup>[51]</sup> Porphyrin **3.24** was then reacted with isocyanate **3.21** to give porphyrin-based PMO precursor **3.25**.<sup>[46]</sup>



\* Y. Li, F. Löbermann, F. Auras, M. Döblinger, J. Schuster, L. Peters, D. Trauner, T. Bein *manuscript in preparation*.

Reagents and conditions: (a) propionic acid, reflux, 39% of **3.24** (b)  $\text{NEt}_3$ , **3.21**, THF, 80 °C, 4h, 40% of **3.25**.

**Scheme 3.10.** Synthesis of porphyrin-based precursor **3.25** from **3.24** and alkoxysilyl isocyanate **3.21**.

The porphyrin-based PMO films were synthesized by the evaporation-induced self-assembly (EISA) approach.<sup>[52]</sup> The mesostructured Por-PMO was obtained as a thin film after spin-coating an acidic solution of the silane precursor **3.25** and block co-polymer F127 in EtOH on flat glass substrates, followed by slow evaporation of the solvent. Figure 3.16 shows the XRD patterns of (a) the as-prepared PMO film (containing the template and denoted as Por-PMO-as prepared), (b) the film after thermal annealing at 120 °C (denoted as Por-PMO-120 °C) and (c) the film after solvent extraction (denoted as Por-PMO-ex). The “Por-PMO-as prepared” gives a diffraction peak at  $2\theta = 0.86^\circ$ , indicating the formation of a periodic mesostructure with a d-spacing of 10.2 nm. After a thermal treatment, followed by solvent extraction, the diffraction peaks are shifted to  $0.92^\circ$  and  $1.33^\circ$ , respectively, corresponding to d-spacings of 9.5 and 6.6 nm. The decreased d-spacings indicate film shrinkage along the direction normal to the substrate, which is commonly observed for mesoporous thin films after template removal, as also observed in the case of Pc-Si-PMO (Figure 3.9).

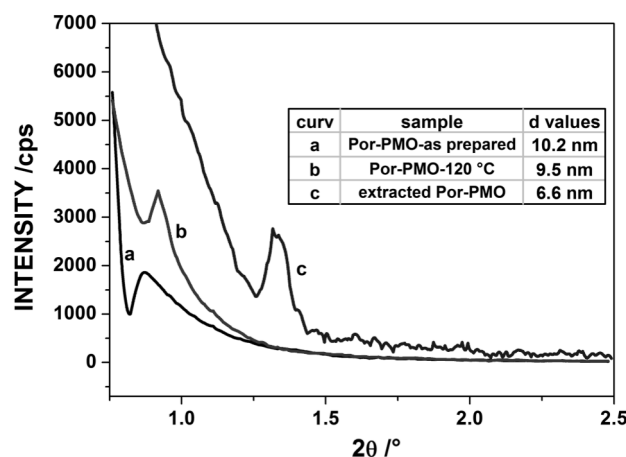


**Figure 3.16.** Small-angle X-ray diffractograms of the Por-PMO films, (a) as prepared, (b) after thermal treatment at 120 °C for 5 hours, (c) after extraction with ethanol. The intensity of the SAXS pattern for the extracted Por-PMO film was multiplied by two for better visibility.

Figure 3.17 shows a representative transmission electron micrograph of the Por-PMO film after solvent extraction. In the plan-view image, the periodic mesostructure of the Por-PMO film can be observed with domain sizes in the range of hundreds of nanometres. The presence of ordered domains in the TEM images confirms that the mesostructure is



preserved after removal of surfactant template and that it is also stable against electron-beam damage during TEM characterisation.

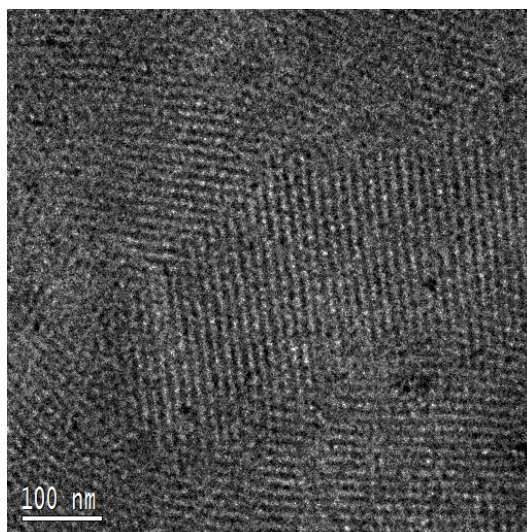


**Figure 3.17.** Plan-view TEM image of the extracted Por-PMO film.

To obtain detailed information about the architecture of the PMO framework, the extracted Por-Si\_PMO material was examined with energy nitrogen sorption measurements, as well as solid-state NMR spectroscopy of both  $^{13}\text{C}$  and  $^{29}\text{Si}$  nuclei. All these data consistently demonstrate the covalent integration of porphyrin molecules into the condensed silica pore walls of the PMO material with pore sizes in the range of 15 nm.

In order to investigate the photoactive and electronic properties of the extracted Por-PMO, films with 220 nm thickness were deposited on ITO-coated glass substrates through spin coating. The set-up of the time-resolved photocurrent response and the spectrally resolved response measurements in an aqueous electrolyte is shown in Figure 3.18.

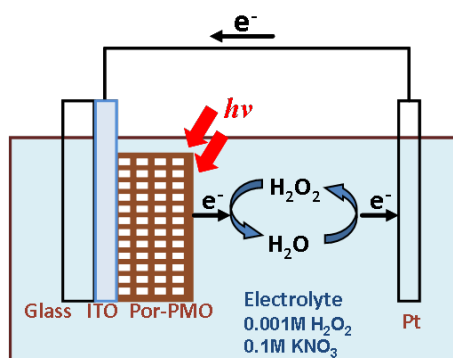


**Figure 3.18.** Illustration of the set up for photo electrochemical experiments in electrolyte containing 0.1 M  $\text{KNO}_3$  and 1 mM  $\text{H}_2\text{O}_2$ .

Current transients were recorded at different intensities of simulated solar light (Figure 3.19A). Observations made are very similar to those previously reported in Chapter 3.4.2. A current pulse is generated upon illumination and quickly decays to a lower steady-state current. A pulse of similar amplitude with opposite sign is observed when switching off the light. These observed anodic and cathodic current spikes are well known for films of organic semiconductors in electrolytes and could originate from charging and discharging of surface states.<sup>[50]</sup> The sign of the photocurrent identifies the Por-PMO film as a p-type semiconductor, indicating that electron–hole pairs are generated upon illumination and the electrons are transferred to the electrolyte, whereas the holes are transported within the Por-PMO film.

The photocurrent excitation spectrum was recorded under short circuit conditions (Figure 3.19B, dashed line). At wavelengths longer than 500 nm, the spectrum of external quantum efficiency (EQE), which is the ratio of collected electrons to incident photons, closely resembles the absorbance spectrum of the Por-PMO film. However, at the position of the Soret absorption band, the EQE is unexpectedly low. A possible explanation is that at around 420 nm the absorbance of the PMO material is far higher than at longer wavelengths, thus leading to absorption of incident photons mainly within a thin surface layer and scarcely in the material underneath. In contrast, at longer wavelengths the light intensity does not vary dramatically through the depth of the film and thus the PMO material over the entire film thickness can be activated by absorbing photons, such that the current output seems to be more favourable in the case that the whole film absorbs light.

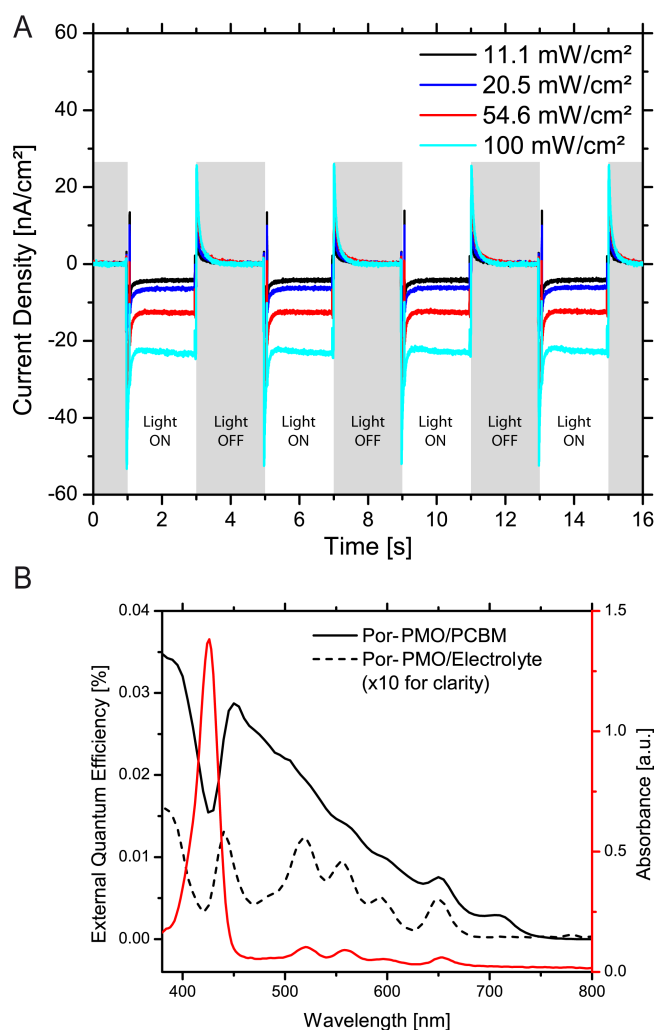


**Figure 3.19.** A) Time-resolved photocurrent response of the extracted Por-PMO film deposited on ITO in an aqueous electrolyte; simulated AM1.5G solar light of different light intensity. B) External quantum efficiency of a Por-PMO film in the electrolyte and of the Por-PMO/PCBM solid-state device, and UV-Vis spectrum of a Por-PMO film. The spectrum measured in the electrolyte was multiplied by ten for clarity.

Next the hole-transporting Por-PMO film was combined with an electron acceptor to form a three-dimensional solid-state heterojunction by soaking the extracted mesoporous film in a solution of PCBM for infiltration of the electron-transporting species into the mesopores. Subsequent spin-coating with the PCBM solution results in an additional PCBM overlayer, which is required for avoiding contact between the Ag back electrode and the hole-transporting material (configuration of the device illustrated in Figure 3.20).

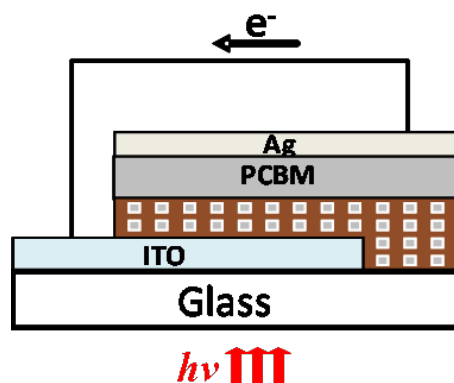


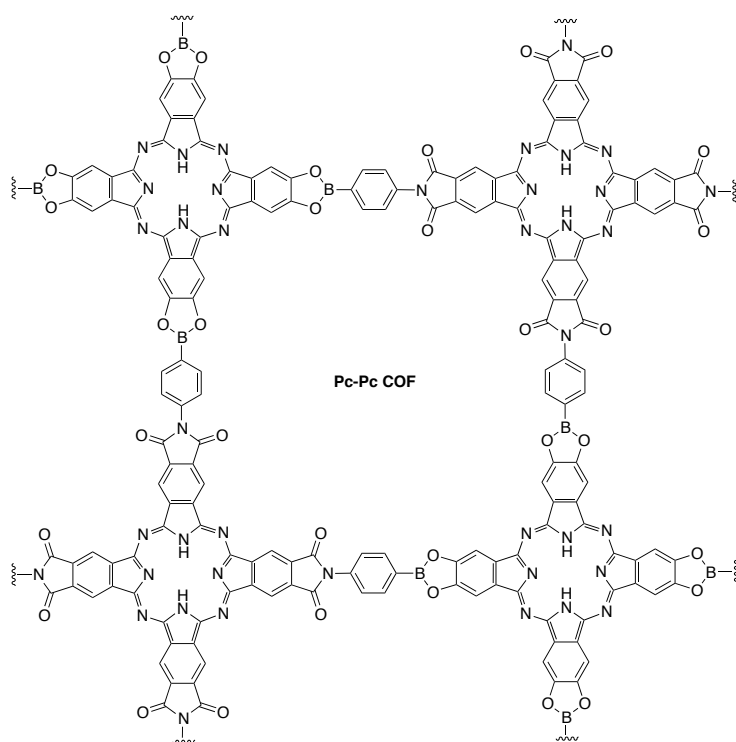
**Figure 3.20.** Illustration of the configuration of the solid-state device based on the mesostructured PMO film. The porous layer on the surface of ITO represents the Por-PMO film.

The external quantum efficiency spectrum of the device follows the absorbance spectrum of the Por-PMO film (Figure 3.18B, solid line). Compared to the measurements in electrolyte, the photocurrent response in the blue and UV part of the spectrum is much higher, which might be due to additional contribution from the PCBM. The observed photocurrent appears to be a superposition of contributions from dissociation of excitons generated in the Por-PMO followed by electron injection into the PCBM, and of excitons generated upon light absorption by the PCBM followed by hole injection into the Por-PMO. As observed for the liquid electrolyte contact, the photocurrent generated at the strong absorption peak of the porphyrin framework is lower than at longer wavelengths. At around 420 nm, since the illumination is through the ITO substrate in this case, most excitons are created close to the contacts and the electrons in PCBM have to diffuse a long way through the interpenetrating networks and might eventually recombine with holes in the PMO film before being collected by the Ag contact. Again, the more uniform charge generation throughout the entire film seems to be more favorable for current output.

In conclusion, a novel periodic mesoporous organosilica film material was successfully synthesized by polycondensation of a porphyrin-containing organosilane precursor in the presence of surfactant template. The resulting PMO film possesses a three-dimensional mesostructure with a large pore size. This architecture allowed the fabrication of a functional device through the incorporation of PCBM as an electron-transporting phase. The optoelectronic measurements showed evidence of light-induced charge generation and hole-conductivity in the PMO material.

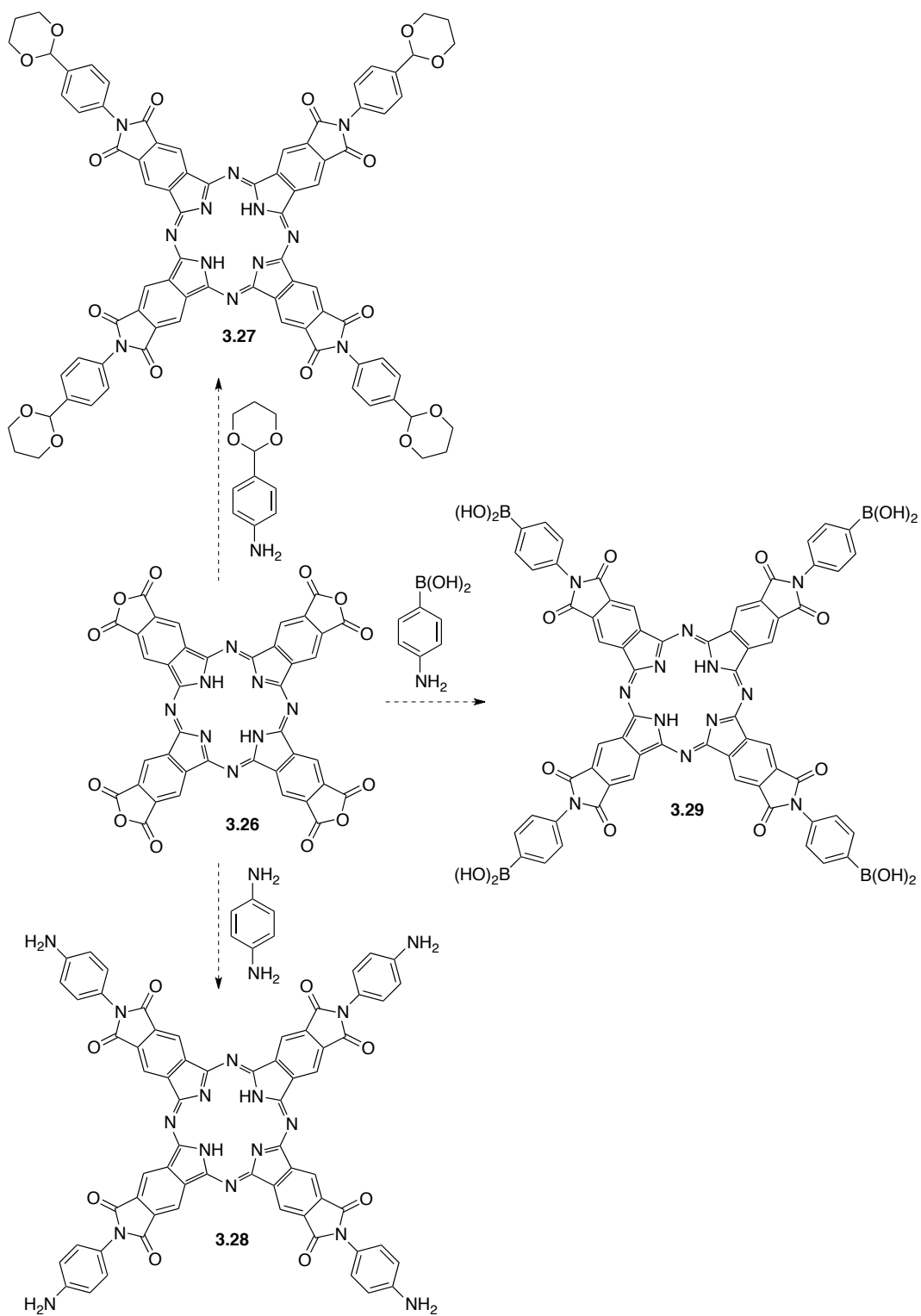
### 3.5 Summary and Outlook\*

Although until now it was not possible to cross-link boronic acid **3.13** with phthalocyanine **3.7** to a COF structure, efforts are still underway. However, it might be necessary consider an alternate synthetic strategy if the formation of the boronate-based COF materials continues fail. A possible solution to achieve COF frameworks would be to employ imine formation as the cross-linking reaction. In order to achieve this, the phthalocyanine precursor needs to be redesigned in a way that allows the incorporation of an aniline or aldehyde functionality while retaining the required symmetry. A potential starting material for this new class of phthalocyanine-based linkers would be literature-known octa-4,5-carboxyphthalocyanine tetraanhydride (**3.26**) (Scheme 3.11).<sup>[53]</sup> This starting material can be prepared in large quantities and it could be used as a platform to obtain both functionalities, aldehyde **3.27** and aniline **3.28**, required for imine-COF formation. Alternatively this approach could also be used to obtain the corresponding boronic acid **3.29**. Hence, broader platform towards Pc-based COF materials can be established. For example, this strategy would allow access to a COF, consisting only of Pc building blocks (Figure 3.20).




---

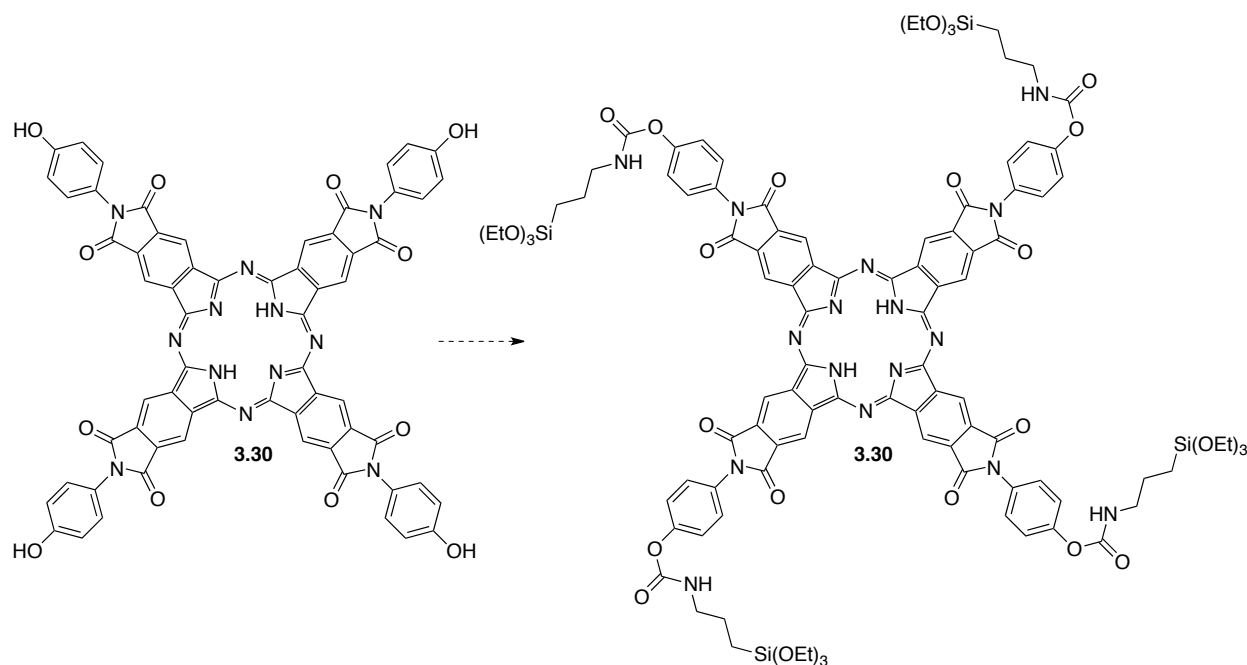
\* Outlook developed together with L. S.

**Figure 3.21.** Illustration of a Pc-Pc COF.**Scheme 3.11.** Synthetic strategy for alternative phthalocyanine precursors 3.27, 3.28 and 3.29.

## CONTRIBUTIONS TO THE CHEMISTRY OF POLYHYDROXYLATED AROMATIC COMPOUNDS

Two novel functional PMO materials, based on Pc and porphyrin precursors, have successfully been synthesised through a evaporation induced self-assembly process. Optoelectronic measurements on this interpenetrating donor-acceptor system unfolded the light-induced charge generation capability and hole-conducting property of the novel PMO films. Those promising results underline the potential of PMO materials for the development of next-generation organic photovoltaic devices.

However, in the case of the Pc-based PMO material, structure could only be obtained after addition of auxiliary silica sources, such as TEOS. Therefore this material is not a material purely based on organic linkers. The additional inorganic silica might form insulating silica domains and thus reducing the effectiveness of the devices fabricated from such precursors. By designing a more rigid PMO precursor, it might be possible to only incorporate organic molecules into the pore walls. Reducing the number of side-chains attached to the phthalocyanine from eight to four, could achieve this task. Scheme 3.12 illustrates the potential synthesis of a Pc-based siloxane precursor **3.30** with only four side-chains attached. Phenol **3.31** could also be derived from tetra-anhydride **3.26**.



**Scheme 3.12.** Synthetic strategy for a more rigid phthalocyanine-based PMO precursor **3.30**.

## 3.6 Experimental Section

### 3.6.1 General Experimental Details

**Chemicals and chromatography.** Unless otherwise noted, all reagents were purchased from commercial suppliers and used without further purification. Unless otherwise noted, all reaction mixtures were magnetically stirred in oven-dried glassware under a blanket of argon. External bath temperatures were used to record all reaction mixture temperatures. Analytical thin layer chromatography (TLC) was carried out on Merck silica gel 60 F<sub>254</sub> TLC plates. TLC visualisation was accomplished using 254 nm UV light or charring solutions of KMnO<sub>4</sub> and ceric ammonium molybdenate. All organic extracts were washed with brine, dried over sodium sulfate and filtered; solvents were then removed with a rotary evaporator at aspirator pressure. Flash chromatography was performed on Merck KGaA Geduran<sup>®</sup> Silica Gel (40–63 μm particle size) using a forced flow of eluent at 1.3–1.5 bar pressure. Yields refer to chromatographically and spectroscopically (<sup>1</sup>H NMR and <sup>13</sup>C NMR) homogenous material.

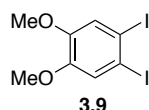
**NMR spectroscopy.** NMR spectra were recorded on Bruker AC 300, WH 400, or AMX 600 instruments (operating at 300 MHz, 400 MHz and 600 MHz for proton nuclei and 75 MHz, 100 MHz, 150 MHz for carbon nuclei respectively). Chemical shifts are reported in ppm with the solvent resonance employed as the internal standard (CDCl<sub>3</sub> at 7.26 and 77.0 ppm; DMSO at 2.50 and 39.5 ppm). Additionally to standard <sup>1</sup>H and <sup>13</sup>C NMR measurements, 2D NMR techniques such as homonuclear correlation spectroscopy (COSY), heteronuclear single quantum coherence (HSQC) and heteronuclear multiple bond coherence (HMBC) was used to assign signals. The following abbreviations are used to explain the multiplicities: s = singlet, d = doublet, t = triplet, q = quartet, m = multiplet, br = broad.

**IR spectroscopy.** IR spectra were recorded 4000–400 cm<sup>-1</sup> on a Perkin Elmer Spectrometer BY FT-IR-System with a Smith Dura sample IR II ATR-unit. Samples were measured as neat materials (neat). The absorption bands are reported in wave numbers (cm<sup>-1</sup>).

**Mass spectroscopy.** Mass spectra were recorded on a Varian MAT CH 7A for electron impact ionisation (EI) and high resolution mass spectra (HRMS) on a Varian MAT 711 spectrometer.

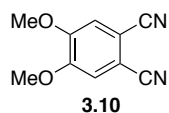


### 3.6.2 Towards Novel Electroactive Covalent Organic Frameworks



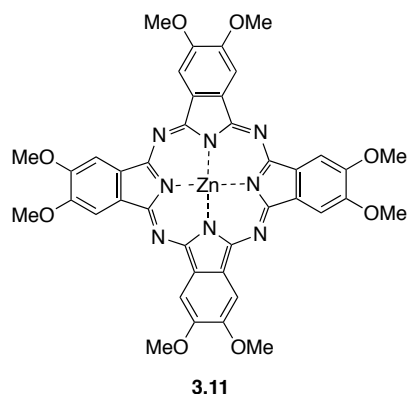
**1,2-diiodo-4,5-dimethoxybenzene (3.9).**<sup>[30]</sup> Periodic acid (8.59 g, 37.7 mmol, 0.4 *eq.*) was stirred in MeOH (60 mL) at room temperature for ca. 20 min. Now iodine (19.84 g, 78.2 mmol, 0.83 *eq.*) was added and the mixture stirred for an additional 10 min. After addition of veratrole (13.02 g, 94.2 mmol, 1.0 *eq.*) the reaction mixture was heated to reflux for 4h, upon which the dark color disappeared. The Reaction mixture was now poured into a diluted sodium pyrosulfite solution (150 mL) and the resulting colorless precipitate was filtered off, dried under high-vacuum to yield 33.5 g (91%) of a **3.9** colorless solid.

**Data for 3.9:** <sup>1</sup>H NMR (300 MHz, CDCl<sub>3</sub>): δ = (400 MHz, CDCl<sub>3</sub>): δ = 7.21 (s, 2H), 3.81 (s, 6H); <sup>13</sup>C NMR (100 MHz, CDCl<sub>3</sub>): δ = 149.6, 121.6, 96.0, 56.1; HRMS (EI) calcd. for C<sub>8</sub>H<sub>8</sub>I<sub>2</sub>O<sub>2</sub> (M<sup>+</sup>): 389.8614; found 389.8621.



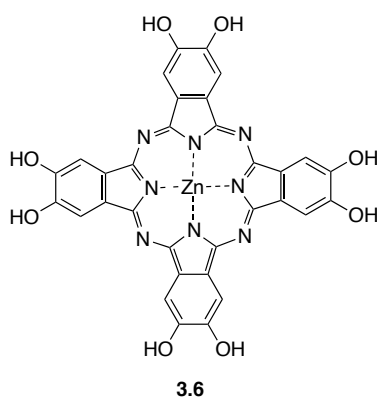
**4,5-dimethoxyphthalonitrile (3.10).** 1,2-Diiodo-4,5-dimethoxybenzene (**3.9**) (5.92 g, 20 mmol, 1.0 *eq.*) and tetrakis(triphenylphosphin)palladium (6.93 g, 6.0 mmol, 0.3 *eq.*) were dissolved in dry DMF (40 mL). After addition of zinc cyanide (5.64 g, 48 mmol, 2.4 *eq.*) the reaction mixture was heated to 90 °C for 2 h. The solution was treated with 25% ammonia (100 mL) after cooling to *rt.* and filtered over a porous glass-filter (pore size 3). The filter cake was washed with additional ammonia (200 mL). All soluble were dissolved in EtOAc (300 mL) and filtered off. The organic phase was dried, filtered and concentrated. The remaining pink solid was purified by silica gel chromatography (33% EtOAc in hexanes) to yield 2.9 g (77%) of title compound **3.10** as colourless solid.

**Data for 3.10:** IR (ATR):  $\tilde{\nu} = 3124, 3068, 2940, 2225, 1742, 1590, 1563, 1517, 1473, 1459, 1449, 1445, 1358, 1292, 1218, 1090, 1018, 984, 972, 879, 866, 829$ ;  $^1\text{H NMR}$  (400 MHz,  $\text{CDCl}_3$ ):  $\delta = 7.21$  (s, 2H), 4.02 (s, 6H);  $^{13}\text{C NMR}$  (75 MHz,  $\text{CDCl}_3$ )  $\delta = 152.6, 115.7, 114.8, 109.0, 56.6$ ; HRMS (EI) calcd. for  $\text{C}_{10}\text{H}_8\text{N}_2\text{O}_2$  ( $\text{M}^+$ ): 188.0586; found 188.0610.



**Zinc-octamethoxyphthalocyanine (3.11).** To a solution of zinc(II)chloride (0.274 g, 2.0 mmol, 0.25 *eq.*), 4,5-dimethoxyphthalonitrile (**3.10**) (1.49 g, 7.9 mmol, 1.0 *eq.*) and urea (0.474 g, 7.9 mmol, 1.0 *eq.*) in ethylene glycol (24 mL) was added a spatula tip of ammonium molybdate. The mixture was heated in a sealed tube to 170 °C under stirring over night. The dark green reaction mixture was diluted with water (50 mL) and centrifuged to obtain a dark green, waxy solid. The precipitate was washed with acetone and dried on air over night. The dark powder was now washed with DMSO, followed by acetone to yield 1.41 g (87%) of zinc-octamethoxyphthalocyanine (**3.11**) as a dark green solid.

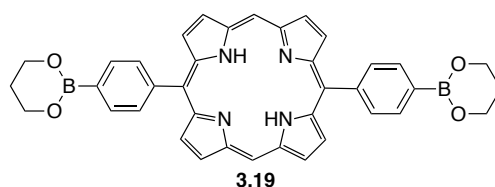
**Data for 3.11:** IR (ATR):  $\tilde{\nu} = 3364$  (br), 3006 (w), 2936 (w), 2218 (w), 1600 (m), 1494 (s), 1476 (s), 1393 (s), 1276 (s), 1205 (s), 1099 (m), 1052 (s), 876 (m), 847 (m), 741 (m);  $^1\text{H NMR}$  (200 MHz,  $\text{DMSO}-d_6$ ):  $\delta = 7.29$  (s, 8H), 3.88 (s, 24H); MS (EI) calcd. for  $\text{C}_{40}\text{H}_{32}\text{N}_8\text{O}_8\text{Zn}$  ( $\text{M}^+$ ): 816.1635; found: 816.1622.



## CONTRIBUTIONS TO THE CHEMISTRY OF POLYHYDROXYLATED AROMATIC COMPOUNDS

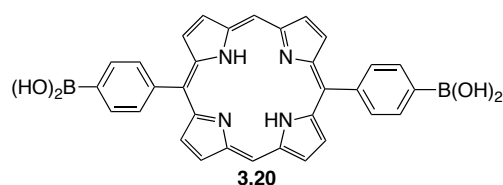
**Zinc-octahydroxyphthalocyanine (3.6).** To a suspension of **3.11** (818 mg, 1.0 mmol, 1.0 *eq.*) in dry CH<sub>2</sub>Cl<sub>2</sub> (20 mL) was added a 1.0 M solution of boron tribromide in CH<sub>2</sub>Cl<sub>2</sub> (40 mL, 40 mmol, 40 *eq.*) drop wise at 0°C. The reaction mixture was stirred at rt for 5 days and subsequently treated with MeOH (200 mL) at 0°C. All volatiles were removed *in vacuo* and the resulting dark solid was suspended in MeOH (100 mL) and centrifuged. The precipitate was filtered off, washed with MeOH and dried *in vacuo* to yield 530 mg (75%) of title compound **3.6**.

**Data for 3.6:** IR (ATR):  $\tilde{\nu}$  = 3196 (br), 2361 (s), 2342 (s), 1647 (m), 1603 (m), 1476 (s), 1380 (br), 1288 (s), 1170 (w), 1087 (m), 1033 (m), 827 (w); MS (EI) calcd for C<sub>32</sub>H<sub>16</sub>N<sub>8</sub>O<sub>8</sub>Zn (M<sup>+</sup>): 704.0383; found 704.0486.



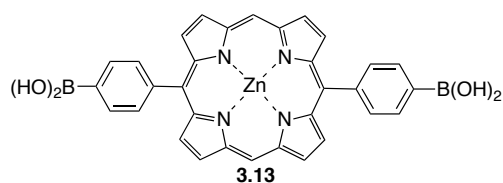
**Porphyrin 3.19.** Dipyrrromethane (1.022 g, 6.99 mmol) and benzaldehyde **3.15** (1.311 g, 6.90 mmol) were dissolved in anhydrous CHCl<sub>3</sub> (700 mL) under Ar, and the mixture degassed with Ar for 15 min. The reaction mixture was cooled to 0 °C, BF<sub>3</sub>·OEt<sub>2</sub> (200 μL, 1.58 mmol) was added drop wise, and the mixture was stirred for 3 h at rt. Then, DDQ (2.452 g, 10.8 mmol) was added in one portion, and the mixture stirred overnight at rt. The mixture was filtered over celite, and poured on to a column of silica (CH<sub>2</sub>Cl<sub>2</sub>; elution CH<sub>2</sub>Cl<sub>2</sub>/MeOH 100:1). The collected purple solid was recrystallized twice from CHCl<sub>3</sub> to give **3.19** (478 mg, 22%) as a dark purple solid.

**Data for 3.19:** IR (ATR):  $\tilde{\nu}$  = 2935, 2884, 1603, 1579, 1546, 1478, 1417, 1389, 1334, 1302, 1272, 1209, 1150, 1123, 1053, 1005, 992, 986, 972, 955, 864, 855, 795, 751, 735, 718, 693, 664; R<sub>f</sub> = 0.44 (CH<sub>2</sub>Cl<sub>2</sub>/MeOH 95:5); <sup>1</sup>H NMR (600 MHz, CDCl<sub>3</sub>)  $\delta$  = 10.31 (s, 2H), 9.39 (d, J = 4.5 Hz, 4H), 9.07 (d, J = 4.5 Hz, 4H), 8.21–8.28 (m, 8H), 4.37 (t, J = 5.6 Hz, 8H), 2.25 (quintett 145.3, 143.7, 134.5, 132.4, 131.7, 131.2, 119.4, 105.4, 62.4, 27.8; MS (EI) calcd for: C<sub>38</sub>H<sub>32</sub>B<sub>2</sub>N<sub>4</sub>O<sub>4</sub>(M<sup>+</sup>): 630.2613; found: 630.2610.



**Porphyrin bisboronic acid 3.20.** Porphyrin **3.19** (630 mg, 1.0 mmol, 1.0 *eq.*) was dissolved in THF (400 mL) and aqueous HCl (400 mL, pH = 1). The mixture was stirred at rt for 18 h and subsequently diluted with CH<sub>2</sub>Cl<sub>2</sub> (400 mL) and sat. NaHCO<sub>3</sub> (100 mL). The organic phase was separated and poured into hexanes (600 mL). The resulting precipitate was collected, dissolved in acetone, dried over Na<sub>2</sub>SO<sub>4</sub> and concentrated to yield 485 mg (88%) of title compound **3.20** as a purple solid.

**Data for 3.20:** IR (ATR):  $\tilde{\nu}$  = 3282, 1604, 1577, 1471, 1395, 1321, 1236, 1197, 1145, 1103, 1008, 973, 954, 850, 786, 745, 732, 718, 688; <sup>1</sup>H NMR (400 MHz, THF-*d*<sub>6</sub>)  $\delta$  = 10.41 (s, 2H), 9.46 (d, *J* = 4.6, 4H), 9.01 (d, *J* = 4.6, 4H), 8.28 (s, 4H), 8.19 (s, 4H); <sup>13</sup>C NMR (100 MHz, THF-*d*<sub>6</sub>)  $\delta$  = 142.82, 133.81, 132.81, 131.60, 130.45, 119.00, 105.05, 48.48; HRMS (ESI) calcd for C<sub>32</sub>H<sub>25</sub>B<sub>2</sub>N<sub>4</sub>O<sub>4</sub> (M+H<sup>+</sup>): 551.2057; found: 551.2048.

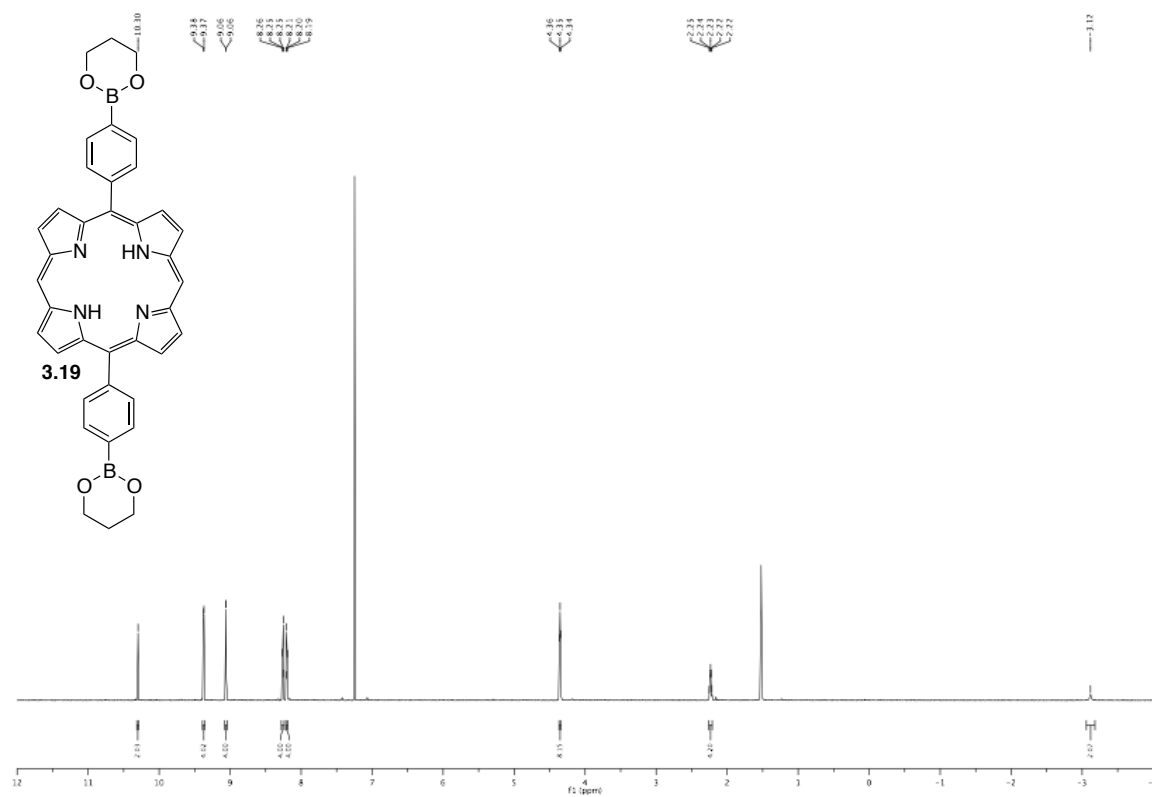


**Zincated Porphyrin Bisboronic Acid (3.13).** Porphyrin **3.20** (440 mg, 0.8 mmol, 1.0 *eq.*) was dissolved in THF (300 mL). To the solution was added a solution of Zn(OAc)<sub>2</sub> (294 mg, 1.6 mmol, 2.0 *eq.*) in MeOH (300 mL). The reaction mixture was stirred at rt for 18 h and then diluted with CHCl<sub>3</sub> (500 mL). The organic phase was dried over Na<sub>2</sub>SO<sub>4</sub> and concentrated to yield 490 mg (99%) of porphyrin **3.13** as a purple solid.

**Data of 3.13:** IR (ATR):  $\tilde{\nu}$  = 3327, 2976, 1704, 1601, 1547, 1520, 1476, 1394, 1335, 1315, 1212, 1192, 1145, 1104, 1063, 1010, 990; <sup>1</sup>H NMR (400 MHz, acetone-*d*<sub>6</sub>)  $\delta$  = 10.30 (s, 2H), 9.43 (d, *J*=4.5, 4H), 8.97 (d, *J*=4.4, 4H), 8.32 – 8.26 (m, 4H), 8.23 – 8.18 (m, 4H); <sup>13</sup>C NMR (100 MHz, acetone-*d*<sub>6</sub>)  $\delta$  = 149.65, 149.44, 145.19, 133.98, 132.39, 131.66, 119.29, 105.81, 48.59; HRMS (ESI) calcd for C<sub>32</sub>H<sub>23</sub>B<sub>2</sub>N<sub>4</sub>O<sub>4</sub>Zn (M+H<sup>+</sup>): 613.1191; found: 613.1191.

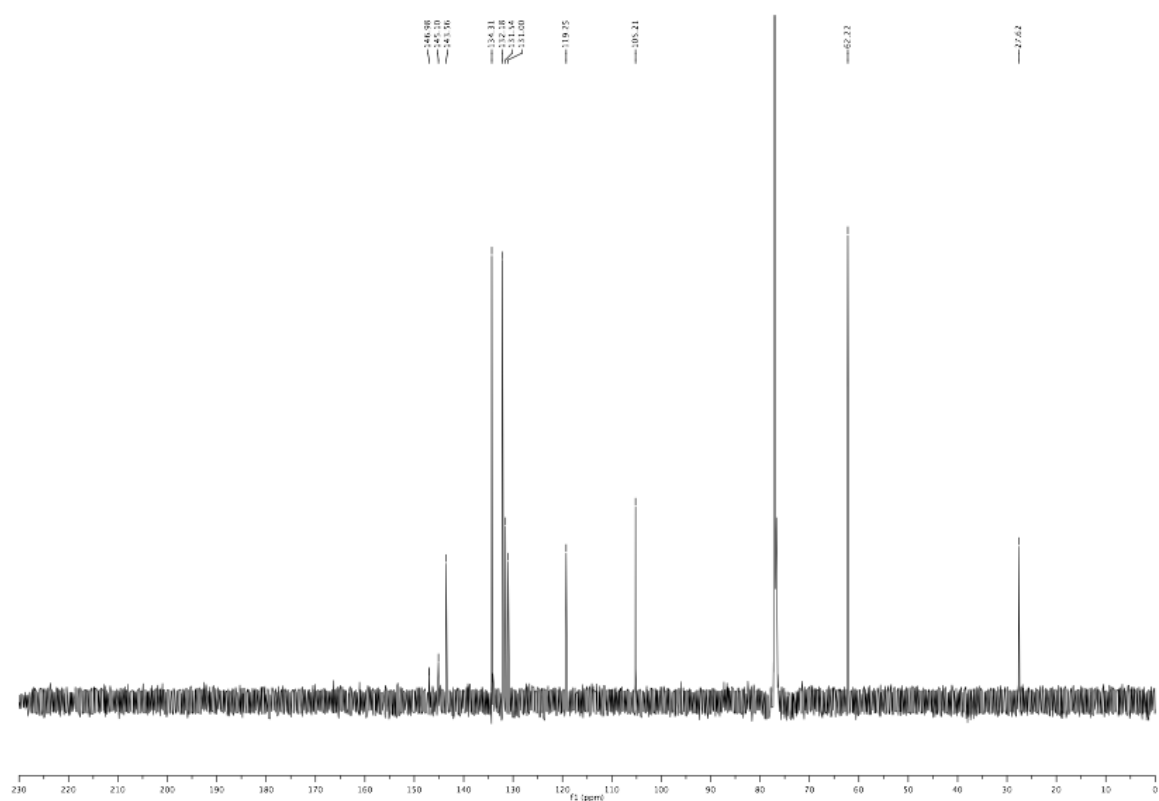
# CONTRIBUTIONS TO THE CHEMISTRY OF POLYHYDROXYLATED AROMATIC COMPOUNDS

$^1\text{H}$  NMR,  $\text{THF-}d_8$ , 400 MHz

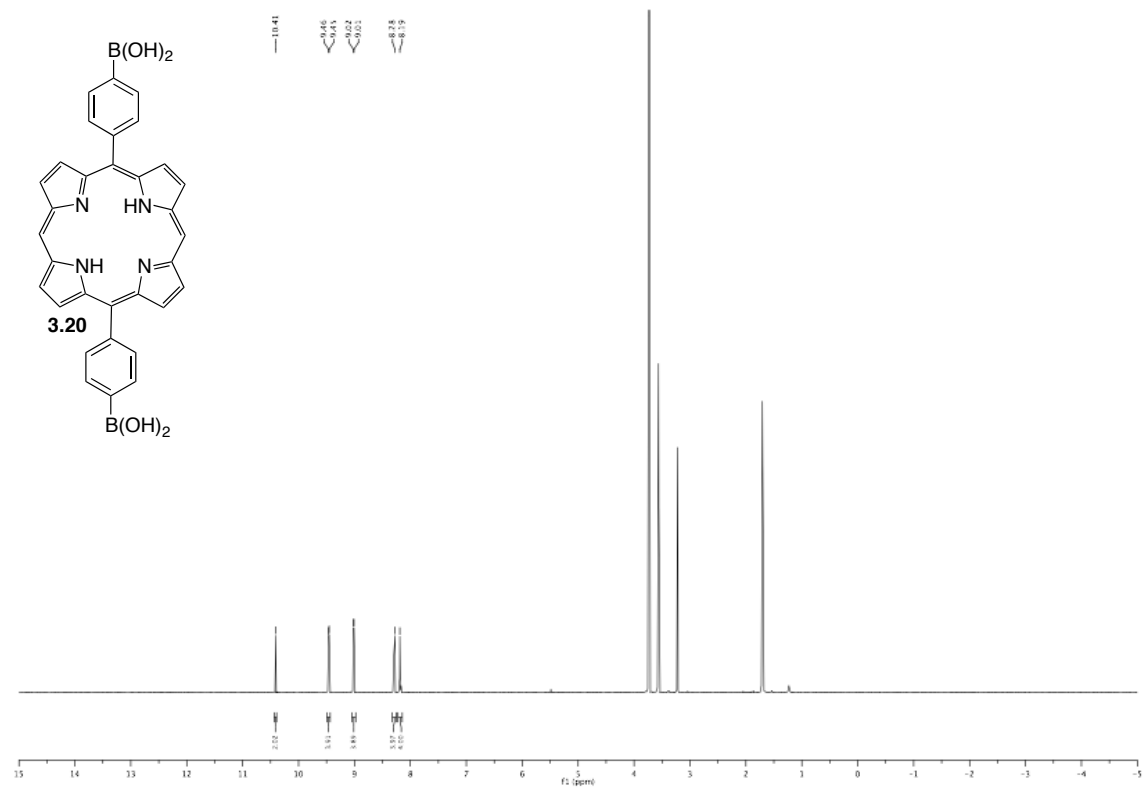


$^{13}\text{C}$  NMR,  $\text{THF-}d_8$ , 100 MHz

### 3.6. Experimental Section

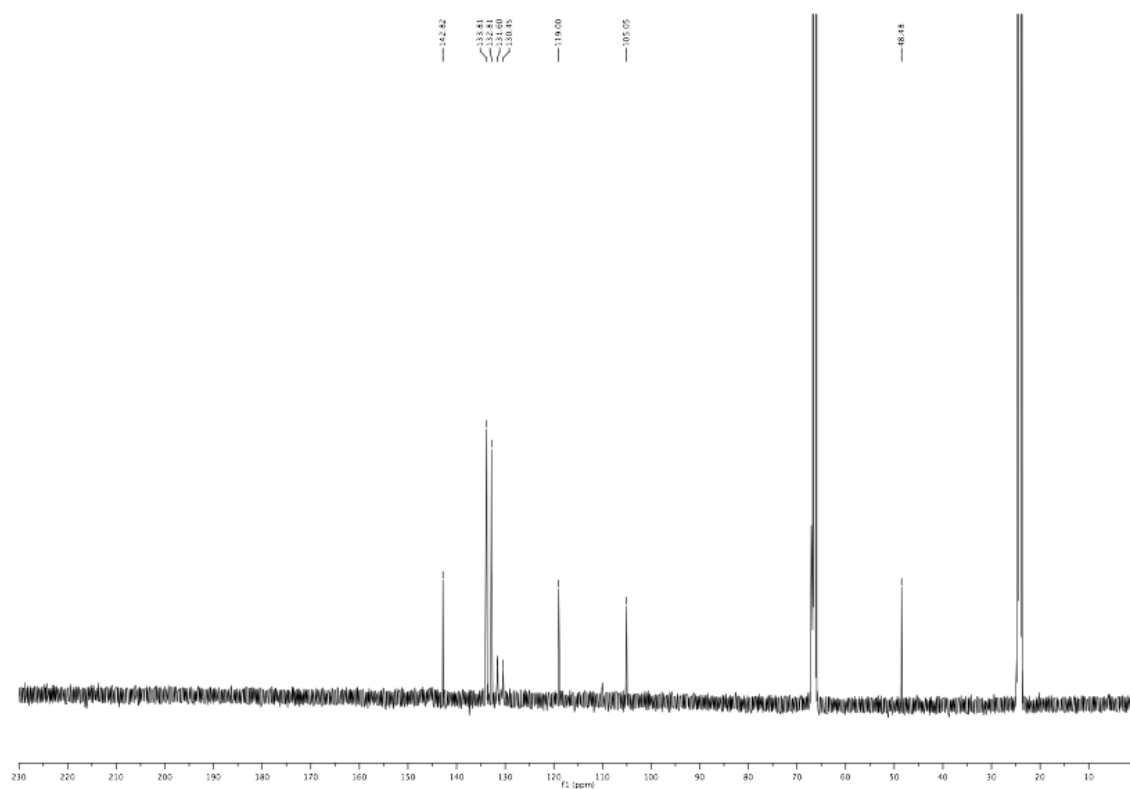


$^1\text{H}$  NMR, THF- $d_8$ , 400 MHz

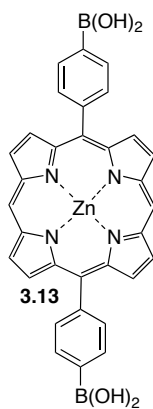
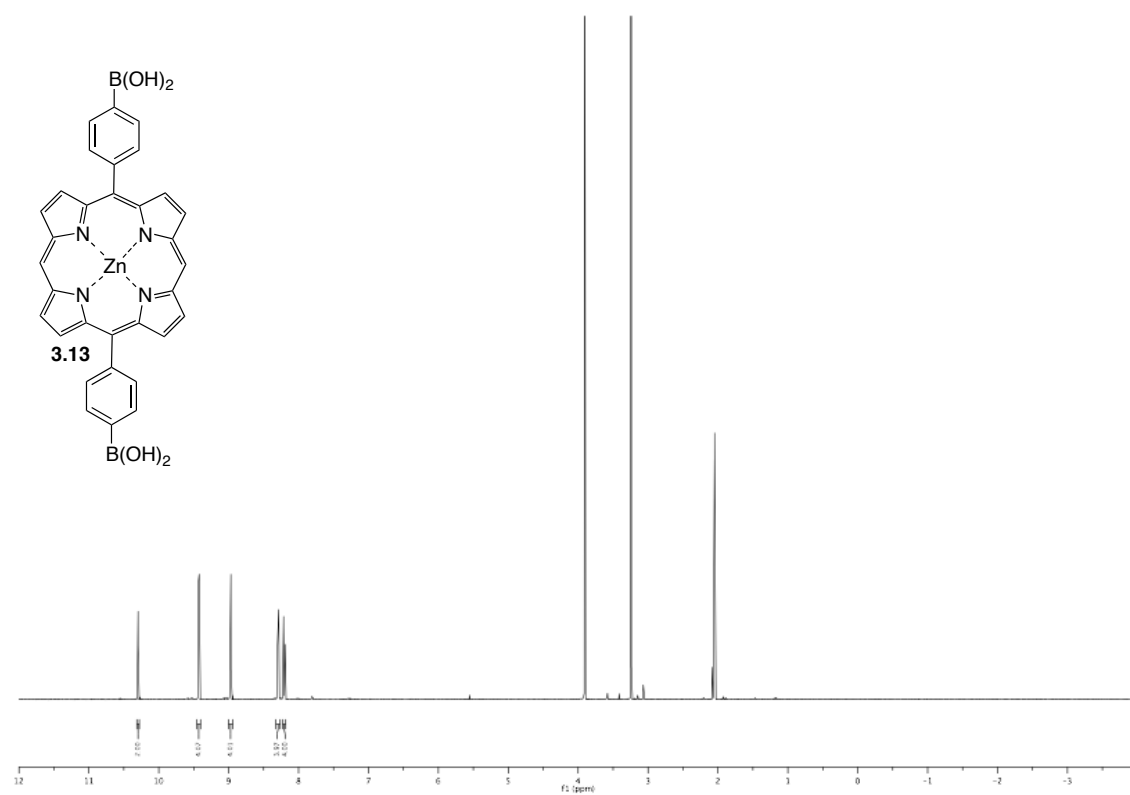


$^{13}\text{C}$  NMR, THF- $d_8$ , 100 MHz

# CONTRIBUTIONS TO THE CHEMISTRY OF POLYHYDROXYLATED AROMATIC COMPOUNDS

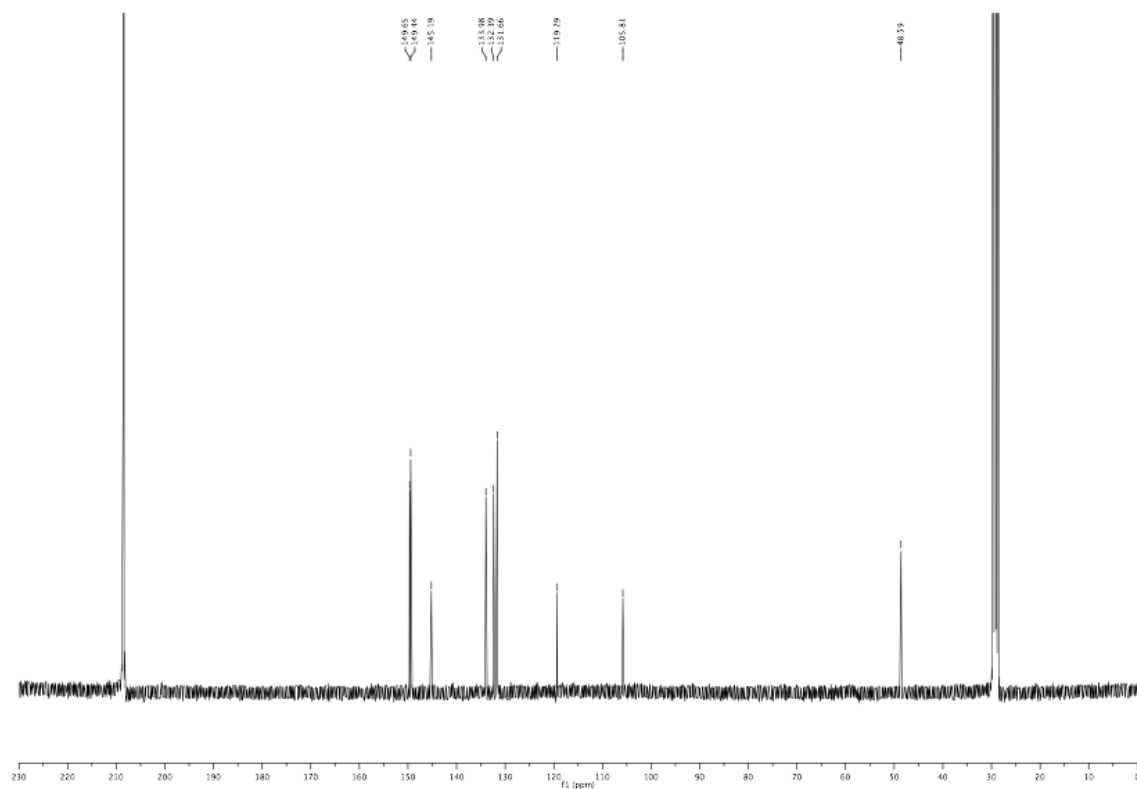


<sup>1</sup>H NMR, acetone-*d*<sub>6</sub>, 400 MHz

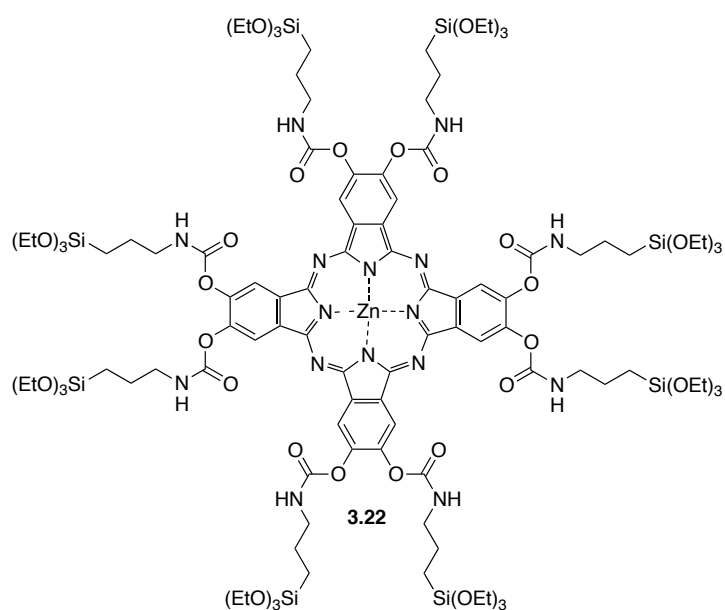


### 3.6. Experimental Section

$^{13}\text{C}$  NMR, acetone- $d_6$ , 100 MHz



#### 3.6.3 Synthesis of a Porphyrin-based 3D Donor-Acceptor Interpenetrating System

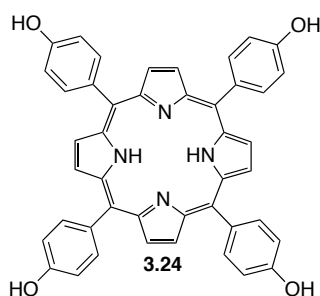




## CONTRIBUTIONS TO THE CHEMISTRY OF POLYHYDROXYLATED AROMATIC COMPOUNDS

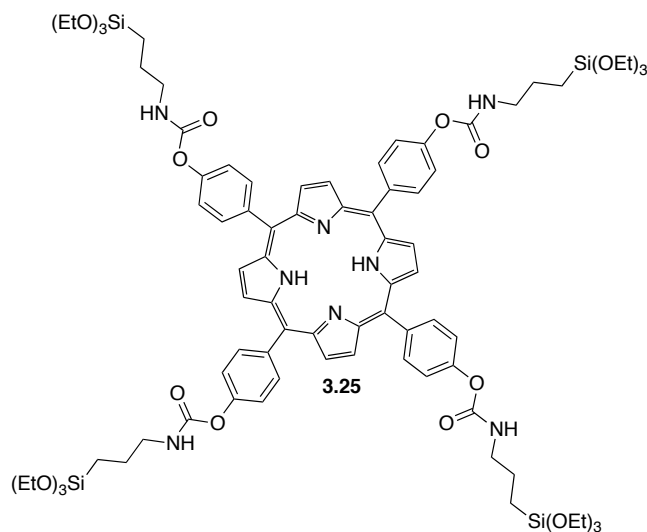
**Phthalocyanine PMO precursor 3.22.** To a suspension of **3.6** (100 mg, 1.0 *eq.*) in dry THF (10 mL) was added TEA (724 mg, 7.15 mmol, 50 *eq.*), followed by 3-isocyanatopropyltriethoxysilane (**3.21**) (566 mg, 2.29 mmol, 16 *eq.*). The reaction mixture was stirred at rt overnight and all volatiles were removed *in vacuo*. The resulting oily residue was taken up in dry toluene and precipitated with hexanes. The suspension was centrifuged and the precipitate was filtered off, dissolved in toluene and precipitated again. After drying 180 mg (47%) of title compound **3.22** were obtained as a green-blue solid.

**Data for 3.22:** IR (neat): IR (ATR):  $\tilde{\nu}$  = 3322 (br), 2973 (m), 2928 (w), 2881 (w), 1714 (vs), 1536 (s), 1453 (m), 1404 (m), 1391 (m), 1244 (s), 1165 (m), 1073 (vs), 938 (vs);  $^1\text{H NMR}$  (400 MHz, DMSO-*d*<sub>6</sub>):  $\delta$  = 9.20 (s, 8H), 8.19 (d, 8H, *J* = 4.8), 3.82 (q, 48H, *J* = 7.0), 7.29 (s, 8H), 3.88 (s, 24H).



**5,10,15,20-Tetrakis(4-hydroxyphenyl)-21H,23H-porphine (3.24).** 4-Hydroxybenzaldehyde (**3.23**) (3.6 g, 30 mmol, 1.0 *eq.*) was dissolved in refluxing propionic acid (150 mL). Upon addition of pyrrole (**3.17**) (2.0 g, 30 mmol, 1.0 *eq.*) the reaction mixture was refluxed for further 30 min. The solution was subsequently slowly cooled 0 °C for 15 min. The resulting precipitate was washed excessively with CHCl<sub>3</sub> (200 mL) and then dissolved in acetone (100 mL) and CHCl<sub>3</sub> (50 mL), washed with saturated sodium bicarbonate solution (2 × 50 mL), brine (3 × 50 mL), dried, filtered and concentrated. The crude product was purified by repetitive silica gel chromatography (1% MeOH in CHCl<sub>3</sub>) to afford 2.5 g (49%) of *meso*-tetra(*p*-hydroxy)phenyl porphyrin **3.24** as a purple solid.

**Data for 3.24:** IR (ATR):  $\tilde{\nu}$  = 3313 (br), 1700 (m), 1607 (s), 1509 (s), 1350 (s), 1213 (vs), 1171 (vs), 966 (s), 794 (vs), 728 (s);  $^1\text{H NMR}$  (300 MHz, DMSO-*d*<sub>6</sub>):  $\delta$  = 9.94 (s, 4H), 8.87 (s, 8H), 8.00 (d, 8H, *J* = 8.5), 7.21 (dd, 8H, *J* = 1.2, 8.5), -2.88 (s, 2H);  $^{13}\text{C NMR}$  (100 MHz, DMSO-*d*<sub>6</sub>):  $\delta$  = 157.8, 157.7, 136.0, 120.4, 116.1, 114.4; MS (EI) calcd. for C<sub>44</sub>H<sub>30</sub>N<sub>4</sub>O<sub>4</sub> (M<sup>+</sup>): 687.2267; found: 687.2271.



**Porphyrin PMO-precursor 3.25.** A dry SCHLENCK-tube was charged with porphyrin **3.24** (204 mg, 0.30 mmol, 1 *eq.*) in dry THF (15 mL). To the solution was added 3-isocyanatopropyltriethoxysilane (445 mg, 1.8 mmol, 6 *eq.*) and TEA (9.11 mg, 0.09 mmol, 0.3 *eq.*) at rt and under argon atmosphere. The reaction mixture was hereafter heated to 80 °C for 4 h. After concentration *in vacuo*, filtration and washing with EtOAc (50 mL), all volatiles were removed. The resulting oily residue was taken up in little EtOAc and precipitated with hexanes. The precipitate was collected after centrifugation and the procedure was repeated five times. The resulting solid was dried under high vacuum to obtain 200 mg (40%) of title compound **3.25** as purple solid.

**Data for 3.25:** IR (ATR):  $\tilde{\nu}$  = 3315 (br), 2971 (w), 2926 (vw), 2884 (vw), 1714 (vs), 1608 (s), 1586 (w), 1498 (s), 1470 (w), 1349 (s), 1205 (vs), 1166 (s), 1069 (vs), 965 (w);  $^1\text{H}$  NMR (400 MHz,  $\text{CDCl}_3$ ):  $\delta$  = 8.88 (s, 8H), 8.18 (d, 8H,  $J$  = 8.4), 7.53 (d, 8H,  $J$  = 8.4), 5.60 (t, 4H,  $J$  = 5.9), 3.91 (dt, 24H,  $J$  = 6.2, 7.0), 3.42 (dd, 8H,  $J$  = 6.6, 13.0), 1.88-1.78 (m, 8H), 1.30 (td, 36H,  $J$  = 1.6, 7.0), 0.82-0.76 (m, 8H), -2.83 (s, 2H);  $^{13}\text{C}$  NMR (100 MHz,  $\text{CDCl}_3$ ):  $\delta$  = 154.7, 151.1, 138.9, 135.7, 135.2, 119.8, 119.3, 113.7, 58.6, 43.7, 23.2, 18.3, 7.8; MS (ESI) calcd. for  $\text{C}_{84}\text{H}_{115}\text{N}_8\text{O}_{20}\text{Si}_4$   $[\text{M}+\text{H}]^+$ : 1667.7305; found: 1667.7306.

### 3.7 Bibliography

- [1] P. Caithamer, *Mathematical Geosciences* **2008**, *40*, 653–670.
- [2] A.-E. Becquerel, *Compte Rendus* **1839**, *9*, 561.
- [3] F. C. Krebs, *Solar Energy Materials and Solar Cells* **2009**, *93*, 394–412.
- [4] J. S. Kim, J. H. Park, J. H. Lee, J. Jo, D.-Y. Kim, K. Cho, *Applied Physics Letters* **2007**, *91*, 112111.
- [5] G. a. Chamberlain, *Solar Cells* **1983**, *8*, 47–83.
- [6] C. W. Tang, *The Journal of Chemical Physics* **1975**, *62*, 2139–2149.
- [7] C. W. Tang, *Applied Physics Letters* **1986**, *48*, 183–185.
- [8] R. R. Lunt, N. C. Giebink, A. a. Belak, J. B. Benziger, S. R. Forrest, *Journal of Applied Physics* **2009**, *105*, 053711.
- [9] K. W. Kolasinski, *Current Opinion in Solid State and Materials Science* **2005**, *9*, 73–83.
- [10] G. M. Whitesides, M. Boncheva, *Proceedings of the National Academy of Sciences of the United States of America* **2002**, *99*, 4769–4774.
- [11] G. M. Whitesides, B. Grzybowski, *Science* **2002**, *295*, 2418–2421.
- [12] A. P. Côté, A. I. Benin, N. W. Ockwig, M. O’Keeffe, A. J. Matzger, O. M. Yaghi, *Science* **2005**, *310*, 1166–1170.
- [13] T. Asefa, M. J. Maclachlan, N. Coombs, G. A. Ozin, *Nature* **1999**, *402*, 867–871.
- [14] T. N. T. Inabe, T. Asari, H. Hasegawa, M. Matsuda, E.H. Gacho, N. Matsumura, S. Takeda, K. Takeda, *Synthetic Metals* **2003**, *134*, 515–518.
- [15] J.-L. Soret, *Compte Rendus* **1883**, *97*, 1269–1270.
- [16] W. Zheng, N. Shan, L. Yu, X. Wang, *Dyes and Pigments* **2008**, *77*, 153–157.

- [17] D. Dini, M. Hanack, in *The Porphyrin Handbook Vol. 17*, Academic Press, San Diego, **2003**, pp. 1–36.
- [18] Gouterman, M., *The Porphyrins*, Dolphin; D.; Ed.; Academic: New York, **1978**.
- [19] E. L. Spitler, W. R. Dichtel, *Nature Chemistry* **2010**, *2*, 672–677.
- [20] D. N. Bunck, W. R. Dichtel, *Angewandte Chemie (Int. Ed. Engl.)* **2012**, *51*, 1885–1889.
- [21] F. J. Uribe-Romo, J. R. Hunt, H. Furukawa, C. Klöck, M. O’Keeffe, O. M. Yaghi, *Journal of the American Chemical Society* **2009**, *131*, 4570–4571.
- [22] E. L. Spitler, J. W. Colson, F. J. Uribe-Romo, A. R. Woll, M. R. Giovino, A. Saldivar, W. R. Dichtel, *Angewandte Chemie (Int. Ed. Engl.)* **2012**, *51*, 2623–2627.
- [23] M. Dogru, A. Sonnauer, A. Gavryushin, P. Knochel, T. Bein, *Chemical Communications* **2011**, *47*, 1707–1709.
- [24] X. Feng, L. Chen, Y. Dong, D. Jiang, *Chemical Communications* **2011**, *47*, 1979–1981.
- [25] S. Wan, F. Gándara, A. Asano, H. Furukawa, A. Saeiki, S. K. Dey, L. Liao, M. W. Ambrogio, Y. Y. Botros, X. Duan, et al., *Chemistry of Materials* **2011**, *23*, 4094–4097.
- [26] J. W. Colson, A. R. Woll, A. Mukherjee, M. P. Levendorf, E. L. Spitler, V. B. Shields, M. G. Spencer, J. Park, W. R. Dichtel, *Science* **2011**, *332*, 228–231.
- [27] A. Nagai, Z. Guo, X. Feng, S. Jin, X. Chen, X. Ding, D. Jiang, *Nature Communications* **2011**, *2*, 1–8.
- [28] N. B. McKeown, in *The Porphyrin Handbook Vol. 15*, Academic Press, San Diego, **2003**, pp. 61–124.
- [29] S. W. Oliver, T. D. Smith, *Journal of the Chemical Society, Perkin Transactions 2* **1987**, 1579–1582.
- [30] J. Lacour, D. Monchaud, G. Bernardinelli, F. Favarger, *Organic Letters* **2001**, *3*, 1407–1410.
- [31] A. Sugasaki, K. Sugiyasu, M. Ikeda, M. Takeuchi, S. Shinkai, *Journal of the American Chemical Society* **2001**, *123*, 10239–10244.

**CONTRIBUTIONS TO THE CHEMISTRY OF POLYHYDROXYLATED  
AROMATIC COMPOUNDS**

---

- [32] M. Ikeda, S. Shinkai, A. Osuka, *Chemical Communications* **2000**, 1047–1048.
- [33] S. Lindsey, C. Hsu, C. Schreiman, *Tetrahedron Letters* **1986**, 27, 4969–4970.
- [34] H. L. Anderson, *Chemical Communications* **1999**, 2323–2330.
- [35] C.-H. Lee, R. Filler, J. Y. Leec, J. Lic, B. K. Mandal, *Renewable Energy* **2010**, 35, 1592–1595.
- [36] E. Bescher, J. D. Mackenzie, *Materials Science and Engineering: C* **1998**, 6, 145–154.
- [37] Q. Yang, J. Liu, L. Zhang, C. Li, *Journal of Materials Chemistry* **2009**, 19, 1945.
- [38] Q. Yang, J. Liu, J. Yang, M. Kapoor, S. Inagaki, C. Li, *Journal of Catalysis* **2004**, 228, 265–272.
- [39] J. Xue, B. P. Rand, S. Uchida, S. R. Forrest, *Advanced Materials* **2005**, 17, 66–71.
- [40] J. R. K. S. W. Sing, D. H. Everett, R. A. W. Haul, L. Moscou, R. A. Pierotti, *Pure and Applied Chemistry* **1985**, 57, 603.
- [41] J. S. Beck, K. D. Schmitt, J. B. Higgins, J. L. Schlenkert, *Journal of the American Chemical Society* **1992**, 114, 10834–10843.
- [42] C. Sanchez, C. Boissière, D. Grosso, C. Laberty, L. Nicole, *Chemistry of Materials* **2008**, 20, 682–737.
- [43] B. J. Melde, B. T. Holland, C. F. Blanford, A. Stein, *Chem. Mater.* **1999**, 11, 3302–3308.
- [44] S. Inagaki, S. Guan, Y. Fukushima, T. Ohsuna, *Journal of the American Chemical Society* **1999**, 9611–9614.
- [45] N. Mizoshita, M. Ikai, T. Tani, S. Inagaki, *Journal of the American Chemical Society* **2009**, 131, 14225–14227.
- [46] N. Mizoshita, Y. Goto, Y. Maegawa, T. Tani, S. Inagaki, *Chemistry of Materials* **2010**, 22, 2548–2554.

- [47] M. Pirouzman, M. M. Amini, N. Safari, *Journal of Colloid and Interface Science* **2008**, *319*, 199–205.
- [48] J. Li, L. Guo, J. Shi, *Physical Chemistry Chemical Physics: PCCP* **2010**, *12*, 5109–5114.
- [49] T. Oekermann, D. Schlettwein, N. I. Jaeger, *Journal of Electroanalytical Chemistry* **1999**, *462*, 222–234.
- [50] T. Oekermann, D. Schlettwein, N. I. Jaeger, *The Journal of Physical Chemistry B* **2001**, *105*, 9524–9532.
- [51] A. Ol'Ga, Z. Sergey, Z. Ol'Ga, U. Nadejda, *Molecular Crystals and Liquid Crystals Science and Technology. Section A*. **2001**, *364*, 611–623.
- [52] C. J. Brinker, Y. Lu, A. Sellinger, H. Fan, *Advanced Materials* **1999**, *11*, 579–585.
- [53] S. A. Mikhalenko, L. I. Solov, E. A. Luk, *Zhurnal Obshchei Khimii* **2004**, *74*, 451–459.